JOURNAL OF APPLIED PHYSICS

JOURNAL OF APPLIED PHYSICS

Vol. 21, No. 4 APRIL, 1950

In This Issue

		Page
High Speed Digital Computers	LOUIS N. RIDENOUR	263

Contributed Original Research

Lapping Technique: To Improve the Image Quality of Electron Microscope Lenses	F. A. HAMM	271
Separation of Gases by Fractional Permeation through Membranes	SOL WELLER AND WALDO A. STEINER	279
D.C. Characteristics of Silicon and Germanium Point Contact Crystal Rectifiers. Part II. The Multicontact Theory	V. A. JOHNSON, R. N. SMITH, AND H. J. YEARIAN	283
Analysis of a Sampling Servo Mechanism	KENNETH S. MILLER AND RALPH J. SCHWARZ	290
Variation of Elastic Moduli and Wave Velocity with Pressure and Temperature in Plastics	D. S. HUGHES, E. B. BLANKENSHIP, AND R. L. MIMS	294
Summation of Fourier Series by Operational Methods	LOUIS A. PIPES	298
Effect of Change of Scale on Sintering Phenomena	CONYERS HERRING	301
Resonant Bar Method for Determining the Elastic Properties of Thin Lamina	A. W. NOLLE AND P. J. WESTERVELT	304
Electronic Isograph for Roots of Polynomials	BYRON O. MARSHALL, JR.	307
Cadmium Sulfide X-Ray Detector	RUDOLF FRERICHS	312
Diffraction by a Cylindrical Obstacle	CHARLES H. PAPAS	318
Air Temperature Modification by Vertical Transport	ROBERT G. FLEAGLE	326
Mode Conversion Losses in Transmission of Circular Electric Waves through Slightly Non-Cylindrical Guides	SAMUEL P. MORGAN, JR.	329
Wettability, a Function of the Polarizability of the Surface Ions	L. R. SONDERS, D. P. ENRIGHT, AND W. A. WEYL	338
Distribution of Ionization in Materials Irradiated by Two and Three Million-Volt Cathode Rays	J. G. TRUMP, K. A. WRIGHT, AND A. M. CLARKE	345

Letters to the Editor:

Metal Transfer in the Cutting Process	MILTON C. SHAW AND CHARLES D. STRANG, JR.	349
Potential Distribution in Pulsed Oxide-Coated Cathodes and Its Consequences for the Velocity Distribution of the Emitted Electrons	R. LOOSJES, H. J. VINK, AND C. G. J. JANSEN	350
Sampling of 1949 Books		352
Index to Advertisers		xxxviii

BOARD OF EDITORS
ELMER HUTCHISSON, *Editor*

Associate Editors
HOWARD H. AIKEN
OTTO BEECK
JAMES HILLIER
W. JAMES LYONS
PHILIP MORRISON
ERIC REISSNER
RAYMOND J. SEEGER
FREDERICK SEITZ
CHARLES S. SMITH

Publication of the
American Institute of Physics

OFFICERS
GEORGE R. HARRISON, *Chairman*
GEORGE B. PEGRAM, *Treasurer*
JOHN T. TATE, *Adviser on Publications*

GOVERNING BOARD
J. W. BEAMS
C. PAUL BONER
WALLACE R. BRODE
W. F. FAIR, JR.
J. B. FISK
G. P. HARNWELL
GEORGE R. HARRISON
W. V. HOUSTON
RUDOLPH KINGSLAKE
PAUL KIRKPATRICK
PAUL E. KLOPSTEG
F. W. LOOMIS
PHILIP M. MORSE
J. R. OPPENHEIMER
GEORGE B. PEGRAM
HAROLD K. SCHILLING
FRANCIS G. SLACK
JOHN C. STEINBERG
JOHN T. TATE

Consultant on Printing
MELVIN LOOS

ADMINISTRATIVE STAFF
HENRY A. BARTON, *Director*
WALLACE WATERFALL, *Executive Secretary*
THEODORE VORBURGER, *Assistant Treasurer and Comptroller*
RUTH F. BRYANS, *Publication Manager*
BETTY HOFSTADTER, *Assistant Secretary*
EILEEN B. NEUBERGER, *Circulation Manager*

The JOURNAL OF APPLIED PHYSICS, published monthly at Prince and Lemon Sts., Lancaster, Pa., is devoted to physics in its role as the science basic to other natural sciences and to the arts and industries. Previous to 1937 this publication was known as PHYSICS. The JOURNAL OF APPLIED PHYSICS publishes editorials and reviews, as well as technical papers of applied physics. Articles appearing in it are indexed regularly, according to their field, by Physics Abstracts, Chemical Abstracts, Engineering Index, Inc., Industrial Arts Index, etc.

Manuscripts should be submitted to Elmer Hutchisson, Editor, Case Institute of Technology, Cleveland 6, Ohio. Unless otherwise stated, submission of a manuscript is a representation that it has been neither copyrighted, published, not submitted for publication elsewhere. The authors' institutions are requested to pay a **publication charge** of $8 per page which, if honored, entitles them to 100 reprints without further charge. Instructions will be sent with galley proofs.

Subscriptions, renewals, and orders for back numbers should be addressed to the American Institute of Physics, 57 East 55 Street, New York 22, New York.

Subscription Price	U.S. and Canada	Elsewhere
To members and associate members of the American Institute of Physics	$7.00	$ 8.00
To all others	9.00	10.00

Back Number Prices

Yearly back number rate when complete year is available: $10.00. Single copies: $1.00 each.

Changes of address should be sent to the Circulation Manager, American Institute of Physics; **corrected proofs** should be sent to the Publication Manager, American Institute of Physics. **Advertising rates** supplied on request. Orders, advertising copy, and cuts should be sent to the American Institute of Physics.

Entered as second class matter January 22, 1937, at the Post Office at Lancaster, Pennsylvania, under the Act of March 3, 1879. Accepted for mailing at the special rate of postage provided for in paragraph (d-2), section 34.40, P. L. & R. of 1948, authorized May 2, 1932.

Journal
of
Applied Physics

Volume 21, Number 4 April, 1950

High Speed Digital Computers

An Elementary Survey of Present Developments and Future Trends

Louis N. Ridenour

University of Illinois, Urbana, Illinois

ONE of the most interesting, and possibly one of the most significant, of the post-war technical developments is the great effort that is currently being expended, both here and abroad, on the design, construction, and improvement of high speed automatic digital computing machines. In accordance with the present pattern of support for technical enterprises, the largest part of the effort on such computers is being financed by the federal government; private industry is investing substantial sums; and, somewhat curiously, the universities of the country do not appear to be supporting with their own resources more than a tiny fraction of the work.

Mechanical aids to computation are an old story, of course. But the high speed, automatic, digital, computer—when each of these qualifying adjectives is taken properly into account—is a very new development. Its practical realization cannot be said to have been achieved earlier than the completion of the celebrated ENIAC in 1945. Of this machine we shall have more to say later. Let us pause now to distinguish from other computing devices the type of machine that will occupy our attention here.

First of all, we shall deal with *digital* machines. This excludes a large class of calculating devices customarily lumped under the name of *analog* machines.[1] An analog machine is one which translates into some physical quantity each of the numbers entering a computation; that is, the physical quantity is the measure of the number. The analog machine then manipulates these physical quantities in accordance with the nature of the computation it is desired to carry out. Finally, the physical quantity resulting from such manipulation is measured—that is, turned back into a number—to obtain the numerical answer for the computation. A slide-rule is an analog machine. Numbers are represented, on the slide-rule, by lengths which are proportional to the logarithms of such numbers. To perform a multiplication, the lengths corresponding to the two factors are added, and the resulting total length corresponds to the product, being in fact proportional to the logarithm of the product. This total length is turned back into a number by means of the scales provided on the rule, and the calculation is finished.

A digital machine also uses physical representations for numbers, of course; but instead of using a single physical quantity as the *entire* representation of the number, and thus depending upon a highly accurate presentation, manipulation, and reproduction of the magnitude of this single physical quantity, a digital machine represents by a separate physical quantity each separate digit of a number. This permits a very much greater latitude in design for the digital machine; to handle numbers of ten digits, no part of a digital machine needs to be built with a precision of one part in 10^{10} An analog machine, on the other hand, has no better over-all accuracy than that conferred on it by the precision with which it is built.

Analog machines have been brought to a high stage of perfection and usefulness. Beginning about 1931, Vannevar Bush and his co-workers at M.I.T. developed the celebrated differential analyzer, which was a mechanical device in its first embodiment. During and since the war, electrical differential analyzers of various designs have been constructed, and some of

[1] For a description of analog computers and their uses, see D. R. Hartree, *Calculating Instruments and Machines* (University of Illinois Press, Urbana, 1949), Chapters 2, 3, and 4.

these machines are currently available on the commercial market. We shall not concern ourselves here, however, with such machines. We shall speak only of *digital* computers.

In fact, we shall speak only of *automatic* digital computers. The meaning of this qualification is that we shall not deal with digital machines of the sort represented by the familiar adding machine, or the Monroe or Marchant type of desk calculator. Such machines are very old in conception and in realization, of course.[2] The first practical adding machine based on the use of number wheels was devised by Blaise Pascal in 1642; a machine capable of multiplication (by repeated addition accompanied by suitable shifts) was designed by Leibnitz in 1671 and built in 1694. In 1820 Charles Thomas, a Frenchman, designed the first commercially successful machine; with minor modifications and improvements, this machine was being built in Paris right up to the Second World War.

We shall not even concern ourselves here with the familiar punched-card machines manufactured by the International Business Machines Company. These machines stem from the work of Herman Hollerith, an employee of the U. S. Census Bureau, who in 1889 conceived the idea of using, for entering numbers into a machine and for reading out the results, holes punched in a card. A similar scheme had long been used for controlling the weaving of complicated fabrics on the Jacquard loom, and its application to computing machines had been proposed two generations earlier by Charles Babbage, of whom we say more later.

Desk calculators and IBM machines are excluded from the present discussion because such a machine performs only one elementary computation at a time, and must be instructed anew before it can perform another. That is, we can enter on a desk machine the two factors entering a multiplication, and then rely on the machine to carry out the operation and display to us the product. But, before another multiplication—or indeed any other operation—is performed, we must ourselves inform the machine what numbers enter the new computation, and which operation is to be performed on these numbers.

In an automatic machine, on the other hand, sufficient instructions are given the machine at the beginning, and the machine has sufficient capabilities within itself, to permit the whole of a complicated sequence of manipulations on many numbers to be performed by the machine without human intervention, once the signal to start has been given. Thus an automatic machine is basically different from a desk calculator; it is more nearly a mechanized simulacrum of the whole complex: human computer plus desk machine plus tables of functions for reference plus work sheet on which the course of the computation is sketched out, and intermediate results can be recorded. The idea for such an automatic machine is more than a century old. Charles Babbage, who was Lucasian Professor of Mathematics at Cambridge, conceived such a device—the Analytical Engine—and began to build it (on British government money) in 1835.[3] The Analytical Engine was never completed, largely because the mechanical engineering of Babbage's day was not equal to the task of realizing his complicated designs, but its plan was astonishingly modern in terms of the ideas which still rule the automatic computer field today.

One more qualifier is left. We shall speak here of *high speed* automatic digital computers. Earlier than the ENIAC, at least two types of automatic digital computers were designed and built. Professor Howard Aiken, of Harvard, built with the help of the IBM Company his so-called Mark I machine which was an electrically controlled, mechanically operated, automatic computer that was hailed as "Babbage's dream come true."[4] About the same time, at Bell Telephone Laboratories, a machine was built which qualified as an automatic digital computer according to the present definitions, and used electromechanical relays as elementary computing and storage elements.[5] Both these machines were of limited speed because of their dependence on mechanical elements whose motion was necessarily slow in comparison with the actions in electrical circuits. In the ENIAC,[6] on the other hand, the operations within the machine are conducted entirely in terms of the circulation through electrical lines of electrical pulses, generated at a base rate of 100,000 per second, and in terms of the registration of the effects of such pulses by means of electronic "flip-flop" circuits which can rest stably in either of two stationary states, yet be transferred from one state to the other in a fraction of a microsecond by a pulse of the correct sign.

The time required in the ENIAC to add together two numbers, each of ten decimal digits, is 200 microseconds—200 millionths of a second. In terms of the times required by machines now under construction, this is long; addition times of about 10 microseconds are common in modern designs. But, in terms of the operation of machines having mechanical elements, this is very fast indeed.

In the remarks to follow, then, whenever the word "machine" is used, it will be understood to refer to a high speed automatic digital computing machine. Let us now turn to some general considerations on the overall design of such machines.

---

[2] For a historical account of the development of desk computing machines, see the article "Calculating machines" in the *Encyclopedia Britannica*.

[3] H. P. Babbage, *Babbage's Calculating Engines* (Spon, Ltd., London, 1889).

[4] *Annals of the Harvard Computation Laboratory* (Harvard University Press, Cambridge, 1946), Vol. I.

[5] S. B. Williams, Bell Lab. Record 25, 49 (1947).

[6] H. H. Goldstine and A. Goldstine, Math. Tables and Aids to Computation, 2, 97 (1946); D. R. Hartree, Nature 158, 500 (1946).

GENERAL REMARKS ON MACHINE DESIGN

While any given machine must be designed as a whole, it is often useful to distinguish as separate various parts of the machine which have various functions. The more important of such parts are:

First, the *arithmetic unit*. This device performs the individual arithmetical operations as required by the schedule of the computation being conducted. It is a very close electronic parallel to the familiar desk computing machine.

Second, the *inner* or *high speed memory unit*. This, which is presently the least satisfactory part of machines in existence or under design, is a device for registering numbers in a permanent way—either the numbers entering the problem or intermediate results—and keeping them accessible for use on demand as the computation proceeds. Any number in the memory must be available on demand in a very few microseconds. The memory is ordinarily so arranged that it can also store *orders*, which are instructions to the machine that govern the course of the computation.

Third, the *control unit*. This part of the machine is in charge of the whole operation. It keeps track of the calculation, determines which individual operation should be performed next, and causes its execution.

Finally, an *input-output unit*. This is necessary to enable the machine to communicate with its human masters. Through this unit, the machine is supplied initially with the data and instructions entering the problem; through this unit, the machine can also read out intermediate or final results. Often, the input-output unit is used to provide a large-capacity low speed storage (on magnetic wire or punched type) for numbers and orders. This outer memory supplements the inner memory, since the latter is seldom as capacious as one would desire.

When a mathematical problem is to be presented to such a machine, it must be programmed; that is, broken down into the individual steps to be performed successively. The numbers entering the problem must be supplied, and so must the *orders*, or instructions to the machine for handling those numbers. The input unit reads the program of numbers and orders into the memory unit of the machine at the beginning, and the work thereafter proceeds entirely within the machine.

A typical order might be translated: "Take the number in stored in memory location 1100 and multiply it by the number stored in memory location 2016. Put the product in memory location 1234 (erasing what stands there now) and then go to memory location 1161 for the next order." Orders are expressed in a code which gives them the appearance of numbers, so far as the machine is concerned. This has two advantages: each memory location can store either a number or an order, indifferently, and arithmetical operations can be performed on the pseudonumbers which are orders, thus changing one order into another when this is required as the computation progresses.

The example of an order just given calls for a multiplication. Similar orders govern addition, subtraction, multiplication, and sometimes certain other arithmetical operations. Another type of order, whose use greatly extends the scope of the machine, is the so-called "*conditional transfer*" order. This provides the machine with a sort of judgment, and enables the further course of a computation to be determined by the results to date, without the explicit intervention of a human operator. A typical conditional transfer order might say: "Compare the result of the last manipulation with the number stored in memory location 1648; if it is larger than that number, or equal to it, go to memory location 1174 for the next order; otherwise, go to memory location 1176 for the next order." Such decisions are a prominent feature of the control of a com plicated calculation by a human computer using conventional methods.

Numbers are represented within the machine by groups of non-linear elements each of which has two stable states: on or off. For electronic machines of the present day, the non-linear elements are ordinarily the so-called "flip-flop" circuits derived from the multivibrator invented in 1919 by Eccles and Jordan.[7] Two tubes are so coupled, in a flip-flop circuit, that when one tube is conducting, the grid of the other tube is biased far beyond cut-off. If a signal is received in such a sense as to swing positive the grid of the cut-off tube, then the current in this tube rises and at the same time the grid of the other tube is driven negative. In a fraction of a microsecond, this action culminates in a stable situation in which the tube that was formerly cut off is carrying full current, while the grid of the tube that was formerly conducting is biased far beyond cut-off. Thus the system has two distinguishable stable states, and can by a pulse be transferred from one of these states to the other.

The flip-flop is not the only device which realizes practically this requirement of having two stable states which we may call on or off. We shall see later that there are other, and sometimes simpler and cheaper, ways of achieving this end. Indeed, it is in this direction that we can expect much of the short-term progress in computing-machine design to lie.

Since numbers are represented by a succession of elements which are either on or off, it seems natural to express numbers, for the purposes of the machine, in terms of the number system based on 2, rather than in the familiar decimal system based on 10. In the binary system—the base-2 system—each digit of a number has either the value 0 or 1, and the digits appearing in neighboring places with reference to the binary point (analogous to the decimal point in the base-10 system) differ in value by a factor 2, rather than by a factor 10

[7] W. H. Eccles and F. W. Jordan, Radio Review **1**, 143 (1919).

as they do in the decimal system. Each number is then represented most economically, by a series of on-off elements, one for each digit of the number. The representation of decimal numbers in terms of on-off elements is somewhat less economical, since it requires the use, to represent each digit, of a collection of on-off elements so arranged that the collection has ten distinguishable stable states. These ten states are then used to represent the values, from 0 to 9, which the digit can assume.

Most of the machines presently under construction use the binary system for internal purposes; this necessitates a transformation of numbers from decimal representation to binary representation at the start and the end of each calculation, but the machine itself can perform this transformation, and the time required for this conversion is small in comparison to the time needed for the internal manipulations of numbers by a machine during the solution of a problem.

There is one other argument for the use of the binary system. Binary arithmetic is the arithmetic of logic, in a universe where a proposition is either true (one) or false (zero). The machine can, then, if it uses the binary representation of numbers, conduct its logical operations in the same formal terms as are used for its arithmetical manipulations.

Let us now pause for a moment to discuss what is called "balance" in the design of a computing machine. This term refers to the simple idea that the most efficient operation will be achieved when the times required to perform the various operations conducted by the machines are related to one another in a reasonable way. To take an absurd example, the requirement that the machine be able to perform whole sequences of computations automatically arises from its internal speed. There would be no sense in performing an addition in 200 microseconds (as the ENIAC does) or in 10 microseconds (as some of the new machines will do), if a slow-moving human operator had, at each stage, to copy off the result and then to enter the next two numbers to be summed.

At a more sophisticated level, we must consider the balance of operating times within the machine. This requires a careful weighing of the relative times required for access to the high speed memory, for addition, for transfer of a number from one place to another in the machine, and for the repeated operations involved in multiplication and division. To a certain extent, decisions on the balance of internal operating times will be made on the basis of the type of problem for which the machine will mainly be used; thus, for example, a machine whose main task was to be addition or comparison of numbers would desirably have a different internal balance of operating times from that appropriate to a machine intended for processes involving many multiplications. But the balance of a general-purpose computing machine can also be specified, and attention to this design consideration is important.

It has already been stated that numbers are ordinarily expressed in the machine in terms of their binary representation. There are two quite different ways of handling such numbers, both of which are in use in machines now building. One is called the serial method, the other the parallel method.[8] In serial operation, a number is transmitted from one place to another in the machine a single digit at a time, until the entire number is spelled out. In parallel operation, each digit of a number is transmitted on its own separate line, and all the digits of a given number are sent simultaneously.

As usual, each of these schemes has its advantages and its disadvantages. The parallel representation is inherently faster, since the entire number is transmitted at once, while in the serial scheme a number is sent one digit at a time. On the other hand, the amount of equipment needed in a parallel machine is greater than that required for a serial machine, since in the former as many lines are needed for transmitting a given number as there are digits in the number, while in serial operation all digits are sent successively down a single line. In a serial machine, exact timing is usually quite significant, since, for example, the successive digits of a number are distinguished from one another by their time of occurrence. In a parallel machine, on the other hand, timing is unimportant, since the place of a digit in a number is distinguished completely by the place at which it occurs in the machine. It is too early to say which of these schemes is the better absolutely, or the better under certain circumstances. They seem today to be competitors of approximately equal promise, and only further work and further development can determine which is the better.

The detailed design of the inner, high speed, memory has a substantial influence on the choice of serial or parallel operation for a machine. The requirements on the inner memory are very simple but very challenging. It must be able to store at least hundreds, and preferably thousands, of separate numbers or orders, and to do this in such a way that each is permanent and may be left stored for long periods without error, while at the same time it is accessible for transmission and use within a very few millionths of a second.

The earliest machines, such as the ENIAC, used for an inner memory banks of flip-flop circuits, so that at least one pair of triodes was required to store each digit of each number in the inner memory. This is such an extravagant scheme that not very many numbers could be so stored; the ENIAC has in its inner memory a capacity of only 20 numbers or orders.

It was clear that greater capacity of the inner memory is needed for achieving proper balance in a general-purpose computing machine. This problem has occupied machine designers for some time, and it still occupies them. The three types of inner memory in use are: first, a rapidly rotating magnetic drum on which the

[8] D. R. Hartree (reference 1, Section 5.6).

digits of numbers can be stored as patterns of magnetization; second, a tube containing mercury or other liquid down which the signals representing digits of numbers can be sent as pulses of sound; and third, electrostatic schemes in which the digits of numbers are stored as patterns of charge on the face of an insulator.

It is worth noticing that the magnetic drum and the sonic delay line are methods of *dynamic* storage in the sense that the numbers stored circulate continuously during storage, while the electrostatic scheme is one of *static* storage. It has therefore sometimes been said that the dynamic storage methods are best suited to a machine of serial type, while the static storage fits best a machine of parallel design. This is only partly true. A dynamic storage method produces one digit after another, to be sure; but a multiplication of the units used for dynamic storage (magnetic drums, mercury delay tubes) permits each digit of a given number or order to be entered on a separate memory unit, so that the whole number can be available at once, as it must be in a parallel machine. On the other hand, static methods of storage are not immediately suitable for use in a serial machine, but can be used if the digits of a number are read off from the static storage one after another.

Let us now turn to a consideration of the capabilities, uses, and limitations of computing machines currently under design or construction.

CAPABILITIES, USES, AND LIMITATIONS OF MACHINES

The nature of the orders presented to a machine has already been mentioned. What we must understand at this juncture is that the number of orders a machine can appreciate and act upon—its vocabulary—is built into it by its designer. An analysis of the operations of arithmetic discloses that the operations of addition, subtraction, multiplication, and division can be defined in terms of the elementary operations "join" and "meet." But the formalism necessary for this reduction is so complicated that it is more sensible to instruct the machine in terms of the four conventional operations of arithmetic than it is to reduce (in programming) every arithmetical operation to its basic terms as expressed by the operations "join" and "meet." How far can we profitably go in this direction of complicated arithmetical operation? Is it worth while, for example, to instruct the machine how to take square roots?

The ENIAC is so instructed. On a single order, the ENIAC will take the square root of a designated number. But the operation of extracting a square root is expressible in terms of the four elementary operations of arithmetic, and thus a machine which does not understand a one-word instruction to take a square root can nevertheless extract such a root if it is provided with a sequence of orders designed to produce such a result, by manipulations which the machine does understand.

This is not a trivial point. To increase the vocabulary of a machine—to increase the number of single orders which it understands—greatly complicates the design of the machine. To simplify the machine by reducing its vocabulary greatly complicates the business of programming a problem for the machine. Here, too, a balance must be struck: between machine complexity and program complexity.

In fact, we meet here one of the major differences of philosophy which has so far occurred in the design of machines. It can be illustrated by noticing that the Harvard Mark I machine is provided with a built-in table of four-place logarithms, so that it has the capability to take the logarithm of a number by looking it up in this table. The designers of other machines have asserted that, since reference to a table of function values is one of the least efficient elementary operations performed by a machine, it is better and faster to have the machine calculate for itself any function values needed, using the infinite series expressing the function. The inefficiency of tabular reference arises because either function values are stored in the inner memory (which is already too small for proper balance in most calculations, and therefore ought not to be used up for function tables), or else function values are stored in an outer memory, where consulting them takes a very long time on the extremely rapid time-scale of the machine. The storage of the form of a function makes far smaller total demands on memory space, and the computation of needed values of the function is, in general, far faster than is consultation of the outer memory to find such values. Thus, in this latter philosophy, tables of functions are an anachronism existing today only because not everyone interested in performing calculations yet has access to a high speed automatic digital computing machine.

Of course, the user of a machine often meets a situation in which he must perform repeated calculations of the same kind. If this calculation is not one comprised in the vocabulary of the machine, it must be programmed for the machine in terms of the elementary operations which are encompassed in that vocabulary. Once this is done, then the program which results can be preserved and used again and again. That is, an extended computation will ordinarily consist of a major routine and a number of sub-routines, the latter being of such a nature that they can be used, if necessary, over and over again as the main computation progresses. If, for example, the machine is not designed to understand an instruction directing it to take the square root of a number, then the square-root operation can be programmed in terms of the four basic operations of arithmetic. If that program is saved, it can be used over and over again whenever the major computation demands that a square root be taken. As a machine is used for extended periods, the number of

such sub-routines which are built up and filed away for future use will be extended; and it is not too much to expect that programming will thereby be greatly simplified.

It is of some interest to compare a high speed automatic digital computing machine to the human brain, and such comparisons have often been made in the past.[9] Such a comparison must be very carefully made. From what we know now, the central nervous system of animals, including men, is composed of individual neurons or nerve cells which are on-or-off devices like the flip-flop. However, man's central nervous system has ten thousand million such elements, while the most complicated computer so far built has only about ten thousand. This factor of a million which separates computing machines from brains is most important. For one thing, it permits the brain to perform its operations with a very considerable redundancy, so that a failure in a single element of a single chain of neurons is not important in terms of the result.

Present day machines, on the other hand, operate in a unitary way. The machine has so few "neurons" that it must use each as if it were infallible. This puts a fantastic premium on reliability in a computing machine. Von Neumann has estimated that, if a machine of the present complexity and design is not to commit errors more frequently than one per four hours, on the average, then its individual parts must have such a reliability that one failure occurs per million million elementary operations. This is some thousand times better reliability than has so far been achieved in conventional telephone practice, where one failure occurs, on the average, per thousand million operations. One of the unanswered questions about computing machines is whether such a reliability can be achieved.

This question has another side. We must ask whether such a reliability needs to be achieved. Are there not methods of checking which can, at every juncture, protect a machine from the consequences of error?

The answer is that there are. Claude Shannon, in his important paper on the "Mathematical theory of communication," has pointed the way to a method of checking which can correct automatically the errors that may be committed by a computer.[10] The scheme involved, which is due to Hamming, requires, to be sure, that other numbers beside those involved in the computation be handled and transmitted, but ensures that failures in the machine will not affect the results of a computation. In effect, the use of such a scheme introduces redundancy for the sake of reliability, and thus moves the logical design of computing machines a step nearer the logical design of the brain. The advantage of Hamming's method is that it provides a prescription for introducing the needed redundancy in the most economical and efficient way, as can be proved by Shannon's communication theory.

Probably one of the most promising directions of development now visible is this matter of evading intolerable requirements for reliability by suitably chosen means of checking. Various rather simple-minded schemes for checking have been proposed in the past—for example, to put the same problem simultaneously on two independent machines, and then to compare the results—but the checking method mentioned above is the first to have a sound theoretical basis.

Let us return to our comparison between computing machines and the brain. The individual on-off elements of a computing machine operate about a thousand times faster than do the neurons of the central nervous system. This constitutes the principal superiority of computing machines to brains; in almost every other respect the computing machines which we now can build are incomparably inferior to the nervous systems which we all possess.

We have already noticed the greatly superior complexity of the brain. Warren McCulloch, a professor of psychiatry at the College of Medicine of the University of Illinois, has observed that the complexity of the ENIAC, the most complicated machine yet built, is about that of the nervous system of the flatworm.

In terms of space and power, there is no comparison. Your brain is contained in your skull, and it dissipates less than twenty-five watts even when it is in full activity. The ENIAC, a million times less complicated, fills a large room and uses 120 kilowatts of power. Twenty kilowatts more are needed to run the blowers which keep it cool.

The great disparity between a machine and a brain must be taken into account in preparing a problem for solution on a machine. In the words of Lady Lovelace, the daughter of the poet Byron (she was speaking of Babbage's Analytical Engine): "The machine can do only what we know how to order it to perform."[11] It can obey instructions exactly, but it must have instructions or it will engage in an absurdity. This means that every possible eventuality of a complicated calculation must be visualized by the human computer when he programs the problem for the machine, and each such eventuality must be provided for in terms of explicit instructions.

Professor Hartree calls this "taking the machine's-eye view" of a computation, and he cites an instance of his own failure to do so.[12] He had failed to foresee that the argument in a trial solution might become negative, since he required finally a positive argument. In the absence of explicit instructions on this point, the machine "did its best, and this was something quite sensible according to its structure and the limited instructions which *had* been given to it, but quite different from the correct small extrapolation of those instruc-

[9] Warren S. McCulloch, Elec. Eng. 68, 492 (1949).
[10] C. E. Shannon and Warren Weaver, *The Mathematical Theory of Communication* (University of Illinois Press, Urbana, 1949), Section 17, p. 48.
[11] H. P. Babbage (reference 3, p. 44).
[12] D. R. Hartree (reference 1, Section 7.9, p. 92).

tions which a human computor would make as a matter of course."

Up to this point we have emphasized, and perhaps overemphasized, the degree to which a computing machine is dependent upon its detailed design and on the orders it receives. The impression has probably been given that these determine entirely the operation of the machine. All this is quite true, under ordinary circumstances, but there is another way of using a machine which is worthy of remark.

I refer to the so-called "Monte Carlo" type of computation.[13] This method replaces the exact analysis of a complicated problem with a sort of statistical experimentation. That is, under properly chosen safeguards to ensure randomness, solutions of the problem at hand are secured for many special cases, and the results are examined to determine the relative probability of various over-all occurrences.

This will be clearer in terms of a specific example. The Monte Carlo technique has been applied to the problem of neutron diffusion in a scattering and absorbing medium. Neutrons of a known energy distribution fall on such a medium in a beam of known intensity; at 10 cm depth (say) what will be the neutron density and velocity distribution? At each encounter with a nucleus, a neutron has a certain chance of being captured, of being elastically scattered in one direction or another, or of being inelastically scattered with energy loss of some amount or other. The probabilities of all these events vary with the energy of the incident neutron and are different for different target nuclei (for the absorber may and usually will contain more than one nuclear type). Rather than seeking an analytical solution for this very complex problem, Ulam[13] has followed the detailed history of many individual neutrons through the absorber, at each encounter with a nucleus determining the outcome by casting dice (in effect), the dice being suitably loaded to reproduce the probability structure appropriate to the event concerned. When this has been done for very many individual neutrons, the statistics of their joint behavior presumably approaches that which would result from a full-dress analytical solution of the problem.

A high speed machine is admirably adapted to apply this method, for its speed enables it to obtain a statistically significant volume of results in a reasonably short time. However, if a machine is to do this, it must be instructed how to gamble. This is accomplished by providing to the machine, at each juncture where gambling is required, a random number whose size determines the result of the play. In fact, schemes exist for the generation by analytical processes—and therefore by and within the machine itself—of "pseudo-random" numbers which have all the necessary properties of randomness. D. H. Lehmer[14] has proposed a particularly elegant and useful scheme of this sort. The pseudorandom numbers produced according to Lehmer's prescription are easy to generate in a machine, and meet all of the standard tests for randomness. After one has made such tests, it comes as a distinct shock to find that all these numbers are divisible by 17.

There are good indications that the Monte Carlo method may be one of the best ways for solving partial differential equations on a machine. Certainly its power and scope seem destined to grow.

FUTURE TRENDS IN COMPUTING MACHINES[15]

There are three important questions which concern the future of computing machinery which I should like to discuss. The first is: "Who is likely to possess large high speed computing machines in the future?" Some workers in the computing-machine field seem quite pessimistic about the ultimate wide availability of such machines, on the grounds that they are complicated, expensive, and difficult to keep in order. This is a point of view with which I entirely disagree. I fully expect that a competent high speed computer will very soon be regarded as an important and inevitable part of the research equipment of any university having even the most modest research pretentions.

Thus, the computing machine is to be viewed not as being in the category of the large astronomical telescope, which is a pleasant but optional luxury for a university, but rather as being in the category of the electronuclear particle accelerator, which is a necessity for any university desiring to cultivate modern nuclear physics. It is a trifle surprising that so few American universities have accepted this view; in fact, only the University of Illinois is presently building a machine on its own funds for its own purposes.

Of course, the wide availability and the general acceptance of high speed computing machines will be greatly forwarded by improvements in reliability and reductions in cost. Such developments can be expected to arise from the continued developments in components and the improvement in the logical design of machines.

Let us now ask: "How large, how fast, and how complicated should a large, high speed, general-purpose computing machine be?" It seems unlikely that machines more involved than the ENIAC will ever be built. More recent machine designs are more ambitious in terms of speed of operation, in terms of the size of inner memory, and in terms of the general competence of the machine. In spite of this, such new machines have fewer tubes than the ENIAC; they use these tubes harder, so to speak. I think that the answer to the question of where to draw the line in designing a general-purpose computing machine is set entirely by con-

[13] S. Ulam, Symposium on Large-Scale Digital Calculating Machinery, Harvard University (September, 1949).

[14] D. H. Lehmer, Symposium on Large-Scale Digital Calculating Machinery, Harvard University (September, 1949).

[15] L. N. Ridenour, Symposium on Large-Scale Digital Calculating Machinery, Harvard University (September, 1949).

siderations of reliability. That is, a large general-purpose machine ought to be as big and complicated and competent as it can be made, subject to the limitation that it must not commit an error oftener than once every few hours. There is no other significant limitation on the total complexity of the device; for the machines which are now in design or construction are still quite inadequate to deal with many problems which we should like to put to them.

One simple example is contained in a remark of Hartree, quoted to me by Professor Aiken. Hartree said that the fastest computing machine available today is still too slow by a factor of 10^{10} to solve the problem of the wave equation for the copper atom. Similarly, the people who are designing the air traffic control plan for the country are proposing to put computers in key locations on the airways of the country, to handle the problems involved in air traffic control. Preliminary estimates of the scope of these problems have indicated that present-day machines will be severely taxed to deal even with the volume of air traffic that exists today.

We want, therefore, to make computing machines as large and as complicated as we can, for the most ambitious machine which we can realize today is powerless in the face of problems that we can readily pose, but not yet solve.

This brings us to my final question: "How can a computing machine be made more reliable, so that its complexity can be increased without increasing the chance of failure?" Much of the answer to this question will depend on the further development and the elaboration of the checking schemes which have already been referred to. However, the obvious way to increase the over-all reliability of present-day machines is to look toward as complete as possible an elimination from such machines of vacuum tubes and electromechanical relays. These two components are presently the major sources of failure in existing machines, partly because they are so numerous, and partly because they wear out with continued use. We need computing elements that can perform the same non-linear functions as those we now achieve with tubes or relays, but elements which are far less prone to depreciation in use.

The vacuum tube also has the disadvantage that it requires large amounts of standby power. McCulloch has remarked that, if a machine built on present principles were to have as many neurons as does the brain, it would require a skyscraper to house it, the power of Niagara to light its tubes, and the full flow of water over the Falls to keep it cool. There are now visible several developments which promise to compete with the vacuum tube for this and other purposes. First, semiconductor devices of the type of the transistor seem to have great promise. Second, magnetic devices like those reported by the Harvard group at the September symposium hold out the hope that they can serve in the place of tubes, with much greater reliability and without requiring power.[16] Finally, the pioneering work of Bowman[17] on electrochemical elements for computers offers a substantial promise in this same direction.

Probably there is no more rewarding direction for computer development than to explore the possibilities of using unconventional elements in the design of such machines. If the vacuum tube can be replaced with a cheaper, simpler, and more durable device, then the over-all competence of practicable computers can be greatly increased. Such a development will being in its train a greater availability for computers of the present sort, and a wider general use of computing machines of all kinds.

---

[16] Way Dong Woo, Symposium on Large-Scale Digital Calculating Machinery, Harvard University (September, 1949).

[17] J. R. Bowman, Symposium on Large-Scale Digital Calculating Machinery, Harvard University (September, 1949).

Contributed Original Research

A Lapping Technique: To Improve the Image Quality of Electron Microscope Lenses

F. A. Hamm
General Aniline and Film Corporation, Central Research Laboratory, Easton, Pennsylvania
(Received July 25, 1949)

One factor inherent in most electron microscopes is the magnetic asymmetry (astigmatism) in the objective lens. This is often due to imperfect machining, localized defects (impurities) in the iron, or grain anisotropies. The lapping technique described herein effectively reduces the effect of imperfect machining (misalignment of components). Critical faces and the bores through the pole piece are lapped with a series of powders (alumina) which increase in fineness until the final process is that of polishing. A set of jigs and laps (brass and hard wood) are described; their specifications and use so as to properly alter the critical pole piece surfaces are also described. Electron micrographs illustrating the value of this lapping procedure in the improvement in objective lens symmetry are included.

INTRODUCTION

DURING the past few years the electron microscope has become an important research tool. Certainly one of the reasons for this is the improvement in specimen preparation techniques. These improvements are the natural results of wider applications and the realization that artifacts must often be considered. However, because most laboratories, and especially the industrial laboratories, are usually hard pressed in applying the electron microscope to their particular urgent problems, relatively little time has been spent in improving the *performance* of the electron microscope itself. For example, each laboratory may have its own condition such as vibration, stray magnetic fields, high humidity and other accidental defects which may limit the performance of that particular instrument. With the ever increasing interest in greater resolution it has become imperative to evaluate more critically the various factors that may impair the instrument's resolution. Hillier and Ramberg[1] have very adequately evaluated both inherent and accidental instrumental defects, and critical investigators have relied heavily on the information already disclosed.

It is the purpose of this paper, first, to describe a lapping technique which has been found useful for eliminating most of the prohibitive magnetic asymmetries inherent in electron microscope objectives, and, secondly, to illustrate the practical results observed after applying this technique. Cognizance of these asymmetries is seldom taken until the investigator becomes interested in resolving structures of 50A or less (or until micrographs are taken at very high instrument magnification). When the electron microscope is used at high magnification (15,000× or greater) the aforementioned defects may be readily observed. Although at times vibration is troublesome, it was observed that the most serious factor limiting the resolution of the electron microscope in this laboratory was the *astigmatism* inherent in the *objective pole piece*. This asymmetry has been almost entirely eliminated by reducing the *mechanical inaccuracies* of an *objective pole piece* by means of a lapping technique. Both projector and objective pole pieces must be handled with care; mistakes in routine cleaning or in haphazard "polishing" techniques may be costly. It is hoped that the information disclosed herein may aid others who are interested in improving their instruments.

The contributions made by Hillier[1,2] and his coworkers should be emphasized again. It is hoped, however, that this paper will stimulate other investigators to report on similar instrumental procedures which they have found to be helpful in eliminating or minimizing conditions which may limit the resolution of their particular instrument. For example, there are undoubtedly some locations which are troubled by building vibrations.

It should be understood that asymmetries in magnetic lenses may also be due to inhomogeneities in the iron (pole pieces). Variations in the grain structure or orientation will obviously affect the distribution of the magnetic flux in the lens. These factors may be especially troublesome if they occur near critical openings. This lapping technique obviously does not eliminate these sources of trouble.

Occasionally small impurities are removed from the faces and the bores of the pole pieces. The small "pits" that remain should be eliminated insofar as possible by lapping until these surfaces are essentially smooth. These mechanical impurities are sometimes quite troublesome

[1] James Hillier and E. G. Ramberg, "The magnetic electron microscope objective: contour phenomena and the attainment of high resolving power," J. App. Phys. 18, 48–71 (January, 1947). James Hillier, "On the adjustment and manipulation of the electron microscope," Paper 32, EMSA Meeting, Toronto, Canada (September 9–11, 1949).

[2] J. Hillier and E. G. Ramberg, "Further studies on the magnetic electron microscope objective," Paper No. 41, joint meeting of EMSA and ASXRED Pittsburgh, Pennsylvania (December 7, 1946).

TABLE I.

A. Jigs (Brass)

(1) One jig to hold (with a slide fit) the sections of both pole pieces when lapping their inside faces. The broad face of the jig that makes contact with the flat glass surface is three and one-half inches in diameter. This face is counterbored 0.031 in. deep with a 1.625-in. diameter. Item 6 in Fig. 1.

(2) One jig equipped with a 0.125-in. bushing. This jig is used to hold the pole piece sections when the bores (holes through) are lapped. The bushing guides the shank of the lap. Item 7.

(3) One jig to hold the short section of the objective pole piece when lapping the outside face. This jig has a hole (0.255 in.) to guide the lap. Item 5.

B. Laps[a] (All laps are about 1 in. long; over-all length including the 0.125-in. shank is 3–4 in.)

(1) *Objective pole piece*
- (a) 0.0610 in.—brass.
- (b) 0.0615 in.—brass. Item 2.
- (c) 0.0620 to 0.0625 in.—oak wood. Item 1.
- (d) 0.255 in.—brass; brass with soft solder babbit on one end—used with *A* and *B* powders. Item 3.

(2) *Projector pole piece*
- (a) *Short section*
  - (i) 0.0630 in.—brass. A section (0.0680 in.) was left ahead of the shank which could have been turned down to the required size if necessary. Item 9.
  - (ii) 0.0650 to 0.0655 in.—oak wood. Item 11.
- (b) *Long section*
  - (i) 0.0700 in.—brass. Item 8.
  - (ii) 0.0710 in.—oak wood. A 0.0720-in. portion was separated from the first (0.0710 in.) portion by means of a deep undercut. The larger diameter lap was included in case it might have become necessary. The undercut prevents the larger lap from rubbing the inside pole piece face. Item 10.

C. Powders

Exolon[b] (aluminum oxide) 600 and 800 abrasives are used to lap. The soft iron in the pole piece is removed.

Linde[c] types *A* and *B* (finest) polishing powders (aluminum oxide) are used on the wooden laps. Little or no metal is removed with the *B* powder. Minute scratches are removed probably by a plastic flow type of deformation. The particle sizes are very uniform; the *B* type is reported to be less than 0.1 micron.

D. Fluid

Singer[d] high grade sewing machine oil was used to make pastes with the powders.

[a] 600 and 800 abrasives used with the brass laps; *A* and *B* polishing powders used with the oak laps.
[b] The Exolon Company, Tonawanda, New York.
[c] The Linde Air Products Company, unit of Carbide and Carbon, New York, New York.
[d] Singer Oil, Type D Stainless Heavy Grade, Singer Sewing Machine Company, New York, New York.

in that more time is required to lap until a glossy surface is observed. It is conceivable that the effect of impurities might never be effectively reduced in some pole pieces; consequently the use of a compensating pole piece spacer would become imperative.

It would be difficult to evaluate the relative importance of grain structure, orientations, impurities, mechanical inaccuracies, etc. Probably these factors are all present in all pole pieces in varying degrees. However, it is worth while to eliminate the last one insofar as possible. The electron microscopist has little control over the other sources of trouble.

Because the lapping technique was done critically and with good success, it was considered worth while to report on it, giving at least the essential details. It should be emphasized that lapping the *projector* pole piece does *not* affect resolution, but it is desirable because it does remove contamination, and it may make projector lens distortion more symmetrical.

DISCUSSION

This paper is concerned only with the *practical* aspects of improving the magnetic asymmetries inherent in perhaps all objective lens pole pieces. The *theoretical* aspects are described in an earlier reference.[1] The term *astigmatism* describes a difference in focus in two mutually perpendicular directions. This difference was originally estimated to be as high as 50 microns in some objective pole pieces. This *degree of astigmatism* could have been more accurately determined by plotting objective coil current against known object displacement. Thus the difference in lens current required to bring the image in one plane into the same focus initially observed along its mutually perpendicular plane would be a measure of the degree of astigmatism as read from a predetermined curve. Such determinations are time consuming and unnecessary *in practice*. A hole in a thin membrane (collodion, silica, polystyrene, etc.) or a round particle such as carbon black (camphor) serves as a convenient subject for evaluating objective lens asymmetries. High instrument magnification is a prerequisite to a study of this kind, and it is assumed that the terms "in focus," "overfocused," and "underfocused" are understood (precluding further discussion).

Since this manuscript was first written a very pertinent investigation has been presented.[3] Through the courtesy of James Hillier the asymmetries exhibited by most of the electron micrographs have been quantitatively evaluated. These asymmetries, expressed in microns, are included in the caption for each figure. These values represent the difference in focus between mutually perpendicular directions. Very slight differences of $\frac{1}{2}\mu$ can be detected.

LAPPING TECHNIQUE

The equipment[4] used in this lapping and polishing technique is listed in Table I with a brief description. The various items are illustrated in Fig. 1.

Hillier[1] has very briefly described his procedure. This technique differs from his in three important respects: (1) The use of a 400 (coarse) lapping powder appears to be undesirable because it sometimes "tears" the soft iron. (The 600 powder removes metal at a good rate.) (2) Unless the pole pieces are dried *immediately*, water corrodes the newly formed iron surfaces. Furthermore,

[3] James Hillier and Henry Froula, "On the testing of electron microscope objectives," Paper No. 4, RCA Laboratories, Princeton, New Jersey, presented at the EMSA meeting, Washington, D. C. (Oct. 6–8, 1949).

[4] The items first used had been made with good precision by the Beeman Manufacturing Company, 1030 Haddon Avenue, Collingswood, New Jersey. Modifications and additional items have since been made in our own machine shop.

it is difficult to maintain a stable water paste of the lapping powders because of evaporation. The highly refined Singer oil does not corrode and lends itself to making stable slurries of varying consistencies. This oil is readily removed with acetone. (3) Straight laps are preferred to tapered (1°) laps because considerably more metal must be removed from one end of the bore when using a tapered lap. This invites trouble. Furthermore, the bores through the pole pieces might become abnormally large if the lapping is repeated. At least 0.004 in. of metal would have to be removed from one end of the bore, whereas only about 0.0015 in. of metal was removed with the straight lap using the 600 powder. Although no deep pits were encountered during the processing of two sets of lenses, it is conceivable that large impurities (pits) might be troublesome. If this is the case, tapered laps would be more desirable because they would preclude the necessity of making several straight laps. Obviously, the amount of metal removed by a lap is a function of the size of the particles in the lapping powder.

It would be desirable to polish with a soft metal lap such as copper or lead. However, this is not feasible because these metals are not rigid enough. Hard wood (oak, maple) was found to serve better than brass for the final polishing with the fine powders.

Before beginning the lapping it is imperative to mark both sections (of each pole piece) with respect to some mark (scratch) on the brass spacer. The pole pieces should always be assembled in the same way using these markings as a guide. This should be done before inserting the pole pieces in the electron microscope or before lapping the bores. The bores through both sections of the *objective* pole piece should be lapped with the pole piece *assembled*.[5] This is not necessary with the projector pole piece; the bore through the long section has always been larger (0.070 in.) than that through the short section (0.063 in.). Should the bores in the objective pole piece not exhibit good alignment, lapping should be continued until good alignment is realized.

A sufficient supply of a fairly thick paste of each powder is prepared so that all surfaces may be lapped before proceeding to the next finer powder. The inside faces (within the spacer when assembled) were lapped first with the 600 powder. The pole piece section does not rotate within the jig; the lapping is done with a rotary motion on a thick glass plate, preferably of good quality (flat). The assembly is lifted occasionally from the plate, turned to a new position, and then lapped as before. The pole piece is also rotated within the jig to eliminate any results due to possible imperfections in the jig. If the assembly is periodically rotated and the lapping done with a rotary motion, all directional effects will be eliminated. This same procedure is carried out with all subsequent grades of powder. All traces of the powder last used should be removed before proceeding to the next one. This can best be done by using lens tissue[6] wet with the oil, wrapped around a toothpick when cleaning the bore. A little pressure (index finger) is used in lapping the faces. The outside of the pole piece may be lubricated with the oil so that it is more readily pressed through the jig (slide fit).

After lapping the faces, especially with the 600 powder, a "burr" usually forms around the lip of the bore. This burr should *not* be removed by inserting the bore lap from either end. Apparently the lap (brass or wood) picks up the soft iron in relatively large pieces; then on withdrawing the lap the bore is scratched and sometimes badly torn. Instead, these burrs are best removed from the entire bore periphery by rolling up a small piece of crocus cloth into a cone shape, inserting the apex of the cone into the bore and gently turning the cone against the burr. At no time was there any evidence of a bevelling action on this lip. *Both* the bores and the faces are lapped to give as smooth a finish as possible with the given powder before proceeding to the next finer powder. Burrs are not usually formed when the finer powders *A* and *B* are used.

Early in this investigation it was observed that the smaller faces (long section of objective pole piece) could always be polished to a higher gloss than the larger faces. It appeared that the larger face was picking up "dirt" from the brass jig which then "stained" the pole piece face. To eliminate this, the large face of the jig, which makes contact with the glass during lapping, was counter-bored 0.031 in. deep to a diameter of 1.625 in. The pole pieces were then lapped with a rotary motion using a *short stroke* so that the lapping paste remained within the counter-bore. This procedure permitted the polishing of the large faces to the same gloss that had been observed earlier on the small faces.

The outside face of the short section of the objective

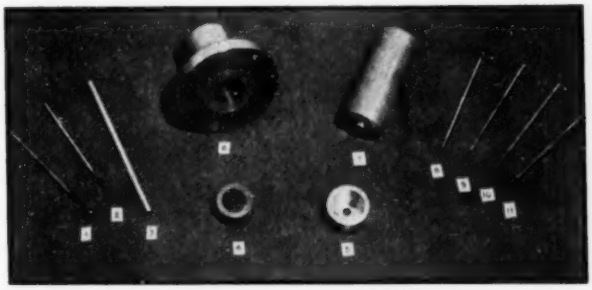

FIG. 1. Laps and jigs described in Table I.

[5] Since originally submitting this paper for publication it has been learned that some RCA e.m.u. electron microscopes have been equipped with objective pole pieces having sections with bores of unequal size. Thus, each section might be lapped separately, but it is almost imperative to lap this pole piece assembled to insure proper alignment of the openings. Consequently the bore through the one section must be carefully enlarged to the same size as the other one.

[6] Ross-Adams lens tissue sold by Clay-Adams Company, Inc., New York, does not readily tear and will not scratch the pole pieces.

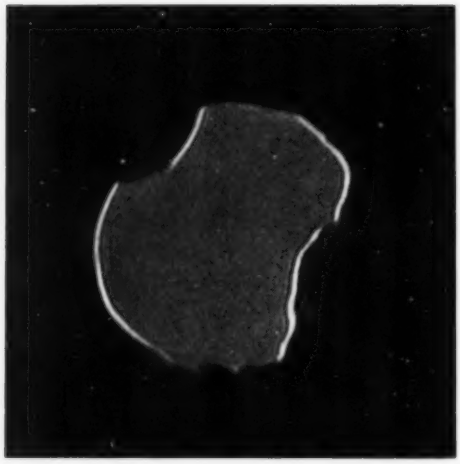

FIG. 2. 100,000×. Diatomaceous earth particle. Severe astigmatism. Note the several orders of Fresnel fringes in the vertical direction. Asymmetry of 20–25μ.

pole piece tarnishes very quickly because it is just below the specimen and because it is sprayed with electrons scattered by the specimen. This face should be polished occasionally, but care must be exercised so as to avoid introducing asymmetries. Furthermore a burr may form around the periphery of the bore when the bore is lapped; this must be removed. To accomplish these purposes, a jig was made to fit over this short section. A hole (0.255 in.) in the exact center guides a brass lap of similar dimension. This lap, used with the 600 and 800 powders, is used to lap the flat face and remove the burr. The lap must be "faced-off" (in a lathe) occasionally because the burr may cut into the brass lap. To polish this pole piece face, a similar lap is made, equipped on one end with a soft solder babbit which must also be faced-off periodically. The *A* powder embeds in the babbit so it must be removed before using the *B* powder. It is suggested that this babbit lap be used quite frequently with the *B* powder to remove the contamination that is the result of the effect of the electron beam.

Lapping the bores of the pole pieces must be done with caution. The hole must be enlarged gradually and symmetrically. The early work on the bores suggested the use of the 600 powder instead of the 400 powder. The Beeman[4] jig served its purpose very well. The 0.125-in. bushing (1.5 in. long) guides the shank of the lap so that it runs "true." The hole for the pole piece is about $1\frac{1}{2}$ in. long (slide fit) so that if the laps are properly made the finished bore should be perfectly symmetrical. In practice the abrasive paste is placed within the bore before inserting the pole piece in the jig. The clean lap is then inserted through the bushing (lubricated) and lapping carefully started when the lap meets the bore. The ends were pointed, merely to aid in starting the lap in the bore. The objective pole piece was inserted in the jig so that the lap went through the short section first.

Lapping is accomplished by rotating the lap back and forth through an arc of about 180°C. The lap is periodically withdrawn, rotated slightly, reinserted, and lapping continued as before. This ensures symmetrical action around the entire bore. The pole piece is tightly held in the jig with the index finger. Occasionally large scratches or tears developed during the early work. This was very probably caused by some hard grit which had accidentally gotten into the system.

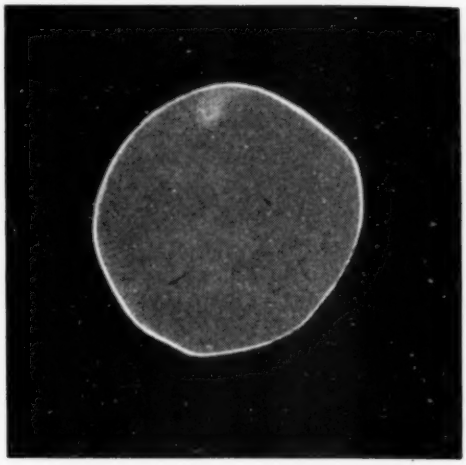

FIG. 3. 112,500×. Compare with Fig. 2. Very slightly underfocused. Different lens. 4–5μ.

The later work was carried out in a cleaner environment, and no trouble was experienced. The bore diameters of the pole pieces in the RCA e.m.u instrument have been varied slightly during the last few years; the bore in the long section of the projector pole piece is apparently always the largest. These bore diameters should, of course, be carefully measured before making the laps.

The hard wooden laps used for the final polishing show signs of wear after some use. By cutting a few grooves (with a razor blade) parallel to the long direction of the lap and soaking the lap in oil, a sufficient increase in diameter results so that these laps may be used repeatedly. It might be expected that these wooden laps do not wear evenly. Although this may be true at times, it is of no significance when polishing with the fine powders.

These wooden laps were used very successfully for polishing the bores. For this reason hard wood laps were made to polish several other surfaces. For example, the bores through the specimen holder and the special Armco iron sleeve in the intermediate screen assembly are occasionally polished with wooden laps (oak) to remove tarnish. This procedure is desirable because polishing these surfaces makes them smoother so that they are more readily cleaned with lens tissue in the routine way employed by many investigators. In both cases, the wooden laps may be held in a small drill press; the polishing is then done by moving the metal

surface up and down over the lap. Hand polishing is preferred because better control is realized.

The cleanliness of the inside conical face of the short section of the projector pole piece is very important, especially at high instrument magnification. At high projector lens current values the imaging beam of electrons is spread so that many of the rays strike the inside of the bottom (short) section of the pole piece. The final image may be of a poor quality if the beam is affected by contamination which may acquire a charge. A wooden lap (maple) was made to polish this face with the *A* or *B* powders. This lap is illustrated as item 4 in Fig. 1. The conical shaped portion (45° cone) is 0.853 in. long, with the sharp apex of the cone rounded. The short section of the projector pole piece is screwed into the brass spacer. The spacer is fitted into the jig

TABLE II. Instrumental operating conditions.

(1) Self-biased gun (saturating between 200 and 250 microamperes), filament distance from grid (gun focusing aperture) about 4 mm. "Home made" filament—sharp apex bent over a razor blade. "Cross-over" image of source approximately normal to the astigmatic plane.
(2) Primary fluorescent viewing screen removed. Brass plate substituted for the usual primary viewing window and copper screen. These changes eliminate some contamination, which may subsequently charge up and cause movement of the beam.
(3) Condenser current[a] = 84 milliamps; this provides an angular aperture of illumination to the specimen of about 4×10^{-4} radian.
(4) Mu-metal shielding between objective and projector lenses to eliminate stray magnetic fields.
(5) Intermediate fluorescent viewing screen removed. Armco iron sleeve in intermediate screen assembly to maintain magnetic symmetry within the upper part of the projector lens (see reference 1).
(6) Objective lens focusing circuit modified to give threefold sensitivity over the standard e.m.u.-2A circuit.
(7) Strict cleanliness of entire microscope column (gun) observed.
(8) Voltage alignment always used. Magnetic alignment is not superimposed; magnetic center of rotation just off the final viewing screen.
(9) No objective aperture.
(10) The micrographs were taken at tap 9 or 10 using the high gain projector spacer.

[a] Some of the data were calculated from information received in a private communication with Dr. James Hillier, RCA Laboratories, Princeton, New Jersey.

with the 0.125-in. bushing, having used tissue paper as a shim. The jig is then placed in the collet of a lathe, which is run at about 400 r.p.m. Polishing is accomplished by moving the wooden lap in and out (by hand) along one side of the cone face. A shoulder at the base of the cone prevents the cone from being inserted too far. Thus, this lap does not touch the bore. This procedure removes the surface contamination, and the tin plating, so that the copper plating is exposed. Sometimes the tin plating on a new pole piece separates from the iron *within* the bore of the pole piece. A burr of this type could be troublesome and might readily tend to catch small contaminating particles. The lapping technique described earlier effectively removes this tin plating.

After carrying out any of the aforementioned steps in the lapping procedure, the oily paste is best removed by wiping the surfaces with a good quality lens tissue.[6] After the lapping has been completed, the oil and last traces of powder are best removed by immersing the lens components in two successive baths of high grade (dirt-free) acetone. The critical surfaces should not be allowed to dry for the last time without first wiping them with lens tissue wet with fresh acetone. No evidence to suggest the incomplete removal of oil has ever been observed. Complete removal of the oil is absolutely imperative for several reasons, the most important being the fact that the electron beam would probably act on the oil (radiation-chemical) so as to cause severe contamination.

FIG. 4. 112,500×. Portion of a diatom. The astigmatism is manifest as a ghost image due to overfocusing along one direction. Before lapping. Abnormally bad asymmetry of about 60μ.

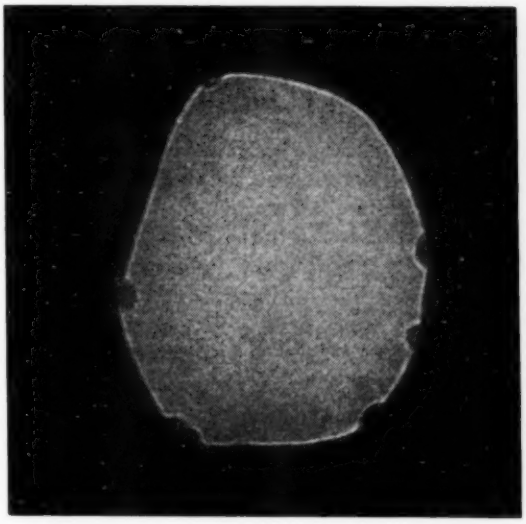

FIG. 5. 112,500×. Diatom very slightly underfocused. Same lens after lapping. 1½μ. This very small asymmetry would have been more obvious at exact focus.

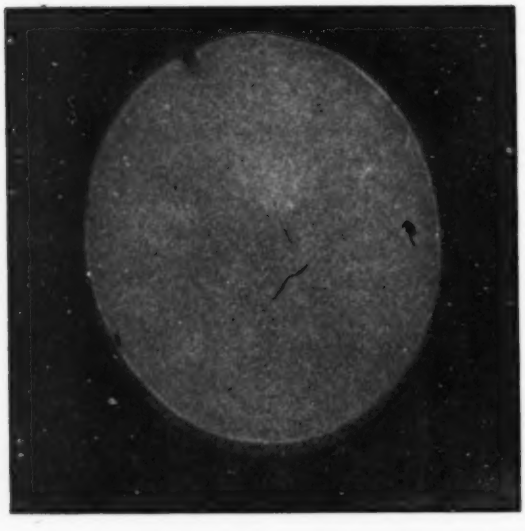

FIG. 6. 112,500×. Thin film of Formvar. 1½μ. Possibly a trace of specimen drift.

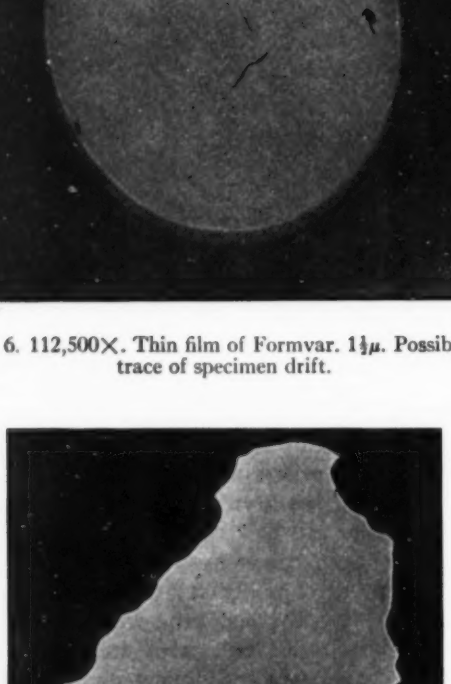

FIG. 7. 48,000×. 200A (calc.) thick film of silica. Too far underfocused to detect the 1½μ-asymmetry.

DISCUSSION OF ELECTRON MICROGRAPHS

The practical use to which the electron microscope is put is very largely based on the photographic record of the images observed. Because it was the purpose of this investigation to increase the "instrumental resolving power" most of the micrographs will be interpreted with this in mind. The "Report of the electron microscope society of America's Committee on Resolution"[7] has been used as a guide in choosing the terminology. Thus, the "instrumental resolving power" is based on measurements made on the photographic record of an image taken under ideal conditions (specimen, photographic, instrumental, etc.). The "quality of the micrograph" is more closely associated with the information revealed in relation to what was hoped for in any given investigation; although it is a function of the performance of the microscope it is probably most closely related to the quality of the electron microscope specimen. A few electron micrographs are illustrated to demonstrate their high quality as a result of better instrument performance. For the sake of convenience the "minimum distance between adjacent particle centers" is used to evaluate the instrumental resolving power. Reliance on micrographs is, of course, necessary. Most of the micrographs are illustrated in an effort to demonstrate the effectiveness of the pole piece lapping technique in eliminating astigmatism rather than to claim some specific optimum resolving power.

In order to make a fair appraisal of the lapping technique it is imperative to eliminate the effects of all other variables. Unless otherwise stated, the operating conditions apropos of these micrographs are briefly summarized in Table II.

Figure 2 illustrates an extreme case of astigmatism. The underfocused portion of the image shows at least

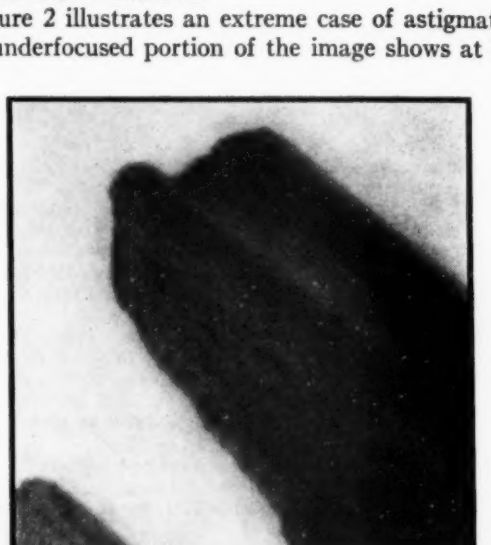

FIG. 8. 160,000×. Sublimed organic pigment. Poor image quality. Before lapping.

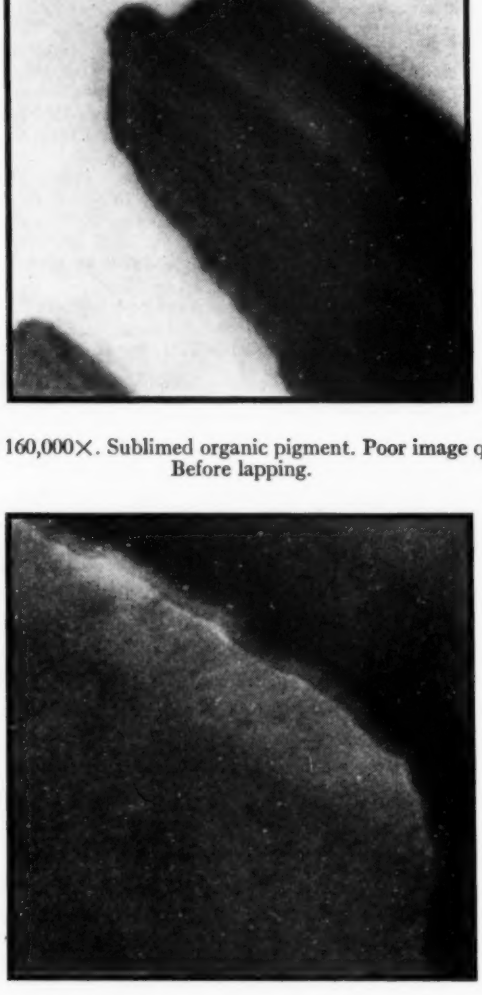

FIG. 9. 160,000×. Unshadowed silica replica of a silver bromide crystal. Good image quality. After lapping.

[7] J. App. Phys. 17, 989–996 (1946).

four orders of Fresnel fringes, indicative of good instrument performance. On the other hand, the image along the horizontal plane is in better focus (exhibiting no diffraction fringes) thereby demonstrating the astigmatism of this objective pole piece. Experience suggests that this amount of asymmetry (20–25μ) is not uncommon in many objective lenses.

Figure 3 is a very slightly underfocused image of the same specimen photographed with a different objective pole piece. The image is too close to being in focus so that only the first-order Fresnel fringe is exhibited. The symmetrical distribution of the white halo around the entire periphery of the hole (diatom) indicates a lens of good quality.

Astigmatism always becomes more pronounced as the image is brought toward exact focus. This is significant because in any critical investigation requiring high resolution, reliance on well-focused images should be made. In cases where the specimen is extremely thin and has little scattering power, a slightly underfocused image reveals more information because of its greater contrast due to phase delay phenomena. By varying the current in the vernier (fourth potentiometer) of the modified objective focusing circuit, the astigmatism can be detected and measured qualitatively in terms of vernier divisions.

Figures 4 and 5 again illustrate the effect of the lapping technique. The holes in diatoms conveniently serve this purpose. The image (Fig. 4) in the plane perpendicular to the arrow is badly overfocused (focal length too short); the parallel direction is in better focus. Figure 5 illustrates a high quality image of the same specimen after lapping. Because diatoms are relatively thick, a thin white halo appears just within the holes even though the image is, for all intents and purposes, in focus. (As a result of the quantitative evaluation[3] this image is now considered to be one or two microns underfocused.)

About one month after the pole pieces had been lapped and polished for the first time it became necessary to polish them again. The bores through and faces (especially on the objective pole piece) had become badly "tarnished." (This tarnish may have been a contamination coming from the particular type of specimen during exposure to the electron beam.) It was decided to lap the objective pole piece again lightly, starting with the 800 powder. The micrographs in Figs. 6 and 7 were taken subsequently. Although the contrast in these figures is poor (no objective aperture) the images still exhibit about the same amount of asymmetry. Because the asymmetries were almost entirely eliminated, it has been unnecessary to use a compensating objective pole piece spacer described earlier by Hillier and Ramberg.[1] It is felt that it is more desirable to eliminate the asymmetries insofar as possible by lapping rather than by using a compensating spacer because laps and jigs must be made anyway in order to occasionally remove the pole piece tarnish by *polishing*. If this is done, only a little more effort is required to complete the job by carrying out the entire lapping procedure. It is conceivable that a compensating objective pole piece spacer might be very desirable for routine work even after lapping, depending upon how badly asymmetrical the pole piece might have been initially due to reasons discussed earlier. In any case, the last traces of astigmatism can perhaps only be removed by compensation.

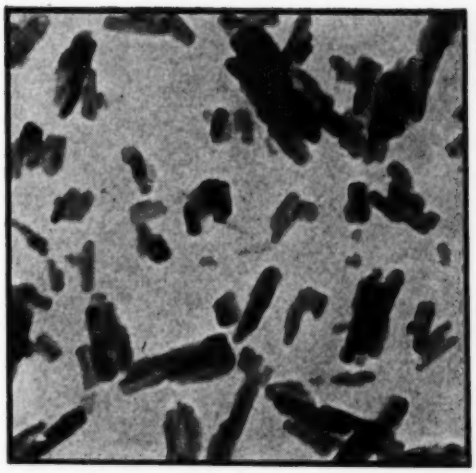

FIG. 10. 56,000×. Dispersed pigment. Poor image quality.

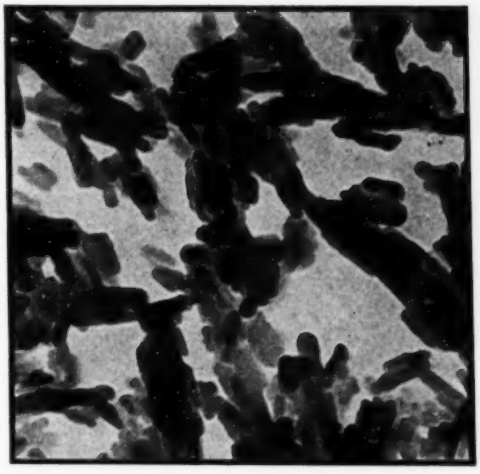

FIG. 11. 56,000×. Same preparation as above. Good image quality.

Admittedly, it is not entirely fair to compare the image quality of micrographs taken of different specimens. However, Figs. 8 and 9 are illustrated for comparison. Both types of samples are very stable in the electron beam, and both micrographs (photographed at 20,000×) represent the optimum quality possible at the time that the micrograph was taken. The difference in image quality is undoubtedly due to the difference in the performances of the lenses. The magnification in both these figures is 200,000 diameters. The absence of

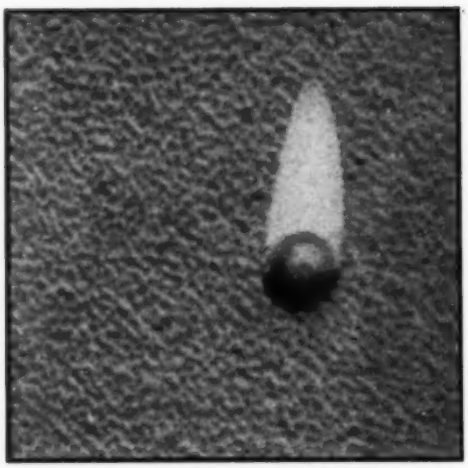

FIG. 12. 160,000×. A silicon monoxide replica of mica shadowed with Pt-Pd. Good image quality.

specimen drift, always a serious problem, should be noted.

Experience during the past several years suggests that image quality is often attributable to the performances of the electron microscope lenses. Figure 8 is several years old, whereas Fig. 9 was taken since the lenses were first lapped and polished. Note how much more "crisp" the latter image is. The contrast is poor; the specimen was not shadowed. The latter image is however, capable of resolving structure at least on the order of 25A.

Figures 10 and 11 represent a comparison of the same specimen, Indanthrene Blue RS, dispersed ultrasonically, demonstrating the "before and after" version of the lapping technique. Figure 10 is slightly underfocused. Underfocusing invariably causes the image to be more crisp and to have more aesthetic appeal. Nevertheless, Fig. 11, taken after the pole pieces had been processed, is much more crisp and suggests, even at this low magnification, the improvement in resolving power due to the lapping technique.

The structure in Fig. 12 was exhibited by a silicon monoxide replica of mica, shadowed at 10° with a platinum-palladium alloy. This structure appears as an undesirable "background grain" when the replica is used as a substrate for other objects (viruses, bacteria, etc.). The structure is typical of platinum-palladium shadowing metal, especially when the metal is relatively thick. Although the image is slightly underfocused, the quality is good and superior to that possible with an "average" objective lens. It should be emphasized that this micrograph and all the others were taken at very high instrument magnification.

CONCLUSION

The effect of astigmatism, an objective lens asymmetry, has been illustrated. A procedure for minimizing this inherent defect is outlined. This process involves lapping and polishing with fine abrasives all critical surfaces on the objective (most important) and projector pole pieces. Routine polishing with the *B* powder should be done frequently to remove contamination. High quality high magnification electron micrographs necessitate routine polishing at least once a month and preferably more often.

Improvement in the instrumental resolving power based on measurements made on micrographs was illustrated. No specific optimum resolving power is claimed. The elimination of astigmatism and the general improvement in image crispness unquestionably permit greater resolution. A reduction in objective lens asymmetry from about 60μ to about $1\frac{1}{2}\mu$ has been illustrated.

Since this initial investigation was completed, another objective pole piece was processed in the same way. The gratifying results add weight to the significance of this technique.

ACKNOWLEDGMENTS

The author is indebted to A. McNevin for his suggestions and care in carrying out much of the lapping procedure. The interest and constructive criticisms expressed by M. C. Banca and James Hillier of the Radio Corporation of America have also been appreciated.

Separation of Gases by Fractional Permeation through Membranes

SOL WELLER* AND WALDO A. STEINER†
Research and Development Branch, Bureau of Mines, Pittsburgh, Pennsylvania
(Received September 19, 1949)

The permeability of a number of thin organic films toward oxygen and nitrogen has been measured. For an ethyl cellulose film the studies were extended to include CO_2, A, He, and H_2. The enrichment of a binary gas mixture in a single stage of permeation has been calculated for the extreme cases of perfect mixing and no mixing. Application of these results indicates that the use of a fractional permeation process may be of practical importance in effecting the separation of oxygen from air, helium from natural gas, and hydrogen from coke-oven gas, as examples.

INTRODUCTION

THE fact that non-porous rubber membranes show a higher permeability to O_2 than to N_2 has been known for almost 120 years[1] and has formed the basis for several old patents for the enrichment of air.[2] Apparently, little attention has been paid in the interim to the possible practical importance of this selective permeability behavior. Most of the work which has been reported on the phenomenon has been done on rubber membranes,[3] although scattered investigations have been made on other materials.[4,5]

In 1942, von Elbe,[6] working with stretched films of natural rubber, found that air, diffusing from a pressure of 4 atmos. to atmospheric pressure, was enriched to an O_2 content of 33 percent, corresponding to a value of 2.4 for the ratio of the permeability constants of O_2 and N_2. Von Elbe's stretched films, which had a thickness of only 0.00038 cm, possessed a permeability coefficient toward O_2 of 1.6×10^{-6} mole O_2 atmos.$^{-1}$ cm^{-2} min.$^{-1}$. Calculations based on these results indicated that a multistage permeation process for obtaining O_2 from air was economically unfavorable compared with the Linde process by a factor of about 2, with the possibility of major improvements if films of superior properties could be found. It was realized that, for possible practical use in effecting the separation of gases, films should have the following qualities: (1) high absolute permeability, to minimize the area of film required; (2) high selective permeability toward the desired gas, to reduce the power required for the separation; and (3) chemical and physical stability. Consideration of literature data[4,5] showed that many types of films probably would not be useful because of failure to satisfy the first requirement; among these were Cellophane, cellulose acetate, Nylon, polyvinyl chloride, polyvinylidene chloride, and rubber hydrochloride. It was considered desirable to test at least rubber, ethyl cellulose, polyethylene, and polystyrene.

EXPERIMENTAL PROCEDURE

The apparatus used to measure permeability was quite simple. A small Seitz bacterial filter was modified to hold the sample of film which was supported on one side by filter paper backed by 30-mesh wire screen. The exposed area of film was 18 sq. cm. In determining permeability to pure gases, the film holder, which was immersed in a thermostated water bath, was simultaneously evacuated on both sides of the film with a rotary oil pump. The pump was then closed off, the pure, dried gas was admitted on the unsupported side of the film to the desired pressure, and the rate of gas permeation was followed by measuring the rate of pressure increase in an enclosed volume on the supported (low pressure) side of the film with a tilting McLeod gauge (0–5 mm range). The enclosed volume on the low pressure side was calibrated so that the permeability could be expressed in standard units. Typical pressure-time curves, in this case for O_2 and N_2 through a 0.023 mm polyethylene film, are shown in Fig. 1.

The determination of pressure-time curves was convenient for the study of pure gases but not for gas mixtures. In several cases when gas mixtures were used, the composition of the permeated gas was determined by connecting the low pressure side of the film holder

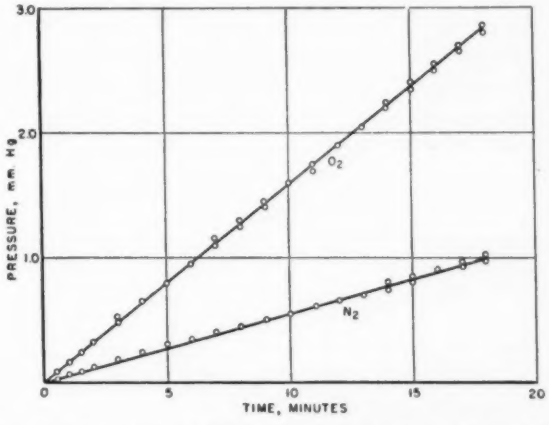

FIG. 1. Permeability of 0.023-mm polyethylene to O_2 and N_2.

* Physical chemist.
† Physicist.
[1] J. V. Mitchell, J. Roy. Inst. **2**, 101, 307 (1831).
[2] P. Margis, D.R.P.17981, Class 12 (August 7, 1881); M. Herzog, U.S. 307,041 (October 21, 1884).
[3] See, for example, G. J. van Amerongen, J. App. Phys. **17**, 972 (1946).
[4] R. M. Barrer, *Diffusion in and through Solids* (Cambridge University Press, London, 1941), Chapter IX.
[5] D. W. Davis, Mod. Packaging **19**, 145 (1946).
[6] G. von Elbe, U. S. Bureau of Mines (unpublished work).

TABLE I. Film permeability to oxygen and nitrogen at 30°C.

Material	Supplier[a]	Film thickness (mm)	Specific permeability, K, at 30°C (cm^2 $min.^{-1}$ $atmos.^{-1}$) $\times 10^8$ K_{O_2}	K_{N_2}	$\frac{K_{O_2}}{K_{N_2}}=\alpha$	Literature[c] K_{O_2} at 21–22°C (cm^2 $min.^{-1}$ $atmos.^{-1}\times 10^8$)
Ethyl cellulose	A	0.026[b]	4.8	2.0	2.4	3.8
Ethyl cellulose	B	0.025[b]	4.6	1.4	3.3	
Ethyl cellulose	C	0.0075[b]	9.4	3.0	3.1	
Polyvinyl chloride-acetate	A	0.051	1.8	1.2	1.5	
Vinyl resin and Buna N rubber	A	0.051	0.70	0.58	1.2	
Natural rubber latex	A	0.19[b]	18.1	8.6	2.1	11.0
Natural rubber latex	G	0.051[b]	11.4	4.4	2.6	
Resproid 1404	E	0.11	3.0	1.1	2.8	
Polyethylene	D	0.038	2.1	0.79	2.7	0.6
Polyethylene	F	0.023	2.2	0.88	2.5	
Polystyrene	D	0.025	1.3	0.44	3.0	0.8
Cellulose acetate	B	0.028	2.1	1.2	1.8	0.4
Cellulose propionate	B	0.023	2.8	0.9	3.2	
Kel-F	H	0.051	2.34	1.17	2.0	
Koroseal	I	0.038	0.37	0.15	2.4	

[a] Suppliers: A, Reynolds Metal Company; B, Celanese Corporation of America; C, cast in laboratory; D, Bakelite Corporation; E, Respro Inc.; F, Plax Corporation; G, cast in laboratory, rubber latex supplied by American Anode Inc.; H, M. W. Kellogg Company; I, B. F. Goodrich Company.
[b] Calculated; density of ethyl cellulose taken as 1.14 g/cu. cm, of rubber as 1.07 g/cu. cm.
[c] Reference 5.

directly to the intake of a mass spectrometer. The procedure was otherwise identical with that outlined. In some experiments with air, superatmospheric pressure (4 atmos.) was used, which resulted in the production of enough sample in 16 hours to permit analysis of the permeated gas by Orsat apparatus.

Most of the films studied were commercial films supplied by the manufacturer (see Table I). Films of ethyl cellulose and of rubber were also cast from solution in the laboratory with the use of Bird film-applicators. It was found possible to make a multiply drawn film of ethyl cellulose, having a total thickness of only 0.0075 mm (0.0003 in.), which did not show any leakage; i.e., the film maintained its selective permeability toward oxygen.

CALCULATION OF ENRICHMENT IN SINGLE STAGE

We assume the permeation of components A and B in a binary gas mixture to obey Fick's law, the rates of permeation of each component through the film area, $d\sum$, being

$$-dn_A=Q_A d\sum[P(n_A)/(n_A+n_B)-p(n_A')/(n_A'+n_B')]$$
$$-dn_B=Q_B d\sum[P(n_B)/(n_A+n_B)-p(n_B')/(n_A'+n_B')]. \quad (1)$$

P is the high pressure, p the low pressure, n_A and n_B the moles of A and B, respectively, flowing per unit time on the high pressure side, n_A' and n_B' the corresponding moles flowing on the low pressure side, and Q_A and Q_B the permeability coefficients (uncorrected for thickness) of A and B.

In the limiting case, where the composition of gas on the high pressure side is held equal to the inlet composition and the permeated gas is immediately removed by evacuation of the low pressure side, maximum enrichment of A is obtained (for $Q_A>Q_B$) and the ratio of molar flow rates for the components of the permeated gas is given by

$$n_A'/n_B'=dn_A/dn_B=Q_A/Q_B\cdot n_A^0/n_B^0=\alpha n_A^0/n_B^0, \quad (2)$$

where $\alpha=Q_A/Q_B$ and n_A^0 and n_B^0 are the entering molar flow rates of A and B.

If a finite fraction of gas entering a stage permeates during that stage, the composition of the permeated gas depends on the nature of the flow conditions on the high and low pressure sides of the film. Only two extreme cases, corresponding to perfect mixing and to no mixing, will be considered.

Case I

Perfect mixing of gases occurs on both sides of the film. The conditions are represented by the following diagram.

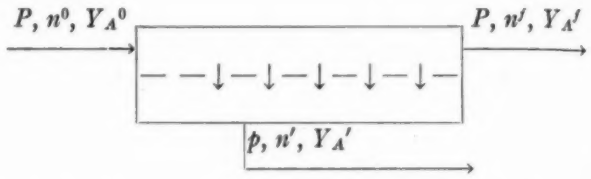

n^0 moles of gas per unit time ($n^0=n_A^0+n_B^0$) of composition Y_A^0 [$Y_A^0=n_A^0/(n_A^0+n_B^0)$] enter the stage at pressure P. Leaving the stage per unit time, still at pressure P, are n' moles of unpermeated gas having a mole fraction of A equal to Y_A'. The n' moles of gas permeating per unit time at pressure p have the composition described by Y_A'. It is assumed that the rate of mixing on the high pressure side is so rapid, compared with the rates of flow, that the unpermeated gas has, at all points in the stage, the same composition as the unpermeated gas leaving the stage. In the steady state, the following equations of continuity and conservation must be satisfied:

$$n'Y_A'=Q_A\sum[PY_A'-pY_A'] \quad (3)$$
$$n'(1-Y_A')=Q_B\sum[P(1-Y_A')-p(1-Y_A')] \quad (4)$$
$$n^0=n'+n' \quad (5)$$
$$n^0Y_A^0=n'Y_A'+n'Y_A'. \quad (6)$$

Let $\alpha=Q_A/Q_B$, $\beta=n'/\sum Q_A$. From Eqs. (3) and (4) is obtained

$$Y_A'=\frac{\alpha-(P-p)/\beta}{\alpha-1}, \quad Y_A'=\frac{(\beta+p)[\alpha-(P-p)/\beta]}{P(\alpha-1)}$$
$$=(\beta+p)Y_A'/P. \quad (7)$$

Y^0 is assumed known, and in any particular case a

value of n'/n^0 may be assumed. Let $n'/n^0=\gamma$; by Eq. (5), $n'/n^0=1-\gamma$. From Eqs. (6) and (7),

$$Y_A{}^0=\gamma Y_A{}'+(1-\gamma)Y_A'$$

$$=\left[\frac{\gamma(\beta+p)}{P}+(1-\gamma)\right]\left[\frac{\gamma-(P-p)/\beta}{\gamma-1}\right]. \quad (8)$$

β is found by solution of this quadratic equation, all the other quantities being known; combination with (7) then gives Y_A'. This solves the problem, since the enrichment of A in the permeated gas is obtained from Y_A', and the area $\sum$ required to sustain an arbitrary rate of permeation is obtained from β.

Case II

Laminar flow (no mixing) occurs on either side of the film; the gas composition at any point on the low pressure side is given by the relative rates of permeation of the individual constituents at that point. From Eq. (1) there results

$$-dn_A=Q_A d\sum\left(P\frac{n_A}{n_A+n_B}-p\frac{dn_A}{dn_A+dn_B}\right) \quad (9)$$

and

$$-dn_B=Q_B d\sum\left(P\frac{n_B}{n_A+n_B}-p\frac{dn_B}{dn_A+dn_B}\right). \quad (10)$$

Let $x=dn_A/dn_B$, $i=n_A/n_B$, and $\alpha=Q_A/Q_B$; divide (9) by (10). Then

$$x=\alpha\left(P\frac{i}{i+1}-p\frac{x}{x+1}\right)\Big/\left(P\frac{1}{i+1}-p\frac{1}{x+1}\right). \quad (11)$$

Solution of this quadratic gives

$$x=f(i)=Ai+C+[A^2i^2+(2AC+\alpha)i+C^2]^{\frac{1}{2}}, \quad (12)$$

where

$$A=\tfrac{1}{2}[(1-\alpha)p/P+\alpha] \quad \text{and} \quad C=\tfrac{1}{2}[(1-\alpha)p/P-1].$$

Separation of variables in (12) can be achieved by noticing that $x=dn_A/dn_B=f(i)=f(n_A/n_B)$. Use of n_B and i as variables results in

$$\frac{dn_B}{n_B}=\frac{di}{f(i)-i}=\frac{di}{(A-1)i+C+[A^2i^2+2Bi+C^2]^{\frac{1}{2}}}, \quad (13)$$

where $2B=2AC+\alpha$. The right side of Eq. (13) can be rationalized by the introduction of a new variable t, defined by $i=\frac{1}{2}(C^2-t^2)/(At-B)$; the result is:

$$\ln\frac{n_B}{n_B{}^0}=-\int_{t^0}^{t}\frac{At^2-2Bt+AC^2}{(At-B)(t-\alpha+C)(t-C)}dt,$$

or

$$\ln\frac{n_B}{n_B{}^0}=R\ln\frac{t^0-B/A}{t-B/A}+S\ln\frac{t^0-\alpha+C}{t-\alpha+C}+T\ln\frac{t^0-C}{t-C}, \quad (14)$$

where $R=1/(2A-1)$, $S=[\alpha(A-1)+C]/(2A-1)[(\alpha/2)-C]$, and $T=1/(1-A-B/C)$; the superscript ^{0} designates entering gas. This solves the problem of determining the enrichment of the permeated gas for an arbitrary choice of n^0 $(=n_A{}^0+n_B{}^0)$, i^0, and i'; for a given $n_B{}^0=n^0/(1+i^0)$, n_B' is then found by Eq. (14), and n_A' is determined by $n_A'=i'n_B'$. The fraction of inlet gas which permeates is $(n^0-n')/n^0$; the fraction of A in the permeated gas is $(n_A{}^0-n_A')/(n^0-n')$.

It may be noted that the solution of Eq. (11) is particularly simple in the case $p=0$, for then $x=\alpha i$, or $dn_A/n_A=\alpha dn_B/n_B$, and

$$n_A/n_A{}^0=(n_B/n_B{}^0)^\alpha. \quad (15)$$

Computation of the permeation area required in Case II is somewhat involved. Assume there are no concentration gradients normal to the direction of gas flow. Use of Eqs. (12) and (13) in Eq. (11) then results in

$$\sum=-\frac{n_B{}^0}{Q_B}\int_{i^0}^{i'}\frac{\text{antiln}[n_B(i)/n_B{}^0]di}{[f(i)-i]\left[P\frac{1}{i+1}-p\frac{1}{f(i)+1}\right]}. \quad (16)$$

The integral on the right side is perhaps most conveniently evaluated numerically or graphically.

Because of the small magnitude of the permeability coefficients, it is probable that any practical design of a permeation process will involve flow conditions corresponding to Case II (laminar) rather than to Case I

TABLE II. Permeability of 0.0075-mm ethyl cellulose toward the constituents of air.

Gas	Permeability coefficient, Q, (moles cm^{-2} min.$^{-1}$ atmos.$^{-1}$) $\times 10^6$	Q_{gas}/Q_{N_2} Pure gas studies	Q_{gas}/Q_{N_2} Mass spectrometer
N_2	0.075	(1.0)	(1.0)
O_2	0.231	3.1	3.2
CO_2	1.07	14.3	—
A	0.170	2.3	3.1

TABLE II. Temperature dependence of permeability of 0.025-mm ethyl cellulose.

Gas	Temperature, °C	Permeability coefficient, Q, (moles cm^{-2} min.$^{-1}$ atmos.$^{-1}$) $\times 10^6$	Q_{gas}/Q_{N_2} at same temperature	Q_{gas}/Q_{O_2} at same temperature
N_2	30	0.025	(1)	0.31
	40	0.032	(1)	0.32
	50	0.045	(1)	0.35
O_2	30	0.081	3.3[a]	(1)
	40	0.100	3.2	(1)
	50	0.130	2.9	(1)
He	30	0.27	10.7	3.3
	40	0.33	10.2	3.3
	50	0.43	9.6	3.3
H_2	30	0.38	15.2	4.6
	40	0.46	14.4	4.6
	50	0.59	13.1	4.6

[a] A value of 3.4 has been obtained on other samples of the same film.

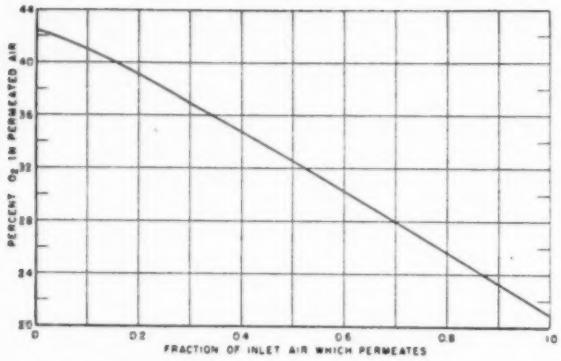

FIG. 2. Enrichment of air in a single stage of permeation. $P=8$, $p=1$, $Q_{O_2}/Q_{N_2}=3.4$.

(perfect mixing). It is interesting to note that, for a given set of conditions, Case II also results in a greater enrichment than does Case I. As an illustration, for the particular situation where normal air at 8 atmos. enters the stage and half of the entering air is permitted to permeate during the stage to the low pressure side at 1 atmos., the composition of the permeated air in Case I is 29.2 percent O_2, and in Case II 32.5 percent O_2. (A value of 3.4 was assumed for α.)

EXPERIMENTAL RESULTS

The permeability of various films toward O_2 and N_2, determined by experiments with the pure gases, is shown in Table I. The specific permeability, K, given is corrected for film thickness; $K=Qd$, where d is the thickness and Q is defined by Eq. (1). Where the comparisons are available, the specific permeability observed is seen to be in reasonable agreement with those previously reported. Of the materials investigated, natural rubber is outstanding in showing the highest permeability; its selectivity, however, as measured by the quantity $\alpha(\alpha=K_{O_2}/K_{N_2})$, is not as great as that of several other materials. Ethyl cellulose appears to satisfy best the joint requirements of high permeability and high selectivity.

Table II shows the permeability coefficients at 30°C of a laboratory-cast ethyl cellulose film toward the major constituents of air. Also shown is a comparison of the relative permeability (with respect to N_2) obtained from the pure gas studies and from the mass spectrometer analysis of air permeating through the film into a vacuum. The concentration of argon is increased along with that of O_2 in the permeated gas, though to a smaller extent than O_2. The permeability toward CO_2 is very high; in a multistage process to obtain high purity oxygen, it would probably be desirable to remove CO_2 after the first permeation stage.

The temperature dependence of the permeability of a 0.025-mm ethyl cellulose film toward several gases is illustrated in Table III. For each gas, the permeability increases with increasing temperature. The temperature dependence (and therefore the activation energy for permeation) is about the same for O_2, He, and H_2 but is greater for N_2. Van Amerongen[3] found a similar situation to hold for the same gases and natural rubber, N_2 having the highese activation energy for permeation and H_2, O_2, and He having lower and approximately equal activation energies. For the enrichment of air, a compromise has to be established between the use of higher temperatures to obtain higher permeability, and lower temperatures to obtain higher selectivity (α).

DISCUSSION

Primary consideration has been given above to a single stage of permeation. In the absence of a perfectly selective film, it is clear that to obtain gases of high purity it would be necessary to employ a multistage recycle system. The principles of such multistage arrangements have been discussed elsewhere.[7,8] Extension of the calculations given for a single stage to a multistage arrangement is straightforward but will not be considered here.

Since a practical permeation process probably would involve flow conditions leading to Eq. (14), calculation has been made of the enrichment of air to be expected from a single stage of permeation under a particular set of conditions. The high pressure has been chosen as 8 atmos., the low pressure as 1 atmos., and the enrichment factor $\alpha(=Q_{O_2}/Q_{N_2})$ as 3.4, the highest value which has been observed. Normal air (20.9 percent O_2) enters the stage. Under these conditions, Fig. 2 shows the composition of the permeated gas as a function of the fraction a of entering gas which permeates $[a=(n^0-n')/n^0]$. For negligible permeation ($a\doteq 0$), maximum enrichment of the permeated gas is observed, and the permeated gas contains 42.5 percent O_2. As $a\doteq 1$, the percent O_2 in the permeated gas approaches 20.9 percent, the inlet composition. For $a=0.5$, the permeated gas contains 32.5 percent O_2. Figure 2 is important for the computation of the net work required for the permeation, since the inlet air must be initially compressed by an imperfect compressor, and the energy of the nonpermeated, compressed gas leaving the stage must be utilized by some machine also of less-than-ideal efficiency.

It is clear from Table III that permeation processes may be of value for systems other than O_2-N_2. The usual separation of He from natural gas involves a relatively easy separation of He from CH_4 in one step, followed by a second step of more intense refrigeration to separate He from residual N_2. For the ethyl cellulose film of Table III, Q_{CH_4}/Q_{N_2} has been found to be about 1.5. The separation factor for He with respect both to N_2 and to CH_4 is quite large, which means that high enrichments can be achieved in each stage. Again, the permeability of ethyl cellulose to H_2 is much larger than to any other permanent gas with the exception of He. This has obvious applications, for example to the

[7] M. Benedict, Chem. Eng. Prog. **43**, 41 (1947).
[8] K. Cohen, U. S. Naval Med. Bull. Supp. **1948**, 6 (1948).

separation of H_2 from coke-oven gas or from the tail-gases of various hydrogenation processes.

ACKNOWLEDGMENTS

The authors gratefully acknowledge the suggestion of the problem and the continuing encouragement by Dr. H. H. Storch. Discussions with Dr. G. von Elbe and E. L. Clark have been most helpful. The authors wish also to thank Dr. R. A. Friedel and J. Sharkey for furnishing the mass-spectrometric analyses, and the companies listed in Table I for their generosity in furnishing samples of films.

D.C. Characteristics of Silicon and Germanium Point Contact Crystal Rectifiers. Part II. The Multicontact Theory*

V. A. Johnson, R. N. Smith,** and H. J. Yearian
Purdue University, Lafayette, Indiana

(Received August 29, 1949)

Part I has described the d.c. current-voltage characteristics obtained for typical Si and Ge crystal rectifiers, has given a summary of the published theories of the rectifier, and has shown that none of these theories accounts for the principal features of the observed characteristics. Part II describes the multicontact theory, an extension of the diode theory, and shows that this theory does account for the behavior of the observed characteristics. There also is described a graphical treatment, based upon the multicontact theory, which may be used in the analysis of experimental characteristics. The multicontact theory assumes that the contact potential at the metal-semiconductor surface varies from spot to spot. It is shown that an exponential distribution function for contact potentials may be used to account for the observed logarithmic slopes and that the observed temperature behavior of the characteristics may be explained by assuming that the distribution function varies with temperature in a manner dependent upon the nature of the contact.

1. INTRODUCTION

In Part I Yearian[1] has described the d.c. current-voltage characteristics obtained for typical silicon and germanium crystal rectifiers. A detailed knowledge of such characteristics and a complete theory of the rectifying behavior of such crystals have been the aim of extensive study in recent years because of the widespread use of silicon and germanium crystal rectifiers in microwave radar. Part I contains a summary of the heretofore published theories of the rectifier, and the discussion shows that none of these theories accounts for the salient features of the observed characteristics.

In Part II an extension of the diode theory, the multicontact theory, is described. It is shown that this theory does account for the essential properties of the observed characteristics. A graphical treatment based upon the multicontact theory is described and its application to the analysis of experimental characteristics is explained. The theory is used in a discussion of the observed change in characteristic for a given point contact with change in temperature of the contact region.

2. MULTICONTACT THEORY

It has been suggested (by Mott, Schottky, Lark-Horovitz, and Bethe) that the small slope of a typical observed log current *vs.* voltage characteristic may be due to a rapid variation in the properties of the blocking layer within the region of contact.[2] Since the thickness of the natural blocking layer is of the order of magnitude of the distance between impurity centers, it is quite probable that the contact potential at the surface of the semiconductor may vary from place to place. It is also likely that external impurities and adsorbed layers may produce fluctuations in contact potential.[3] The currents flowing across regions of low (negative or small positive) contact potential are essentially ohmic. In such regions the rate of change of current with applied voltage is much smaller than the exponential variation which occurs for higher contact potentials. The total current is the sum of the currents for regions of low and high contact potentials; hence, if the region of low contact potential is large enough in comparison to the region of high contact potential, the variation in total current with voltage rise is much less than the value predicted by pure diode theory for a contact with constant positive contact potential.

The multicontact theory assumes that the contact area consists of a number of spots, that the contact potential φ varies from spot to spot, and that the observed current is the sum of the contributions of

* This work was performed under OSRD Contract OEMsr-362 with Purdue University, and was reported in an NDRC Div. 14 Report dated August 14, 1943.

** Now at Boeing Aircraft Company, Seattle, Washington.

[1] H. J. Yearian, J. App. Phys. **21**, 214 (1950), referred to as Part I in the current discussion.

[2] Preliminary studies based upon the multicontact theory have been discussed by R. G. Sachs, NDRC Div. 14 Report No. 168, Purdue University (June 15, 1943); Phys. Rev. **69**, 682 (1946).

[3] For a different approach to the problem of how surface imperfections, foreign atoms on the surface, etc., may affect rectification, see John Bardeen, "Surface states and rectification at a metal semiconductor contact," Phys. Rev. **71**, 717 (1947).

the partial currents from these spots. The number of spots may be considered to be quite small with discretely separated contact potentials; in this case a graphical treatment of the summation is convenient. Or, a continuous distribution may be assumed such that the probability of finding a given contact potential between φ and $\varphi+d\varphi$ can be represented by a continuous probability density which is a function of φ, and so that the area of the spot having contact potential φ can also be represented as a probability function of φ. The spreading resistance in series with each spot is taken as $(2\sigma d)^{-1}$, where σ is the bulk conductivity of the semiconductor and d is the spot diameter. It follows that the spreading resistance is a function of φ determined by the dependence of spot area upon φ.

A graphical study shows that the addition of diode type currents for a group of spots corresponding to very few (three or four) different contact potentials produces a total current which is closely exponential, or linear on a semilogarithmic plot, over an appreciable voltage range. Any value of the logarithmic slope, less than e/kT, may be obtained by a suitable choice of the parameters governing the distribution. The graphical treatment is extended to provide a method whereby a total current curve may be rapidly synthesized to fit any given experimental characteristic.

One assumes that the contact consists of a number of small diodes, each with its own spreading resistance in series. These diodes are effectively in parallel, and so the total current is given by

$$i=\sum_j i_j, \tag{1}$$

where

$$i_j=j_0 a_j(\varphi_j)n_j(\varphi_j)\exp(-e\varphi_j/kT) \times[\exp\{(e/kT)(V_a-i_jR_{sj})\}-1] \tag{2}$$

is the current flowing through all spots for which the contact potential is φ_j. V_a is the applied voltage; j_0 denotes the current density due to the N free electrons (or holes) per unit volume in the semiconductor traveling with mean thermal velocity:

$$j_0=Ne\bar{v}/4=Ne(kT/2\pi m)^{\frac{1}{2}} \tag{3}$$

$a_j(\varphi_j)$ is the area of each spot having contact potential φ_j, and $n_j(\varphi_j)$ is the number of spots having contact potential φ_j. The spreading resistance R_{sj} for all spots with contact potential φ_j is calculated by considering the spreading resistances of such spots to be in parallel with one another. Then

$$R_{sj}=(\pi/a_j)^{\frac{1}{2}}(4\sigma n_j)^{-1}. \tag{4}$$

A template of a master curve (Fig. 1) to be used in the analysis of experimental characteristics, in the forward direction with $V_a>0.1$ volt, may be designed as follows: Using semilogarithmic paper with the same choice of scales as is made in plotting the experimental log$i$ *vs.* V_a characteristics, draw a straight line with logarithmic slope e/kT, i.e., the characteristic of a diode of single contact potential and zero spreading resistance. Choose an arbitrary value for the spreading resistance, compute the corresponding potential drops in the spreading resistance for a series of current values, and plot the characteristic of log$i$ *vs.* V_a, using the relation $V_a=V+R_{sj}i$. Mark on the template the point at which the iR_{sj} potential drop has a known value, such as 0.01 volt. This template may be used to reproduce the current-voltage curve for any diode of any φ_j; R_{sj} refers to the local series spreading resistance rather than to the equivalent spreading resistance of the whole contact.

In order to analyze a given experimental characteristic, by trial and error slide the template into several positions such that the sum of the partial currents so obtained closely approximates the given curve. Each partial current corresponds to a group of spots on the contact having the same contact potential, φ_j. The simplest numerical interpretation of the partial currents is made by assuming $a_j(\varphi_j)$ to be a constant with a reasonable value such as $a=10^{-10}$ cm^2. Then φ_j and $n_j(\varphi_j)$ may be evaluated as follows: Let i_j' represent the value of the partial current for which the potential drop in the spreading resistance is 0.01 volt, i.e., i_j' is the current at the index mark on the template. Then $R_{sj}=(100i_j')^{-1}$ ohm. Extend the low voltage straight

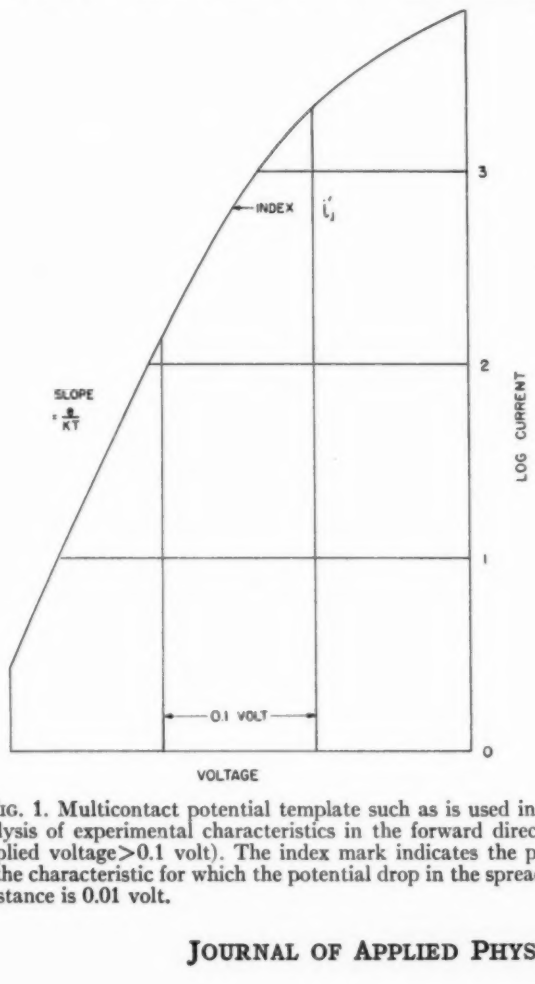

FIG. 1. Multicontact potential template such as is used in the analysis of experimental characteristics in the forward direction (applied voltage>0.1 volt). The index mark indicates the point on the characteristic for which the potential drop in the spreading resistance is 0.01 volt.

portion of the partial current back to find its intersection, i_{j0}, with the $V_a=0$ axis. Eq. (2) indicates that

$$i_{j0}=j_0 a n_j \exp(-e\varphi_j/kT). \qquad (2')$$

When σ and j_0 are known from resistivity and Hall effect measurements on the semiconductor, n_j may be computed by use of Eq. (4) and then Eq. (2′) is used to determine φ_j. The product an_j represents the total area of the spots having contact potential φ_j. The choice of a different value for the area a will yield different values for the n_j, but the distribution of total areas (an_j) over the φ_j values will be much the same.

Figure 2 illustrates the application of the graphical method just described to the analysis of the characteristic obtained for contact in vacuum between a tungsten whisker and a germanium sample prepared in vacuum.[4] It is found that the observed characteristic may be treated as due to three groups of spots with $\varphi_j=0.1$, 0.4, and 0.8 volt, respectively.

Analogous templates and equivalent treatments may be designed for the analysis of experimental characteristics in the back direction and in the forward direction for $V_a<0.1$ volt.

It is to be noted that, in a construction of the type illustrated by Fig. 2, the chief contribution by a spot of contact potential φ_j to the approximately linear portion of the total current curve is made only over a range of V_a in the immediate neighborhood of φ_j. This affords an interpretation of any abnormal characteristic curve; e.g., if the curve of Fig. 2 were slightly concave upward in the region about $V_a=0.4$ volt, there would be a corresponding decrease in the total area corresponding to "B" spots. It is evident that, if the observed current-voltage curve is linear (on semilogarithmic plot) over a considerable range, the distribution of numbers of spots (for the simplest case of assumed constant area) must cover a similar range of φ and that, to obtain the linear total curve, the value of n_j must increase very rapidly with increasing φ_j.

The forward current intercept I_F is determined almost completely by the spots for which φ_j is greater than about 0.05 to 0.1 volt, and it may be seen that I_F is necessarily larger than the sum of the i_{j0} intercepts of the partial currents, $\sum_j i_{j0}$, where i_{j0} is given by Eq. (2). This sum is the contribution of these spots to the limiting diode current in the back direction. Thus one expects the observed diode back current I_B to be less than I_F. This is usually the case (Part I). The sum may be increased to give an I_B approaching I_F by introduction of spots of very low φ_j; this will affect I_F and the logarithmic slope α only slightly, but it will contribute noticeably to the observed diode current in the back direction. The ohmic component of the current in the back direction can be reproduced by any suitable distribution of spots having negative contact potentials; for such spots there is no barrier and only

[4] This figure and its analysis were supplied by Dr. R. M. Whaley of Purdue University; the authors thank him for this courtesy.

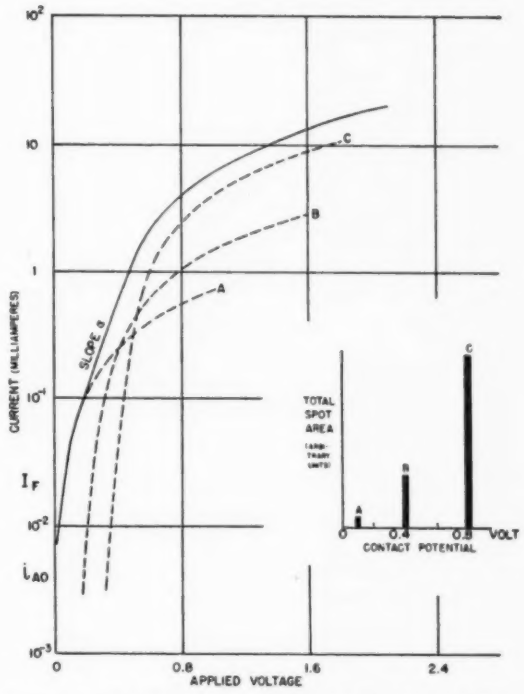

FIG. 2. Application of the multicontact theory to the analysis of an experimental characteristic. The solid line, indicating the experimental curve, is synthesized in a non-unique manner from three partial currents, A, B, and C, which correspond to three discrete contact potential groups. The insert indicates the distribution of spot area among the contact potentials 0.1, 0.4, and 0.8 volt, respectively.

R_{sj} need be considered. The observed back resistance usually can be accounted for by the existence of a very small total area of spots with negative φ_j. If the barrier lowering due to image force and tunneling effects (Part I) is considered, the spots of very small positive contact potenial will also be essentially ohmic in nature for current in the back direction.

3. EXPONENTIAL DISTRIBUTION

If a distribution function $P(\varphi)$ is introduced to describe the dependence of spot area upon contact potential, it is found that the theoretical current-voltage characteristic calculated with the use of such a distribution is essentially independent of the details of the function $P(\varphi)$. Only the tail of the distribution function at low contact potentials influences the shape of the characteristic in that part of the voltage range which is of practical interest. Hence it is not possible to determine the shape of the entire distribution function by use of an experimental characteristic. Since the theoretical characteristic depends only upon the tail of the distribution, one is free to choose a distribution function primarily on the basis of convenience in calculation. An exponential type distribution function is simple and convenient to use.

Hence it is assumed that

(1) The spot area depends upon φ_j according to

$$a(\varphi_j)=a_0 \exp(q\varphi_j). \qquad (5)$$

(2) The number of spots having contact potential φ_j is given by

$$n(\varphi_j)=n_0\exp(p\varphi_j). \tag{6}$$

p and q are parameters which may be chosen to fit experimental data.

(3) Insertions of Eqs. (5) and (6) into Eq. (4) yields for the spreading resistance due to all spots having contact potential φ_j:

$$R_{sj}=(4\sigma n_0)^{-1}(\pi a_0)^{\frac{1}{2}}\exp(-p\varphi_j-q\varphi_j/2). \tag{7}$$

Equation (2) may now be written

$$i_j=n_0a_0j_0\exp\{(p+q-e/kT)\varphi_j\}\times[\exp(e/kT)(V_a-R_{sj}i_j)-1]. \tag{8}$$

If V_a is greater than about 0.1 volt, the -1 in the last bracket may be neglected, and Eq. (8) becomes

$$i_j=n_0a_0j_0\exp\{eV_a/kT-(e/kT-p-q)\varphi_j-R_{sj}i_j\}. \tag{9}$$

Figure 3 illustrates the construction of a total current curve by the summation of partial currents as given by Eq. (9) with $p=20$ volt^{-1} and $q=0$. Such a construction yields a total current curve which is straight over an appreciable range on a semilogarithmic plot and which is parallel to the envelope of the partial current curves. The logarithmic slope of the envelope can be shown to be

$$\alpha=\frac{p+q/2}{e/kT-q/2}\cdot\frac{e}{kT}\ \text{volt}^{-1};\quad (p+q)\leqq e/kT. \tag{10}$$

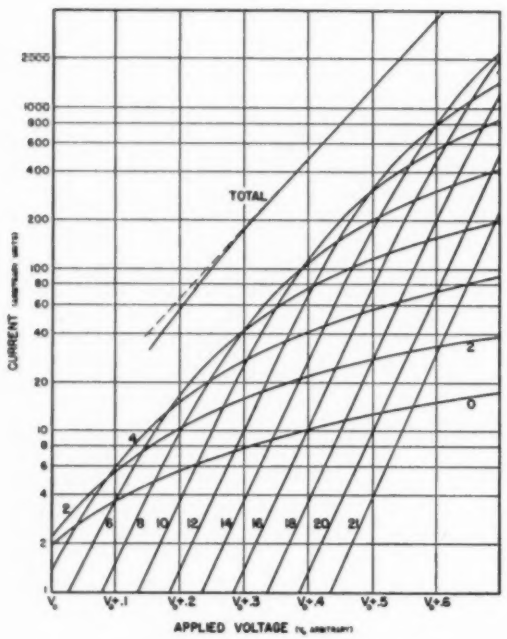

FIG. 3. Construction of a total current by the summation of partial currents. In this case the spot area is taken as constant and the number of spots having contact potential φ-volts is taken as $n_0\exp(20\varphi)$. The partial currents identified by $k=0, 2, \cdots$ are to be identified as passing through spots having $\varphi=\varphi_0+k/40$ volts, where φ_0 is an arbitrary contact potential.

By suitable choice of p and q, any value of α between 0 and e/kT may be obtained. The magnitude of i, but not the slope of the characteristic, depends upon constants of the material, such as σ, j_0, a_0, and n_0.

The assumptions used in the preceding analysis are the basis for the following theoretical treatment in which continuous distribution functions are employed. The dependence of spot area on contact potential is written

$$a(\varphi)=a_0\exp(q\varphi). \tag{11}$$

The number of spots having contact potential between φ and $\varphi+d\varphi$ is given by

$$n(\varphi)d\varphi=n_0\exp(p\varphi)d\varphi. \tag{12}$$

The spreading resistance due to all spots having contact potential φ is

$$R_s(\varphi)=(\pi/a_0)^{\frac{1}{2}}(4\sigma n_0)^{-1}\exp(-p\varphi-q\varphi/2). \tag{13}$$

Equations (11)–(13) may be used to set up an expression for the current in the forward direction. It is considered that the tendency is for diode type currents to flow through spots for which φ is positive and for ohmic currents to flow through spots for which φ is negative. These tendencies are restricted by the fact that the current density flowing through any group of spots is limited to the current density j_0 due to N electrons per unit volume traveling with thermal velocity. Reference to Eq. (2) for a diode type current shows that the current density cannot exceed j_0 if $\varphi>V$, but the current density will exceed j_0 if $\varphi<V$ unless some restriction is introduced. In order to conveniently express the total forward current, it is assumed that if V is large enough to produce the limiting current through a given group of spots, then further increase in V does not change the current. Since the current through a single spot is limited to $j_0a(\varphi)$, the corresponding potential drop in the spreading resistance in series with this spot is $j_0\{\pi a(\varphi)\}^{\frac{1}{2}}/4\pi\sigma$. This quantity has a small magnitude (usually less than 0.01 volt) and so the $iR_s(\varphi)$ drop may be neglected without serious error. V is assumed to be large enough ($\gg kT/e$) so that one may replace $\{\exp(eV/kT)-1\}$ by $\exp(eV/kT)$. Then the forward current ($V>0$) becomes

$$\begin{aligned}i(V)&=j_0a_0n_0\exp(eV/kT)\\&\quad\times\int_V^\infty\exp\{-(e/kT-p-q)\varphi\}d\varphi\\&\quad+j_0a_0n_0\int_{-\infty}^V\exp\{(p+q)\varphi\}d\varphi \qquad (14)\\&=\frac{j_0a_0n_0}{\alpha(e/kT-\alpha)}\frac{e}{kT}\exp(\alpha V),\end{aligned}$$

where $\alpha=p+q$. By setting $V=0$ in Eq. (14) one ob-

TABLE I. Values obtained from study of the d.c. characteristics at various temperatures for germanium crystals in contact with tungsten whiskers. Columns 2, 3, 4, 5, and 7 give measured slopes, intercepts, and back resistances. Columns 6 and 7 permit checking the predicted relation $I_B = sI_F$. Columns 8, 9, and 10 list bulk properties of the germanium samples. Columns 11, 12, and 13 give calculated quantities characteristic of the exponential distribution used in applying the multicontact theory to these samples.

	1	2	3	4	5	6	7	8	9	10	11	12	13
Sample	T °K	α volt^{-1}	$s=\alpha kT/e$	I_F ma	I_B ma	sI_F ma	R_B ohms	σ mho/cm	Hall Constant cm^3/clmb	j_0 10^4 amp./cm^2	n_0a_0 10^{-10} cm^3/volt	Minimum a_0 10^{-8} cm^2	n_0 volt^{-1}
$5I-d4$	243	22	0.46	0.0003	0.0004	0.00014	254000	28.2	64.5	4.43	0.813	0.35	0.023
	295	20	0.52	0.003	0.0032	0.0016	77000	23.5	61.5	5.09	5.74	1.34	0.043
	394	8.9–6.2	0.30–0.21	0.25–0.40	0.24	0.08	5800	16.8	58.5	6.18	291	72	0.040
	549	7.0–5.0	0.33–0.24	2.0 –3.0	0.3–0.5	0.29	90	18.7	23	17.8	607	15	0.41
$5I-d2$	286	7.4	0.18	0.20	0.025	0.04	1100	24.0	61.5	5.01	241	3.8	0.63
	436	6.3	0.24	1.0	0.35	0.24	2000	14.8	56.0	6.81	703	56	0.13
	505	4.9–2.8	0.21–0.12	2.0 –4.0	0.6	0.5	200	15.1	37	11.5	833	2.2	3.7
$9H-a$	298	7.8	0.20	0.80	0.013	0.16	32000	15.4	280	1.13	4420	400000	0.00011
	358	11.9	0.36	0.71	0.28	0.25	4980	12.3	277	1.25	4380	2600	0.017
	391	11.5	0.38	0.95	0.87	0.36	1670	11.2	275	1.32	5130	360	0.14
	426	9.0	0.33	2.5	3.0	0.8	495	10.6	217	1.68	8970	140	0.64
	468	6.6	0.27	5.5	7.1	1.5	145	11.0	105	2.20	12100	44	2.8
	521	7.0	0.31	10.2	7.8	3.2	19	15.4	37	4.17	11800	1.2	95
	574	4.4	0.22	22	?	4.8	7	27.0	16.5	9.41	8030	0.6	132

tains the forward current intercept

$$I_F = \frac{j_0 a_0 n_0}{\alpha(e/kT-\alpha)} \frac{e}{kT}. \tag{15}$$

The diode type current in the back direction is due to all spots having positive contact potentials. Current limitation need not be considered because of the smallness of the diode current for $V<0$, and for the same reason the $R_s i$ potential drop may be neglected. Then the diode current in the back direction ($V<0$) becomes

$$i(V) = j_0 a_0 n_0 \{\exp(eV/kT)-1\} \times \int_0^\infty \exp\{-(e/kT-p-q)\varphi\} d\varphi$$

$$= \frac{j_0 a_0 n_0}{e/kT-\alpha}\{\exp(eV/kT)-1\}. \tag{16}$$

The magnitude of the limiting current in the back direction is found by letting $V \to -\infty$; hence

$$I_B = j_0 a_0 n_0 (e/kT-\alpha)^{-1}. \tag{17}$$

The ohmic current in the back direction is due to all spots having negative contact potentials. The resistance in the back direction is given by

$$1/R_B = 4\sigma n_0 (a_0/\pi)^{\frac{1}{2}} \int_{-\infty}^0 \exp\{(p+q/2)\varphi\} d\varphi$$

$$= 4\sigma n_0 (a_0/\pi)^{\frac{1}{2}} (p+q/2)^{-1}. \tag{18}$$

The value of the quantity $n_0 a_0$ may be found directly from either Eq. (15) or Eq. (17); Eq. (15) is preferable because I_F is usually determined with greater accuracy than I_B. A consistency test for the theory is provided by the fact that the values of $n_0 a_0$ obtained by use of Eqs. (15) and (17) should agree within limits dependent upon the experimental errors in the values of I_F and I_B. These values of $n_0 a_0$ will be equal if

$$I_B = sI_F, \tag{19}$$

where s is the fractional slope $\alpha kT/e$. Table I shows corresponding values of I_B and sI_F, which are found to agree in order of magnitude. For the same reasons as given in the discussion on the discrete distribution of spots of various contact potentials, I_F is determined by only the spots for which the contact potential is greater than about 0.1 volt, whereas I_B is increased by the presence of spots of lower positive contact potential. Hence I_B may exceed the value given in Eq. (19). In addition, the effect of barrier lowering on the spots of low contact potential tends to increase the measured value of I_B.

The maximum value of $n_0 a_0^{\frac{1}{2}}$ may be calculated from Eq. (18) by setting $q=0$; the minimum value of $n_0 a_0^{\frac{1}{2}}$ is one-half of the maximum value and corresponds to setting $p=0$. A combination of $n_0 a_0$ and $n_0 a_0^{\frac{1}{2}}$ values yields values for a_0 and n_0; such values are listed in Table I.

In general the values of $n_0 a_0$ are reasonable, i.e., they are small compared to the total whisker area of 10^{-6} to 10^{-5} cm^2. There is a noticeable tendency for $n_0 a_0$ values to increase with rising temperature. At the lower temperatures the a_0 values tend to exceed the $n_0 a_0$ values, thus yielding fractional values for n in the neighborhood of zero contact potentials. Such a result is contradictory to the basic assumption of a statistical distribution of a very large number of spots.

One possible explanation of the small n_0 values is that the assumed exponential distribution may not be valid in the region of negative contact potential. The back resistance determines the value of

$$\int_{-\infty}^0 n(\varphi)\{a(\varphi)\}^{\frac{1}{2}} d\varphi$$

and, for any assumed distribution, the value of $n_0 a_0^{\frac{1}{2}}$.

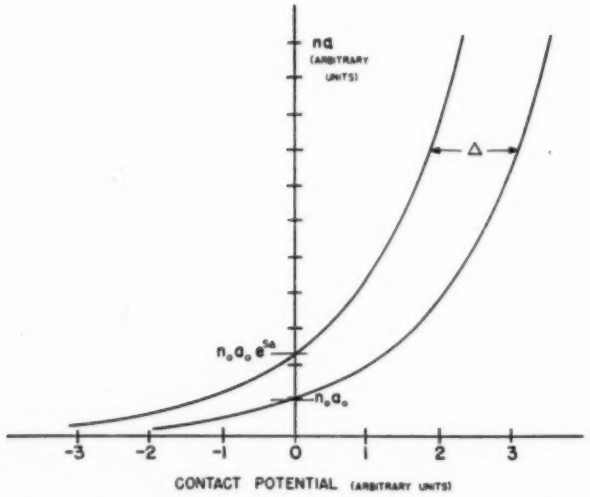

FIG. 4. Effect of temperature change upon the distribution function for "welded" contacts. Ordinates represent the contact areas corresponding to various contact potentials.

A distribution falling off more rapidly with increasing negative φ than an exponential distribution leads to a larger value of n_0a_0 for a fixed n_0a_0. This produces a smaller calculated value of a_0 and hence a larger value of n_0, as is desired.

A second explanation is that the effective conductivity of the small ohmic spots is less than the measured bulk conductivity of the sample. Then a_0 is less in proportion as σ^2 drops below the bulk value. Weisskopf[5] has advanced the hypothesis that the small spots with negative contact potential may be "overloaded" and that "overloading" decreases the effective conductivity. The exponential dependence of spot area on contact potential may lead, for negative φ, to spot diameters equal to or smaller than the electronic mean-free-path in the semiconductor; Lark-Horovitz has pointed out that in such a case a reduction in conductivity is to be expected.

A section of Part I described the effect of image force and tunneling in producing a barrier lowering in the point contact rectifier. A quantitative introduction of barrier lowering into the diode rectifier theory has been made by Courant.[6] Since the multicontact theory is based upon the diode theory, calculations have been made to ascertain the effects of introducing barrier lowering into the multicontact theory. For the forward direction the changes are small and may be summarized as follows: (1) at high voltage the logarithmic slope is constant at the same value given by the multicontact theory without barrier lowering, but at lower voltages (less than about 0.4 volt) the logarithmic slope with lowering considered decreases slightly with decreasing voltage; (2) for a fixed n_0a_0 value the current calculated with barrier lowering considered is greater than the current at the same voltage without lowering; the factor varies from 1.0 to 1.2, increasing with increasing α; (3) for a fixed n_0a_0 value one obtains a higher I_F intercept on the theoretical curve including barrier lowering; I_F is higher by about 5 percent to 20 percent, depending upon α. Another way of stating this result is to say that, for an I_F value taken from a measured characteristic, one calculates on the basis of barrier lowering a value for n_0a_0 that is from 5 percent to 20 percent lower than he would obtain by neglecting barrier lowering.

Since the effect of tunneling alone is to give rectification in the opposite direction from the observed direction, one would expect the inclusion of tunneling, through barrier lowering, in the multicontact theory to give rather marked effects in the back direction characteristic. Such is found to be the case; both the ohmic and diode contributions as calculated without barrier lowering are altered. The back resistance corresponding to the ohmic current is considerably reduced and hence the ohmic current considerably increased. The diode contribution is markedly changed; the extent of the change depends upon the electron concentration with the change greatest for the highest concentration. The tunneling produces an exponentially increasing current that, at higher voltages, has a logarithmic slope equal to or even greater than the forward slope. This exponential current tends to cover up the saturation current, denoted by I_B. The tendency is for the ohmic current to dominate at the lower back voltages; the extent of barrier lowering determines the voltage at which the exponential current surpasses the ohmic current.

The barrier lowering calculations of Courant assume an electron concentration of 5×10^{18} cm^{-3}; the use of these results in the multicontact theory yields calculated back currents too high to agree with experiment. The agreement would be improved by noting that the actual electron concentrations in germanium and silicon point contact rectifiers are one or two orders of magnitude less than that assumed by Courant, and hence the effect of barrier lowering would not be as great as calculated by Courant.

4. TEMPERATURE BEHAVIOR

In Part I a description was given of the changes in characteristic observed for a given contact as the temperature is varied. Sets of characteristics for different temperatures were obtained both for "free" contacts between tungsten whiskers and germanium and for "welded" contacts between whisker and germanium in General Electric cartridges. The temperature behavior of α is dependent upon the type of contact. For free contacts, α decreases with increasing temperature in such a way that the fractional slope is approximately constant. For welded contacts, the value of α is prac-

[5] V. F. Weisskopf, Radiation Laboratory Report 133 (May, 1943).

[6] E. Courant, NDRC Div. 14, Cornell University Report, Contract OEMsr-429 (May 17, 1943); Phys. Rev. **69**, 684 (1946). A report of Courant's results is given in a paper by W. E. Meyerhof, Phys. Rev. **71**, 727 (1947).

tically independent of temperature. Figures of Part I show that the back resistance R_B decreases with increasing temperature and that the forward intercept I_F and limiting diode current in the back direction, I_B, increase with rising temperature. The plot of $\log R_B$ against temperature can be represented by a straight line of negative slope; the plots of $\log I_F$ and $\log I_B$ against T can be approximated by straight lines of positive slope.

Equation (14) shows that the forward logarithmic slope α is equal to the sum of the distribution parameters p and q, and so α determines the shape of the distribution. The constancy of α with changing temperature for the "welded" contacts suggests that the shape of the distribution is independent of T for these contacts, but the dependence of R_B, I_F, and I_B on T implies that the distribution has some type of temperature dependence. Assume that, although the shape of the distribution curve is unchanged, the whole curve is shifted by an amount Δ depending upon the temperature change. Let φ' be contact potential, at the new temperature, corresponding to the ordinate of the distribution curve at φ at the original temperature (see Fig. 4). Then

$$\varphi' = \varphi - \Delta. \tag{20}$$

Introducing this assumption into Eqs. (14), (16), and (18) yields

$$I_F' = \frac{j_0' a_0 n_0}{\alpha(e/kT' - \alpha)} \frac{e}{kT'} \exp(\alpha\Delta) \approx I_F \exp(\alpha\Delta) \tag{21}$$

$$I_B' = j_0' a_0 n_0 (e/kT' - \alpha)^{-1} \exp(\alpha\Delta) \approx I_B \exp(\alpha\Delta) \tag{22}$$

$$R_B' = (\pi/a_0)^{\frac{1}{2}} (4\sigma' n_0)^{-1} (\alpha - q/2) \exp\{-(\alpha - q/2)\Delta\}$$
$$\approx R_B \exp\{-(\alpha - q/2)\Delta\}. \tag{23}$$

The introduction of the shift Δ makes it possible to treat n_0 and a_0 as temperature independent in Eqs. (21), (22), and (23). If j_0 is taken as proportional to $T^{\frac{1}{2}}$, the temperature dependence predicted by Eq. (21) is

$$(T')^{\frac{1}{2}}(e/kT' - \alpha) I_F' \sim \exp(\alpha\Delta).$$

Plots against T of $\log I_F'$ and $\log\{(T')^{\frac{1}{2}}(e/kT' - \alpha) I_F'\}$ give lines of equal slopes and so justify the use of the simpler expression. As shown in Part I, the plots of $\log I_F'$, $\log I_B'$, and $\log R_B'$ against T are quite straight over a considerable temperature range. This suggests the relation

$$\Delta = B(T' - T) \tag{24}$$

that is, the distribution curve is shifted laterally by an amount proportional to the temperature change. A change in temperature shifts the distribution so that the total area corresponding to negative contact potential increases with rising temperature. The value of B may be found from the known values of α and of the slopes of $\log I_F'$ *vs.* T and $\log I_B'$ *vs.* T lines. For the welded samples, $B = 1.1$–1.2 millivolts per degree as determined from the I_F plot and $B = 1.8$–2.0 mv per degree from the I_B plot.

The foregoing discussion does not apply to free contacts. Since the value of α decreases with rising temperature, the shape of the distribution curve changes and p and q are functions of temperature. The approximately constant value of the fractional slope implies that α, p, and q are inversely proportional to T. In order to explain the temperature behavior of the characteristics for free contacts, one must assume that the distribution curve for φ is not only shifted but is also flattened as the temperature rises.

5. SUMMARY

In conclusion, one can say that (1) the multicontact theory accounts for the frequently observed forward logarithmic slopes much less than e/kT, and for the diode and ohmic components of current in the back direction, (2) a distribution of spots with discrete contact potentials can readily be found such that it will yield any given observed characteristic; although such a discrete distribution is non-unique, it is useful in interpretation of the given characteristic, (3) an exponential distribution function, with parameters determined by experimental values, is satisfactory and convenient, and (4) the observed temperature behavior may be accounted for by assuming that the distribution function varies with temperature in a manner dependent on the nature of the contact. It should be noted that the treatment just described is incomplete in the sense that the constants of the distribution may be found empirically from the observed characteristics, but the constants cannot be determined by independent physical reasoning.

Analysis of a Sampling Servo Mechanism

KENNETH S. MILLER* AND RALPH J. SCHWARZ†
Columbia University, New York, New York
(Received October 3, 1949)

An analysis of a sampling servo mechanism with an error-clamping device and linear forward and return paths is given. The method leads to a determination of the continuous output of the system in terms of quadratures and gives explicitly the value of the output at the discrete sampling instants. Frequently this is all that is needed in order to study the output variation with time. The question of stability is discussed and a criterion for testing the stability of the system is given in terms of the system parameters.

I. INTRODUCTION

IN a large class of servo mechanisms, error data are supplied continuously, the error being a measure of the instantaneous deviation of some function of the output from the input. In another important class of servos, called sampling servo mechanisms,[1,2] error data are supplied at discrete, equally spaced instants only. The servo mechanism is then given no information about the error in the intermediate periods. Such systems may be analyzed by using the theory of filters with pulsed data.[3]

In many applications, the error data, supplied only at discrete sampling instants, are passed through a device whose output at any time is equal to the input at the preceding sampling instant. Such a mechanism is called a "clamping device." The output of the error-clamping device is thus constant for a period equal to the interval between sampling instants. This interval will be called the sampling period, T_s. Sampling occurs at the instants $t=0, T_s, 2T_s, \cdots, NT_s, \cdots$.

The mathematical analysis below is carried out by employing the "one-sided Green's function." Using this and associated concepts, explicit relations are derived for the error, response to a step input, and asymptotic value of the output; further, a stability criterion is formulated. The output is a continuous function of time, and an integral representation is obtained. An explicit formula, however, can be given for the output at the sampling instants.

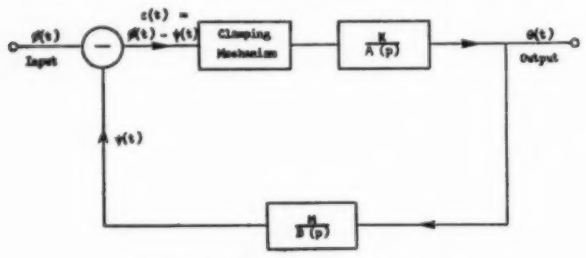

$$A(p)=p^n+a_1p^{n-1}+\cdots+a_{n-1}p+a_n$$
$$B(p)=p^m+b_1p^{m-1}+\cdots+b_{m-1}p+b_m$$

FIG. 1. Sampling servo system.

II. MATHEMATICAL ANALYSIS

1. Introduction

The feed-back system which is to be operated as a sampling servo mechanism in the sense of the definition given in Section I is illustrated in Fig. 1. $A(p)$ and $B(p)$ are polynomials in p with constant coefficients. p is the differential operator d/dt. Explicitly,

$$A(p)=p^n+a_1p^{n-1}+\cdots+a_{n-1}p+a_n \tag{1}$$
$$B(p)=p^m+b_1p^{m-1}+\cdots+b_{m-1}p+b_m. \tag{2}$$

K and M are constants and

$$R=KM$$

is defined as the "loop gain."

It will be assumed that the system is initially unexcited. This implies that

$$\psi^{(\alpha)}(0)=0, \quad \alpha=0, 1, \cdots, m+n-1 \tag{3}$$

where $\psi(t)$ is defined in Fig. 1.

In accordance with Fig. 1,

$$A(p)\theta(t)=K\cdot\epsilon(t) \tag{4}$$

and

$$B(p)\psi(t)=M\cdot\theta(t).$$

Hence

$$A(p)B(p)\psi(t)=MK\cdot\epsilon(t)\equiv R\cdot\epsilon(t). \tag{5}$$

Since the initial conditions (3) have been specified, the inverse operator $[A(p)B(p)]^{-1}$ is well defined. In fact,

$$\psi(t)=\int_0^t G(t,\zeta)[R\cdot\epsilon(\zeta)]d\zeta \tag{6}$$

where $G(t,\zeta)$ is the "one-sided Green's function" for the incompatible system[4]

$$\left.\begin{aligned} A(p)B(p)\psi(t)&=0 \\ \psi^{(\alpha)}(0)&=0, \quad \alpha=0, 1, \cdots, m+n-1 \end{aligned}\right\} \tag{7}$$

* Present address: School of Mathematics, Institute for Advanced Study, Princeton, New Jersey.
† Department of Electrical Engineering.
[1] L. A. MacColl, *Fundamental Theory of Servomechanisms* (D. Van Nostrand Company, Inc., New York, 1945), Chapter 10.
[2] R. C. Oldenbourg and H. Sartorius, *The Dynamics of Automatic Controls*, translated and edited by H. L. Mason (American Society of Mechanical Engineers, New York, 1948), Chapter 5.
[3] James, Nichols, and Philips, *Theory of Servomechanisms*, Vol. 25 of M.I.T. Radiation Laboratory Series (McGraw-Hill Book Company, Inc., New York, 1947), Chapter 5.
[4] E. L. Ince, *Ordinary Differential Equations* (Dover Publications, New York, 1944), p. 254 ff.

and is given by

$$G(t,\zeta)=(-1)^{m+n-1}\frac{\begin{vmatrix}\phi_1(t) & \phi_2(t) & \cdots & \phi_{m+n}(t)\\ \phi_1(\zeta) & \phi_2(\zeta) & \cdots & \phi_{m+n}(\zeta)\\ \phi_1'(\zeta) & \phi_2'(\zeta) & \cdots & \phi_{m+n}'(\zeta)\\ \cdots & \cdots & \cdots & \cdots\\ \phi_1^{(m+n-2)}(\zeta) & \phi_2^{(m+n-2)}(\zeta) & \cdots & \phi_{m+n}^{(m+n-2)}(\zeta)\end{vmatrix}}{\begin{vmatrix}\phi_1(\zeta) & \phi_2(\zeta) & \cdots & \phi_{m+n}(\zeta)\\ \cdots & \cdots & \cdots & \cdots\\ \phi_1^{(m+n-1)}(\zeta) & \phi_2^{(m+n-1)}(\zeta) & \cdots & \phi_{m+n}^{(m+n-1)}(\zeta)\end{vmatrix}}. \tag{8}$$

In this determinant, $\phi_\alpha(t)$, $\alpha=1, 2, \cdots, m+n$, are $m+n$ linearly independent solutions of $A(p)B(p)\psi(t)=0$.

It should be noted that no loss of generality results by considering R a constant. For if R were a polynomial in p,

$$R\equiv R(p)=p^q+c_1p^{q-1}+\cdots+c_{q-1}p+c_q \tag{9}$$

then

$$R(p)\epsilon(t)\equiv c_q\epsilon_{N-1}$$

in any sampling interval $(N-1)T_s<t\leqq NT_s$ since $\epsilon(t)$ is a "staircase function" (see Section I). Also, it is permissible to use a "one-sided Green's function" instead of the more familiar "two-sided" one[4] since symmetric properties of the integral operator of Eq. (6) are of no interest in this paper.

Since the operator $A(p)B(p)$ has constant coefficients, the linearly independent solutions $\phi_\alpha(t)$ are of the form

$$\phi_\alpha(t)=t^re^{st},\quad \alpha=1, 2, \cdots, m+n. \tag{10}$$

It will now be assumed that the $m+n$ roots, v_α, $\alpha=1, 2, \cdots, m+n$ of the characteristic equation for $A(p)B(p)$ are all distinct and non-zero. The analysis of cases not in this category will be readily apparent from the treatment given here.

With this assumption,

$$\phi_\alpha(t)=e^{v_\alpha t},\quad \alpha=1, 2, \cdots, m+n. \tag{11}$$

Substituting these values of $\phi_\alpha(t)$ in the Green's function, Eq. (8), yields

$$G(t,\zeta)=(-1)^{m+n}\sum_{\beta=1}^{m+n}(-1)^\beta e^{v_\beta t}e^{-v_\beta\zeta}W_\beta W^{-1} \tag{12}$$

where W is the Vandermonde determinant[5]

$$W=\begin{vmatrix}1 & 1 & \cdots & 1\\ v_1 & v_2 & \cdots & v_{m+n}\\ \cdots & \cdots & \cdots & \cdots\\ v_1^{m+n-1} & v_2^{m+n-1} & \cdots & v_{m+n}^{m+n-1}\end{vmatrix}=\prod_{\substack{\alpha,\beta=1\\ \alpha>\beta}}^{m+n}(v_\alpha-v_\beta) \tag{13}$$

and W_β is the minor of the element in the last row and β^{TH} column of W.

$$W_\beta=\prod_{\substack{i,j=1\\ i>j\\ i,j\neq\beta}}^{m+n}(v_i-v_j),\quad \beta=1, 2, \cdots, m+n. \tag{14}$$

2. The Linear Recurrent Relation for $\epsilon(t)$

Since $\epsilon(t)$ is a staircase function, the value of $\psi(t)$ at the sampling instant $t=NT_s$ is

$$\psi(NT_s)\equiv\psi_N=R\sum_{\alpha=0}^{N-1}\epsilon_\alpha\int_{\alpha T_s}^{(\alpha+1)T_s}G(NT_s,\zeta)d\zeta \tag{15}$$

where $\epsilon(t)=\epsilon_\alpha$ for $\alpha T_s<t\leqq(\alpha+1)T_s$. Introducing the notation

$$\left.\begin{aligned}&\omega_\beta=e^{v_\beta T_s}\\ &X_\beta=(-1)^{m+n+\beta}W_\beta W^{-1}(1-\omega_\beta^{-1})v_\beta^{-1}\end{aligned}\right\}\quad \beta=1, 2, \cdots, m+n, \tag{16}$$

Eq. (15) becomes, after a few simple algebraic reductions,

$$\psi_N=R\sum_{\alpha=0}^{N-1}\epsilon_\alpha\sum_{\beta=1}^{m+n}X_\beta\omega_\beta^{N-\alpha},\quad \beta=1, 2, \cdots, m+n. \tag{17}$$

Letting

$$Z_{j,N}=\sum_{\alpha=0}^{N-1}\epsilon_\alpha\omega_j^{-\alpha},\quad j=1, 2, \cdots, m+n, \tag{18}$$

yields

$$Z_{j,N+q}=Z_{j,N}+\sum_{\beta=0}^{q-1}\epsilon_{N+\beta}\omega_j^{-(N+\beta)},\quad \begin{matrix}j=1, 2, \cdots, m+n\\ q=1, 2, \cdots.\end{matrix} \tag{19}$$

The second term of Eq. (19) does not involve any summation "up to N." It is desired to obtain a relation among the ψ_N's which is free of $Z_{j,N}$. Toward this end the ψ_{N+q}'s are considered.

$$\psi_{N+q}=R\sum_{\alpha=1}^{m+n}X_\alpha\omega_\alpha{}^{N+q}Z_{\alpha,N}+R\sum_{\alpha=1}^{m+n}X_\alpha\sum_{\beta=0}^{q-1}\epsilon_{N+\beta}\omega_\alpha{}^{q-\beta}. \tag{20}$$

Introducing the $m+n+1$ multipliers λ_q and summing

[5] G. Kowalewski, *Einführung in die Determinantentheorie* (Chelsea Publishing Company, New York, 1948), p. 38.

the products $\lambda_q\psi_{N+q}$ up to $m+n$ yields

$$\sum_{q=0}^{m+n}\lambda_q\psi_{N+q}=R\sum_{q=0}^{m+n}\lambda_q\sum_{\alpha=1}^{m+n}X_\alpha\omega_\alpha{}^{N+q}Z_{\alpha,N}$$

$$+R\sum_{q=0}^{m+n}\lambda_q\sum_{\alpha=1}^{m+n}X_\alpha\sum_{\beta=0}^{q-1}\epsilon_{N+\beta}\omega_\alpha{}^{q-\beta}. \quad (21)$$

The λ_α, $\alpha=0, 1, \cdots, m+n$ will be so determined that the first member of Eq. (21) on the right vanishes without all the λ_α being identically zero. It is seen that

$$\sum_{q=0}^{m+n}\lambda_q\omega_\alpha{}^q=0, \quad \alpha=1, 2, \cdots, m+n \quad (22)$$

is a sufficient condition. If $\lambda_{m+n}\equiv 1$, then Eq. (22) becomes a system [Eq. (23)] of $(m+n)$ equations for the $(m+n)$ unknowns $\lambda_0, \lambda_1, \cdots, \lambda_{m+n-1}$:

$$\sum_{q=0}^{m+n-1}\lambda_q\omega_\alpha{}^q=-\omega_\alpha{}^{m+n}, \quad \alpha=1, 2, \cdots, m+n. \quad (23)$$

Since the determinant of this system is again a Vandermonde determinant, it is $\neq 0$ since $\omega_\alpha\neq\omega_\beta$ (and $\alpha\neq\beta$) by hypothesis. Hence the system of equations is consistent. Since $\lambda_{m+n}=1\neq 0$, not all the λ_α vanish. With this choice of the λ's, Eq. (21) reduces (after some algebraic manipulations) to

$$\epsilon_{N+m+n}+\sum_{\beta=0}^{m+n-1}\{\lambda_\beta+R\sum_{q=\beta+1}^{m+n}\sum_{\alpha=1}^{m+n}\lambda_qX_\alpha\omega_\alpha{}^{q-\beta}\}\epsilon_{N+\beta}$$

$$=\sum_{q=0}^{m+n}\lambda_q\phi_{N+q}. \quad (24)$$

Equation (24) is an equation for the ϵ_N's with constant coefficients. It is not a difference equation in the usual sense since it is valid only at the sampling instants $0, T_s, 2T_s, 3T_s, \cdots$. Hence, strictly speaking, Eq. (24) is a linear recurrence formula.[6]

From Eq. (23) it is seen that the λ's are the indicated coefficients of the algebraic equation

$$x^{m+n}+\lambda_{m+n-1}x^{m+n-1}+\cdots+\lambda_1x+\lambda_0=0, \quad \lambda_{m+n}=1 \quad (25)$$

whose roots are ω_α, $\alpha=1, 2, \cdots, m+n$.

If Eq. (24) is written in the compact form

$$\sum_{\alpha=0}^{m+n}A_\alpha\epsilon_{N+\alpha}=\sum_{q=0}^{m+n}\lambda_q\phi_{N+q} \quad (26)$$

where

$$A_{m+n}=1, \quad A_\beta=\lambda_\beta+R\sum_{q=\beta+1}^{m+n}\sum_{\alpha=1}^{m+n}\lambda_qX_\alpha\omega_\alpha{}^{q-\beta}, \quad (27)$$

$$\beta=0, 1, \cdots, m+n-1,$$

[6] T. Fort, *Finite Differences* (Oxford University Press, London, 1948), p. 115.

it is seen that the solution of the homogeneous equation

$$\sum_{\alpha=0}^{m+n}A_\alpha\epsilon_{N+\alpha}=0 \quad (28)$$

is

$$\epsilon_N=\sum_{\beta=1}^{m+n}P_\beta r_\beta{}^N \quad (29)$$

where the r_β are the roots of the algebraic equation

$$\sum_{\alpha=0}^{m+n}A_\alpha r^\alpha=0 \quad (30)$$

and P_β are periodic constants of period T_s. Since Eq. (24) is a linear recurrence formula and not a difference equation, the P_β are precisely constants in the ordinary sense. In writing Eq. (29), it has been tacitly assumed that all the roots of Eq. (30) are distinct. If this is not the case, the obvious modification

$$\epsilon_N=\sum_{\beta=1}^{k}[P_\beta N^{\beta-1}]r_1{}^N+\sum_{\alpha=k+1}^{m+n}P_\alpha r_\alpha{}^N$$

is made, where r_1 is a root of multiplicity k.

The particular integral $h(N)$ corresponding to the non-homogeneous equation can be obtained by the usual method of undetermined coefficients.[7] Hence the solution of Eq. (26) is

$$\epsilon_N=\sum_{\beta=1}^{m+n}P_\beta r_\beta{}^N+h(N). \quad (31)$$

The constants P_β in the solution [Eq. (31)] corresponding to the boundary conditions of Eq. (3) can readily be obtained in the following manner.

At the time $t=0$, $\psi(0)=0$; hence

$$\phi(0)=\epsilon(0) \quad \text{or} \quad \phi_0=\epsilon_0. \quad (32)$$

From Eq. (15)

$$\psi_1=R\epsilon_0\int_0^{T_s}G(T_s, \zeta)d\zeta. \quad (33)$$

Since ϵ_0, $\int_0^{T_s}G(T_s, \zeta)d\zeta$ and R are known, ψ_1 is known. ϕ_1 is known since the input $\phi(t)$ is a given function. Since at the sampling instants

$$\epsilon_N=\phi_N-\psi_N, \quad (34)$$

in particular

$$\epsilon_1=\phi_1-\psi_1 \quad (35)$$

and hence ϵ_1 is known. Proceeding in this pedestrian fashion, $\epsilon_0, \epsilon_1, \cdots, \epsilon_{m+n-1}$ are calculated. From Eq. (29)

$$\epsilon_\alpha=\sum_{\beta=1}^{m+n}P_\beta r_\beta{}^\alpha+h(\alpha), \quad \alpha=0, 1, \cdots, m+n-1. \quad (36)$$

The determinant of the P_β is non-zero. (It is a Vander-

[7] T. Fort (reference 6, p. 126).

monde determinant if the r_β are distinct and non-zero.) Hence the system (36) may be solved for P_β, $\beta=1, 2, \cdots, m+n$.

3. Stability of the Sampling Servo Mechanism

The servo system illustrated in Fig. 1 will be said to be stable if $\epsilon_N \to 0$ as $N \to \infty$ for any bounded input $\phi(t)$ of finite duration. If $\phi^*(t)$ is such a function, $\phi_N{}^*=0$ and $h(N)=0$ for N sufficiently large. Therefore, Eq. (31) may be written as

$$\epsilon_N = \sum_{\beta=1}^{m+n} P_\beta r_\beta{}^N. \tag{37}$$

It is evident from Eq. (37) that a necessary and sufficient condition that $\epsilon_N \to 0$ as $N \to \infty$ is that $|r_\beta|<1$. In other words, all the roots r_β, $\beta=1, 2, \cdots, m+n$ must lie inside the unit circle in the complex domain. Since the unit circle in the z plane can be transformed into the left half-plane of the complex w plane, the Nyquist criterion can be applied to determine the stability of the system without actually calculating the roots.

4. Determination of the Output $\theta(t)$

To determine the output $\theta(t)$, it is noted from Fig. 1 that

$$A(p)\theta(t)=K\epsilon(t). \tag{38}$$

Also, from the feed-back loop

$$B(p)\psi(t)=M\theta(t). \tag{39}$$

Since $\psi^{(\alpha)}(0)=0$, $\alpha=0, 1, \cdots, m+n-1$ by Eq. (3), it follows that

$$\theta^{(\alpha)}(0)=0, \quad \alpha=0, 1, \cdots, n-1. \tag{40}$$

Hence the "Green's function method" is applicable and

$$\theta(t)=K\int_0^t g(t,\zeta)\epsilon(\zeta)d\zeta \tag{41}$$

where $g(t, \zeta)$ is a one-sided Green's function.

If it is desired to compute $\theta(t)$ at the sampling instants nT_s, a method exactly analogous to the one discussed for $\epsilon(t)$ leads to the equation

$$\sum_{q=0}^{n} l_q\theta_{N+q}=M\sum_{q=0}^{n} l_q\sum_{\alpha=1}^{n} Y_\alpha\sigma_\alpha{}^q\sum_{\beta=0}^{q-1}\epsilon_{N+\beta}\sigma_\alpha{}^{-\beta} \tag{42}$$

where

$$\sigma_\alpha=e^{u_\alpha T_s}, \tag{43}$$

$u_1, u_2, \cdots, u_n$ are the distinct non-zero roots of the algebraic equation

$$x^n+a_1x^{n-1}+\cdots+a_{n-1}x+a_n=0, \tag{44}$$

$$Y_\alpha=(-1)^{n+\alpha}\Delta_\alpha\Delta^{-1}(1-\sigma_\alpha{}^{-1})u_\alpha{}^{-1}, \quad \alpha=1, 2, \cdots, n, \tag{45}$$

$$\Delta=\prod_{\substack{i,j=1\\ i>j}}^{n}(u_i-u_j), \tag{46}$$

$$\Delta_\alpha=\prod_{\substack{i,j=1\\ i>j\\ i,j\neq\alpha}}^{n}(u_i-u_j), \quad \alpha=1, 2, \cdots, n, \tag{47}$$

and l_α are the indicated coefficients of the algebraic equation

$$x^n+l_{n-1}x^{n-1}+\cdots+l_1x+l_0=0, \quad l_n\equiv 1, \tag{48}$$

whose roots are $\sigma_1, \sigma_2, \cdots, \sigma_n$. Hence if $f(N)$ is any particular solution of the non-homogeneous Eq. (42),

$$\theta_N=\sum_{\alpha=1}^{n} Q_\alpha\sigma_\alpha{}^N+f(N). \tag{49}$$

The constants Q_α, $\alpha=1, 2, \cdots, n$ can be obtained in the same manner in which the P_β were determined in Section II.2.

5. Response to a Step Input

If the input $\phi(t)$ to a stable system is given by $u(t)$ where $u(t)$ is the unit step function defined by

$$\left.\begin{aligned} u(t-\alpha)&=0 \quad t<\alpha\\ u(t-\alpha)&=1 \quad t>\alpha\end{aligned}\right\}, \tag{50}$$

then

$$\phi_0=\phi_1=\cdots=\phi_N=\cdots=1 \tag{51}$$

and

$$\sum_{q=0}^{m+n}\lambda_q\phi_N=\sum_{q=0}^{m+n}\lambda_q. \tag{52}$$

Hence,

$$h(N)=[\sum_{q=0}^{m+n}\lambda_q][\sum_{\alpha=0}^{m+n}A_\alpha]^{-1}\equiv H \tag{53}$$

is a particular solution of Eq. (26).

As $N\to\infty$, $\epsilon_N\to H$ since $|r_\beta|<1$, $\beta=1, 2, \cdots, m+n$. Hence it is seen that the system does not close out the error arising from a step function input. In order to adjust the system so that it will close out the steady state error, it is sufficient for $A(p)$ to have a simple zero at $p=0$. In this case

$$\omega_1=e^{w_1T_s}\equiv 1, \tag{54}$$

and the only modification of Eq. (24) is that X_1 becomes

$$X_1=(-1)^{m+n-1}W_1W^{-1}T_s. \tag{55}$$

From Eq. (23) for $\omega_1=1$,

$$\sum_{q=0}^{m+n-1}\lambda_q=-1 \quad \text{or} \quad \sum_{q=0}^{m+n}\lambda_q=0 \tag{56}$$

since $\lambda_{m+n}=1$. Hence Eq. (26) reduces to a homogeneous equation and, if the system is stable,

$$\epsilon_N=\sum_{\beta=1}^{m+n}P_\beta r_\beta{}^N\to 0 \quad \text{as} \quad N\to\infty. \tag{57}$$

Now the output θ_N satisfies Eq. (42). Since $\epsilon_N \to 0$ as $N \to \infty$, Eq. (49) can be written

$$\theta_N = \sum_{\alpha=1}^{n} Q_\alpha \sigma_\alpha{}^N + \delta \tag{58}$$

where δ is an infinitesimal for $N \to \infty$. Equation (58) gives the output at the sampling instants for a step input.

The asymptotic value of the output is readily obtained. Since the system is stable by hypothesis and $\phi(t)$ is bounded, $\theta(t)$ must be bounded. This implies

$$|\sigma_\alpha| \leqq 1, \quad \alpha = 1, 2, \cdots, n. \tag{59}$$

But $\sigma_\beta = \omega_\beta$, $\beta = 1, 2, \cdots, n$ and since $\omega_1 = 1$, $\sigma_1 = 1$. All the other σ_α must be less than one since $v_1 = 0$ is the only pole of $M/A(p)$ at $p = 0$. Hence

$$\theta_N = Q_1 + \sum_{\alpha=2}^{n} \sigma_\alpha{}^N + \delta, \tag{60}$$

and thus

$$\theta_\infty = Q_1. \tag{61}$$

It is noted that the condition $|\sigma_\alpha| \leqq 1$ implies Real part $(u_\alpha) \leqq 0$, $\alpha = 1, 2, \cdots, n$. In other words, a necessary condition that the system be stable is that the forward transmission have no poles in the right-half of the complex p plane.

Variation of Elastic Moduli and Wave Velocity with Pressure and Temperature in Plastics*

D. S. Hughes, E. B. Blankenship, and R. L. Mims†
Department of Physics, University of Texas, Austin, Texas
(Received September 6, 1949)

The variations in velocity of dilatational waves in the pressure range 0 to 15,000 lb./in.² and temperature range 30° to 90°C have been measured for samples of polystyrene, Lucite, and polyethylene. The velocity of rotational waves was also measured for polystyrene and Lucite. In polyethylene no trace of a rotational wave could be identified. The elastic moduli and Poisson's ratio are computed over the experimental range.

INTRODUCTION

A QUICK and simple method of measuring the velocity of waves in rods is to measure the time of transmission of a pulse through a known length. This pulse in long thin rods usually travels with the "acoustic" velocity given by

$$V_S = (E/\rho)^{\frac{1}{2}} \tag{1}$$

where E is the Young's modulus of the material and ρ is the density. For short, relatively thick rods the first arrival is the dilatational wave whose velocity is given by

$$V_D = [(K + \tfrac{4}{3}\mu)/\rho]^{\frac{1}{2}} \tag{2}$$

where K is the bulk modulus and μ is the rigidity modulus. It has been found that following the dilatational wave[1] there are other arrivals which arise by transformation of the original dilatational pulse at the boundaries of the rod into rotational waves. These rotational waves cross the rod and at the opposite boundary give rise again to a dilatational wave traveling parallel to the axis of the rod. The angle between the normal to the rotational waves and the axis of the rod is given by

$$\sin\Theta = V_R/V_D. \tag{3}$$

In reference 1 it is shown that the arrival times to be expected are given by

$$t_{nm} = m\alpha D + n\beta L \tag{4}$$

where n is any odd integer and m is subject to the condition

$$0 \leqq mD \tan\Theta \leqq nL$$

$$\beta = 1/V_D \quad \alpha = [(V_D{}^2 - V_R{}^2)/V_D V_R]^{\frac{1}{2}}. \tag{5}$$

Thus t_{10} is the direct dilatational wave, t_{11} is a dilatational wave that was transformed into a rotational wave and back into a dilatational wave, t_{12} has been transformed twice into a rotational wave, t_{30} is a dilatational wave that has traversed the rod three times without transformation, t_{31} has traversed the rod three times with one transformation, etc.

In practice, values of m greater than five or six are rarely observed even with metals of good acoustic properties. With polystyrene, t_{10}, t_{11}, and t_{30} could always be identified. With Lucite, only t_{10} and t_{11} could be read dependably, and with polyethylene, only t_{10}.

The values of α and β are computed from Eq. (4) and the observed times, and from these, the dilatational and rotational velocities may be derived.

$$V_D = \beta^{-1}$$
$$V_R = (\alpha^2 + \beta^2)^{-\frac{1}{2}}. \tag{6}$$

From these velocities and the density ρ, the elastic constants may be derived.

Define

$$R = V_D/V_R. \tag{7}$$

* This work was supported by the ONR under Contract N6-onr-266, Task Order VIII.
† Employed under research grant from Shell Oil Company.
[1] D. S. Hughes, W. L. Pondrom, and R. L. Mims, Phys. Rev. **75**, 1552 (1949).

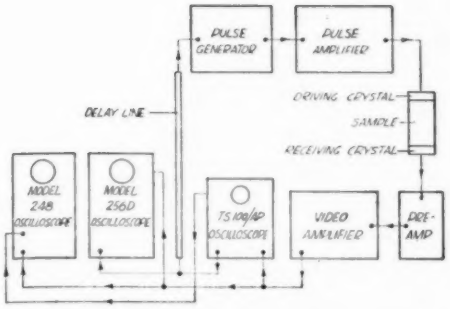

FIG. 1. Block diagram of electronic equipment.

Then, Poisson's ratio is

$$\sigma=(\tfrac{1}{2}R^2-1)/(R^2-1),$$

the rigidity modulus is

$$\mu=\rho V_R^2,$$

the Young's modulus is

$$E=2(1+\sigma)\mu,$$

and the bulk modulus is

$$K=E/3(1-2\sigma).$$

APPARATUS

Figure 1 shows a block diagram of the apparatus. This is essentially the same as described in reference 1. The TS-100/AP oscilloscope is used as standard for all time measurements. This instrument has a circular sweep of 80.86-kc frequency of 12.368 μsec. per revolution. A trigger circuit is provided that operates at submultiples of this frequency in the range 150 to 500 pulses per second. This trigger is accurately synchronized with the circular sweep. The instrument is also provided with an intensity gate so that any one selected revolution, after the trigger, appears on the screen. The trigger is sent through a delay line to synchronize the pulse generator. The pulse generator provides pulses with a rise time of about 0.3 μsec., 180-v amplitude and length from 0.5 to 60 μsec. A volume control was added so that the amplitude could be varied from 20 to 180 v. For materials with poor transmission these pulses are insufficient. A pulse amplifier consisting of a 6AG7 tube to invert and sharpen the pulse, an 807 as an amplifier, and a second 807 as a cathode follower for an output tube was constructed. This amplifier when driven by the pulse generator will provide pulses of about 800-v amplitude and rise time of 0.2 μsec., with an exponential decay of about 5 μsec. This sharp rise and slow decay both impressed on the driving crystal give a very simple pulse in the sample. The driving and receiving crystals are 3.5 Mc, x-cut, quartz crystals, 1.125 in. in diameter.

The signal from the receiving crystals is amplified by a preamplifier similar to that described by Jordan and Bell[2] but modified so that the gain is about 10 and the band width extends to some 5 Mc. This is followed by a video amplifier[3] which has a gain of about 800 and an upper frequency limit of about 8 Mc. The output of this amplifier is sent to the radial deflection electrode of the TS-100/AP and the vertical plates of the 248 and 256D oscilloscopes. The 25-μsec. R sweep of the 256D is triggered by the TS-100/AP generator. This scope is used for qualitative observations of wave form and approximate time checks. The 248 is triggered by the delayed intensity gate of the TS-100/AP so that any delayed 25- or 100-μsec. portion of the record may be displayed. This scope is fitted with a blue tube and camera for photography.

The sample may be used either in open air or placed in the pressure chamber, Fig. 2. The pressure chamber is constructed of Type 309 stainless steel, 4 in. in diameter by 12 in. high. The inner chamber is 2 in. in diameter by 7 in. high. The cylinder sets in a brass tank filled with SAE 30 oil and fitted with heating element, circulating stirrer, and cooling coils. The leads from the crystals are brought out through the head of the cylinder.

DATA

Figure 3 shows records of the waves received through polystyrene, Lucite, and polyethelene at room tem-

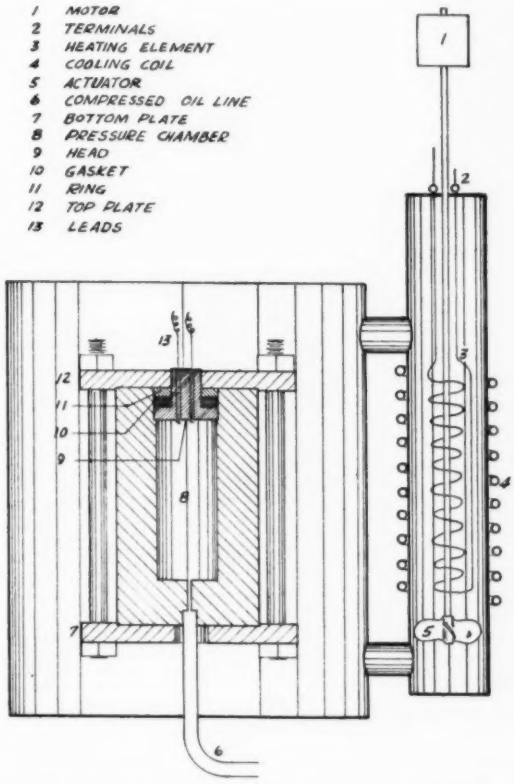

FIG. 2. Schematic diagram of pressure chamber.

[2] W. H. Jordan and P. R. Bell, Rev. Sci. Inst. **18**, 703 (1947).
[3] Research Laboratory Series, *Electronic Instruments* (McGraw-Hill Book Company, Inc., New York, 1948), Vol. 21, p. 602.

TABLE I. Material: polystyrene.

Pressure lb./in.²	L=5.090 cm V_D m/sec.	V_R m/sec.	ρ=1.046 g/cc $E\times10^{11}$ dynes/cm²	$\mu\times10^{11}$ dynes/cm²	D=2.626 cm $K\times10^{11}$ dynes/cm²	σ
			Temperature 31°C			
P_0	2295	1139	0.3627	0.1358	0.3699	0.336
2500	2336	1149	0.3703	0.1381	0.3880	0.340
5000	2375	1157	0.3777	0.1404	0.4056	0.342
7500	2413	1169	0.3874	0.1435	0.4233	0.345
10000	2448	1181	0.3952	0.1465	0.4348	0.348
12500	2481	1187	0.4012	0.1484	0.4520	0.351
15000	2515	1194	0.4063	0.1500	0.4598	0.353
			Temperature 51°C			
P_0	2256	1121	0.3505	0.1311	0.3572	0.337
2500	2304	1134	0.3604	0.1345	0.3749	0.341
5000	2344	1147	0.3709	0.1382	0.3976	0.344
7500	2380	1156	0.3773	0.1402	0.4079	0.347
10000	2418	1167	0.3816	0.1427	0.4256	0.349
12500	2449	1174	0.3923	0.1453	0.4382	0.352
15000	2488	1185	0.3989	0.1476	0.4551	0.354
			Temperature 72°C			
P_0	2238	1106	0.3422	0.1278	0.3532	0.339
2500	2275	1118	0.3506	0.1307	0.3675	0.342
5000	2325	1129	0.3586	0.1332	0.3837	0.346
7500	2359	1142	0.3675	0.1364	0.4024	0.348
10000	2399	1153	0.3743	0.1385	0.4151	0.351
12500	2420	1158	0.3815	0.1409	0.4300	0.353
15000	2456	1167	0.3876	0.1428	0.4457	0.355
			Temperature 82°C			
P_0	2205	1090	0.3328	0.1242	0.3390	0.339
2500	2250	1108	0.3444	0.1284	0.3588	0.341
5000	2296	1125	0.3560	0.1321	0.3768	0.347
7500	2339	1136	0.3631	0.1349	0.3945	0.350
10000	2384	1149	0.3723	0.1376	0.4136	0.352
12500	2407	1154	0.3779	0.1398	0.4237	0.354
15000	2434	1163	0.3832	0.1419	0.4352	0.355
			Temperature 92°C			
P_0	2177	1074	0.3237	0.1208	0.3345	0.340
2500	2231	1097	0.3376	0.1258	0.3557	0.344
5000	2277	1118	0.3504	0.1305	0.3703	0.348
7500	2323	1128	0.3578	0.1328	0.3893	0.350
10000	2364	1140	0.3669	0.1359	0.4059	0.351
12500	2398	1149	0.3751	0.1383	0.4217	0.355
15000	2436	1159	0.3809	0.1409	0.4305	0.356

TABLE II. Material: Lucite.

Pressure lb./in.²	L=7.976 cm V_D m/sec.	V_R m/sec.	ρ=1.171 g/cc $\mu\times10^{11}$ dynes/cm²	$E\times10^{11}$ dynes/cm²	D=2.540 cm $K\times10^{11}$ dynes/cm²	σ
			Temperature 33°C			
P_0	2621	1296	0.1968	0.5226	0.5422	0.338
2500	2666	1320	0.2038	0.5453	0.5602	0.338
5000	2702	1336	0.2102	0.5622	0.5768	0.338
7500	2744	1361	0.2175	0.5816	0.5944	0.337
10000	2782	1375	0.2222	0.5949	0.6135	0.338
12500	2820	1390	0.2274	0.6091	0.6324	0.340
15000	2853	1400	0.2310	0.6195	0.6505	0.341
			Temperature 48°C			
P_0	2538	—	—	—	—	—
2500	2585	—	—	—	—	—
5000	2632	1276	0.1912	0.5150	0.5580	0.347
7500	2681	1294	0.1972	0.5312	0.5798	0.347
10000	2719	1315	0.2029	0.5469	0.5978	0.348
12500	2763	1329	0.2075	0.5595	0.6141	0.348
15000	2800	1336	0.2116	0.5719	0.6405	0.351
			Temperature 71°C			
P_0	2468	—	—	—	—	—
2500	2496	—	—	—	—	—
5000	2547	—	—	—	—	—
7500	2620	1249	0.1840	0.4966	0.5505	0.350
10000	2652	1266	0.1889	0.5228	0.5866	0.352
12500	2705	1289	0.1951	0.5386	0.6091	0.353
15000	2738	1305	0.2008	0.5446	0.6308	0.356

perature and pressure. With increase in pressure the arrivals become slightly sharper and, with increase in temperature, somewhat less sharp; but the changes are minor except that with Lucite the t_{11} arrival disappears at low pressures and elevated temperatures. The trace length is about 100 μsec. The arrivals falling in this range are indicated.

The arrivals can be read on the TS-100/AP with a probable error of about ±0.03 μsec. This permits a determination of V_D and V_R with a probable error of about 0.2 percent. From these velocites and the density ρ, Poisson's ratio σ, the rigidity modulus μ, Young's modulus E, and the bulk modulus K, may be computed using Eq. (7). These values are slightly erroneous since the length, diameter, and density as measured at room temperature and pressure are used. However, this first computation gives an approximate value for K as a function of pressure at a given temperature. The length at any given temperature and room pressure may be computed from a knowledge of the coefficient of thermal expansion. Thus,

$$L_{T_0}=L_0[1+\alpha(T-T_0)], \tag{8}$$

where α is the coefficient of thermal expansion, T_0 is room temperature, T is temperature at which the run was made, L_0 is the length or diameter at room temperature and pressure, and L_{T_0} is the computed length at temperature T and room pressure. From the approximate value of K already computed, the length at any temperature and pressure is given by

$$L_{T_P}=L_{T_0}[1-(P/3\bar{K})], \tag{9}$$

where P is the pressure and $\bar{K}$ is average bulk modulus over the pressure range zero to P. Using Eqs. (8) and (9), the length and diameter were computed for all pressures and temperatures. The density ρ and the velocities V_D and V_R were recomputed as a function of pressure and temperature and then Eq. (8) used to re-

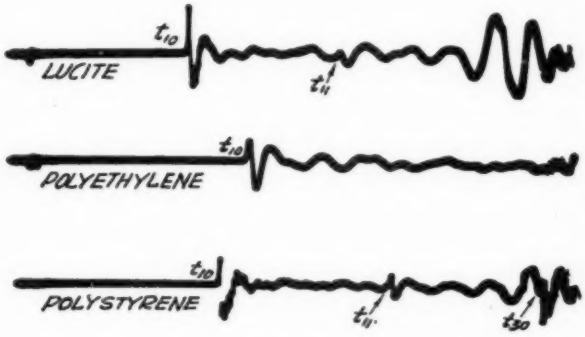

FIG. 3. Pulse transmission in plastics.

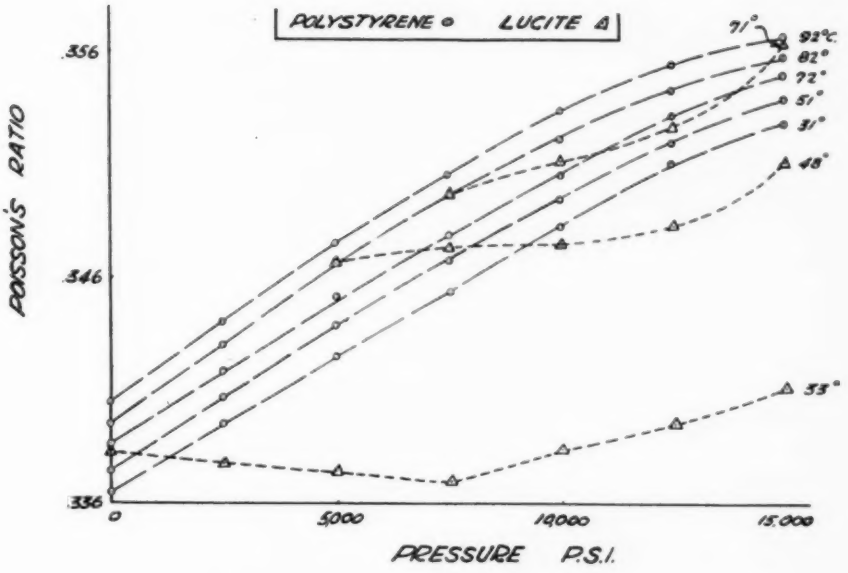

FIG. 4. Comparison of Poisson's ratio for Lucite and polystyrene.

compute values of σ, μ, E, and K. The largest correction is about two percent. It is assumed that for the purpose of this correction the differences between the adiabatic and isothermal moduli can be neglected.

Table I lists the velocities and elastic moduli for polystyrene over the range of pressures and temperatures. The variation in the rotational velocity with both temperature and pressure is very much less than that in the dilatational velocity. Similarly, the rigidity modulus increases by approximately six percent for an increase in pressure of 15,000 p.s.i. whereas the bulk modulus increases over the same range by about 30 percent. Corresponding to this rise in bulk modulus, Poisson's ratio, σ, increases uniformly.

Table II lists the velocities and elastic moduli for Lucite. Although the elastic moduli vary in a somewhat similar way to those of polystyrene there are fundamental differences. At room temperature Poisson's ratio decreases slightly as the pressure is raised reaching a minimum at 7500 p.s.i. and then increases slightly thereafter. At 48°C the first transformed wave cannot be read until a pressure of 5000 p.s.i. is reached and at 71°C a pressure of 7500 p.s.i. is required.

This almost certainly indicates a large change in viscous damping of the rotational waves. The first appearance of the transformed waves as the pressure increases is not sudden but gradual. The pressures listed above are those at which a clear definite arrival can be identified. At the elevated temperatures, Poisson's ratio rises very rapidly with pressure in contrast to its behavior at room temperature for Lucite and polystyrene over the experimental range as shown by Fig. 4.

TABLE III. Material: polyethylene.

Pressure lb./in.² / Temp.	L = 5.093 cm 31°C	45°C	ρ = 0.9069 g/cc V_D m/sec. 51°C	55°C	D = 2.535 cm 68°C	73°C
P_0	1979	1844	1807	1725	1678	1643
2500	2064	1918	1876	1837	1753	1716
5000	2129	1991	1939	1904	1829	1792
7500	2193	2061	2010	1973	1897	1864
10000	2257	2123	2079	2034	1961	1925
12500	2320	2179	2137	2095	2027	1986
15000	2374	2227	2191	2152	2082	2040

Table III lists the dilatational velocity for polyethylene. No trace of a transformed wave could be detected and the elastic constants could not be computed.

The Summation of Fourier Series by Operational Methods

LOUIS A. PIPES
Department of Engineering, University of California, Los Angeles, California
(Received September 26, 1949)

A method for the summation of certain types of Fourier series by the use of Laplace transforms is presented. The procedure enables one to easily obtain graphical representations of functions defined by Fourier series in many cases of practical importance.

I. INTRODUCTION

IN the mathematical analysis of problems in electric circuit theory, mechanical vibrations, heat conduction, and other branches of mathematical physics, one frequently arrives at solutions that are expressed in the form of infinite Fourier series. In many cases, it is more convenient to have the solutions of these problems expressed in closed form for purposes of calculation.

Oliver Heaviside[1] in the second volume of his *Electromagnetic Theory* used his rather informal "resistance operator" methods to interpret and sum Fourier series. As is well known, his mathematical processes were sometimes open to question. However, his methods frequently lead to useful results most simply, and he himself said in several instances, "I feel quite certain that this could be shown by conventional mathematics."

It is the purpose of this discussion to present a method for summing certain types of Fourier series of frequent occurrence in applied mathematics by the use of the modern Laplace method of the "Operational Calculus."

II. FUNDAMENTAL TRANSFORMATIONS

The method to be described is based upon the fact that certain hyperbolic functions can be expressed as an infinite series of exponential functions. If we use the notation,

$$A_k = e^{-kap} = \exp(-kap) \tag{2.1}$$

then the following expansions may be written

$$\tanh(ap) = 1 - 2A_2 + 2A_4 - 2A_6 + \ldots, \tag{2.2}$$

$$\coth(ap) = 1 + 2A_2 + 2A_4 + 2A_6 + \ldots, \tag{2.3}$$

$$\frac{1}{\sinh(ap)} = 2(A_1 + A_3 + A_5 + A_7 + \cdots) \tag{2.4}$$

$$\frac{1}{\cosh(ap)} = 2(A_1 - A_3 + A_5 - A_7 + \cdots), \tag{2.5}$$

a is a positive real number, and p is a number whose real part is positive.

By the use of a method due to Mittag-Leffler,[2] it is possible to obtain the following expansions,

$$\tanh(ap) = \frac{2}{ap}\left\{\frac{1}{1+(\pi/2ap)^2} + \frac{1}{1+(3\pi/2ap)^2} + \frac{1}{1+(5\pi/2ap)^2} + \cdots\right\} = \frac{2}{ap}\sum_{n=1}^{\infty}\frac{1}{1+\{[(2n-1)\pi]/2ap\}^2}, \tag{2.6}$$

$$\coth(ap) = \frac{1}{ap}\left\{1 + \frac{1}{1+(\pi/ap)^2} + \frac{2}{1+(2\pi/ap)^2} + \cdots\right\} = \frac{1}{ap}\left\{1 + \sum_{n=1}^{\infty}\frac{2}{1+(n\pi/ap)^2}\right\}, \tag{2.7}$$

$$\frac{1}{\cosh(ap)} = \frac{1}{a^2p^2}\left\{\frac{\pi}{1+(\pi/2ap)^2} - \frac{3\pi}{1+(3\pi/2ap)^2} + \cdots\right\} = \frac{1}{a^2p^2}\sum_{n=1}^{\infty}\frac{(-1)(2n-1)\pi}{1+(n\pi/2ap)^2}, \tag{2.8}$$

$$\frac{1}{\sinh(ap)} = \frac{1}{ap}\left\{1 - \frac{2}{1+(\pi/ap)^2} + \frac{2}{1+(2\pi/ap)^2} - \cdots\right\} = \frac{1}{ap}\left\{1 + \sum_{n=1}^{\infty}(-1)^n\frac{2}{1+(n\pi/ap)^2}\right\}. \tag{2.9}$$

It is possible to expand other combinations of hyperbolic functions in a similar manner, however, the above expansions are sufficient to illustrate the general principles of the method to be described.

III. THE LAPLACE TRANSFORMATION

Modern rigorous "operational calculus" is based upon the Fourier-Mellin integral equations.[3]

[1] O. Heaviside, *Electromagnetic Theory* (D. Van Nostrand Company, Inc., New York, 1925), Vol. II, pp. 107–119.
[2] E. T. Whittaker, and G. N. Watson, *Modern Analysis* (Cambridge University Press, London, 1927), pp. 134–136.
[3] L. A. Pipes, *Applied Mathematics for Engineers and Physicists* (McGraw-Hill Book Company, Inc., New York, 1946), Chapter XXI.

These equations state that, if

$$g(p)=p\int_0^\infty e^{-pt}h(t)dt, \tag{3.1}$$

then

$$h(t)=\frac{1}{2\pi j}\int_{c-j\infty}^{c+j\infty}\frac{g(p)e^{pt}dp}{p}, \tag{3.2}$$

where $j=(-1)^{\frac{1}{2}}$ and c is a real constant of such magnitude that the poles of the integrand lie entirely to the left of the path of integration. For brevity, the notation

$$g(p)=Lh(t) \quad \text{or} \quad h(t)=L^{-1}g(p) \tag{3.3}$$

is used to denote the above relations between the functions $g(p)$ and $h(t)$. The function $g(p)$ is said to be the Laplace transform of $h(t)$ and the function $h(t)$ is said to be the inverse Laplace transform of $g(p)$. Extensive tables of Laplace transforms have been compiled.[3] In this discussion we require the transforms of the sine and the cosine. These transforms are given by

$$L\sin(nwt)=\frac{nwp}{p^2+n^2w^2}=\frac{nw}{p}\cdot\frac{1}{1+(nw/p)^2} \tag{3.4}$$

and

$$L\cos(nwt)=\frac{p^2}{p^2+(nw)^2}=\frac{1}{1+(nw/p)^2}. \tag{3.5}$$

Another result of the theory of Laplace transform that is required is the following one.[3]

If

$$L^{-1}g(p)=h(t) \tag{3.6}$$

then

$$L^{-1}e^{-kp}g(p)=\begin{cases}0 & t<k\\ h(t-k) & t>k,\end{cases} \tag{3.7}$$

where k is a positive constant.

IV. SUMMATION OF FOURIER SERIES

The general method of summation will now be illustrated by applying it to several special cases.

Example I

In certain investigations of physical problems the following Fourier series is obtained:

$$F_1(t)=4[(\sin t/1)+(\sin 3t/3)+(\sin 5t/5)+\cdots]$$

$$=4\sum_{n=1}^{\infty}\frac{\sin(2n-1)t}{(2n-1)} \quad t>0. \tag{4.1}$$

The Laplace transform of the function $F(t)$ represented by the series (4.1) may be obtained by taking the Laplace transform of each term of the series using (3.4). In this manner one obtains

$$LF_1(t)=\frac{4}{p}\left[\frac{1}{1+(1/p)^2}+\frac{1}{1+(3/p)^2}+\frac{1}{1+(5/p)^2}+\cdots\right]. \tag{4.2}$$

We now note that, if in Eq. (2.6) we let

$$a=\pi/2, \tag{4.3}$$

then we can express the series term of (4.2) in the following form:

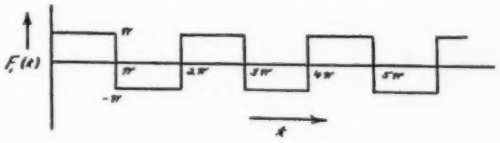

FIG. 1.

$$\left[\frac{1}{1+(1/p)^2}+\frac{1}{1+(3/p)^2}+\frac{1}{1+(5/p)^2}+\cdots\right]$$

$$=ap/2\tanh(ap). \tag{4.4}$$

Hence, comparing (4.2) and (4.4) we see that

$$LF_1(t)=2a\tanh(ap)=\tanh(\pi p/2). \tag{4.5}$$

We now use the expansion (2.2) and obtain

$$LF_1(t)=\pi[1-2e^{-\pi p}+2e^{-2\pi p}-2e^{-3\pi p}+\ldots]. \tag{4.6}$$

This is the Laplace transform of the Fourier series (4.1). To obtain the inverse Laplace transform of (4.6) and then obtain a representation of the series (4.1) we use the result (3.7). The inverse Laplace transform of the first term of (4.6) is a step function of height π formed at $t=0$. The inverse transform of the second term is a step function of height -2π formed at $t=\pi$. The inverse transform of the third term is a step function of height $+2\pi$ formed at $t=2$ and so on. The sum of all these step functions is illustrated in Fig. 1.

Example II

As a second example let it be required to interpret the following Fourier series that occurs in certain electrical and heat conduction problems.

$$F_2(t)=\frac{2}{\pi}\sum_{n=1}^{\infty}\frac{1}{n}\sin\left(\frac{n\pi t}{s}\right). \tag{4.7}$$

By the use of (3.4), the Laplace transform of (4.7) is obtained and is given by:

$$LF_2(t)=\frac{2}{\pi}\sum_{n=1}^{\infty}\frac{n\pi}{nsp}\frac{1}{1+(n\pi/sp)^2}$$

$$=\frac{1}{sp}\sum_{n=1}^{\infty}\frac{2}{1+(n\pi/sp)^2}. \tag{4.8}$$

If we now compare (4.8) with (2.7) it is seen that we have,

$$LF_2(t)=\coth(sp)-1/sp. \tag{4.9}$$

By the use of (2.3) this may be written in the following form,

$$LF_2(t)=(1-1/sp+2e^{-2sp}+2e^{-4sp}+2e^{-6sp}+\ldots). \tag{4.10}$$

To obtain the inverse transform of F_2 we note that the inverse transform of the first term is a unit step function, the inverse transform of the term $-1/sp$ is $-t/s$, the inverse transform of $+2e^{-2sp}$ is a step function of height that begins at $t=2s$, etc. The sum of the various transforms gives the function $F_2(t)$. The result is given graphically in Fig. 2.
This figure is a graphical representation of the Fourier series $F_2(t)$.

Example III

As another example, let it be required to obtain the graph of the following Fourier series:

$$F_3(t)=(\sin t-\tfrac{1}{2}\sin 2t+\tfrac{1}{3}\sin 3t-\cdots)$$

$$=-\sum_{n=1}^{\infty}(-1)^n\frac{1}{n}\sin(nt). \tag{4.11}$$

In this case we transform (4.11) by the use of Eq. (3.4) and note the similarity to Eq. (2.8). Then the expansion (2.4) gives the result

$$LF_3(t)=(1/p-2\pi e^{-\pi p}-2\pi e^{-3\pi p}-2\pi e^{-5\pi p}+\ldots). \tag{4.12}$$

Now the inverse transform of $1/p$ is t, the inverse transform of $-2\pi e^{-\pi p}$ is a step function of height -2π that begins at $t=\pi$, etc. The sum of the various inverse transforms is $F_3(t)$. This function is given graphically in Fig. 3.

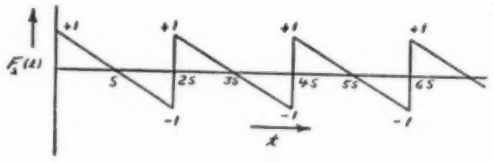

FIG. 2.

Example IV

An interesting series which arises in the analysis of the propagation of charge along a cable will now be considered. This series represents a row of impulses and the function it represents is important in the analysis of the disturbances created when lightning hits a transmission line. The series to be considered is the following one:

$$F_4(x)=\frac{2}{s}\sum_{n=1}^{n=\infty}\sin\left(\frac{n\pi x}{s}\right)\sin\left(\frac{n\pi b}{s}\right). \tag{4.13}$$

To study this series more easily, the product of sines may be transformed into two cosines and written in the following form:

$$F_4(x)=\frac{1}{s}\sum_{n=1}^{n=\infty}\left[\cos\frac{n\pi(x-b)}{s}-\cos\frac{n\pi(x+b)}{s}\right]. \tag{4.14}$$

Let us first consider the first series of (4.14) and let,

$$t=x-b. \tag{4.15}$$

This series may be written in the form:

$$\phi(t)=\frac{1}{s}\sum_{n=1}^{\infty}\cos\left(\frac{n\pi st}{s}\right). \tag{4.16}$$

By (3.5) it can be transformed to:

$$L\phi(t)=\frac{1}{s}\sum_{n=1}^{\infty}\cos\frac{1}{1+(n/sp)}. \tag{4.17}$$

By the use of Eqs. (2.7) and (2.3) this may be written in the form,

$$L\phi(t)=p/s(1+2e^{-2sp}+2e^{-4sp}+\ldots). \tag{4.18}$$

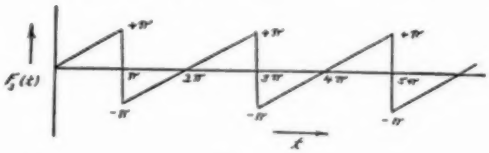

FIG. 3.

To obtain the inverse transform of this function we note that,[3]

$$L^{-1}p=\delta(t). \tag{4.19}$$

The function, $\delta(t)$, is an impulse function known in the literature as the Dirac function. It has the following properties:

$$\delta(t)=\begin{cases}0 & t\neq 0\\ \infty & t=0\end{cases} \tag{4.20}$$

and

$$\int_{-\infty}^{+\infty}\delta(t)dt=1. \tag{4.21}$$

As a consequence of (3.7), the inverse transform of (4.18) is

$$\phi(t)=1/s[\delta(t)+2\delta(t-2s)+2\delta(t-4s)+\ldots]. \tag{4.22}$$

We note that the first term is an impulse at $t=x-b=0$ or at $x=b$. The second term is an impulse located at $t=2s$ or $x=2s+b$, and so forth. The second series of (4.14) may be transformed in a similar manner if the substitution $t=x+b$ is made and it can be shown that this series represents a row of negative impulses at $x=-b$, $x=2s-b$, etc. A graphical representation of the function $F_4(x)$ defined by (4.13) is given in Fig. 4.

The function $F_4(x)$ is zero for all values of x except at the places where it has the values of positive and negative pulses of the Dirac type.

V. GENERAL CONSIDERATIONS

The general Fourier series may be written in the form:

$$F(t)=A_0+\sum_{n=1}^{\infty} A_n \cos(nwt)+\sum_{n=1}^{\infty} B_n \sin(nwt). \quad (5.1)$$

The coefficients A_n and B_n are known functions of n. By the use of Eqs. (3.4) and (3.5), it is possible to transform (5.1) into

$$LF(t)=A_0+\sum_{n=1}^{\infty} \frac{An}{1+(nw/p)^2}+\frac{w}{p}\sum_{n=1}^{\infty} \frac{nBn}{1+(nw/p)^2}. \quad (5.2)$$

The success of the method of interpretation described in this discussion depends upon the possibility of effecting the summations of (5.2) by the use of the Eqs. (2.6)–(2.9) or by formulas derivable from them.

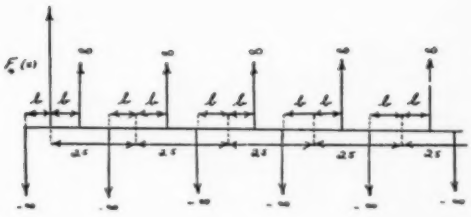

FIG. 4.

The interpretation of the Fourier series can then be carried out by the use of Eqs. (2.2)–(2.5) or combinations of these expansions.

In many cases, however, the summation of the fractions of (5.2) may present insurmountable difficulties and in such cases, this method of interpretation is not applicable.

Effect of Change of Scale on Sintering Phenomena

CONYERS HERRING
Bell Telephone Laboratories, Murray Hill, New Jersey
(Received November 16, 1949)

It is shown that when certain plausible assumptions are fulfilled simple scaling laws govern the times required to produce, by sintering at a given temperature, geometrically similar changes in two or more systems of solid particles which are identical geometrically except for a difference of scale. It is suggested that experimental studies of the effect of such a change of scale may prove valuable in identifying the predominant mechanism responsible for sintering under any particular set of conditions, and may also help to decide certain fundamental questions in fields such as creep and crystal growth.

FOR the purposes of this paper "sintering" will be understood to mean any change in shape which a small particle or a cluster of particles of uniform composition undergoes when held at high temperature. In the absence of externally applied stresses, such changes are believed to be motivated by surface tension, since the surface free energy decreases as the particles grow together and assume a more compact shape. The transport of matter which is involved can take place by any of four mechanisms: viscous or plastic flow, evaporation and condensation, volume diffusion, and surface migration. With the aid of certain plausible assumptions the rates of transport by each of these mechanisms can be computed in terms of the geometrical parameters and certain constants of the material such as surface tensions, diffusion coefficients, etc.[1] Foremost among the assumptions involved is the assumption that the building up or tearing down of the surface can occur quite readily in response to conditions in the immediately adjoining solid or vapor phase. This assumption is closely related to the controversial problem of the mechanism of crystal growth, and it would be incorrect, at least in cases involving plane crystal facets, if growth normal to such facets required a "two-dimensional nucleation" process.[1,2] It is the purpose of this note to point out that useful information can probably be obtained, both on the fundamental question of the way in which crystals grow and on the more specific question of the relative importance of the four transport mechanisms in specific cases, by a comparison of sintering rates for particles or clusters of different sizes but geometrically similar shapes.

THE SCALING LAWS

We shall use the term "cluster" to refer to any particle or to a number of particles which have started to grow together. Consider two partially sintered clusters which are geometrically similar, the linear dimensions of number two being λ times those of number one. For example, if each cluster consists of spherical

[1] C. Herring, paper presented at the Symposium on the Physics of Powder Metallurgy organized by Sylvania Electric Products, Inc., Bayside, Long Island, New York (August 24–26, 1949). Plans have been made to publish the papers of the Symposium in book form.

[2] The theory of growth by two-dimensional nucleation is summarized in the book of M. Volmer, *Kinetik der Phasenbildung* (Verlag von Theodor Steinkopff, Dresden and Leipzig, 1939; Edwards Brothers, Inc., Ann Arbor, 1945). An alternative theory of crystal growth has been proposed by F. C. Frank, to appear in *Trans. Faraday Soc.* (paper presented at the Discussion on Crystal Growth sponsored by the Faraday Society and held at Bristol, England, April, 1949).

grains of radius R, sintered until the radius of the area of contact of adjacent grains is a, similarity will require $R_2=\lambda R_1$, $a_2=\lambda a_1$. The question to be considered is, how is the time Δt_1 required to produce a given change in shape of cluster number one in the sintering process related to the time Δt_2 required, at the same temperature, to produce a geometrically similar change in the second cluster? This relation turns out to be quite simple in the following four cases, if the same one of the basic mechanisms predominates for both clusters and if the above-mentioned assumption of facile growth and recession of the surface is valid.

Viscous Flow of an Amorphous Material

It is well known that the surface tension γ of a spherical drop of liquid of radius R produces a pressure p in the interior of the drop, given by

$$2\pi R\gamma=\pi R^2 p$$

or

$$p=2\gamma/R. \tag{1}$$

This equation can be shown to give, in more general cases, the normal stress p_{zz} immediately under a curved surface of any shape, provided R^{-1} is interpreted as the mean of the principal curvatures of the surface, these being counted positive if convex, negative if concave. It can be applied to "amorphous solids" provided the temperature is high enough so that the surface layers of atoms are reasonably free to rearrange themselves; however, the simple form (1) is not valid for crystals.[1]

If the surface of a cluster is inhomogeneously curved, the normal stresses given by (1) will vary over the surface, and to compensate this there must be shearing stresses in the interior. For the two sizes of cluster mentioned, the stress tensors at corresponding points, being determined by (1) and the linear conditions of equilibrium, must satisfy

$$p_{ij}^{(2)}(\lambda\mathbf{r})=p_{ij}^{(1)}(\mathbf{r})/\lambda. \tag{2}$$

Thus assuming viscous behavior the strain rates ds_{ij}/dt at corresponding points will satisfy

$$(ds_{ij}/dt)_2=(1/\lambda)(ds_{ij}/dt)_1$$

and so the times required for a given change of shape to take place will be related by

$$\Delta t_2=\lambda\Delta t_1. \tag{3}$$

Evaporation and Condensation

It will be assumed that the mean free path of an atom or molecule in the vapor is long compared with the dimensions of the particles being sintered, and that only one kind of atom or molecule is involved. For a liquid or an amorphous solid it is well known that the equilibrium vapor pressure over a spherically curved surface of radius R is greater than that over a flat surface by the ratio[3]

$$p_R/p_\infty=\exp(2\Omega_0\gamma/kTR), \tag{4}$$

where Ω_0 is the atomic or molecular volume and γ the surface tension. Application of a similar thermodynamic argument to crystals yields a relation which, though more complicated, agrees with (4) in having an exponent which varies inversely with the first power of the linear scale.[1] If the exponent is small, as is likely to be the case if R is of the order of 10^{-5} cm or greater, (4) can be written

$$p_R=p_\infty(1+2\Omega_0\gamma/kTR). \tag{5}$$

Now consider any two elements of surface dS_a and dS_b on nearby portions of the cluster being sintered. The evaporation rates from these two will be in the ratio of their areas and of their equilibrium vapor pressures.* If these vapor pressures are different, as they will be if the radii of curvature R_a and R_b are different, the amount of material which in any given time is evaporated from a, passes directly to b, and condenses there, will be different from the amount passing in the reverse direction. Ignoring factors of proportionality which are independent of the linear scale factor λ, one may write

$$\text{rate } (a\to b)-\text{rate } (b\to a)\propto dS_a dS_b(p_a-p_b)/r_{ab}^2$$

where r_{ab} is the distance of dS_a from dS_b. Thus the rates for the two geometrically similar aggregates we are considering bear the ratio

$$\frac{\text{rate } (a\to b)_2-\text{rate } (b\to a)_2}{\text{rate } (a\to b)_1-\text{rate } (b\to a)_1}=\lambda^2\cdot\lambda^2\cdot\lambda^{-1}\cdot\lambda^{-2}=\lambda. \tag{6}$$

A similar equation obviously holds for material transported from a to b by any type of trajectory involving reflection from some intermediate surface. Since the total amount of material which must be transported in these ways to produce geometrically similar changes in cluster 2 is λ^3 times that for cluster 1, the intervals of time required will be related by

$$\Delta t_2=\Delta t_1\lambda^3/\lambda=\lambda^2\Delta t_1. \tag{7}$$

Volume Diffusion

It can be shown that in a crystal the diffusive flux of matter, i.e., of interstitial atoms or lattice vacancies, is proportional to the local gradient of the chemical potential of the diffusing substance. (Use of the chemical potential takes account of the effects of both pressure gradients and concentration gradients.) Now the value of this chemical potential at any place on the boundary

[3] See, for example, E. A. Guggenheim, *Modern Thermodynamics by The Methods of Willard Gibbs* (Methuen and Company, Ltd., London, 1933), p. 172.

* This statement may not be true if the "sticking coefficients" α_a and α_b for the two surface elements are different. However, since both the probability of evaporation and the probability of condensation contain the sticking coefficient as a factor, (6) will be correct in any case.

of the crystal must coincide with the chemical potential of the vapor which is in equilibrium with that portion of the crystal surface. For a one-component substance we have from (4), or from its extension to the crystalline case[1]

$$\text{chemical potential at surface} = \text{const.} + kT \ln(p_R/p_\infty) = \text{const.} + B/(\text{linear dimension}), \quad (7)$$

where B is a quantity which is the same at corresponding points of the surfaces of the geometrically similar clusters 1 and 2. Thus, when a quasi-steady distribution of diffusion currents has been set up we have at corresponding points of the interiors of the two clusters

$$(\text{chem. pot.})_2 = (\text{chem. pot.})_1/\lambda$$

and

$$(\text{flux})_2 = (\text{flux})_1/\lambda. \quad (8)$$

Since corresponding areas in the two clusters bear the ratio λ^2 and the amount of material which must be transported goes as λ^3, the times required to produce corresponding amounts of sintering satisfy

$$\Delta t_2 = (\lambda^3 \cdot \lambda^2/\lambda^2)\Delta t_1 = \lambda^3 \Delta t_1. \quad (9)$$

Surface Migration

The scaling law for sintering due to surface migration can be derived in a similar way, by starting from the assumption that the rate of migration over a given type of surface is proportional to the gradient of the chemical potential in the plane of the surface. Thus (8) will hold for the surface flux as well as for the volume flux. In the present case, however, the total rate of transport is the product of the flux not by an area but by a length in the plane of the surface and normal to the flux direction. Thus, instead of (9) we have

$$\Delta t_2 = (\lambda^3 \cdot \lambda^2/\lambda)\Delta t_1 = \lambda^4 \Delta t_1. \quad (10)$$

DISCUSSION

In attempting to draw conclusions from experimental comparisons of sintering times for similar systems of different sizes, several obvious precautions must be observed. One must be sure that the factors determining the degree of contamination of the surface are kept the same for all the cases being compared. If possible, the orientations of the various crystals making up each cluster should be the same for the clusters of different sizes which are being compared: surface tension, surface mobilities, evaporation rates, etc., can be quite different for differently oriented surfaces, the more so because preferential adsorption can cause different surfaces to acquire widely different degrees of contamination. If there is an appreciable delay in the formation of the initial bond between two particles, time should be measured from the moment when this bond is first established.

When experimental data fail to follow one of the scaling laws one must decide whether this is merely because more than one of the above mechanisms is operative over the range of sizes covered by the experiment or whether mechanisms basically different from those assumed above are involved. In the former case there will usually be certain accessible ranges of temperatures and particle sizes over which only one of the four mechanisms contributes appreciably to the changes involved, and if data from these ranges are available, the transition ranges can easily be identified as such. If basically different mechanisms are involved, on the other hand, the variation of sintering time with linear scale may be of a sort quite inconsistent with the hypothesis of a gradual transition from one of the above power laws to another. For example, if a change were produced by slip or creep which set in abruptly at a given critical stress, the sintering time might vary discontinuously with linear scale. An almost discontinuous variation might also result if growth of crystal facets by two-dimensional nucleation were involved.

If a given type of sintering experiment is found to obey one of the scaling laws, the predominant mechanism of transport can be inferred. This inference can probably be drawn with less ambiguity than in the method used by Kuczynski,[4] who inferred the mechanism of sintering by comparing the observed rate of growth of the neck between a particle and a flat block with rates computed theoretically according to each of the above mechanisms. According to Kuczynski's calculations, the radius of the neck varies as the nth root of the sintering time, where $n=2$ for viscous flow, 3 for evaporation and condensation, 5 for volume diffusion, and 7 for surface migration. Although these exponents cannot be far from the truth if the assumptions used in the present paper are correct, uncertainties in geometrical details of the calculations could perhaps affect the values of n by as much as 0.5. The exponents in the present scaling laws, on the other hand, are subject to no such uncertainty.

[4] G. C. Kuczynski, J. Met. 1, 169 (1949).

A Resonant Bar Method for Determining the Elastic Properties of Thin Lamina

A. W. Nolle and P. J. Westervelt
Acoustics Laboratory, Massachusetts Institute of Technology, Cambridge, Massachusetts
(Received September 9, 1949)

A resonant bar method for obtaining the dynamic elastic properties of a thin cement layer is discussed. Formulas are deduced for the calculation of Young's modulus from the measured resonant frequency and band width of two similar steel bars, cemented end-to-end. The accuracy of the method is discussed.

I. INTRODUCTION

THE method to be described has proved useful in obtaining the effective elastic properties of a thin layer of cement. In this application two cylindrical steel bars (see Fig. 1) of equal length $l/2$ are cemented end-to-end forming a single bar. By suitable means the frequency and Q of the fundamental resonance of the cemented bar are measured and compared with similar quantities measured for a continuous bar of length l. From this comparison it is possible to obtain an effective complex Young's modulus for the thin cement film.

For a discussion of the concept of a complex modulus the reader is referred to a recent paper by Nolle.[1] Briefly, the complex modulus is defined as the stress-to-strain ratio for sinusoidal displacements. Provided the displacements are proportional to $e^{-i\omega t}$, the complex modulus E can be expressed as $E=E_1-iE_2$ where E_1 is the ordinary Young's elastic modulus, and $E_2=\omega\gamma$ (γ=normal viscosity coefficient).

The moduli are termed "effective" for two reasons. In the first place, E_1 and γ are presumed to vary with frequency, whereas for a true modulus, E_1 and γ would be independent of frequency. Secondly, in laterally constrained lamina, the measured modulus might lie between that of a Young's modulus and a bulk modulus.

Approximate formulae will first be derived for E_1 and E_2 under the assumption that the resonant frequency of the cemented bar does not differ much from the value for the continuous bar.

II. APPROXIMATE FORMULA FOR E_1

The fundamental resonant frequency ν_0 of a bar of length l is given by

$$l\nu_0=c/2, \tag{1}$$

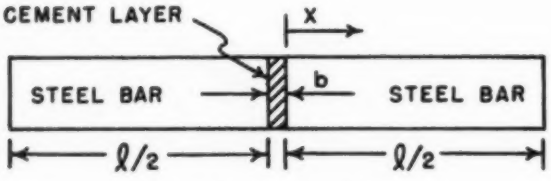

FIG. 1. Sketch of cemented bars.

where the velocity of sound $c=(E/\rho)^{\frac{1}{2}}$ (E=Young's modulus; ρ=density for the bar).

Increasing the length of the bar by δl will result in a decrease $\delta\nu$ of the resonant frequency, given by:

$$\delta\nu/\nu_0=\delta l/l, \tag{2}$$

as can be verified by differentiating Eq. (1). Next, suppose the element $\delta l \ll l$ lies in the middle of the rod. The effect of δl can be visualized as that of a spring, coupling the two halves of the rod together. If the element had a Young's modulus E_1 instead of the modulus E of the bar, its length would have to be $(E_1/E)\delta l$ in order to give the same fractional change in frequency; thus the fractional change due to an element b with modulus E_1 is:

$$\delta\nu/\nu_0=(E/E_1)(b/l). \tag{3}$$

From Eqs. (1), (3) and the expression $E=\rho c^2$, we obtain an expression for the real part of the complex Young's modulus, E_1, of a lamina of thickness b:

$$E_1=4\rho l b\nu_0^2(\nu_0/\delta\nu). \tag{4}$$

It can be shown that Eq. (4) is valid to within 10 percent provided the band width $\Delta\nu$ of the resonance of the cemented bar is small enough to satisfy $(\Delta\nu)^2 \ll(\delta\nu)^2$, and provided $(\delta\nu/\nu_0)<0.1$. These restrictions are met in many cases. Formulas that hold when the first restriction does not apply will be given in the Appendix.

In the event that $\delta\nu/\nu_0$ is not small with respect to unity but that $(\Delta\nu)^2\ll(\delta\nu)^2$ and $b\ll l$, it can be shown that a more precise value of E_1 is obtained by multiplying the value given by Eq. (4) by the function $F(\delta\nu/\nu_0)$:

$$F\left(\frac{\delta\nu}{\nu_0}\right)=\frac{\pi}{2}\left(1-\frac{\delta\nu}{\nu_0}\right)\left(\frac{\delta\nu}{\nu_0}\right)\cot\frac{\pi\delta\nu}{\nu_0}. \tag{5}$$

From Eq. (5), $F(0.1)=0.90$. Hence, when $\delta\nu/\nu_0=0.1$, the value of E_1 obtained from Eq. (4) will be too high by 10 percent.

Another approximate form results from expanding the cotangent in Eq. (5) and retaining the first term in the expansion. This leads to the following expression which is accurate to within 10 percent, provided $\delta\nu/\nu_0<0.3$:

$$E_1=4\rho l b\nu_0^2\left(\frac{\nu_0}{\delta\nu}-1\right), \tag{6}$$

[1] A. W. Nolle, "Method for measuring dynamic mechanical properties of rubber-like materials," J. App. Phys. **19**, 753 (1948).

which may be written:

$$E_1 = 4\rho l b \nu_0^2 (\nu/\delta\nu), \tag{7}$$

where $\nu = \nu_0 - \delta\nu$, the resonant frequency of the cemented bars.

III. APPROXIMATE FORMULA FOR E_2

We shall look for a relation between E_2 (which is a measure of the damping of the lamina), the resonant frequency of the cemented bar ν and the band width $\Delta\nu$ of the resonance peak. The quantity E_2 can be expressed in terms of the mechanical resistance, R, of the lamina which is supposed to have a thickness $b \ll l$ and the same area S as that of the bar:

$$E_2 = (2\pi\nu R b)/S. \tag{8}$$

Provided that the Q of the fundamental mode is at all times large compared with unity, the band width $\Delta\nu$ is given by:[2]

$$\Delta\nu = \frac{\nu}{2\pi} \times \frac{\text{Decrease of Energy of Free Vibration per Cycle}}{\text{Total Energy of Vibration}}. \tag{9}$$

The total energy of vibration in the bar is the maximum kinetic energy, or:

$$\text{total energy} = (MV_0^2)/2, \tag{10}$$

where M is the equivalent mass of the bar, vibrating in its first mode

$$M = (\rho l S)/2, \tag{11}$$

and V_0 is the amplitude of the velocity configuration $V(x)$ at a point $x < l/2$ along the bar, measured from the plane joining the bar and the sample:

$$V(x) = V_0 \cos\left[\left(1 - \frac{\delta\nu}{\nu_0}\right)\left(\frac{\pi x}{l} - \frac{\pi}{2}\right)\right].$$

The energy loss per cycle in the lamina is given by:

$$\text{loss per cycle} = \frac{1}{2}\frac{R 2V(x-l/2)^2}{\nu},$$

or, for $\delta\nu/\nu_0 \ll 1$:

$$\text{loss per cycle} = \pi^2 V_0^2 \frac{R}{2\nu_0}\left(\frac{\delta\nu}{\nu_0}\right)^2. \tag{12}$$

Introducing Eqs. (10) and (12) into (9) we obtain:

$$\Delta\nu = \frac{\pi}{2}\frac{R}{M}\left(\frac{\delta\nu}{\nu_0}\right)^2,$$

then, solving for R and using Eq. (11)

$$R = \frac{\rho l S}{\pi}\left(\frac{\nu_0}{\delta\nu}\right)^2 \Delta\nu.$$

Introducing the above expression into Eq. (8):

$$E_2 = 2\rho l b \nu_0 (\nu_0/\delta\nu)^2 \Delta\nu,$$

or in terms of E_1, given in Eq. (4):

$$E_2 = (E_1/2)\Delta\nu/\delta\nu. \tag{13}$$

Any loss inherent in the continuous unloaded bar is effectively added to the loss introduced by the sample. Therefore, if the band width of the unloaded rod is not negligible in comparison to the band width observed with the sample in place, the quantity $\Delta\nu$ to be used in Eq. (12) should be obtained from the relation:

$$\Delta\nu = \Delta\nu_{\text{loaded}} - \Delta\nu_{\text{unloaded}}. \tag{14}$$

The term "band width" as used above denotes the difference between the two frequencies for which the displacement amplitude of the system is $\frac{1}{2}\sqrt{2}$ times the value found at resonance, under the condition that the system is excited by a sinusoidal force whose amplitude is independent of frequency.

IV. APPLICATIONS

The method described here may be employed successfully in conjunction with any of the known techniques for measuring the fundamental resonant frequency and the band width of a rod with free ends. A technique that is suitable when the rod is made of magnetostrictive metal has been described in a previous publication.[1] The completely electrostatic technique of Bordoni[3] is also well suited to this application. This method is being used by a group at M.I.T. for the study of deterioration of adhesives.*

In general, this method is suitable for investigating the elastic properties of thin samples whose mechanical impedance per unit area is large compared to the specific acoustic impedance, ρc, of the rod material, provided of course that the samples can be bonded suitably to the rod metal. For the study of samples whose mechanical impedance per unit area is small compared to the specific acoustic impedance of the rod material, it is necessary to place the sample at a position of low impedance (that is, at an antinode of displacement) with respect to the wave pattern in the rod. This case has been discussed in connection with the magnetostriction technique to which reference has already been made.[1]

[2] Slater and Frank, *Mechanics* (McGraw-Hill Book Company, Inc., New York, 1947), p. 32.

[3] P. G. Bordoni, "Metodo Elettroacustico per Ricerche Sperimentali sulla Elasticita," Nuovo Cimento **4**, 177 (1947).

* Ordnance Dept. Project No. TB4-601, Professor A. G. H. Dietz, Supervisor.

APPENDIX

More Rigorous Treatment of the Vibration of a Split Rod

It is assumed that the Q of the vibrating system is at least of the order of 10 to 100. The motion, then, is closely symmetrical about a plane normal to the rod and through the center of the viscoelastic sample. This plane of symmetry contains a displacement node which may be replaced by a termination of infinite impedance. The problem resolves into the treatment of a rod whose length is that of one-half of the actual rod, terminated by a rigidly backed viscoelastic sample whose thickness is half that of the actual sample. The analysis is easily performed by the hyperbolic tangent method of Morse[4] and is given below in the terminology established by him.

In the plane joining the sample and the metal rod ($x=0$), the specific acoustic impedance $2(E_2+iE_1)/b\omega$ of the half-thickness viscoelastic sample must equal the transmission-line impedance at this location as given by the function

$$z=\rho c \tanh\pi(\alpha-i\beta_0). \tag{15}$$

Here β_0 represents the value at $x=0$ of the phase parameter β which obeys the relation

$$\beta_{l/2}=\beta_0+l/\lambda. \tag{16}$$

Evidently the dynamic modulus, E_1-iE_2, can be calculated from a knowledge of the quantities α and β_0.

It will be shown that these quantities may be evaluated by measurement of the resonant frequency and the band width of the system.

Let $K\omega$ represent the amplitude of an alternating pressure whose magnitude is proportional to frequency, applied to the free end of the rod at $x=l/2$. The displacement amplitude at $x=l/2$ is $K/z_{l/2}$. Expansion of the hyperbolic tangent Eq. (15) shows that the square of this displacement amplitude is proportional to

$$\frac{A\cos^2\pi\beta_{l/2}+B\sin^2\pi\beta_{l/2}}{B\cos^2\pi\beta_{l/2}+A\sin^2\pi\beta_{l/2}} \tag{17}$$

where $A=\cosh^2\pi\alpha$, $B=\sinh^2\pi\alpha$. It may be verified by differentiation that this squared amplitude is maximum for $\beta_{l/2}=0$. Thus the parameter β_0 is given immediately as

$$\beta_0=-\nu l/c=-\nu/2\nu_0=-\tfrac{1}{2}\left(1+\frac{\delta\nu}{\nu_0}\right), \tag{18}$$

where ν and ν_0 are the frequencies of maximum amplitude for the compound rod and for an unmodified rod of length l respectively.

At the amplitude maximum, the quantity (17) has the value A/B, but this value must reduce to $A/2B$ at either of the two frequencies which define the band width. By setting the expression (17) equal to $A/2B$, we obtain

$$\tan\beta'_{l/2}=\pm(AB/(A^2-2B^2))^{\frac{1}{2}}, \tag{19}$$

where $\tan\beta'_{l/2}$, which equals $\pm l\Delta\nu/2c$, denotes the values of $\beta_{l/2}$ obtaining at the limits of the "pass band." This expression results in the following transcendental equation for α:

$$\tanh^2\pi\alpha/(1-2\tanh^2\pi\alpha)=\tan^2(\pi\Delta\nu/4\nu_0). \tag{20}$$

By means of Eqs. (15), (18), and (20) it is possible to compute the specific acoustic impedance or the complex modulus of the cement layer from measurements of the resonance frequency and the band width of the compound rod.

Since the above equations are unwieldy for purposes of calculation, it is convenient to introduce approximations. Suppose that the fractional frequency change $\delta\nu/\nu_0$ and the fractional band width $\Delta\nu/\nu_0$ are each small compared to unity. In this case the equations reduce to

$$E_1=4\rho lb\nu_0^2(1+\delta\nu/\nu_0)(\delta\nu/\nu_0)/[(\delta\nu/\nu_0)^2+(\Delta\nu/2\nu_0)^2], \tag{21}$$

$$E_2/E_1=\tfrac{1}{2}(\Delta\nu/\delta\nu). \tag{22}$$

These equations are valid for any ratio E_2/E_1. Where this ratio is small compared to unity, as is the case for many cements, Eq. (21) may be replaced by Eq. (7), obtained in the simpler derivation.

The assumption that the driving-force amplitude is proportional to frequency, made in the derivation leading to Eqs. (21) and (22), is introduced solely to achieve a considerable simplification in the derivation and in the results. This condition can be achieved easily in the design of the apparatus, but the distinction involved is unimportant when the resonance is sharp, as will be the case for hard cements. Results identical to Eqs. (21) and (22) are also obtained if it is assumed that the driving-force amplitude is independent of frequency and that the detection device responds to velocity rather than to amplitude.

[4] P. M. Morse, *Vibration and Sound* (McGraw-Hill Book Company, Inc., New York, 1948), second edition.

The Electronic Isograph for Roots of Polynomials

BYRON O. MARSHALL, JR.
Air Force Cambridge Research Laboratories, Cambridge, Massachusetts
(Received August 10, 1949)

An electronic apparatus which assists in the finding of the roots of polynomials is described. The device accepts the coefficients of polynomials of degree 10 or less and yields the absolute magnitude of the roots to a precision of 0.01 relative to the largest coefficient in the polynomial and an angular accuracy of 0.3 degree on the angle of the root.

The method used is the electronic analog of the expression

$$\omega=\Sigma a_n z^n$$
$$=\Sigma a_n r^n \cos n\theta+j\Sigma a_n r^n \sin n\theta.$$

$\sin n\theta$ and $\cos n\theta$ are generated by a motor-driven commutator. The radius r is controlled manually. Hence a plot of ω is placed on the oscilloscope for a fixed r as a function of θ. To find the root r is manipulated until ω crosses the origin in the ω-plane. The value of θ is found by inserting a pip on the intensity of the oscilloscope under a variable phase control. When this pip is moved to the origin of the ω-plane the phase meter indicates the angle of the root in the z plane.

I. INTRODUCTION

THE great interest in the location of the roots of polynomials is partly evidenced by the great number of methods that have been devised for the process. The most common "pencil and paper" methods include the binomial formula for quadratics, the rather awkward formulas for cubics and quartics, Graffe's root squaring method, the various methods of successive approximation (Newton's Birge-Vieta, etc.[1]) and several more complicated procedures. These methods, however useful for low degree polynomials, are laborious and time consuming for greater than fourth or fifth degree. A convenient process for finding the roots of polynomials of perhaps tenth degree or so would have several fold applications: (1) for the solution to the great variety of engineering problems that may be expressed as functions of polynomials, (2) as an aid to large-scale computing machines for which the roots of a polynomials must be isolated before further calculation can be performed, (3) possibly to give new approaches to problems difficult by other mathematical procedures, since any analytic function may be expressed as a power series, many of which converge rapidly, (4) as an adjunct to other mathematical processes: complementary solution to differential equations, the study of transforms, the determination of latent roots of a matrix, and the like.

Several electrical and mechanical methods have been developed for finding the roots of polynomials, some of which are: the Bell Laboratories isograph,[2] the Stibitz electrolytic isograph,[3] and the University of Texas[4] mechanical synthesizer. The system herein described will possess the advantages: (a) of being able to evaluate a polynomial to three significant figures for all values of the complex variables in a matter of minutes, (b) of being extendable to operation with automatic computers, and (c) of allowing additional operations such as Fourier synthesis.

II. THEORY OF OPERATION

Given the polynomial

$$a_n z^n+a_{n-1}z^{n-1}\cdots a_0=f(z),$$

it is desired to find the values of complex z for which $f(z)=0$. That is, $f(z)$ will have one value for each point $z=x+jy$ of the complex plane. In particular, $f(z)$ will be zero for some values of z (the roots) and the number of roots will equal the degree of the polynomial. By de Moivre's theorem we can set

$$z=re^{j\theta}=r(\cos\theta+j\sin\theta) \quad r,\ \theta \text{ real},\ \geq 0$$

and the polynomial becomes

$$\sum_0^n a_k r^k e^{jk\theta}=f(z).$$

Let θ now be varied periodically from 0 to 2π at a frequency $\omega/2\pi$ cycles per second. It can be seen that the kth term may be represented by a sinusoid of frequency $k\omega/2\pi$ amplified or attenuated by the amount $a_k r^k$. It is possible to investigate $f(z)$ for all values of z by summing these weighted sinusoids and varying r from zero to infinity continuously. Also

$$f(z)=\sum_{k=0}^n a_k r^k \cos k\omega t+j\sum_{k=0}^n a_k r^k \sin k\omega t,$$

and a root will obtain when both

$$\sum_{k=0}^n a_k r^k \cos k\omega t=0$$

$$\sum_{k=0}^n a_k r^k \sin k\omega t=0.$$

[1] J. B. Scarborough, *Numerical Mathematical Analysis* (Johns Hopkins Press, Baltimore, Maryland, 1930).
[2] R. L. Diezold, "The isograph, a mechanical root finder," Bell Lab. Record (1937).
[3] G. R. Stibitz, "An electric root finder," Memo., Burlington, Vermont.
[4] S. Leroy Brown and R. G. Packard, Phys. Rev. **73**, 646 (1948).

In other words, both real and imaginary components must be zero simultaneously. This situation and the value of $f(z)$ for all z are indicated by the isograph.

Physically, then, the method of solution consists of (1) generating the required sinusoids, constant in phase relationships and amplitude, (2) multiplying the amplitude of each sinusoid by its corresponding coefficient, a_k, (3) multiplying each of these quantities by the appropriate r^k, r being continuously variable from zero to infinity, (4) presentation of the sum by some convenient means.

There are many existing techniques for performing each of the above operations; those for the isograph were chosen for ease of operation, reliability and accuracy of circuits.

III. PHYSICAL DESIGN

Although it would be possible to introduce complex coefficients through phase shifting of each frequency, the present model operates with real coefficients only, since a method exists (described in a later paragraph) for obtaining a polynomial with real coefficients from one with complex ones. Let this polynomial be divided through by its largest coefficient. All the remaining coefficients are now one or smaller and so may be obtained electrically with potentiometers. Coefficients are inverted in sign by reversing the phase of the corresponding sinusoid.

Again, it will be shown possible to construct an equivalent polynomial

$$\sum_{k=0}^{n} a_k' r'^k e^{jk\omega} = f(z),$$

such that $r=1/r'$. We can investigate $f(z)$ from 0 to 1 and $f'(z')$ in the same range, covering the whole z plane. If R designates r when $|z| \leq 1$, and r' when $|z| \geq 1$, then R will be everywhere less than one and may also be obtained with potential dividers. The value of R^n may be formed by the ganged potentiometers shown in Fig. 1. Each potentiometer is separated from the following one by buffing amplifiers of gain one. One could use a gang of k potentiometers for the kth frequency, $k+1$ for the $(k+1)$th frequency, and so on, but a more convenient method is to produce d.c. voltages proportional to R^k, k between 0 and n, with a gang of n potentiometers. It then remains to control the amplitude of each voltage of frequency $k\omega$ with the d.c. voltage R^k.

As to the number of frequencies to be generated, or the degree of polynomial that may be generated, ten has been chosen for the electronic isograph, since most frequent polynomials are of this degree or less. Also, as will be shown, the roots of polynomials of higher degree may be found if the roots are sufficiently removed from 1. It is necessary, then to produce the first ten harmonics of the base frequency in constant phase relationships and of controlled amplitude. Some of the many methods of this generation are:

1. Mixing and remixing of the base frequency.
2. Synchronized oscillators or trigger circuits.
3. Magnetic pick-up from revolving gears.
4. The photoelectric analogy of (3).
5. The electrostatic analogy of (3).
6. Square wave generators using commutators.

The commutators (6) possess the unique property of having a large output that is a linear function of the applied d.c. voltage, since the d.c. voltage is the amplitude of the square wave output. Other types of generators must be followed by a linear modulator for multiplication of their output by the d.c. voltage, R^k. This consideration eliminated 30 vacuum tubes from the first design of the isograph. Operation using method (2) is being considered for another model.

The ten commutators, Fig. 1, being driven by a 3600 r.p.m. synchronous motor, have been found to have optimum operation with from one to ten segments.

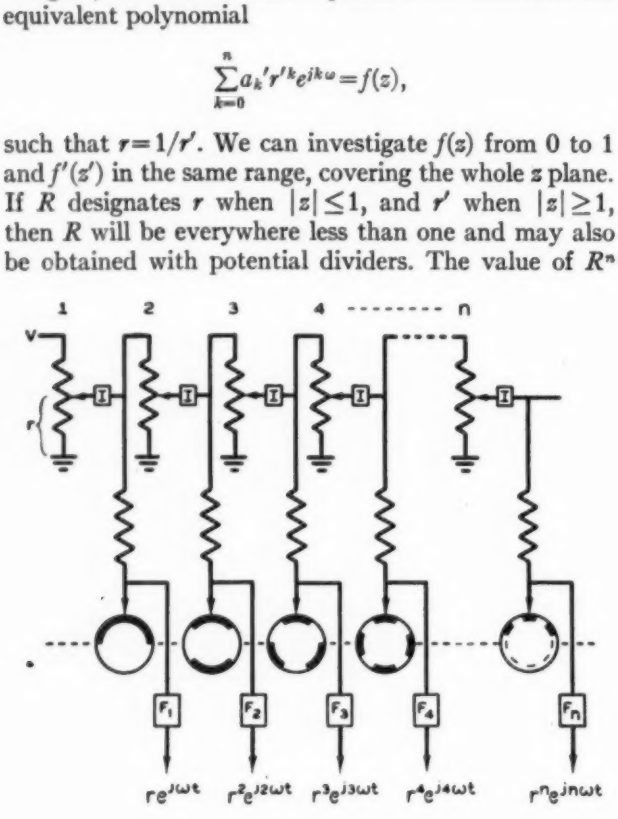

FIG. 1. Generation of terms.

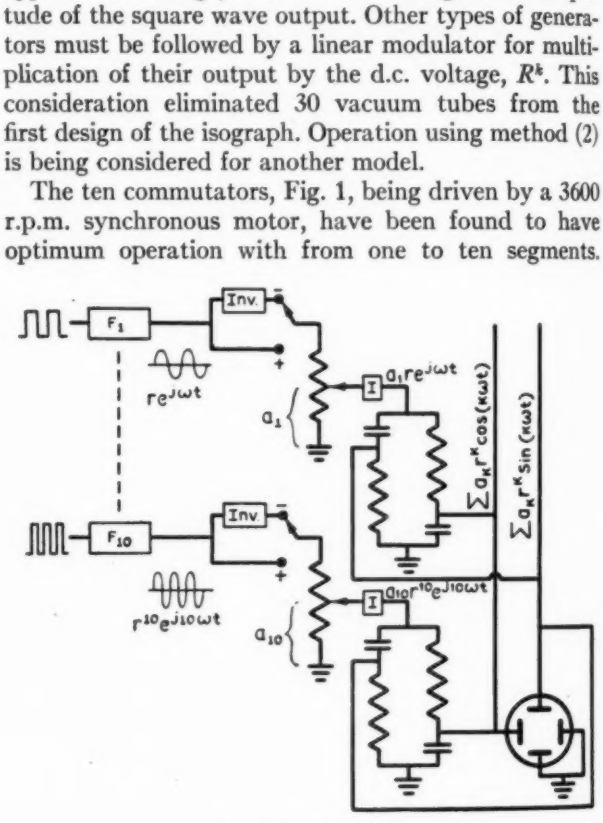

FIG. 2. Block diagram.

The output frequencies are therefore 60,120$\cdots$540 and 600 cycles, each of which will be at least as constant as the line frequency and will have permanent relative phase. The d.c. voltages from the ganged potentiometer are applied to the commutators and each output square wave, proportional to R^k, is filtered to obtain a sinusoidal voltage with harmonics less than 0.1 percent. The potentiometer for multiplication by the fractional a_n may be introduced at a convenient point in the subsequent circuit.

In view of the range of frequencies employed, the type of presentation that immediately suggests itself is an oscilloscope. It is convenient to separate the polynomial into:

$$f(z)=\sum_{k=0}^{\infty} a_k R^k e^{jk\omega t}=\sum_{k=0}^{\infty} a_k R^k \cos k\omega t+j\sum_{k=0}^{\infty} a_k R^k \sin k\omega t,$$

which may be achieved electrically by splitting each frequency into $\sin k\omega t$ and $\cos k\omega t$ and summing the ten of each in linear mixers. If the sum of the cosine voltages is supplied to the horizontal deflection circuit of the oscilloscope and the sines to the vertical, it is seen that a root of the polynomial will occur when the trace of $f(z)$ crosses the zero point of the oscilloscope. Such a representation has the convenient properties that: (a) The complex value of $f(z)$ is the vector from the origin to that particular point of the trace, (b) the region of greatest interest occurs at the center of the scope face, and hence the presentation may be greatly amplified for greater precision, and (c) since the parameter of the presentation is θ, varying periodically, a particular θ may be indicated by a marker in the proper phase relationship to the fundamental frequency. In the isograph, this marker is produced with a differential selsyn to shift the phase of the fundamental by any given angle, a clipper and peaker and then intensity modulation of the trace with the peaked pulse. In addition, the vector from the origin of the oscilloscope face to a point of the trace is the value of $f(z)$ at that setting of R and the indicated θ.

Using the elements described above, the electronic isograph appears as shown in the block diagram, Fig. 2. It can be seen that the channel for each frequency consists of rather elementary circuits, linear throughout. The zero degree term, the constant in the polynomial, is introduced by horizontal and vertical displacements of the oscilloscope pattern relative to the etched axes. Since all potentiometers have errors of less than 0.07 percent and all circuits are linear, it is possible to align the channels to evaluate a tenth degree polynomial with a constant term to three significant digits. Figure 3(a) shows the physical appearance of the isograph.

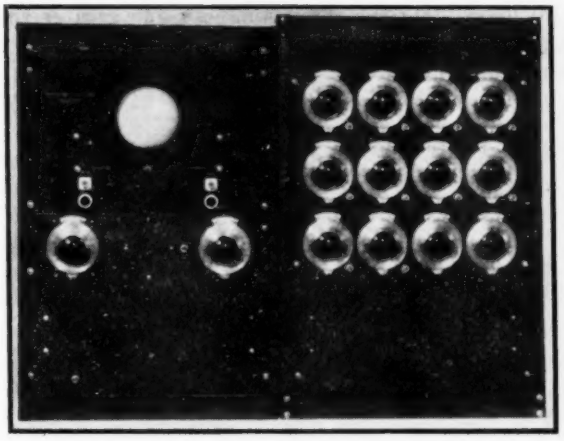

(a)

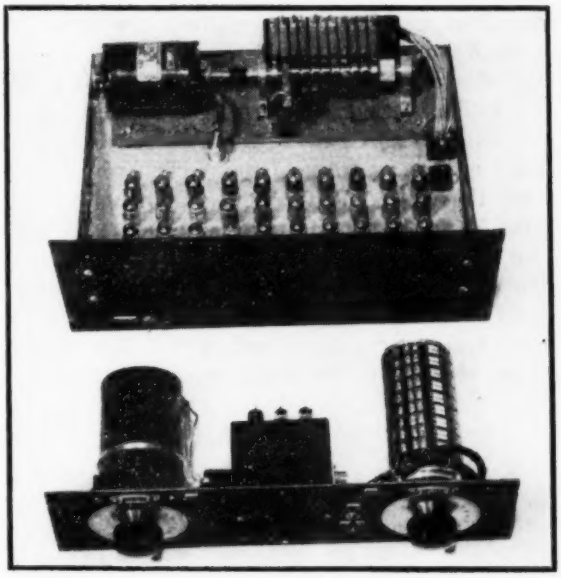

(b)

FIG. 3. Appearance of isograph.

IV. OPERATION

Basic Function—Zeros of Tenth Degree Polynomial With Real Coefficients

The only operation that must be performed externally is to divide the polynomial by its largest coefficient, the new polynomial having the same roots as the original. These coefficients are now entered on the vernier coefficient dials, which can be set with an accuracy of one part in two thousand. The values of $f(z)$ for $|z|$ from zero to one are investigated by the R potentiometer through this range. The oscilloscope presentation gives at once a trace representing the values complex $f(z)$ for all z lying on the circle $|z|=R$ for the particular R entered on that dial. A root will be indicated by the trace crossing the origin of the presentation, the magnitude of the root being the R setting when this situation obtains. The argument, or phase angle, of the root may be read from the θ-scale after the θ-marker has been placed on the portion of the trace at the origin. The precision of the root magnitude measurement is 0.05 percent and of the argument, 0.1 degree, which, of course, is one limit of the attainable accuracy.

To investigate the polynomial for $|z|$ greater than one, a slightly different procedure is employed. If the transformation

$$z=1/Z=1/(re^{j\theta})$$

is made, the polynomial becomes

$$\sum_{k=0}^{n} a_k z^k=\sum_{k=0}^{n} a_k/Z^k=\sum_{k=0}^{n} a_k/(r^k e^{jk\theta})$$

which may be multiplied by $r^n e^{jn\theta}$ to give

$$\sum_{k=0}^{n} a_k r^{n-k} e^{j(n-k)\theta}=a_n+a_{n-1}re^{j\theta}+\cdots+a_0 r^n e^{jn\theta}.$$

This transformation is performed simply by inverting the order of the coefficients, allowing the completion of the investigation of the z plane from 1 to ∞. The reciprocal of r, r', and the argument are again read from the R and θ scales, respectively.

Since the figure traversed in the z plane is a circle with a radius r (determined by the ganged potentiometer setting), the figure on the oscilloscope face (the w plane) is the transform of the circle. From complex variable theory, a line through a branch point of a function is transformed into a cusp. The branch points are the roots of the derivative, and another method of finding roots presents itself. It is merely necessary to integrate the polynomial (a simple multiplication by integers) and observe the occurrence of cusps on the w plane, as shown by the seven simultaneous roots of Fig. 4.

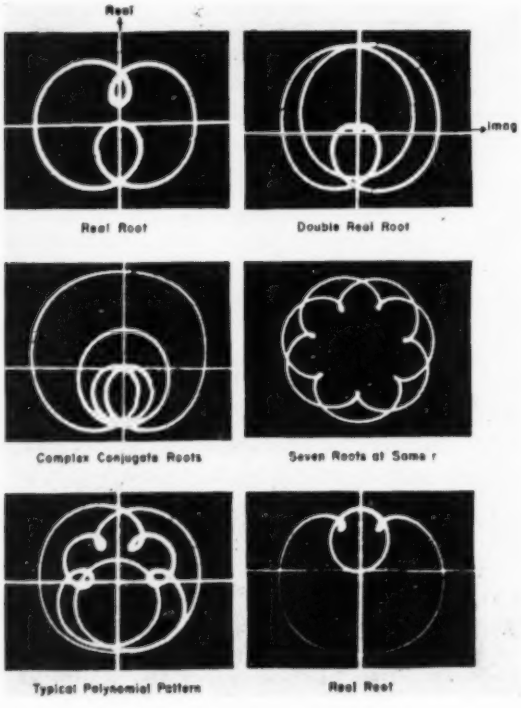

FIG. 4. Real, complex conjugate, double roots, etc.

The accuracy of the isograph is greater near $(z)=1$, so that large or small roots should be brought to this neighborhood by constructing a polynomial in z', z' being defined as Mz when M is some large (or small) real number.

Many of the properties of the polynomial may be observed on the $f(z)$ presentation. The investigation of $f(z)$ is carried out over circles about the origin in the z plane, since r is constant at any instant and θ is being scanned. Any polynomial, $P_n(z)$, may be expressed as the product

$$P_n(z)=A(z-p_1)(z-p_2)\cdots(z-p_n),$$

where $p_1\cdots p_n$ are the roots of $P_n(z)$. The quantity $(z-p_k)$ will change its argument by 2π as z moves around a circle enclosing p_k. If the circle C encloses m roots, the argument of $P_n(z)$ will change by $2m\pi$ for each circuit or z on C, or the trace of $P_n(z)$ will enclose the origin m times. In other words, the number of loops made by the trace of $P_n(z)$ about the origin of the oscilloscope is equal to the number of roots of absolute value less than the r then entered in the isograph.

The character of each root may also be determined from the presentation. Real, complex conjugate, double roots, etc., have the characteristic appearance shown in Fig. 4. It is also possible to determine some of the properties of the derivative at the root from the presentation.

If it is desired to obtain greater accuracy, the polynomial may be differentiated and the resulting $f'(z)$ entered in the isograph as a new polynomial to be evaluated at the R and θ of the root's approximation given by the first process. One can then apply Newton's formula:

$$z_1=z_0-[f(z_0)/f'(z_0)],$$

where z_0 is the first approximation, z_1 a better value. It is necessary to calculate the value of $f(z_0)$ by some auxiliary means; but since each application of Newton's formula usually doubles the number of significant figures, the additional calculation is efficient.

Roots of Polynomials with Complex Coefficients

A necessary and sufficient condition for a polynomial to have real coefficients is that its roots be distributed symmetrically about the real axis in the z plane. A polynomial with complex coefficients may be changed to one with real coefficients by introducing the conjugates of the roots of the original. Since it may be shown that

$$f(\bar{z})=\langle f(z)\rangle_{Av}$$

the conjugate roots may be introduced by forming the product

$$F(z)=f(z)\cdot\langle f(z)\rangle_{Av}.$$

The new polynomial will in general be of twice the degree of the original and have twice the number of roots. The additional roots are the conjugates of the

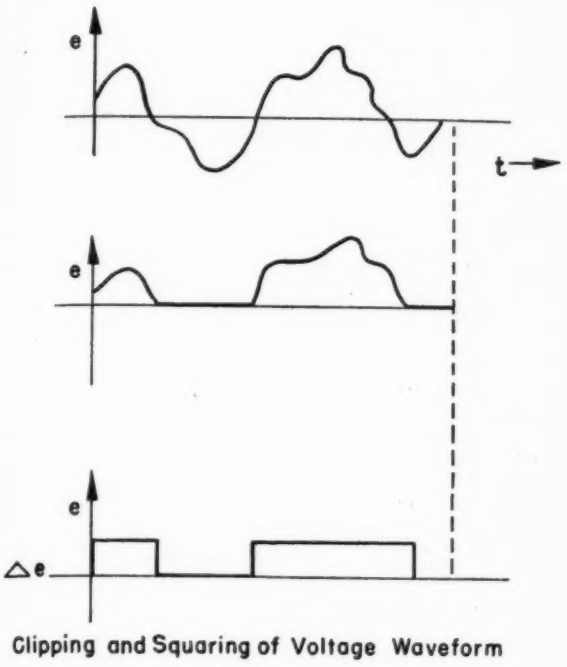

FIG. 5.

desired ones and may be eliminated by substitutions in the original polynomial. The roots of $F(z)$ are found by as described in the first paragraphs of Section IV.

Polynomials of Degree Higher Than Ten

A polynomial of degree $10+n$ may have all of its roots found by the isograph if n of its roots are sufficiently removed from one. The upper ten terms will give perhaps ten of the roots correct to three places if the roots are greater than 1.6 or less than 0.6, assuming reasonable coefficients. The terms neglected will contribute little to the root determination since $(1.6)^{10}$ is greater than 1000 and $(0.6)^{10}$ is less than $1/1000$, meaning that the lower terms' contributions are outside the accuracy of the instrument. The larger roots, discovered by using the upper ten terms, may be divided out of the original polynomial, resulting in one of lower degree which may then be solved by the isograph for the remaining roots.

Again, if the roots are too close to one for the above conditions to obtain, it is possible to remove them from this neighborhood by defining a new variable or by using Horner's method.

V. EXTENSIONS

It is possible to give a presentation much easier to interpret by mapping the polynomial over the z plane. This is a familiar type of representation and would be much more recognizable by mathematicians and engineers. It is difficult to accomplish but a method which would indicate the important points of the map would be valuable. One way of doing this, which it is believed will give considerable information to the engineer, would be as follows.

The previously mentioned oscilloscope presentation was developed by having a voltage on the horizontal plates proportional to the sum of the cosines of the various terms of the polynomial and was some periodic voltage centered about 0. The voltage on the vertical plates is the same type representing the sum of the sines. If each voltage were clipped at zero and at some small voltage above zero (see Fig. 5), and the resulting rectangular wave form were placed on the z axis of an oscilloscope while at the same time tracing on the face of the oscilloscope the circle corresponding to z magnitude$=r$ (r the setting of the r potentiometer), then this intensity modulation defines the regions of positive real (or imaginary) $P_n(z)$. This means that as r is varied from 0 to 1 there is obtained on the face of the oscilloscope a set of zones corresponding roughly to the surface of real (or imaginary) $P_n(z)$. The edges of these zones, of course, represent the lines real $P_n(z)=0$ (or imaginary $P_n(z)=0$). Although this is an approximation to the surface $P_n(z)$ mapped above the z plane, the significant points, roots, and branch points are given accurately. It is possible to put both surfaces on the face of the oscilloscope by simply adding the two intensity modulating voltages. There are then displayed on the z plane, intersections of the zero lines indicating the roots, and other shapes, the branch points of the

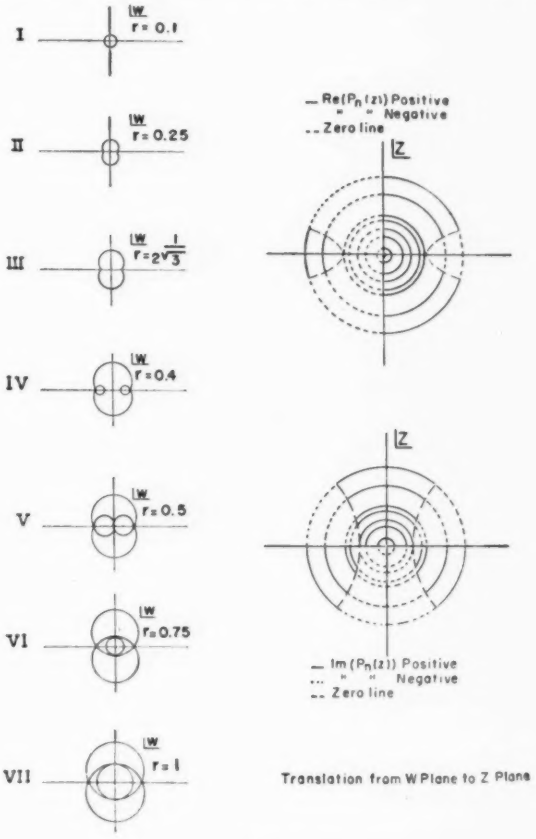

FIG. 6.

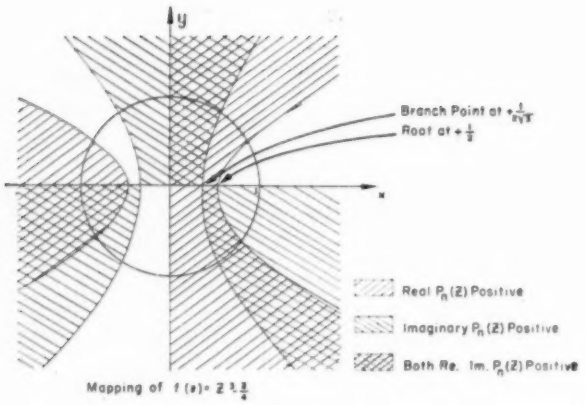

FIG. 7.

polynomial, and it will be possible to trace the behavior of these significant points as coefficients of the input polynomial are varied. Figure 6 is an illustration of what would be obtained using this presentation on the polynomial $z^3-z/4$. On the left are the series of illustrations representing the transforms of circles in the z plane to the w plane which are the usual isograph presentation. To the right are the two presentations representing the surface real $P_n(z)$ and imaginary $P_n(z)$ and Fig. 7 is the sum of the two upon which may be seen the roots and the branch points of this function. It is believed that this is the first attempt at mapping a function electronically. Instrumentation of this presentation is presently being completed.

Also, the coincidences of zeros in both real and imaginary parts of $P_n(z)$ may be detected electronically and presented on the z axis of the oscilloscope representing the z plane. The horizontal and vertical voltages again sweep the oscilloscope beam in a circle of $r=z$. The trace is brightened at the roots and the presentation is one in which the roots are indicated by bright spots on the z plane.[5] Again it will be possible to trace the movement of the roots as coefficients are varied.

VI. CONCLUSION

The electronic isograph can give rapid solutions to reasonably well-behaved polynomials to three places. With the addition of a small amount of paper work it is possible to find the zeros of all but a very small number of polynomials. It is hoped that the isograph will prove extremely valuable in servomechanism and other fields where the problem may be represented as a polynomial and that theoretical analysis of engineering problems will be furthered by its use.

VII. ACKNOWLEDGMENTS

The author wishes to thank co-workers of Special Studies Laboratory, A.F.C.R.L., for suggestions and assistance in the construction of this first model, especially Mr. Eugene F. Grant, whose suggestions inspired the project.

[5] Presentation of this type used by O. Vierlins, Germany. No reference available.

The Cadmium Sulfide X-Ray Detector*

RUDOLF FRERICHS
Department of Physics, Northwestern University, Evanston, Illinois
(Received September 12, 1949)

The CdS x-ray detector is compared with the photo-multiplier x-ray detector. Reduced to the same solid angle the sensitivity of the CdS x-ray detector is of the same order of magnitude as the sensitivity of the photo-multiplier x-ray detector. As the internal amplification of the primarily released electron currents in CdS is of the order 10^2 to 10^4 compared with the amplification in the multiplier tube of $\frac{1}{2}\times10^6$ the conversion process of x-ray quanta in slow electrons in CdS must be more efficient than the corresponding processes in the combination crystal phosphor screen photo-multiplier. Calibration curves show a linear relation between photo-current and intensity of x-rays at low irradiation levels. At high irradiation saturation effects occur. Oscilloscope curves of the response at 60 x-ray pulses per second are given. At strong irradiation the photo-current over a long time increases in a completely reversible way. X-ray intensities as low as 150 quanta CuK_α per second are registered with a circuit employing a WL 759 trigger tube.

INTRODUCTION

THE measurement of x-rays with a combination of a crystal phosphor screen and a photoelectric cell has been introduced by Herz in 1936.[1] Since this time every progress in the development of new phosphor screens or photo-cells has increased the sensitivity of this method. A great step was achieved in 1941, when Hodges and Morgan[2] introduced the photo-multiplier tube x-ray detector. Subsequently this combination

* This investigation was sponsored by the U. S. Navy, Bureau of Ships.

[1] R. H. Herz, Fortschr. Gebiete Röntgenstrahlen **54**, 6 (1936). It is interesting to note that in his first papers Röntgen tried to determine the distribution in space of the x-rays around the tube by photometrie of barium platino cyanide screens. Now the expensive and unstable barium platino cyanide screens have generally been replaced by crystal phosphors.

[2] R. H. Morgan, Am. J. Roent. Rad. Ther. **47**, 777 (1942).

has been thoroughly investigated[3] and the photo-multiplier x-ray detector is now a sensitive and reliable x-ray measuring device.

On the other hand, it was shown in 1946 by the author that synthetic CdS crystals show a large photo-conductivity under irradiation with x-rays.[4] In the photo-multiplier x-ray detector the energy of the absorbed x-rays is transformed at first in energy of slow electrons of a few ev. These electrons raised into the conduction band, subsequently recombine with the activating impurities and produce photons. A part of these photons is absorbed in the photo-cathode of the multiplier and releases a small yield of photo-electrons. These in turn release increasing cascades of secondary electrons at the consecutive stages of the multiplier. One photo-electron, liberated from the cathode, yields up to $\frac{1}{2}\times10^6$ electrons in the anode circuit. In the CdS crystal the same primary process of raising a number of slow electrons into the conduction band takes place. But in contradistinction to the man-made photo-multiplier arrangement the nature of the crystal provides the subsequent amplification of these electron currents.[5]

While in the photo-multiplier the rate of amplification in the different stages can be easily investigated, in CdS the amplification factor is only approximately known. Estimates made under rather plausible assumptions yield values of 10^3 to 10^4. Exact figures could be obtained by a simultaneous study of the light emission and the photo-conductivity of the irradiated CdS crystal. The light emission is determined by the number of electrons in the conduction band which recombine with the activating impurities. The photo-conductivity is related to the lifetime of the positive stationary space charges at the activating impurities. They make the presence of an additional electron in the conduction band possible.[6] As their lifetime is large, compared with the time one electron needs for passing through the crystal, a chain of up to 10^4 electrons cross the crystal, until the positive charge is neutralized by recombination. This amplification of the primary photo-current appears to be less favorable in the CdS crystal than in the multiplier tube. The primary processes, however, are simpler and are apparently connected with smaller losses than the corresponding processes in the combination phosphor screen photo-multiplier.

The purpose of this investigation to compare the two devices under identical conditions in order to find out for which purpose the one or the other might be best applied.

TABLE I. X-ray absorption in CdS crystals.

Wave-length	Crystal thickness: 99 percent absorption	Crystal thickness: 99.9 percent absorption
0.13A	7.4 mm	11.1 mm
0.20	2.16	3.24
0.31	0.66	0.99
0.40	0.36	0.54
0.45	0.25	0.37
0.47 (*K* edge)	1.30	1.95
0.51	1.06	1.59
0.61	0.62	0.93
0.71	0.42	0.63
0.83	0.28	0.42
0.92	0.20	0.30
1.04	0.14	0.21
2.09	0.02	0.03
3.02	0.009	0.013
3.72 (*L* edge)	0.028	0.042
6.14	0.008	0.012
9.86	0.002	0.003

D.C. MEASUREMENTS OF THE PHOTO-CURRENT

Measurements were performed with copper target tubes provided with beryllium windows.[7] The tubes were used with half-wave and with full wave rectification but without condensors. They furnished 60 (half-wave), 120 (full wave) x-ray pulses per second.

For a comparison at higher intensities the crystal, as well as the photo-multiplier x-ray detector, were placed in the beam at a distance of 50 cm from the target. For this informatory experiment no filtering other than 1.5-mm beryllium window was used. The photo-multiplier tube was used with 102 volts across each dynode corresponding to an over-all amplification of the electron current by a factor of 1.3×10^6. The d.c. currents were measured with a sensitive micro-amperemeter (full scale 5, 50, 500, 5000×10^{-6} amp.). The photo-multiplier tube was shielded in a brass container, and a fluoroscopic screen, Patterson Type B, was attached at the tube surface behind a black, paper window. The dark current of the tube was about 1×10^{-7} amp. When the multiplier was irradiated without the phosphor screen at 24 kv and 10 ma, the current rose to $3.8\pm0.2\times10^{-6}$ amp. The crystals to be investigated have sensitive areas of the order of 1 mm^2. Accordingly, a comparable size of the phosphor screen was used. The phosphor layer was scratched from the supporting cardboard leaving an area of 1×5 mm. Under these conditions the current obtained under x-ray irradiation amounted to 12.5×10^{-6} amp., but quickly dropped to 9×10^{-6} amp. because of the fatigue effects extensively discussed by Marshall, Coltman, and Hunter.[3]

The CdS crystal showed a bright red luminescence under irradiation with filtered ultraviolet. It is known

[3] H. M. Smith, Gen. Elec. Rev. **48**, 13–17 (1945). Marshall, Coltman, and Hunter, Rev. Sci. Inst. **18**, 504 (1947). J. W. Coltman, Proc. I. R. E. **37**, 671 (1949).

[4] R. Frerichs, Naturwiss. **33**, 281 (1946). R. Frerichs, Phys. Rev. **72**, 594 (1947).

[5] Natural amplification phenomena will play a more important role as the number of electronic devices applied in complicated mechanism (electronic calculators, electronic brains) reaches values which make it necessary to reduce the size and the labor involved in the individual device. An example is the recently developed transistor, which can replace complicated electron tubes. See furthermore: V. K. Zworykin and E. G. Ramberg, *Photoelectricity*, p. 469.

[6] R. Frerichs, Phys. Rev. **76**, 1869 (1949).

[7] The author is greatly indebted to Dr. J. C. M. Brentano, who made the equipment of his x-ray laboratory available to him.

TABLE II. Current through crystal and multiplier as a function of the x-ray intensity.

X-ray tube Potential	X-ray tube Current	r per min.	Current $\times 10^{-9}$ amp. Crystal	Current $\times 10^{-9}$ amp. Photo-multiplier
70 kv	2.1 ma	0.063	0.487	0.463
65	2.1		0.450	0.390
60	2.1		0.425	0.325
50	2.1	0.031	0.375	0.270
45	2.1		0.306	0.220
40	2.1		0.250	0.165
35	2.1		0.175	0.110
30	2.1	0.014	0.100	0.068
25	2.1		0.037	0.037
20	2.1		0.005	0.011
15	2.1		0.000	0.002

(0.5 mm Cu filter)

that luminescent CdS crystals yield large amplification.[8] The sensitive area between the Aquadag electrodes was 0.3×1.5 mm². It was mounted in a brass tube with a black, paper window. The leads were well insulated and shielded. At an applied potential of 280 volts the dark current remained smaller than 1×10^{-8}; it could not be observed with the microamperemeter used. Within five seconds the current rose under irradiation to $27\pm1\times10^{-6}$ amp. The amount of energy absorbed in the phosphor layer or in the crystal was not determined. The thickness of the crystals was not uniform. These crystals show a ribbon-like structure. Therefore, exact measurements of the absorption are difficult to perform. It was observed, however, with a fluoroscopic screen that only a small amount of incident soft x-rays passed through the crystal at its average thickness of 0.2 mm. Table I shows the thickness which is necessary to absorb 99 or 99.9 percent of the incident irradiation at different wave-lengths. The values are calculated from the mass absorption coefficients of cadmium determined by Laubert and Biermann.[8a] In the range between 1 and 2A no data were available.

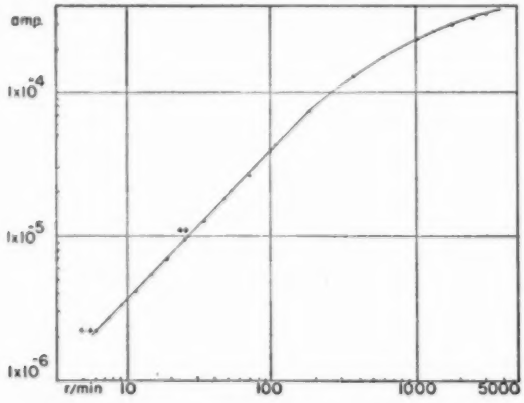

FIG. 1. Photo-current in CdS as a function of the x-ray intensity.

[8] This is to be expected from the theory outlined in reference 6. High luminescence proves that sufficient activating impurities are present which furnish the positive stationary space charges necessary for the compensation of the transported negative charges.

[8a] S. Laubert, Ann. d. Physik **40**, 553–578 (1941). H. H. Biermann, Ann. d. Physik **26**, 740 (1936).

It was not attempted to consider the influence of the scattering coefficient which is contained in these measurements but which is usually much smaller than the coefficient of true absorption. In contradistinction to other photo-conductors with larger dark currents, it is not necessary to chose the thinnest crystals. For short wave-lengths it is recommended to irradiate the ribbon-like crystals ($a>b>c$) through the surfaces $a\times c$ or even $b\times c$ in order to obtain high absorption. Thus, the effective area can be small, which is an advantage for measuring narrow bundles of x-rays.

From these experiments it follows that reduced to the same solid angle which corresponds to an effective area of 0.5 mm², the photo-currents obtained in CdS are one order of magnitude larger than those obtained with the multiplier.

The luminescent screen used (Patterson B) is not the most efficient. The photo-multiplier responds about three times better to the blue luminescent screen, Type C. It should be possible to use the entire light emitted by the phosphor. For instance, with a spherical mirror such as Coltman[3] used. Furthermore, the sensitive area of the phosphor screen generally should be larger (50 mm²) in order to increase the solid angle without increasing the dark current.

On the other hand, the potential applied at the CdS crystal can be increased until the dark current reaches values comparable with the photo-multiplier dark current. Furthermore, it is possible to assemble different crystals in one plane and to connect the electrodes parallel.

In conclusion we might state that using d.c. currents the CdS crystal can be made one order of magnitude more sensitive per unit area than the photo-multiplier x-ray detector. The experiments show that the mechanism of transforming x-ray quanta into slow electrons in CdS is apparently much more effective than the transforming of x-rays→slow electrons→photons→photoelectrons at the photo-cathode since a deficiency in amplification of 10^{-2} to 10^{-3} is more than compensated.

THE PHOTO-CURRENT IN CdS AS A FUNCTION OF THE X-RAY IRRADIATION

A few measurements were made to study the photocurrent in CdS as a function of the irradiation. It was previously observed by the author[6] that at high irradiation levels—for instance, with gamma-rays—the current produced in CdS crystals is proportional to the square root of the intensity of irradiation. This relation follows theoretically from the recombination processes involved in these secondary photo-currents. In equilibrium after prolonged and strong irradiation, the number n of the electrons in the conduction band and thus the current is determined by

$$dn/dt = aI - bn^2 = 0.$$

I is intensity of the impinging radiation; a is a factor which contains the absorption in the crystal and the

efficiency of conversing x-rays in slow electrons. The factor b determines the recombination rate between electrons in the conduction band and activating impurities in the lattice. At the first approximation trapping and releasing of electrons, which play such an important role in persistent phosphorescence, do not need to be considered in the equilibrium state. The number of the electrons which are trapped per second is equal to the number of electrons which are released from the traps into the conduction band per second. We make the assumption that first-order processes do not take part. Nail, Pearlman, and Urbach[9] recently pointed out that at low irradiation levels in crystal phosphors first-order processes such as energy transfer from trapped electrons to the lattice by direct transition can occur. Under certain circumstances a region of proportionality to the square root of the exciting intensity is situated between linear regions at low and extremely high intensities. Therefore, the dependence of the photo-current from the incident radiation should not be linear at high intensities. It might be pointed out here that the same is to be expected for the photomultiplier x-ray detector if a crystal phosphor is used.[10] The combination with a fluorescent emitter, for instance, barium platino cyanide, yields a linear characteristic as fluorescent substances do not show any saturation effects.[11]

Some measurements were taken with the copper target tube at 40 kv and 20 ma. The crystal was used with 22.5 volts. The distance between crystal and target was varied from 8 to 147 cm. The results are plotted in the log-log diagram Fig. 1. The abscissa contains the true x-ray intensities. According to the manufacturer of the apparatus, at 40 kv and 20 ma the intensity of the unfiltered x-rays at 50-cm distance from the target amounts to 100 r per min. According to the measurements of Day and Taylor,[12] considerable corrections have to be applied at the simple distance square relation, if the tube potential is low and if no filters are interposed. The intensity values in Fig. 2 are corrected, using Fig. 4 of Day and Taylor, assuming a value of 40 kv and 1.5-mm beryllium window. The curve covers the range 10 r per min. up to 5000 r per min. It is straight at low values and becomes curved above 100 r per min. The tube used in our experiments with 40-kv peak current emits a spectrum, the distribution of which shifts periodically with the alternating voltage applied. In Fig. 1 the size of corrections is marked under the conservative assumption that the actual average voltage would be as low as 20 kv. Another possible correction, the slow change of the photocurrent with time, will be discussed later.

TABLE III. Current through crystal and multiplier at different filtering.

X-ray tube Potential	X-ray tube Current	Thickness of Al filter	Current $\times 10^{-6}$ amp. Crystal	Current $\times 10^{-6}$ amp. Photo-multiplier
60 kv	2.2 ma	0	0.475	0.355
60	2.2	$\frac{1}{4}$ in.	0.200	0.080
60	2.2	$\frac{1}{2}$ in.	0.100	0.032
60	2.2	$\frac{3}{4}$ in.	0.042	0.012
60	2.2	1 in.	0.017	0.005
60	2.2	5/4 in.	0.005	0.002

Measurements at low intensity levels have been performed by Mr. J. E. Jacobs of the Department of Electrical Engineering, Northwestern Technological Institute.[13] The measurements were taken with a tungsten target tube. The x-rays in Table II are filtered by 0.5 mm Cu. The r values were determined by a Victoreen r meter. The crystal had a sensitive area of 3×1.5 mm^2; the field strength applied was low and equal 90 volts per 3 mm. The currents were measured with a d.c. amplifier. The photo-multiplier tube 931A was selected from a large number. The potential at the single dynodes was 105 volts. A Patterson E_2 industrial screen was used behind a lead aperture of 3×1.5 mm. This limited the solid angle to the value of the crystal.

With increasing potential the efficiency becomes smaller similarly as the efficiency of an ionization chamber decreases with increasing hardness or radiation. As the radiation was not homogeneous, it is not possible to construct a curve, sensitivity *versus* wavelength.[14] The general shape of such a curve should indicate that ionization in air and photo-conductivity in CdS are not parallel, if the hardness of the x-rays is changed.[15] Furthermore, the K absorption edge of cadmium at 0.460A should produce a discontinuity in this curve analogous to the discontinuity produced in the photographic plate due to the silver K edge. Similar

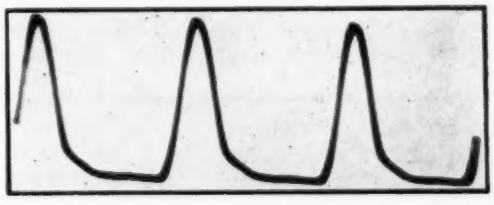

FIG. 2. 30 kv, 20 ma, distance target-crystal=17 cm, CdS crystal area=0.3×1.5 mm, applied potential=1.55 volts, current amplitude=5.5×10^{-8} amp.

[9] Nail, Perlman, and Urbach, "Preparation and characteristics of solid luminescent materials," Cornell University, Symposium (1946), p. 190.

[10] O. Glasser, *Medical Physics* (Chicago 1944), p. 1293. Figure 1, Patterson Type B screens show an increase of brightness which is less than proportional to the impinging radiation at high intensities (3–4 r per min.) especially at lower x-ray tube potentials.

[11] W. de Groot, Physica **6**, 393 (1939).

[12] F. H. Day and L. S. Taylor, J. Research Nat. Bur. Stand. **40**, 393 (1948).

[13] The author is much indebted to Mr. Jacobs for the facility of using these values in the present investigation.

[14] It might be useful to determine this dependency, for instance, with the powerful filter method developed by H. Kustner, Zeits. f. Physik **70**, 324 (1931). According to his measurements monochromatic radiations $\Delta\lambda=0.005$A with intensities from 5×10^{-4} to 27×10^{-3} r per min. can be produced in the wave-length region 0.128 to 2.50A.

[15] For a comparison of the effects produced by x-rays of different wave-lengths at ionization in air, at fluorescent screens and at the photographic plate see: G. L. Clark, *Applied X-Rays* (New York, 1940), p. 68, Fig. 48.

discontinuities are to be expected with the crystal phosphor photo-multiplier x-ray detector at the zinc and cadmium K absorption edges.

Table III contains further measurements with the photo-multiplier and the CdS crystal obtained by Mr. Jacobs. The potential was constant, and different thicknesses of aluminum filtering were applied. Crystal and photo-multiplier were used in 150-cm distance from the tungsten target tube.

THE SPEED OF RESPONSE

As the photo-multiplier can follow light pulses of the order of 10^{-8} sec. the speed of the photo-multiplier x-ray detector is determined by the properties of the screen used. Fast responding phosphors (calcium tungstate) show, according to Marshall, Coltman, and Hunter, a fast and exponential decline of the photo-current, after irradiation with x-ray pulses of 1 μsec. duration. The somewhat persistent sulfide screens, Patterson B and C, are slower. According to their oscillograms the response of the phosphor screen does not match the short x-ray pulse applied. It is not possible to determine its exact shape from such measurements.

Identical experiments could not be performed with the CdS crystal, as the necessary radar pulsing equipment was not available. However, the usual chopping of the x-ray output with 60, respectively, 120 pulses per second, which is obtained by one way or two way rectifiers is very useful for the oscilloscopic observation of the currents in CdS.

A comparison was made of the current *versus* time curves obtained with the photo-multiplier x-ray detector and the CdS crystal at the half-wave tube. The comparison of Figs. 2 and 3 shows that the reproduction of the x-ray intensity curve obtained with these two devices is nearly identical. The declining branch in the photo-multiplier curve approaches the ideal curve more perfectly,[16] but also at these low frequencies the slow decline of the phosphor in the photo-multiplier can be observed. According to Marshall, Coltman, and Hunter, the screens, Type B and C, are somewhat persistent. This dissymmetry is to be attributed to the afterglow of the phosphor. The curves show that at these rather low frequencies the CdS crystal follows the x-ray intensity distribution with good approximation. Figure 4 has been taken with the CdS crystal connected directly to the input resistance of the oscilloscope without battery. In the polar crystal the x-rays produce a small e.m.f., which can be observed with the oscilloscope, if the irradiation is strong enough.[16a]

FIG. 3. 30 kv, 8 ma, distance 50 cm, photo-multiplier x-ray detector, screen size = 1 mm², Patterson Type B, dynode potential = 123 volts, current amplitude = 1.3×10^{-7} amp.

[16] The intensity of the afterglow of the phosphor is proportional to the number of recombination processes bn^2. The photo-current is proportional to the number n of electrons in the conduction band. Hence the optical decay is faster than the decay of the photo-current. Verified by L. Gildart and A. W. Ewald in a paper given at the Oak Ridge meeting of the Physical Society (March, 1950).

Curve 4 shows the current in the crystal under weak irradiation. As it has been observed with the luminescence of crystal phosphors, the slope of the raising and declining branch of these curves depends upon the intensity of irradiation. At low intensities the current rises and declines slowly, and the x-ray curve is badly reproduced. One should expect that at low intensities the curve of the photo-multiplier x-ray detector should show some similar shape.

From these experiments it can be concluded that for x-ray pulses of 60 per sec. the CdS crystal can replace the photo-multiplier x-ray detector.

FIG. 4. 40 kv, 20 ma, 17 cm distance, CdS crystal without potential applied, crystal photo-current amplitude = 4.8×10^{-9} amp.

EFFECTS DUE TO PROLONGED IRRADIATION

The fatigue effects observed in photo-multiplier x-ray detectors are due to the multiplier tube. With sufficiently low levels of irradiation they can be greatly reduced. The phosphor screen used with the photo-multiplier shows no change in its sensitivity with prolonged irradiation. An experiment was made to find out whether small changes in the brightness of the phosphor screen take place at prolonged irradiation with intense x-rays. The detector was irradiated with 36,000 r at 60 pulses per sec. In order to avoid fatigue of the multiplier the potential at the dynodes was interrupted during this irradiation. The currents observed at the beginning and at the end of this irradiation agreed within 0.6 percent. This proves that the Patterson B screen does not undergo any observable changes in its luminosity. Such effects could be due to a slow rearrangement of the electrons in the traps of different depths.

A CdS crystal was adjusted so that it showed a photo-current of 85×10^{-6} amp., after a few seconds of irradiation. This current slowly increased during 11 hr. of continuous irradiation until it finally reached 182×10^{-6} amp. The irradiation during this period amounted to 2.5×10^{5} r. The x-rays were pulsed (60 per sec.) and the potential at the crystal was kept constant. The dark current remained throughout this experiment below 10^{-8} amp. After about 12 hr. recovery the crystal

[16a] T. Broser and R. Warminsky, Zeits. f. Naturforschung **5A**, 63 (1950).

FIG. 5. 40 kv, 20 ma, 130 cm distance, CdS crystal, potential applied at crystal = 45 volts, current amplitude = 1.2×10^{-8} amp.

reassumed its original value, corresponding to 85×10^{-6} amp. at that particular level of irradiation; and no permanent changes remained. This slow change of the resistance has been investigated with gamma-rays.[6] It is attributed to a rearrangement in the occupancy of deep and shallow traps during prolonged and intermittent irradiation.

The slow increase in the final current has to be considered at all d.c. measurements with these crystals. In the measurements of Fig. 1 the currents were always read after 5 sec. irradiation.

It has been shown by the author that the original high dark resistance can be quickly restored by irradiation with infra-red light.

MEASURING OF SMALL X-RAY INTENSITIES WITH CdS CRYSTALS

Measurements of very weak x-rays were made using a trigger tube (Westinghouse WL759) in a circuit developed by Dr. R. J. Cashman.[17] The current in the crystals (active area 0.5×6 mm^2) charges a well-insulated condensor. As soon as the potential across the condensor reaches a defined value, the trigger tube starts, and the resultant impulse is counted by a suitable amplifier and an electromagnetic counting device. The frequency of this periodic discharging is a scale for the intensity of the impinging radiation and currents of the order of 10^{-11} amp. can easily be measured.

The copper target x-ray tube, used in a full wave rectifier circuit, was applied with reduced heating current. The number of quanta emitted by the tube were determined by a Geiger-Müller counter with a measured efficiency of 40 percent for the copper K_α line monochromatized by a simple rocksalt spectrometer. The exit slit in front of the Geiger-Müller tube of 3 mm^2 defined the same bundle of x-rays with the crystal and with the counter.

With 1900 quanta hitting the crystal the condensor was charged within 12 to 13 sec. to the starting potential of the trigger tube. With this irradiation (about 150 quanta per sec.) a periodical trigging every 12 to 13 sec. is produced. This state is reached three minutes after the irradiation of the crystal has started. However, 20 min. after the x-ray irradiation was interrupted the crystal was still counting with a rate of one triggering in 55 to 59 sec. This persistent conductivity can be quickly reduced to zero, if a small amount of infra-red simultaneously illuminates the crystal during the irradiation with x-rays. The conductivity reached under x-ray irradiation is lowered somewhat by the simultaneous infra-red irradiation. 2300 quanta are necessary to charge the smallest capacity so that the trigger tube starts every 11 sec. Under the additional infra-red irradiation the trigger tube stops after counting two or three more counts (equivalent to 2300 quanta each), as soon as the x-ray irradiation is interrupted. No more counts were observed in the following 10 hr. The additional infra-red irradiation can also be applied between the different triggerings. It should be possible to design a circuit where each triggering flashes a small infra-red lamp (for instance, a xenon discharge), which reduces the persistent conductivity.

Thus, the trigger circuit is quite promising for the measuring of small numbers of x-ray quanta. Further experiments have to be made to find the actual limit of this method. As the current at 150 x-ray quanta per sec. is of the order of 1×10^{-11} amp. $=6.3\times10^7$ electron charges per sec. the efficiency in this case is 4.2×10^5 electrons per x-ray quantum.

CONCLUSIONS

The measurements show that the sensitivity of the CdS crystal can be compared directly with the sensitivity of the photo-multiplier x-ray detector. The crystal has in its present form the disadvantage that the response to x-ray pulses is apparently slower and that the current reaches a final value only after long irradiation. As the persistence in the original zinc sulfide screens has been greatly reduced by "killers," it might be possible to reduce the inertial of CdS by suitable impurities. On the other hand, the crystals do not show the fatigue effects observed with multiplier tubes. Their small size is a further advantage in some applications. As the crystal size defines the sensitive volume, it is not necessary to screen the receiver with lead slits.

The crystals can be grown in large numbers. They afford no treatment but a suitable mounting, for instance on a polystyrene strip, and the application of the Aquadag electrodes. As the crystal current is proportional to the first power of the potential applied no power of supply of extreme constancy is necessary.

The present measurements deal with such intensities that the effects of single x-ray quanta have not been considered. The regularities of electron pulses produced in these crystals afford further detailed investigations.[18]

[17] W. B. Nottingham, Rev. Sci. Inst. **11**, 2 (1940). R. J. Cashman, reference 10, p. 918, Fig. 20.

[18] S. G. Zizzo and J. B. Platt, Phys. Rev. **76**, 704 (1949) studied the pulses due to x-ray quanta as well as the continuous photocurrent in CdS crystals obtained from the author.

Note added in proof: Measurements of the efficiency of the photocurrents produced in CdS crystals by irradiation with x-rays have been recently published by Y. Fassbender and O. Hachenberg, Ann. d. Physik (6) **6**, 229 (1949). They confirm our results regarding the amplification factor in CdS.

Diffraction by a Cylindrical Obstacle*

CHARLES H. PAPAS
Cruft Laboratory, Harvard University, Cambridge, Massachusetts
(Received September 23, 1949)

The diffraction of a plane electromagnetic wave by an infinitely long, perfectly conducting cylinder has been treated by a variational method (see the two papers by H. Levine and J. Schwinger). The incident field is assumed to be polarized in the direction of the cylinder axis, and thus the entire field is of two-dimensional nature. This formulation yields an expression for the diffracted cylindrical wave amplitude, at distances from the cylinder large compared to its transverse dimension and the wave-length, which is stationary relative to small independent variations of the surface currents arising from plane-wave excitation along a pair of directions in space; furthermore, the stationary form of the diffracted amplitude is independent of the scale of the surface currents. In accordance with a theorem of Levine and Schwinger, the total plane-wave scattering cross section is simply related to the diffracted cylindrical wave amplitude in the direction of incidence. To examine the high frequency behavior of the cross section, the surface current induced by a plane wave is taken different from zero only on the illuminated part of the cylinder, where its value is derived from the tangential component of the incident magnetic field. The resulting cross section is obtained and is shown to approach $4a$ when ka approaches infinity ($k=2\pi\div$wave-length, a equals the radius of cylinder).

I. INTRODUCTION

THE theoretical examination of the diffraction of a steady-state plane electromagnetic wave by a cylindrical obstacle has interested many investigators. One of the earliest treatments proceeds according to the Fourier-Lamé eigenfunction method. The incident electromagnetic wave is assumed to be polarized parallel to the axis of the perfectly conducting, circular cylinder. The axis of the cylinder lies along the x axis, and the incident wave has only an x component of the electric field, $E_x^{\text{inc}}(\rho,\phi)$, and a y component of the magnetic field, $H_y^{\text{inc}}(\rho,\phi)$ (Fig. 1). For an incident wave whose electric field is of unit amplitude and propagating in the direction ϕ_1, i.e., $E_x^{\text{inc}}=\exp[ik\rho\cos(\phi-\phi_1)]$, the corresponding scattered electric field is given by

$$E_x^{sc}(\rho,\phi-\phi_1)=-\sum_{-\infty}^{\infty}(i)^m\frac{J_m(ka)}{H_m^{(1)}(ka)}H_m^{(1)}(k\rho)\cos m(\phi-\phi_1), \quad (1)$$

where $J_m(x)$ are the Bessel functions, and $H_m^{(1)}(x)$ are the Hankel functions of the first kind, and $k=2\pi\div$wave-length.

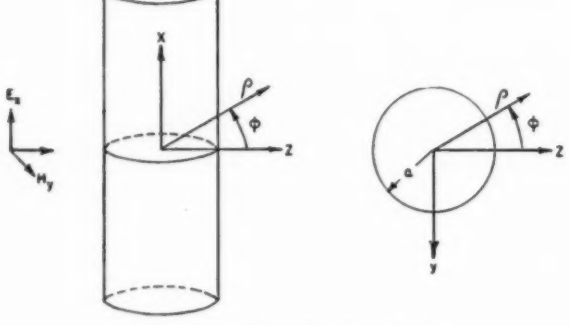

FIG. 1. Diffracting circular cylinder.

The inadequacy of the rigorous representation (1) stems from the fact that its convergence becomes slower with increasing values of ka, i.e., at high frequencies. To avoid this difficulty, Debye[1] represented the scattered field by a Fourier integral in the following manner. Let

$$f(m)=\frac{H_m^{(1)}(k\rho)}{H_m^{(1)}(ka)}\cos m(\phi-\phi_1),$$

where m can be considered to be a continuous real variable. According to the Fourier integral theorem,

$$f(m)=\frac{1}{2\pi}\int_{-\infty}^{\infty}d\mu\int_{-\infty}^{\infty}f(\alpha)\exp[i\mu(m-\alpha)]d\alpha$$

$$=\frac{1}{\pi}\int_{-\infty}^{\infty}d\mu\exp(i\mu m)\int_{0}^{\infty}f(\alpha)\cdot\cos\mu\alpha\cdot d\alpha$$

$$=\frac{1}{\pi}\int_{-\infty}^{\infty}d\mu\exp(i\mu m)\int_{0}^{\infty}\frac{H_\alpha^{(1)}(k\rho)}{H_\alpha^{(1)}(ka)}\cdot\cos\alpha(\phi-\phi_1)\cdot\cos\mu\alpha\cdot d\alpha.$$

Then,

$$E_x^{sc}(\rho,\phi-\phi_1)=-\frac{1}{\pi}\sum_{m=-\infty}^{\infty}(i)^mJ_m(ka)$$

$$\cdot\int_{-\infty}^{\infty}d\mu\exp(i\mu m)\int_{0}^{\infty}\frac{H_\alpha^{(1)}(k\rho)}{H_\alpha^{(1)}(ka)}\cos\alpha(\phi-\phi_1)\cdot\cos\mu\alpha\cdot d\alpha.$$

Since

$$\sum_{m=-\infty}^{\infty}(i)^mJ_m(ka)\exp(im\mu)=\exp(ika\cos\mu),$$

by interchanging the order of summation and integra-

* The research reported in this document was made possible through support extended Cruft Laboratory, Harvard University, jointly by the Navy Department (ONR), the Signal Corps of the U. S. Army, and the U. S. Air Force, under ONR Contract N5ori-76, T. O. I.

[1] P. Debye, "Das electromagnetische Feld um einem Zylinder und die Theorie des Regenbogens," Physik. Zeits. 9, 775-778 (1908).

tion Debye's integral representation is obtained:

$$E_x^{sc}(\rho,\phi-\phi_1)=-\frac{1}{\pi}\int_{-\infty}^{\infty}\exp(ika\cos\mu)d\mu \times\int_0^{\infty}\frac{H_\alpha^{(1)}(k\rho)}{H_\alpha^{(1)}(ka)}\cos\alpha(\phi-\phi_1)\cdot\cos\mu\alpha\cdot d\alpha. \quad (2)$$

By an approximate evaluation of (2) for large ka, he obtained

$$E_x^{sc}(\rho,\phi)=-\left(\frac{ka\cos(\phi/2)}{2k\rho}\right)^{\frac{1}{2}}\exp\left[ik\left(\rho-2a\cos\frac{\phi}{2}\right)\right] \quad (3)$$

for the scattered electric field resulting from a plane wave incident in the direction $\phi_1=0$.

Up to the present we have had the rigorous eigenfunction expansion of the scattered field (1) which suffers from convergence difficulties for large ka, and the Debye summation scheme yielding the expression (3) for the high frequency far-zone scattered field, valid for directions not in the neighborhood of $\phi=\pi$. Consequently (3) cannot be used to calculate the total scattering cross section of the cylinder; (1) can be used, however, even for large values of ka, i.e., at high frequencies, but only with considerable heuristic manipulation of the slowly convergent eigenfunction expansion.

It is the purpose of this paper to show that the aforementioned difficulties can be avoided if the problem is formulated from the start using a variational principle in the manner of Levine and Schwinger.[2,3] This formulation yields an expression for the diffracted cylindrical wave amplitude, at distances from the cylinder large compared to its transverse dimension and the wavelength, which is stationary relative to small independent variations of the surface currents arising from plane-wave excitation along a pair of directions in space. Furthermore, the stationary form of the diffracted amplitude is independent of the scale of the surface currents. The total plane-wave scattering cross section is simply related to the diffracted cylindrical wave amplitude in the direction of incidence. To examine the high frequency behavior of the cross section ($ka\gg1$), the surface current induced by a plane wave is taken different from zero only on the illuminated part of the cylinder, where its value is derived from the tangential component of the incident magnetic field.

II. INTEGRAL EQUATION FORMULATION

Consider a plane electromagnetic wave incident upon a perfectly conducting circular cylinder of radius a, whose axis lies along the x axis of a rectangular coordinate system, Fig. 1. The incident wave is polarized parallel to the axis of this cylinder, its electric field

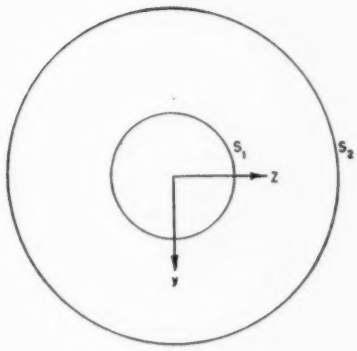

FIG. 2. Integration domain.

being given by

$$E_x^{inc}(\rho,\phi)=\exp[ik\rho\cos(\phi-\phi_1)], \quad (1)$$

where ρ,ϕ are cylindrical coordinates, $k=2\pi\div$ wavelength, and ϕ_1 is the direction of propagation. The scattered electric field, $E_x^{sc}(\rho,\phi)$, is also polarized parallel to the cylinder axis. The electric field at any point r, r being a two-dimensional vector from the origin to any point (ρ,ϕ), is the sum of the incident and scattered fields, $E_x(r)=E_x^{inc}(r)+E_x^{sc}(r)$. The problem is formulated in terms of these electric fields. To emphasize their two-dimensional scalar nature, denote them by $\psi(r)\equiv E_x(r)$, $\psi^{inc}(r)\equiv E_x^{inc}(r)$, and $\psi^{sc}(r)\equiv E_x^{sc}(r)$.

Note that $\psi(r)$ satisfies the scalar wave equation

$$(\nabla^2+k^2)\psi(r)=0, \quad (2)$$

and the two-dimensional scalar Green's function $G(r,r')$ satisfies the inhomogeneous scalar wave equation

$$(\nabla^2+k^2)G(r,r')=-\delta(r-r'), \quad (3)$$

where the inhomogeneous term is the two-dimensional Dirac delta-function. Applying Green's second scalar identity to $\psi(r)$ and $G(r,r')$, we obtain

$$\int_v[G(r',r)(\nabla'^2+k^2)\psi(r')-\psi(r')(\nabla'^2+k^2)G(r',r)]d\tau =\int_{s_1+s_2}\left[G(r',r)\frac{\partial}{\partial n'}\psi(r')-\psi(r')\frac{\partial}{\partial n'}G(r',r)\right]ds', \quad (4)$$

where the derivative in the surface integral is taken in the direction of the outward normal (Fig. 2). The surface integral extends over the surface of the scattering cylinder, s_1, and a concentric cylinder, s_2, of very large radius. In view of (2) and (3) the volume integral becomes $\psi(r)$, and since $\psi(r)=0$ when r lies on the scattering cylinder, it follows that

$$\psi(r)=\int_{s_1}G(r',r)\frac{\partial}{\partial n'}\psi(r')ds' +\int_{s_2}\left[G(r',r)\frac{\partial}{\partial n'}\psi(r')-\psi(r')\frac{\partial}{\partial n'}G(r',r)\right]ds'. \quad (5)$$

Recalling that $\psi(r)=\psi^{inc}(r)+\psi^{sc}(r)$, the integral over s_2

[2] H. Levine and J. Schwinger, "On the theory of diffraction by an aperture in an infinite plane screen, I," Phys. Rev. 74, 958–974 (1948).

[3] H. Levine and J. Schwinger, "On the theory of diffraction by an aperture in an infinite plane screen, II," Phys. Rev. 75, 1423–1432 (1949).

in (5) becomes

$$\int_{s_2}\left[G(r',r)\frac{\partial}{\partial n'}\psi^{\text{inc}}(r')-\psi^{\text{inc}}(r')\frac{\partial}{\partial n'}G(r',r)\right]ds'$$

$$+\int_{s_2}\left[G(r',r)\frac{\partial}{\partial n'}\psi^{sc}(r')-\psi^{sc}(r')\frac{\partial}{\partial n'}G(r',r)\right]ds'.$$

The first integral yields $\psi^{\text{inc}}(r)$ and the second disappears due to the asymptotic behavior of the integrand for $r'\to\infty$, and (5) takes the form

$$\psi(r)=\psi^{\text{inc}}(r)+\int_{s_1}G(r',r)\frac{\partial}{\partial n'}\psi(r')ds'. \tag{6}$$

Since $(\partial/\partial n')\psi(r')=-(\partial/\partial\rho')E_z(\rho',\phi')=i\omega\mu H_\phi(\rho',\phi')$ and $ds'=ad\phi'$, (6) becomes

$$\psi(\rho,\phi)=\psi^{\text{inc}}(\rho,\phi)$$

$$+\int_0^{2\pi}i\omega\mu H_\phi(a,\phi')G(a,\phi';\rho,\phi)\cdot ad\phi'. \tag{7}$$

$H_\phi(a,\phi')$ is numerically equal to the surface-current density at the point (a,ϕ') on the cylinder. Let $I_{\phi_1}(\phi')=i\omega\mu aH_\phi(a,\phi')$, where $I_{\phi_1}(\phi')$ is proportional to the current density at the point (a,ϕ') due to the incident wave (1) propagating in the direction ϕ_1. With this notation, (7) becomes

$$\psi(\rho,\phi)=\psi^{\text{inc}}(\rho,\phi)+\int_0^{2\pi}I_{\phi_1}(\phi')G(a,\phi';\rho,\phi)d\phi'. \tag{8}$$

Since $\psi(a,\phi)=0$, i.e., E_z must disappear at the surface of the cylinder, the following integral equation is obtained by placing $\rho=a$ in (8):

$$0=\psi^{\text{inc}}(\rho,\phi)+\int_0^{2\pi}I_{\phi_1}(\phi')G(a,\phi';a,\phi)d\phi'$$

or

$$-\exp[ika\cos(\phi-\phi_1)]=\int_0^{2\pi}I_{\phi_1}(\phi')G(a,\phi';a,\phi)d\phi'. \tag{9}$$

The solution of this integral equation would yield $I_{\phi_1}(\phi)$, i.e., the current except for a numerical factor, produced by a plane incident wave traveling in the direction ϕ_1. By substituting this solution back into (8) and carrying out the indicated integration, the diffracted field $\psi(\rho,\phi)$ could be determined. Two objections are immediately apparent, the first is the difficult problem of solving (9) for $I_{\phi_1}(\phi')$, the second is the evaluation of the integral in (8) once $I_{\phi_1}(\phi')$ is determined. Moreover, to obtain the total scattering cross section, still another integration would have to be performed. Use will be made of the integral equation (9) to formulate a variational principle for the scattered wave amplitude.

III. VARIATIONAL PRINCIPLE FOR SCATTERED WAVE AMPLITUDE

Since the two-dimensional Green's function, $G(r,r')$, has to satisfy the inhomogeneous wave equation (3) and the radiation condition, i.e., it must represent at large distances from the cylinder outwardly propagating cylindrical waves, it follows that $G(r,r')=(i/4)H_0\times(k|r-r'|)$. For large r, the leading term of the asymptotic expansion is

$$r\to\infty:\quad G(r,r')$$

$$\sim\frac{i}{4}\left(\frac{2}{\pi k|r-r'|}\right)^{\frac{1}{2}}\exp(ik)|r-r'|\exp\left(-i\frac{\pi}{4}\right),$$

where

$$|r-r'|=[\rho^2+\rho'^2-2\rho\rho'\cos(\phi-\phi')]$$

$$\to\rho\left(1-\frac{\rho'}{\rho}\cos(\phi-\phi')\right).$$

With these asymptotic values the scattered field, which is given by the integral in (8), at large distances becomes

$$\psi^{sc}(\rho,\phi)\sim\frac{i}{4}\left(\frac{2}{\pi ik\rho}\right)^{\frac{1}{2}}\exp(ik\rho)$$

$$\times\left[\int_0^{2\pi}\exp[-ika\cos(\phi-\phi')]I_{\phi_1}(\phi')d\phi'\right].$$

The scattered wave amplitude is represented by the quantity in square brackets. We denote it by $A(\phi,\phi_1)$:

$$A(\phi,\phi_1)=\int_0^{2\pi}\exp[-ika\cos(\phi-\phi')]I_{\phi_1}(\phi')d\phi'. \tag{10}$$

As the notation explicitly denotes, $A(\phi,\phi_1)$ is the scattered wave amplitude in the direction ϕ for an incident wave traveling in the direction ϕ_1.

Multiplication of the integral equation (9) by $I_{\phi_2}(\phi)$ and integration with respect to ϕ (in accordance with the notation that $I_{\phi_2}(\phi)$ is $i\omega\mu a$ times the surface-current density at the point (a,ϕ) due to an incident plane wave traveling in the direction ϕ_2) leads to

$$-\int_0^{2\pi}\exp[ika\cos(\phi-\phi_1)]I_{\phi_2}(\phi)d\phi$$

$$=\int_0^{2\pi}\int_0^{2\pi}d\phi I_{\phi_2}(\phi)G(a,\phi';a,\phi)I_{\phi_1}(\phi')d\phi'. \tag{11}$$

But according to (10),

$$\int_0^{2\pi}\exp[ika\cos(\phi-\phi_1)]I_{\phi_2}(\phi)d\phi$$

$$=\int_0^{2\pi}\exp[-ika\cos(\pi+\phi_1-\phi)]I_{\phi_2}(\phi)d\phi$$

$$=A(\pi+\phi_1,\phi_2). \tag{12}$$

$A(\pi+\phi_1,\phi_2)$ represents the scattered wave amplitude in the direction of $\pi+\phi_1$ due to an incident wave traveling in the direction ϕ_2, and it is clear that it must equal the scattered wave amplitude in the direction $\pi+\phi_2$ due to an incident wave traveling in the direction ϕ_1. This reciprocity relation is given by the equality,

$$A(\pi+\phi_1,\phi_2)=A(\pi+\phi_2,\phi_1). \tag{13}$$

Dividing (11) by

$$\int_0^{2\pi}\exp[ika\cos(\phi-\phi_1)]I_{\phi_2}(\phi)d\phi \times\int_0^{2\pi}\exp[ika\cos(\phi-\phi_2)]I_{\phi_1}(\phi)d\phi,$$

and taking into consideration (12) and (13),

$$\frac{1}{A(\pi+\phi_2,\phi_1)}=\frac{1}{A(\pi+\phi_1,\phi_2)}=-\frac{\int_0^{2\pi}\int_0^{2\pi}d\phi I_{\phi_2}(\phi)G(a,\phi';a,\phi)I_{\phi_1}(\phi')d\phi'}{\int_0^{2\pi}\exp[ika\cos(\phi-\phi_1)]I_{\phi_2}(\phi)d\phi\int_0^{2\pi}\exp[ika\cos(\phi-\phi_2)]I_{\phi_1}(\phi)d\phi}. \tag{14}$$

The expression (14) is homogeneous in $I_{\phi_1}(\phi)$, $I_{\phi_2}(\phi)$ and stationary with respect to independent first-order variations about their correct values (determined by integral equations of the form (9)). The property of homogeneity is clear. To show the stationary property of (14), proceed as follows. Clearing fractions in (14),

$$\int_0^{2\pi}\exp[ika\cos(\phi-\phi_1)]I_{\phi_2}(\phi)d\phi \times\int_0^{2\pi}\exp[ika\cos(\phi-\phi_2)]I_{\phi_1}(\phi)d\phi =-A\int_0^{2\pi}\int_0^{2\pi}d\phi I_{\phi_2}(\phi)G(\phi,\phi')I_{\phi_1}(\phi')d\phi',$$

where $A\equiv A(\pi+\phi_1,\phi_2)$, $G(\phi',\phi)\equiv G(a,\phi';a,\phi)$. Now take the variations of $I_{\phi_2}(\phi)$, $I_{\phi_1}(\phi)$, and A.

$$\int_0^{2\pi}\exp[ika\cos(\phi-\phi_1)]\delta I_{\phi_2}(\phi)d\phi \times\int_0^{2\pi}\exp[ika\cos(\phi-\phi_2)]I_{\phi_1}(\phi)d\phi +\int_0^{2\pi}\exp[ika\cos(\phi-\phi_1)]I_{\phi_2}(\phi)d\phi \times\int_0^{2\pi}\exp[ika\cos(\phi-\phi_2)]\delta I_{\phi_1}(\phi)d\phi_1$$
$$=-\delta A\int_0^{2\pi}\int_0^{2\pi}d\phi I_{\phi_2}(\phi)G(\phi,\phi')I_{\phi_1}(\phi')d\phi' -A\int_0^{2\pi}\int^{2\pi}d\phi\delta I_{\phi_2}(\phi)G(\phi,\phi')I_{\phi_1}(\phi')d\phi' -A\int_0^{2\pi}\int_0^{2\pi}d\phi I_{\phi_2}(\phi)G(\phi,\phi')\delta I_{\phi_1}(\phi')d\phi'.$$

Using (12) and (13) this can be written in the form

$$A\int_0^{2\pi}\exp[ika\cos(\phi-\phi_1)]\delta I_{\phi_2}(\phi)d\phi +A\int_0^{2\pi}\exp[ika\cos(\phi-\phi_2)]\delta I_{\phi_1}(\phi)d\phi$$
$$=-\delta A\int_0^{2\pi}\int_0^{2\pi}d\phi I_{\phi_2}(\phi)G(\phi,\phi')I_{\phi_1}(\phi')d\phi' -A\int_0^{2\pi}\int_0^{2\pi}d\phi\delta I_{\phi_2}(\phi)G(\phi,\phi')I_{\phi_1}(\phi')d\phi' -A\int_0^{2\pi}\int_0^{2\pi}d\phi I_{\phi_2}(\phi)G(\phi,\phi')\delta I_{\phi_1}(\phi')d\phi'.$$

Combining terms, this equation becomes

$$\delta A\int_0^{2\pi}\int_0^{2\pi}d\phi I_{\phi_2}(\phi)G(\phi,\phi')I_{\phi_1}(\phi')d\phi' =-A\int_0^{2\pi}d\phi\delta I_{\phi_2}(\phi)\Big[\int_0^{2\pi}d\phi'G(\phi,\phi')I_{\phi_1}(\phi') +\exp[ika\cos(\phi-\phi_1)]\Big]-A\int_0^{2\pi}d\phi'\delta I_{\phi_1}(\phi') \Big[\int_0^{2\pi}d\phi G(\phi,\phi')I_{\phi_2}(\phi) +\exp[ika\cos(\phi'-\phi_2)]\Big]. \tag{15}$$

If $I_{\phi_1}(\phi)$ and $I_{\phi_2}(\phi)$ satisfy integral equations of the form (9), then the square-bracket terms in (15) vanish identically. Hence A is stationary with respect to first-order independent variations of $I_{\phi_1}(\phi)$ and $I_{\phi_2}(\phi)$.

IV. A THEOREM CONCERNING THE TOTAL SCATTERING CROSS SECTION AND SCATTERED WAVE AMPLITUDE

The total scattering cross section is defined by the ratio of the total scattered power per unit length of

cylinder to the incident power per unit area. The time-average incident power per unit area, $\bar{S}^{inc}$, is given by $\frac{1}{2}\,\mathrm{Re}E\times H^*=\frac{1}{2}\,\mathrm{Re}E^*\times H$, where the asterisk indicates the conjugate complex and Re the real part. Since

$$E_z^{inc}=\exp(ikz)$$

and

$$H_y^{inc}=\frac{1}{i\omega\mu}\frac{\partial}{\partial z}E_z^{inc}=\frac{k}{\omega\mu}\exp(ikz),$$

then

$$\bar{S}^{inc}=\tfrac{1}{2}\,\mathrm{Re}E_z^{*inc}H_y^{inc}=\frac{k}{2\omega\mu}.$$

The time-average scattered power, $\bar{P}^{sc}$, passing through a cylinder s_2 of large radius is equal to the time-average power leaving the cylindrical surface s_1, i.e.,

$$\bar{P}^{sc}=\mathrm{Re}\int_{s_2}\tfrac{1}{2}(E_z^{sc}(\rho,\phi))(-H_\phi^{sc}(\rho,\phi))\rho d\phi$$

$$=\mathrm{Re}\int_{s_1}\tfrac{1}{2}(E_z^{sc}(a,\phi))(-H_\phi^{sc}(a,\phi))ad\phi.$$

The total scattering cross section, σ, is then given by the expression

$$\sigma=\frac{\bar{P}^{sc}}{\bar{S}^{inc}}=\frac{1}{k}\,\mathrm{Re}\frac{1}{i}\int_0^{2\pi}E_z^{*sc}(a,\phi)\frac{\partial}{\partial\rho}E_z^{sc}(a,\phi)ad\phi. \quad (16)$$

At the surface of the cylinder, $E_z^{*sc}(a,\phi)=-E_z^{*inc}(a,\phi)$; hence

$$\sigma=\frac{1}{k}\,\mathrm{Re}\frac{1}{i}\int_0^{2\pi}-E_z^{*inc}(a,\phi)\frac{\partial}{\partial\rho}[E_z(a,\phi)-E_z^{inc}(a,\phi)]ad\phi.$$

But

$$\int_0^{2\pi}E_z^{*inc}(a,\phi)\frac{\partial}{\partial\rho}E_z^{inc}(a,\phi)ad\phi=0,$$

and consequently

$$\sigma=\frac{1}{k}\,\mathrm{Re}\frac{1}{i}\int_0^{2\pi}\exp[-ika\cos(\phi-\phi_1)]I_{\phi_1}(\phi)d\phi, \quad (17)$$

where use has been made of $a(\partial/\partial\rho)E_z(a,\phi)=-i\omega\mu aH_\phi\times(a,\phi)=-I_{\phi_1}(\phi)$. In view of (10) and (17) σ can be represented in terms of the scattered wave amplitude:

$$\sigma=\frac{1}{k}\,\mathrm{Re}\frac{1}{i}A(\phi_1,\phi_1)=\frac{1}{k}\,\mathrm{Im}A(\phi_1,\phi_1), \quad (18)$$

where Im means imaginary part.

V. LOW FREQUENCY SCATTERING CROSS SECTION

To find the total scattering cross section it is necessary first to compute $A(\phi_1,\phi_1)$ from (14) and then to use (18). Let $\phi_1=0$ and $\phi_2=\pi$ in (14); then

$$\frac{1}{A(\pi,\pi)}=-\frac{\int_0^{2\pi}\int_0^{2\pi}d\phi I_\pi(\phi)G(a,\phi';a,\phi)I_0(\phi')d\phi'}{\int_0^{2\pi}\exp(ika\cos\phi)I_\pi(\phi)d\phi\int_0^{2\pi}\exp(-ika\cos\phi)I_0(\phi)d\phi}. \quad (19)$$

At low frequencies $ka\ll1$; also choose $I_\pi(\phi)=I_0(\phi)=1$. The numerator then becomes

$$\int_0^{2\pi}\int_0^{2\pi}d\phi G(a,\phi';a,\phi)d\phi'=\frac{i}{4}\int_0^{2\pi}\int_0^{2\pi}d\phi d\phi' H_0(k|r-r'|)$$

$$=\frac{i}{4}\int_0^{2\pi}\int_0^{2\pi}d\phi d\phi'\sum_{m=0}^{\infty}\epsilon_m J_m(ka)H_m^{(1)}(ka)\cos m(\phi-\phi')$$

$$=i\pi^2J_0(ka)H_0(ka).$$

and

$$\int_0^{2\pi}\exp(ika\cos\phi)d\phi=2\pi J_0(ka),$$

$$\int_0^{2\pi}\exp(-ika\cos\phi)d\phi=2\pi J_0(ka).$$

Consequently

$$\frac{1}{A(\pi,\pi)}=-\frac{i\pi^2J_0(ka)H_0(ka)}{[2\pi J_0(ka)]^2}=-\frac{i}{4}\frac{H_0(ka)}{J_0(ka)},$$

and

$$\sigma=-\frac{4}{k}\frac{J_0^2(ka)}{J_0^2(ka)+N_0^2(ka)}. \quad (20)$$

Suppose, instead of taking $I_\pi(\phi)=I_0(\phi)=1$, the following more general representation is used:

$$I_0(\phi)=\sum_0^\infty A_m\cos m\phi,$$

$$I_\pi(\phi)=\sum_0^\infty A_m\cos m(\phi-\pi)=\sum_0^\infty A_m(-1)^m\cos m\phi,$$

where the A_m's are constants. Substitution in (19) gives for the numerator:

$$\int_0^{2\pi}\int_0^{2\pi}d\phi I_\pi(\phi)G(a,\phi';a,\phi)I_0(\phi')d\phi'$$

$$=\frac{i}{4}\int_0^{2\pi}\int_0^{2\pi}d\phi d\phi'\left(\sum_{m=0}^{\infty}A_m(-1)^m\cos m\phi\right)$$

$$\times\left(\sum_{p=0}^{\infty}\epsilon_p J_p(ka)H_p^{(1)}(ka)\cos p(\phi-\phi')\right)$$

$$\times\left(\sum_{n=0}^{\infty}A_n\cos n\phi'\right).$$

Let

$$C_{mn}=(-1)^m\frac{i}{4}\int_0^{2\pi}\int_0^{2\pi}d\phi d\phi'\cos m\phi \times\left(\sum_{p=0}^{\infty}\epsilon_p J_p(ka)H_p^{(1)}(ka)\cos p(\phi-\phi')\right)\cos n\phi'.$$

But

$$\int_0^{2\pi}\int_0^{2\pi}d\phi d\phi'\cos m\phi\cos p(\phi-\phi')\cos n\phi'=\frac{4\pi^2\delta_p{}^n\delta_p{}^m}{\epsilon_p{}^2},$$

where

$$\delta_n{}^m=\begin{cases}1 & m=n\\ 0 & m\neq n\end{cases}\quad\text{and}\quad \epsilon_m=\begin{cases}1 & m=0\\ 2 & m\geq 1\end{cases},$$

and hence

$$C_{mn}=\frac{(-1)^m i\pi^2}{(\epsilon_m)}\delta_n{}^m J_m(ka)H_m^{(1)}(ka).$$

The numerator becomes the double series,

$$\sum_{m=0}^{\infty}\sum_{n=0}^{\infty}A_m C_{mn}A_n.$$

For the denominator the following is obtained:

$$\int_0^{2\pi}\exp(ika\cos\phi)I_\pi(\phi)d\phi\int_0^{2\pi}\exp(-ika\cos\phi)I_0(\phi)d\phi$$

$$=\int_0^{2\pi}\exp(ika\cos)\phi\sum_{m=0}^{\infty}A_m(-1)^m\cos m\phi d\phi$$

$$\times\int_0^{2\pi}\exp(-ika\cos)\phi\sum_{n=0}^{\infty}A_n\cos n\phi d\phi$$

$$=\left(\sum_{m=0}^{\infty}A_m(-1)^m 2\pi(i)^m J_m(ka)\right)\times\left(\sum_{n=0}^{\infty}A_n 2\pi(-i)^m J_n(ka)\right).$$

By setting $B_m=2\pi(-i)^m J_m(ka)$, it follows that

$$\frac{1}{A(\pi,\pi)}=-\frac{\sum_{m=0}^{\infty}\sum_{n=0}^{\infty}A_m C_{mn}A_n}{\left(\sum_{l=0}^{\infty}A_l B_l\right)^2}. \tag{21}$$

In view of the stationary character of $A(\pi,\pi)$, differentiation of (21) with respect to A_m gives

$$A(\pi,\pi)\sum_{n=0}^{\infty}A_n C_{mn}=-B_m\sum_{n=0}^{\infty}A_n B_n,\quad m=0,1,2,\cdots \tag{22}$$

To simplify (22) the coefficients D_n are introduced so that

$$A(\pi,\pi)=-\sum_{n=0}^{\infty}B_n D_n, \tag{23}$$

where the D_n's are determined by the simultaneous equations

$$\sum_{n=0}^{\infty}C_{mn}D_n=B_m,\quad m=0,1,2,\cdots \tag{24}$$

Since $C_{mn}=0$ when $m\neq n$ only the diagonal terms of (24) are different from zero, i.e., $D_n=B_n/C_{nn}$, and hence

$$A(\pi,\pi)=-\sum_{n=0}^{\infty}\frac{B_n{}^2}{C_{nn}}=\sum_{n=0}^{\infty}\frac{(\epsilon_n 2\pi(-i)^n J_n(ka))^2}{i\pi^2(-1)^n J_n(ka)H_n^{(1)}(ka)}$$

$$=4i\sum_{n=0}^{\infty}\epsilon_n\frac{J_n(ka)}{H_n^{(1)}(ka)}. \tag{25}$$

Applying the theorem (18) to (25) the total scattering cross section is obtained. It is

$$\sigma=-\frac{4}{k}\sum_{n=0}^{\infty}\frac{\epsilon_n J_n{}^2(ka)}{J_n{}^2(ka)+N_n{}^2(ka)}, \tag{26}$$

where use has been made of the form $H_n^{(1)}(ka)=J_n(ka)+iN_n(ka)$. Since $ka\ll 1$, only the first term of (26) contributes appreciably to the value of σ. Therefore

$$\sigma=-\frac{4}{k}\frac{J_0{}^2(ka)}{J_0{}^2(ka)+N_0{}^2(ka)}. \tag{27}$$

Comparing (20) with (27) it is seen that the expressions are identical. It appears that for low frequencies ($ka\ll 1$) very accurate results are obtained by taking the current on the cylinder to be independent of ϕ.

VI. HIGH FREQUENCY SCATTERING CROSS SECTION

Now consider the frequency of the incident wave to be high, i.e., $ka\gg 1$. In (14) let $\phi_1=3\pi/2$, $\phi_2=\pi/2$, and for this choice the following result is obtained:

$$\frac{1}{A\left(\pi+\frac{3\pi}{2},\frac{\pi}{2}\right)}=-\frac{\int_0^{2\pi}\int_0^{2\pi}d\phi I_{\pi/2}(\phi)G(a,\phi';a,\phi)I_{3\pi/2}(\phi')d\phi'}{\int_0^{2\pi}\exp\left[ika\cos\left(\phi-\frac{3\pi}{2}\right)\right]I_{\pi/2}(\phi)d\phi\int_0^{2\pi}\exp\left[ika\cos\left(\phi-\frac{\pi}{2}\right)\right]I_{3\pi/2}(\phi)d\phi}. \tag{28}$$

In accordance with the assumed convention, $I_{\pi/2}(\phi)$ and $I_{3\pi/2}(\phi)$ are proportional to the surface currents induced by incident waves propagating in the directions $\pi/2$ and $3\pi/2$ respectively. For an incident wave propagating in the direction ϕ_1, $H_z^{\text{inc}}(\rho,\phi)=-(k/\omega\mu)\times\cos(\phi-\phi_1)\exp[ik\rho\cos(\phi-\phi_1)]$. It is assumed that the high frequency current induced by a plane wave is different from zero only on the illuminated half of the cylinder, where its value is numerically equal to the tangential component of the incident magnetic field. That is, for a trial function we take

$$I_{\phi_1}(\phi)=\text{const.}\cos(\phi-\phi_1)\exp[ika\cos(\phi-\phi_1)]. \quad (29)$$

Hence,

$$I_{\pi/2}(\phi)=\text{const.}\sin\phi\exp[ika\sin\phi] \text{ for } \pi\leq\phi\leq 2\pi$$
$$=0 \text{ for } 0\leq\phi\leq\pi,$$

and

$$I_{3\pi/2}(\phi)=-\text{const.}\sin\phi\exp[-ika\sin\phi] \text{ for } 0\leq\phi\leq\pi$$
$$=0 \text{ for } \pi\leq\phi\leq 2\pi.$$

Substituting these trial functions in (28) and noting that $A(\pi+3\pi/2,\pi/2)=A(\pi/2,\pi/2)$, we get

$$\frac{1}{A\left(\frac{\pi}{2},\frac{\pi}{2}\right)}=-\frac{\int_0^{\pi}d\phi'\sin\phi'\exp[-ika\sin\phi']\int_{\pi}^{2\pi}\sin\phi\exp(ika\sin\phi)G(a,\phi';a,\phi)}{\int_{\pi}^{2\pi}\sin\phi d\phi\int_0^{\pi}\sin\phi d\phi}.$$

Since

$$G(a,\phi';a,\phi)=\frac{i}{4}H_0^{(1)}\left(2ka\left|\sin\left(\frac{\phi-\phi'}{2}\right)\right|\right),$$

then

$$\frac{1}{A\left(\frac{\pi}{2},\frac{\pi}{2}\right)}=\frac{i}{16}\int_0^{\pi}d\phi'\int_{\pi}^{2\pi}d\phi\sin\phi'\sin\phi\exp[-ika(\sin\phi'-\sin\phi)]H_0^{(1)}\left(2ka\left|\sin\left(\frac{\phi-\phi'}{2}\right)\right|\right). \quad (30)$$

Let $\phi=2\pi-\xi$. Then $\sin\phi=-\sin\xi$, $d\phi=-d\xi$, and

$$\left|\sin\left(\frac{\phi-\phi'}{2}\right)\right|=\left|\sin\left(\frac{\xi+\phi'}{2}\right)\right|.$$

With this change of variables (30) becomes*

$$\frac{1}{A\left(\frac{\pi}{2},\frac{\pi}{2}\right)}=-\frac{i}{16}\int_0^{\pi}d\phi'\int_0^{\pi}d\xi\sin\phi'\sin\xi$$
$$\times\exp[-ika(\sin\phi'+\sin\xi)]H_0^{(1)}\left(2ka\left|\sin\left(\frac{\xi+\phi'}{2}\right)\right|\right).$$

Let the variables be changed again according to the following transformation

$$(\phi'+\xi^2)/2=\beta+\pi/2, \quad (\phi'-\xi)/2=\alpha.$$

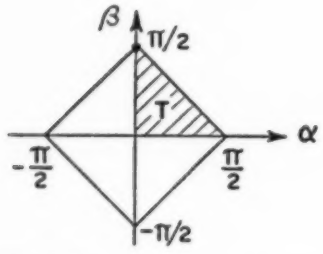

FIG. 3. Integration domain.

Then

$$\sin\phi'\sin\xi=\tfrac{1}{2}(\cos 2\alpha+\cos 2\beta), \quad \sin\phi'+\sin\xi=2\cos\alpha\cos\beta,$$
$$\frac{\partial(\phi',\xi)}{\partial(\alpha,\beta)}=2, \quad \text{and} \quad |\sin((\xi+\phi')/2)|=\cos\beta.$$

It follows that in terms of α and β,

$$\frac{1}{A\left(\frac{\pi}{2},\frac{\pi}{2}\right)}=-\frac{i}{16}\iint_Q\exp(-2ika\cos\alpha\cos\beta)$$
$$\times(\cos^2\alpha+\cos 2\beta)H_0^{(1)}(2ka\cos\beta), \quad (31)$$

where Q is the square region in the α, β plane shown in Fig. 3. In view of the symmetry in α and β about $\alpha=\beta=0$, we can confine the integration to the triangular region T, Consequently,

$$\frac{1}{A\left(\frac{\pi}{2},\frac{\pi}{2}\right)}=-\frac{i}{4}\int_0^{\pi/2}d\beta\int_0^{\pi/2-\beta}d\alpha\exp(-2ika\cos\alpha\cos\beta)$$
$$\times(\cos 2\alpha+\cos 2\beta)H_0^{(1)}(2kR\cos\beta). \quad (32)$$

Consider first the integration with respect to α. Since $ka\gg 1$, the main contribution to the value of this integral occurs in the neighborhood of $\alpha=0$ (provided $\beta\neq\pi/2$). An approximate evaluation is obtained by

* The author received enlightening discussions on integrals of this class from Professor F. Tricomi.

the method of stationary phase:

$$\int_0^{\pi/2-\beta} d\alpha \exp(-2ika\cos\alpha\cos\beta)(\cos2\alpha+\cos2\beta)$$
$$=\left(\frac{\pi}{ka}\right)^{\frac{1}{2}}\frac{\cos^2\beta}{(\cos\beta)^{\frac{1}{2}}}\exp(-2ika\cos\beta)\exp\left(i\frac{\pi}{4}\right).$$

There remains the task of evaluating the following integral:

$$\frac{1}{A\left(\frac{\pi}{2},\frac{\pi}{2}\right)}=-\frac{i}{4}\left(\frac{\pi}{ka}\right)^{\frac{1}{2}}\exp\left(i\frac{\pi}{4}\right)\int_0^{\pi/2}d\beta\frac{\cos^2\beta}{(\cos\beta)^{\frac{1}{2}}}$$
$$\times\exp[-2ika\cos\beta]H_0^{(1)}(2ka\cos\beta). \quad (33)$$

As $\beta\to\pi/2$ the integrand disappears, and hence the contribution to the integral in the neighborhood of $\beta=\pi/2$ is very small. When $\beta\neq\pi/2$ and $ka\to\infty$,

$$H_0^{(1)}(2ka\cos\beta)$$
$$\sim\left(\frac{2}{2\pi ka\cos\beta}\right)^{\frac{1}{2}}\exp(2ika\cos\beta)\exp(-i\pi/4). \quad (34)$$

After substituting this asymptotic form into (33) and changing the upper limit from $\pi/2$ to β_0, the result is

$$\frac{1}{A(\pi/2,\pi/2)}\sim-\frac{i}{4}\frac{1}{ka}\int_0^{\beta_0}d\beta\cos\beta=-\frac{i}{4ka}\sin\beta_0 \quad (35)$$

for the leading term of the asymptotic development of $[1/A(\pi/2,\pi/2)]$ in reciprocal powers of ka. Application of the theorem (18) to (35) gives for the total scattering cross section

$$\sigma=\frac{1}{k}\operatorname{Im}A\left(\frac{\pi}{2},\frac{\pi}{2}\right)\sim\frac{4a}{\sin\beta_0}=\frac{4a}{(1-(4/ka)^2)^{\frac{1}{2}}}. \quad (36)$$

Choose β_0 such that $\cos\beta_0=4/ka$. This choice guarantees the argument of the Hankel function to be equal to or greater than 8 for the entire range of values from $\beta=0$ to $\beta=\beta_0$, and thereby allows the replacement of the Hankel function by the first term of its asymptotic development. It is seen that as $ka\to\infty$, $\sigma\to4a$ which is the geometric optics scattering cross section and physically equal to twice the projected area of a unit length of the scattering cylinder. Figure 4 shows a plot of σk *versus* ka. For values of ka less than 10, Eq. (26) was used to compute σk; for ka larger than 8, Eq. (36) was used. In the region $8<ka<10$ the broken and solid curves overlap.

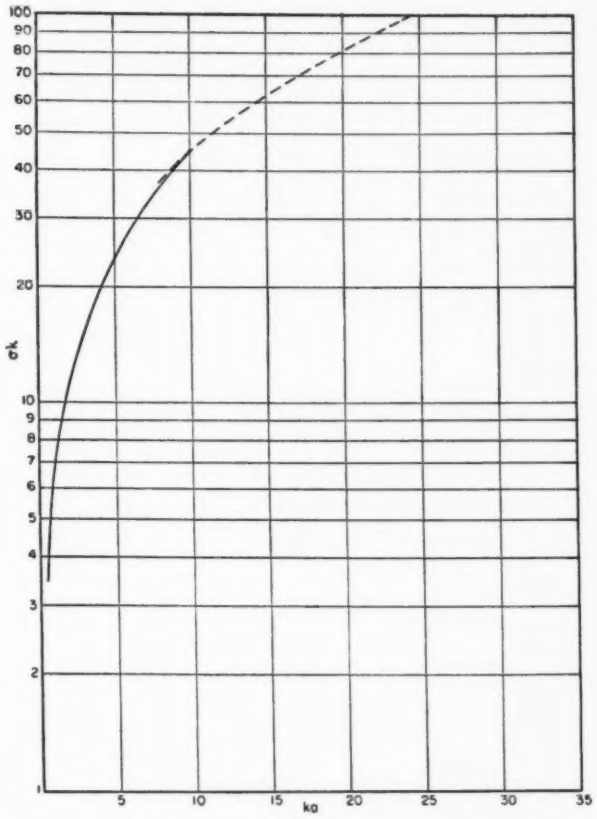

FIG. 4. σk *versus* ka. Solid curve computed from (26). Broken curve computed from (36).

The author wishes to acknowledge the generous help of Dr. Harold Levine of Harvard University, without whose patient and clear explanations this paper would never have been completed. The assistance of Miss J. Klimas and Mrs. R. Stokey with numerical calculations is gratefully acknowledged.

Air Temperature Modification by Vertical Transport*

ROBERT G. FLEAGLE
University of Washington, Seattle, Washington
(Received October 3, 1949)

It is suggested that when the air temperature increases upward an efficient and economical method for modifying low temperatures near the ground is to force air downward through vertical stacks from the relatively warm air aloft. Theory is developed which shows that the necessary power per unit mass is mainly a function of the air velocity in the stack. The energy required by this method is compared with the energy required to heat the air originally near the ground, and it is shown that under a strong temperature inversion the power method requires considerably less energy than the heating method.

INTRODUCTION

TEMPERATURE modification by a combination of radiational cooling and direct application of heat (both accomplished by smudge pots) is the standard method used by fruit growers in avoiding low nocturnal temperatures near the ground. Under conditions requiring the use of smudge pots the temperature of the air usually increases rapidly with height; at 100–200 feet above the ground the temperature may be 5 to 10° C higher than the temperature near the ground. Recently, this normal temperature inversion has been utilized in modifying the temperatures near the ground; large fans have been set up above the trees to mix the cold and warm air.[1] It appears that a more effective and better controlled method would be to conduct the warm air downward through vertical stacks and exhaust it within the orchard. It is proposed to investigate the energy required for this process and to compare it with the energy required by direct heating. The application to maintenance of outdoor temperature-sensitive installations, machinery, and supplies is obvious.

THEORY

Consider the energy required to force a unit mass of air through a vertical stack at a speed, v_2. Some energy is converted into kinetic energy, some is lost in friction at the sides of the stack, and some is required to overcome the buoyant force experienced by the warm air in being displaced downward into colder air. Where M represents the energy per gram supplied by the fan; F_r, the energy per gram dissipated by friction; and W, the energy per gram required to overcome atmospheric stability, the principle of conservation of energy requires that,

$$M=\tfrac{1}{2}v_2^2+F_r+W. \tag{1}$$

The mass of air passing through the stack per second is given by $\pi r^2\rho v_2$, where ρ represents air density and r represents radius of the stack. We therefore have for the power required of the motor,

$$P(\text{ergs/sec.})=\pi r^2\rho v_2\{\tfrac{1}{2}v_2^2+F_r+W\}. \tag{2}$$

The frictional loss of energy per unit mass in fundamental c.g.s. units is given by the empirical expression,

$$F_r=\frac{fhv_2^2}{4r}, \tag{3}$$

where f represents a dimensionless coefficient depending upon roughness of conduit and the Reynolds number and h represents length of the conduit.[2] Several values of f are shown in Table I below.[3] Table I shows that f is not sensitive to changes in r or v_2 within the ranges applicable to this problem. The single value of 0.02 will be used in future computations.

The work required to bring air down the stack against the buoyant force due to atmospheric stability remains to be computed. Where F represents the net upward

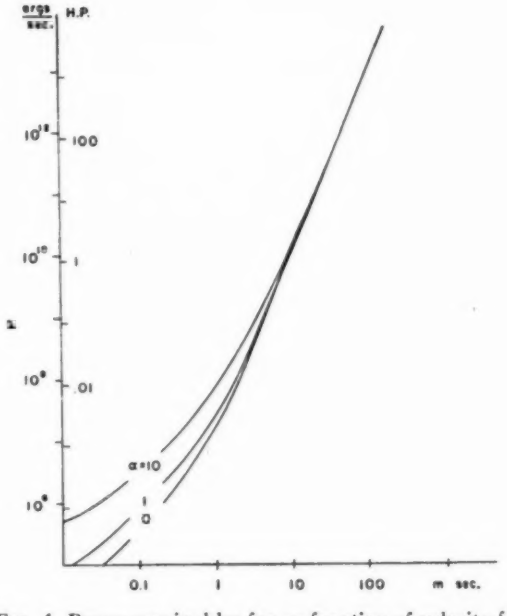

FIG. 1. Power required by fan as function of velocity for $\alpha=0$, 1, $10K/(100\text{ m})$ as computed from Eq. (12).

* Contribution No. 5, Department of Meteorology and Climatology, University of Washington.

[1] R. E. Ahrens, "Breath of steel," *Steelways*, No. 12, 32 (1947).

[2] Am. Soc. Heating and Ventilating Eng., *Heating, Ventilating, Air Conditioning Guide* (Waverly Press, Inc., Baltimore, Maryland, 1949), pp. 807–808.

[3] Computed from (3) using data supplied in Am. Soc. Heating and Ventilating Eng. (see reference 2).

force per gram on the displaced air, we have,

$$W=-\int_h^0 F dz. \tag{4}$$

The net force per gram is given by,

$$F=\frac{\rho-\rho'}{\rho'}g=\frac{(p/RT)-(p/RT')}{p/RT'}g=\frac{T'-T}{T}g, \tag{5}$$

where the prime indicates a property of the moving air, p represents pressure; T, absolute temperature; and R, the gas constant for air. Substitution of (5) in (4) gives,

$$W=-g\int_h^0 \frac{T'-T}{T}dz. \tag{6}$$

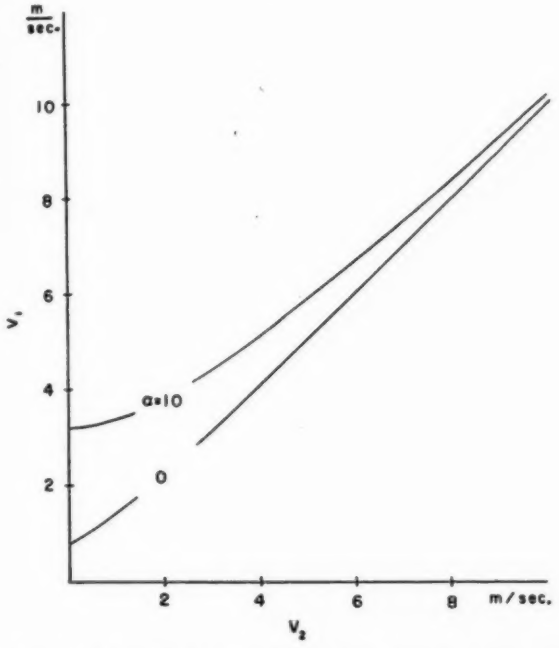

FIG. 2. Air speed within stack, (v_2), as a function of horizontal wind speed at the top of the stack, (v_1) for $\alpha=0$ and $10K/(100\text{ m})$ as computed from Eq. (13).

We shall assume that the temperature in the undisturbed air may be expressed by a linear function of elevation and that the disturbed air neither gains nor loses heat to the stack walls. Thus, the descending air increases in temperature at the adiabatic rate. We may express these assumptions by the following:

$$T=T_0+\alpha z \tag{7}$$

$$T'=T_0+\alpha h+\frac{g}{c_p}(h-z). \tag{8}$$

Equation (6) now may be written, for $\alpha\neq 0$

$$W=-\frac{g(\alpha+(g/c_p))}{\alpha}\int_h^0 \frac{(h-z)\partial z}{(T_0/\alpha)+z}. \tag{9}$$

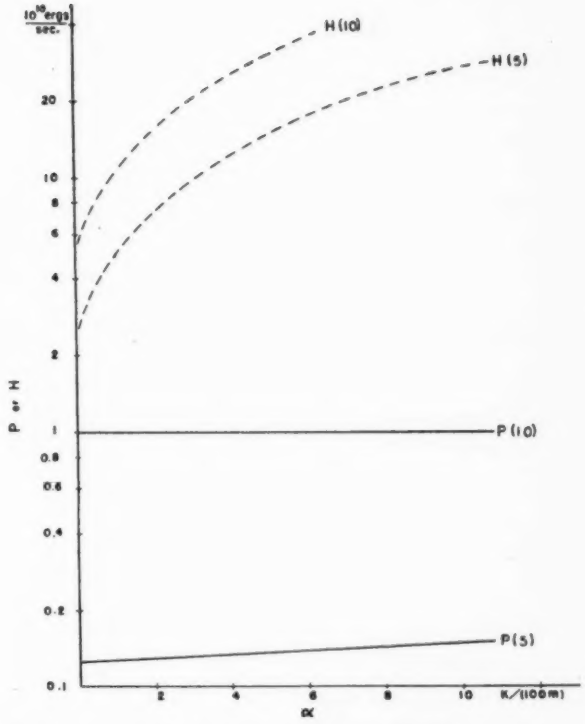

FIG. 3. Power required by fan compared with rate of energy required for heating (H) as function of rate of temperature increase with height (α). The bracketed numbers indicate the air speed within the stack in m/sec.

Integration gives,

$$W=-g\left(1+\frac{g}{\alpha c_p}\right)\left\{-\left(h+\frac{T_0}{\alpha}\right)\log_e\frac{T_h}{T_0}+h\right\}, \tag{10}$$

where T_h represents the temperature at the height of the top of the stack. For purposes of computation it is sufficiently accurate to replace $T_0+\alpha z$ by T_0 in the denominator of (9). This leads to,

$$W=gh^2/2T_0(\alpha+(g/c_p)). \tag{11}$$

Equation (11) holds for $\alpha=0$ since division by α is not required in the integration.

Finally, substituting (3) and (11) in (2) results in,

$$P=\pi r^2\rho v_2\left\{0.5v_2^2(1+0.01h/r)+\frac{gh^2}{2T_0}\left(\alpha+\frac{g}{c_p}\right)\right\}. \tag{12}$$

In order to visualize the relative importance of the individual terms in this rather cumbersome equation, P is plotted as a function of v_2 and α in Fig. 1 using the following arbitrary values:

$r=0.5$ meter
$h=50$ meters
$T_0=270°$ K

Figure 1 shows that within the power range between 0.1 and 100 horsepower the lapse rate does not affect seriously the air speed within the stack.

TABLE I.

r(cm)	v_2(m/sec.)	f
15	2.5	0.022
15	5.1	0.021
15	50.8	0.018
46	2.5	0.019
46	5.1	0.016
46	50.8	0.013

It is of interest to investigate the speed within the stack which is possible without the use of a fan. A horizontal opening at the top of the stack free to rotate so that it always faces the wind stream is assumed. For this case, the kinetic energy of the moving air must be added to the left side of (1) and M set equal to zero. Equation (12) then becomes,

$$0.5v_2^2\left(1+0.01\frac{h}{r}\right)+\frac{gh^2}{2T_0}\left(\alpha+\frac{g}{c_p}\right)=0.5v_1^2. \quad (13)$$

In Fig. 2, v_2 is plotted as a function of v_1 and α using the same arbitrary values listed above. Figure 2 indicates that the air speed within the stack is of the same order of magnitude as the wind speed. It appears that where only a small quantity of air is required, the kinetic energy of the wind at the height of the top of the stack might be sufficient to do the job alone. However, it should be realized that when the wind speed at the top of the stack exceeds about 5 m.p.sec. the resulting mechanical turbulence is likely to prevent the creation of a large temperature inversion. In other words, at high wind speeds the warm air is conducted to the ground without the assistance of fan and stack.

POWER COMPARISON

It is important to compare the energy required to produce at the ground a certain temperature increase by the method described here with the energy required to heat the original air through the same temperature interval. The rate of expenditure of heat required by the latter process may be written,

$$H=\pi r^2\rho v_2 c_p[T_h+(gh/c_p)-T_0]. \quad (14)$$

Substitution of $T_0+\alpha h$ for T_h leads to,

$$H=\pi r^2\rho v_2 c_p h(\alpha+(g/c_p)). \quad (15)$$

This energy requirement may be compared with P by plotting P and H as functions of α for certain arbitrary values of v_2, say 5 and 10 m/sec. In Fig. 3 P and H have been computed for air at sea level using the same values of r, h, and T_0 used before. Inspection of Fig. 3 shows that economy of the power method over the heating method ranges from a factor of about 5 to a factor of about 100. The relative economy varies in a direct sense with the strength of the temperature inversion. Economy of power is greater at the lower velocity (5 m/sec.) than at the higher velocity (10 m/sec.). It follows that maximum efficiency would be attained with fans operating at slow speed in stacks of large radius. Of course the economy in energy expended by the power method must be balanced against the greater cost of mechanical energy. Also, the greater efficiency attained with large stacks must be balanced against the greater initial cost of large stacks. Determination of the economy of cost of installation and operation depends upon local factors beyond the scope of this paper.

Aside from the question of economy, advantages of the power method over the heating method include: greater uniformity in temperature, absence of smoke, gas, and dirt, less attention required, and the possibility of utilizing the kinetic energy of the wind. Disadvantages include: more critical dependence on a large temperature inversion, greater initial expense (unless existing stacks may be used).

ACKNOWLEDGMENT

The writer is indebted to Mr. G. E. Ledbetter of the Department of Aeronautical Engineering for discussing with him the problem of frictional loss of energy.

Mode Conversion Losses in Transmission of Circular Electric Waves through Slightly Non-Cylindrical Guides

SAMUEL P. MORGAN, JR.
Bell Telephone Laboratories, Murray Hill, New Jersey
(Received July 8, 1949)

A general expression is derived for the effective attenuation of circular electric (TE_{01}) waves owing to mode conversions in a section of wave guide whose shape deviates slightly in any specified manner from a perfect circular cylinder. Numerical predictions are in good agreement with experiment for the special case of transmission through an elliptically deformed section of pipe. The effect of random distortions in a long wave guide line is analyzed in terms of the mean-square values of the Fourier coefficients describing the distortions; and from the general formulas it appears that the mode conversion losses depend in large measure upon the statistical distribution of the various types of distortion. Under certain rather arbitrary simplifying assumptions about this distribution, it is calculated that mode conversions in a 4.732-inch copper pipe whose radius deviates by 1 mil r.m.s. from that of an average cylinder will increase the attenuation of the TE_{01} mode at 3.2 cm by an amount equal to 8 percent of the theoretical copper losses. The dependence on frequency of mode conversion losses in such a guide is discussed.

I. INTRODUCTION

THE propagation of electromagnetic energy through a perfectly conducting cylindrical guide may take place at sufficiently high frequencies in any one of a number of independent transmission modes, the field pattern for a given mode being the same, up to phase, at every cross section of the guide. The natural modes in circular and rectangular guides are well known, and it has been shown[1,2] that for a cylindrical guide whose uniform cross section deviates but slightly from circular, the natural modes are only slightly different in field configuration from the corresponding modes for a circular cylinder. If however the size or shape of the cross section varies slightly from point to point, so that the guide is not strictly cylindrical, then although one may still represent the field at any given section by an expansion in terms of the natural modes of a circular cylinder, these modes are no longer independent but coupled to each other by the distortion. Electromagnetic energy in any mode will, on passing through a distorted section of guide, be partially converted into other modes, of which those above cut-off can be expected to propagate through the guide with different phase velocities from the original mode and, in the case of a physical guide, with different attenuations due to the finite conductivity of the walls. Thus the original mode exhibits an increase in effective attenuation owing to mode conversions in the distorted section, provided of course that no other mode is present at a sufficiently high level to return an appreciable amount of energy by reconversion.

Mode conversion losses become of practical importance when one attempts to transmit a mode which has intrinsically low copper loss, such as the lowest order circular electric (TE_{01}) wave in a round pipe, through a guide so large that many other modes are freely propagated at the chosen frequency. It is easy to imagine that in transmission of the TE_{01} mode through commercial copper pipe of diameter several times the wave-length, mode conversion losses might under some conditions be an appreciable fraction of the total loss; and it seems desirable to have a theoretical estimate of the magnitude of this effect. In the present paper we treat the following problem:

A pure TE_{01} wave propagating in the forward direction through a perfectly conducting circular pipe passes through a distorted section, the only restrictions on the form of the distortion being that the deviation from perfect circularity is small compared to the pipe radius, and there are no discontinuities in the surface of the pipe. No real generality is lost by the assumption of infinite conductivity, since to first approximation the losses from the TE_{01} mode due to finite conductivity and due to mode conversions are additive.* The distorted section will in general couple an infinite number of other modes to the circular electric mode; but if this section is of finite length then at sufficient distances on each side of it we shall find only those modes which propagate freely in the original circular pipe, and the power carried in each direction by these propagating modes can be calculated. The power which has been abstracted from the incident TE_{01} mode can be expressed in terms of an effective attenuation or, if desired, in terms of an average attenuation per unit length caused by mode conversions in the distorted section. In the present analysis the mode conversions are supposed to take place either in an infinitely long pipe or in one where each undesired mode is terminated

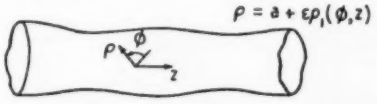

FIG. 1. Longitudinal section of slightly non-cylindrical wave guide.

[1] S. A. Schelkunoff, J. App. Phys. **9**, 484 (1938).
[2] M. Jouguet, Comptes Rendus **266**, 1436 (1948).

* Inhomogeneity in the conductivity of the inner wall of the guide would couple the TE_{01} mode to other modes even if the walls were perfectly smooth and circular; but an order-of-magnitude calculation has shown that for such variations in conductivity as are likely to occur in practice the coupling would be far smaller than the anticipated geometrical mode coupling effects.

in its own characteristic impedance, and it is assumed that the level of unwanted modes never becomes high enough in the distorted pipe so that reconversion from these modes into TE_{01} needs to be taken into account.

Since the following sections of this paper are largely mathematical, it may be well to indicate their contents in advance. In Section II a general formula is derived, to the first order of approximation, for the power scattered into modes other than TE_{01} by an arbitrarily distorted section of pipe. In Section III this formula is applied to a pipe a short section of which has been squeezed into elliptical shape, and good numerical agreement is obtained with experiment. In Section IV we calculate the average mode conversion losses in sections of pipe whose departures from circularity may be described by finite Fourier series with randomly distributed coefficients, and under certain simplifying assumptions we obtain numerical results for a few specific cases. The appendices include certain formal mathematical work and a tabulation of some numerical constants.

II. GENERAL FORMULA FOR MODE CONVERSION LOSSES

Consider a perfectly conducting wave guide (Fig. 1) whose inner surface is defined by

$$\rho=a+\epsilon\rho_1(\varphi,z), \quad 0\leq\varphi\leq 2\pi, \quad -\infty<z<\infty, \qquad (1)$$

where $\rho_1(\varphi,z)$ is a continuous function of φ and z, and ϵ is a small dimensionless parameter such that $\epsilon\rho_1(\varphi,z)$ measures the departure of the guide from perfect circularity at any point. The inward unit normal to the guide surface is given by

$$\mathbf{n}=\mathbf{n}_0+\epsilon\mathbf{n}_1=-\mathbf{e}_\rho+\epsilon[(\partial\rho_1/a\partial\varphi)\mathbf{e}_\varphi+(\partial\rho_1/\partial z)\mathbf{e}_z]$$

up to terms of order ϵ, where $\mathbf{e}_\rho$, $\mathbf{e}_\varphi$, $\mathbf{e}_z$ are unit vectors in the direction of increasing ρ, φ, z respectively.

The electric vector of a possible electromagnetic field in the guide defined by (1) may be taken as

$$\mathbf{E}(\rho,\varphi,z)=\mathbf{E}_0(\rho,\varphi,z)+\epsilon\mathbf{E}_1(\rho,\varphi,z),$$

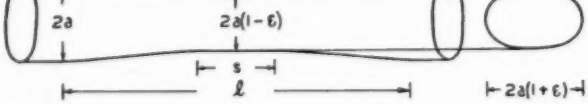

FIG. 2. Longitudinal section of circular guide whose center section has been deformed into elliptical shape.

where all fields are assumed to satisfy Maxwell's equations and to vary harmonically with time. $\mathbf{E}_0$ is chosen to satisfy the appropriate boundary conditions for a conducting cylinder of radius a; in particular it may represent any of the progressive waves which are possible in a circular wave guide. The perturbation field $\mathbf{E}_1$ is chosen so that in the distorted guide the total field satisfies the condition

$$\mathbf{n}\times\mathbf{E}=0 \text{ at } \rho=a+\epsilon\rho_1(\varphi,z). \qquad (2)$$

If we write

$$\mathbf{E}_0(a+\epsilon\rho_1,\varphi,z)=\mathbf{E}_0(a,\varphi,z)+\epsilon\rho_1(\varphi,z)[\partial\mathbf{E}_0(\rho,\varphi,z)/\partial\rho]_{\rho=a},$$

we find that (2) becomes, up to first order in ϵ,

$$[\mathbf{n}\times\mathbf{E}_0]_{a,\varphi,z}+\epsilon[\mathbf{n}_0\times\rho_1\partial\mathbf{E}_0/\partial\rho+\mathbf{n}_0\times\mathbf{E}_1+\mathbf{n}_1\times\mathbf{E}_0]_{a,\varphi,z}=0, \qquad (3)$$

and the zero-order term vanishes automatically since it merely expresses the boundary condition on $\mathbf{E}_0$ in the undistorted guide. If we equate to zero the first order terms in (3) we obtain expressions for the φ- and z-components of $\mathbf{E}_1$ at $\rho=a$ in terms of ρ_1 and the components of $\mathbf{E}_0$ and of their derivatives at $\rho=a$. The relations are somewhat simplified if, as in the present analysis, we take $\mathbf{E}_0$ to be the field of a circular electric wave. Thus if

$$\mathbf{E}_0=E_0(\rho,z)\mathbf{e}_\varphi, \quad \mathbf{E}_0(a,z)=0,$$

then on writing out the components of (3) we have

$$E_{1\varphi}(a,\varphi,z)=-[\rho_1\partial E_0/\partial\rho]_{a,\varphi,z}; \quad E_{1z}(a,\varphi,z)=0. \qquad (4)$$

The problem of determining the fields in a wave guide, given the tangential component of the electric field at the wall, has recently been treated in the literature;[3] we give here a development sufficient for our purpose. The boundary conditions (4) require that the perturbation field be purely transverse electric and hence derivable from a stream function $\Psi_1(\rho,\varphi,z)$ satisfying the wave equation and such that[4]

$$E_{1\rho}=-\partial\Psi_1/\rho\partial\varphi, \quad E_{1\varphi}=\partial\Psi_1/\partial\rho.$$

We write for Ψ_1 a series of the form

$$\Psi_1(\rho,\varphi,z)=\sum_{n=0}^{\infty}\sum_{m=1}^{\infty}A_{nm}\Psi_{nm}(\rho,\varphi,z),$$

where the functions Ψ_{nm} correspond to the natural transverse electric waves in a conducting circular guide; thus [5]

$$\Psi_{nm}(\rho,\varphi,z)=J_n(\chi_{nm}\rho)\begin{matrix}\cos\\ \sin\end{matrix}n\varphi\,\exp(\pm\Gamma_{nm}z),$$

$$\Gamma_{nm}=(\chi_{nm}^2-\beta^2)^{\frac{1}{2}}, \quad \beta=2\pi/\lambda,$$

where λ is the free-space wave-length corresponding to the given frequency and $\chi_{nm}a=k_{nm}$ is the mth positive root of $J_n'(x)=0$. It is shown formally in Appendix I that

$$A_{nm}\Psi_{nm}(\rho,\varphi,z)=(\epsilon_n k_{nm}^2 J_n(\chi_{nm}\rho))/(2\pi\Gamma_{nm}a(k_{nm}^2-n^2)J_n(k_{nm}))\times\int\int E_{1\varphi}(a,\varphi',z')\exp(-\Gamma_{nm}|z-z'|)\times\cos n(\varphi-\varphi')dz'd\varphi', \qquad (5)$$

[3] A. F. Stevenson, J. App. Phys. **19**, 24 (1948), Section II.
[4] S. A. Schelkunoff, *Electromagnetic Waves* (D. van Nostrand Company, Inc., New York, 1943), p. 380.
[5] Reference 4, pp. 389–390.

where φ' and z' are coordinates covering that part of the surface $\rho=a$ on which $E_{1\varphi}$ is different from zero, and where

$$\epsilon_n=\begin{cases}1, & n=0,\\ 2, & n\neq 0.\end{cases}$$

Suppose now that the field $\mathbf{E}_0$ is that of a pure TE_{01} wave traveling in the positive z-direction; i.e.,

$$\Psi_0=AJ_0(\chi_{01}\rho)\exp(-\Gamma_{01}z),$$
$$E_0=-A\chi_{01}J_1(\chi_{01}\rho)\exp(-\Gamma_{01}z),$$
$$[\partial E_0/\partial\rho]_{\rho=a}=-A\chi_{01}{}^2J_0(k_{01})\exp(-\Gamma_{01}z),$$

so that from (4),

$$E_{1\varphi}(a,\varphi,z)=A\chi_{01}{}^2J_0(k_{01})\rho_1(\varphi,z)\exp(-\Gamma_{01}z). \quad (6)$$

Now supposing further that the distorted section of the guide is of finite length l, so that

$$\rho_1(\varphi,z)\equiv 0 \quad \text{for} \quad |z|\geq\tfrac{1}{2}l,$$

we shall find that at sufficient distances from the distorted section the field $\mathbf{E}_1$ consists only of progressive TE_{nm} waves propagating *away* from it. Thus setting

$$\Gamma_{nm}=ih_{nm}=i(\beta^2-\chi_{nm}{}^2)^{\frac{1}{2}}$$

for the waves which are above cut-off, we find from (5) and (6) after some manipulation

$$[A_{nm}\Psi_{nm}]^{\pm}=-iAB_{nm}J_n(\chi_{nm}\rho)[C_{nm}{}^{\pm}\cos n\varphi + S_{nm}{}^{\pm}\sin n\varphi]\exp(\mp ih_{nm}z), \quad (7)$$

$$B_{nm}=\frac{\epsilon_n k_{nm}{}^2k_{01}{}^2J_0(k_{01})}{h_{nm}a(k_{nm}{}^2-n^2)J_n(k_{nm})},$$

$$\begin{matrix}C_{nm}{}^{\pm}\\ S_{nm}{}^{\pm}\end{matrix}=\frac{1}{2\pi a^2}\int_0^{2\pi}\int_{-\frac{1}{2}l}^{\frac{1}{2}l}\rho_1(\varphi',z')\exp(-i(h_{01}\mp h_{nm})z')\times\begin{matrix}\cos\\ \sin\end{matrix}n\varphi'dz'd\varphi'. \quad (8)$$

In these equations the upper signs refer to waves traveling in the positive z direction for $z>\frac{1}{2}l$ and the lower signs to waves traveling in the negative z direction for $z<-\frac{1}{2}l$.

The average power carried past any cross section of the guide by the TE_{nm} mode whose stream function is given by (7) is [6]

$$P_{nm}{}^{\pm}=\frac{\chi_{nm}{}^2h_{nm}}{2\omega\mu}\int_0^{2\pi}\int_0^a|A_{nm}{}^{\pm}\Psi_{nm}{}^{\pm}|^2\rho d\rho d\varphi$$
$$=\frac{1}{\epsilon_n}\frac{\pi h_{nm}}{2\omega\mu}A^2B_{nm}{}^2(k_{nm}{}^2-n^2)J_n{}^2(k_{nm})\times[|C_{nm}{}^{\pm}|^2+|S_{nm}{}^{\pm}|^2],$$

where ω and μ are respectively the angular frequency and the permeability of the medium filling the guide. Since the total power carried by the incident TE_{01} wave is

$$P_0=\frac{\pi h_{01}}{2\omega\mu}A^2k_{01}{}^2J_0{}^2(k_{01}),$$

the relative power in the two "scattered" TE_{nm} waves is

$$\frac{\epsilon^2P_{nm}{}^{\pm}}{P_0}=\epsilon^2D_{nm}[|C_{nm}{}^{\pm}|^2+|S_{nm}{}^{\pm}|^2], \quad (9)$$

where

$$D_{nm}=\frac{\epsilon_nk_{01}{}^2k_{nm}{}^4}{(h_{01}a)(h_{nm}a)(k_{nm}{}^2-n^2)}. \quad (10)$$

The fraction of the total power which is lost from the original TE_{01} wave through mode conversions is

$$\Delta P/P_0=\epsilon^2\sum_{n,m}(P_{nm}{}^{+}+P_{nm}{}^{-})/P_0, \quad (11)$$

where the summation is extended over all the modes which are above cut-off except $TE_{01}{}^{+}$.

The attenuation of the TE_{01} mode caused by mode conversions in the distorted section is evidently just

$$N=-\ln(1-\Delta P/P_0)\approx\Delta P/P_0 \text{ nepers}$$
$$=4.343\Delta P/P_0 \text{ decibels}, \quad (12)$$

where $\Delta P/P_0$ is given by (11). The average attenuation per unit length of distorted section is

$$\alpha=4.343\Delta P/(P_0l) \text{ db/unit length}. \quad (13)$$

TABLE I. Increase in attenuation of TE_{01} mode due to 30 round trips through elliptically distorted section of wave guide.

d_{max}	d_{min}	ϵ	$60N$ (theoretical)	$60N$ (experimental)
4.774″	4.674″	0.0106	1.11 db	0.95 db
4.790″	4.659″	0.0139	1.91 db	1.85 db
4.822″	4.624″	0.0210	4.36 db	4.15 db
4.851″	4.590″	0.0276	7.59 db	8.0 db

III. SHORT ELLIPTICAL SECTION IN CIRCULAR GUIDE

A measurement under controlled conditions of the mode conversion losses exhibited by the TE_{01} wave in a slightly non-circular pipe has been made by A. C. Beck and A. P. King at Bell Telephone Laboratories.[7] Their experiment consisted in placing two steel plates each somewhat more than 6 inches long on opposite sides of the center section of a 2½-foot piece of 5-inch (outside diameter) pipe and applying pressure with C clamps, then measuring the increase in attenuation caused by the pipe as a function of the increase in the major axis of the distorted section over the diameter of the original pipe. It is not difficult to apply the theory of the preceding section to this special case.

Consider a slightly non-cylindrical pipe, as in Fig. 2,

[6] Reference 4, p. 385.

[7] A. C. Beck and A. P. King (unpublished observations).

whose deviation from perfect circularity is given by:

$$\epsilon\rho_1(\varphi,z)=\epsilon a f(z)\cos 2\varphi, \tag{14}$$

$$f(z)=\begin{cases}1, & 0\le|z|\le\frac{1}{2}s;\\ (l-2|z|)/(l-s), & \frac{1}{2}s\le|z|\le\frac{1}{2}l;\\ 0, & |z|\ge\frac{1}{2}l.\end{cases} \tag{15}$$

These equations represent a section of pipe, of length l, which is held with circular pipe clamps at each end and whose center section, of length s, is squeezed into an approximately elliptical shape of the same perimeter as the original pipe, the transition between the clamped ends and the distorted center section being linear. Measurements of the section of pipe used in the experiments showed that this transition was in fact very nearly linear. Of course a real pipe would not have the discontinuities in slope exhibited by (15) at $z=\pm\frac{1}{2}s$ and $z=\pm\frac{1}{2}l$; but in view of the other idealizations present in our formulation of the problem we do not feel that much would be gained by choosing a more complicated shape function with continuous slope.

In order to obtain the mode conversion losses in a pipe whose deformation is given by (14), we have to calculate the coefficients $C_{nm}^{\pm}$ and $S_{nm}^{\pm}$ defined by (8) of the preceding section. It is easily seen that all of these quantities vanish except

$$\begin{aligned}C_{2m}^{\pm}&=\frac{1}{2\pi a}\int_0^{2\pi}\int_{-\frac{1}{2}l}^{\frac{1}{2}l}f(z')\exp(-i(h_{01}\mp h_{2m})z')\cos^2 2\varphi'\,dz'\,d\varphi'\\ &=\frac{1}{a}\int_0^{\frac{1}{2}l}f(z')\cos(h_{01}\mp h_{2m})z'\,dz'\\ &=\frac{2[\cos\frac{1}{2}(h_{01}\mp h_{2m})s-\cos\frac{1}{2}(h_{01}\mp h_{2m})l]}{(h_{01}\mp h_{2m})^2 a(l-s)}.\end{aligned}$$

As might have been anticipated, an elliptical deformation couples only TE_{2m} modes to the TE_{01} wave. The attenuation of the circular electric mode by a single passage through the distorted section is, using Eqs. (9) to (12) of Section II,

$$N=4.343\epsilon^2\sum_m D_{2m}[|C_{2m}^{+}|^2+|C_{2m}^{-}|^2]\ \text{db}, \tag{16}$$

where the summation includes all TE_{2m} modes which are above cut-off in the circular pipe.

Using the numerical values which prevailed in the experimental work, namely

$$\lambda=3.20\ \text{cm},\quad a=2.366\ \text{in.}=6.010\ \text{cm},$$
$$l=77\ \text{cm},\quad s=17\ \text{cm},$$

we find that the only TE_{2m} waves which are above cut-off are TE_{21}, TE_{22}, and TE_{23}. A calculation the details of which will be omitted gives for the value of the sum on the right side of (16):

$$\sum_{m=1}^{3} D_{2m}[|C_{2m}^{+}|^2+|C_{2m}^{-}|^2]=38.12,$$

of which the TE_{21}^{+} mode contributes over 99.9 percent and the TE_{22}^{+} about 0.09 percent, while the TE_{23}^{+} and the three "backward" waves contribute entirely negligible amounts. Thus from (16) the attenuation per one-way trip through the elliptical section is

$$N=165.6\epsilon^2\ \text{db}. \tag{17}$$

If the distortion of the pipe is given by (14) and (15), then the parameter ϵ is related to the major and minor axes $d_{\max}$ and $d_{\min}$ of the center section by

$$\epsilon=\frac{d_{\max}-d_{\min}}{d_{\max}+d_{\min}}. \tag{18}$$

When ϵ has been determined* by (18), the theoretical attenuation is easily calculated from (17). The comparison between the values so calculated and representative experimental values, for a total of 30 round trips through the distorted section, is set forth in Table I. We regard the agreement between theory and experiment as quite satisfactory.

IV. RANDOM DISTORTIONS IN CIRCULAR GUIDE

A complete specification of the inner surface of a given section of pipe by means of the function $\epsilon\rho_1(\varphi,z)$ would allow us, at least in principle, to calculate by the formulas of Section II the mode conversion losses in that particular pipe. To obtain such detailed knowledge of $\epsilon\rho_1(\varphi,z)$ by actual measurement would, however, be highly impracticable, and at any rate we are not likely to be so interested in the properties of a single section of pipe as in the average properties of a line composed of many sections of pipe whose deviations from circularity will be more or less random. In the following paragraphs we shall calculate, for sections of pipe having a certain degree of randomness in shape, the average mode conversion loss per unit length in terms of the root-mean-square departure of the pipe from a perfect circular cylinder.

We shall begin by describing the deformation of a specific section of pipe in terms of a double Fourier series in the circumferential variable φ and the axial distance z. The deformation is thus characterized by its Fourier coefficients, which for an arbitrary continuous distortion will be a doubly infinite set of constants. In the subsequent numerical calculations, however, it will be necessary to deal with only a finite number of Fourier components; this will essentially restrict us to sections of pipe which exhibit only gradual changes in shape and no very closely spaced "ripples".

We shall proceed to express the mode conversion losses associated with the given pipe in terms of the Fourier coefficients of the distortion. We then consider

* The sample of pipe squeezed by Beck and King evidently had a radius $a=\frac{1}{4}(d_{\max}+d_{\min})$ smaller by about 0.005 in. than the nominal radius, namely 2.366 in., of the wave guide line from which it was taken. Our results should not be appreciably affected by the fact that we used the latter value of a in the calculations leading to (17).

a large number of different sections of pipe (all of equal length for simplicity), whose shapes are defined by different sets of Fourier amplitudes. We suppose that any particular Fourier coefficient is as likely to be negative as positive, so that the mean value of each coefficient, averaged over all the sections of pipe, is zero. It is also assumed that the various coefficients describing an individual section of pipe are uncorrelated, i.e., that the mean value of the product of any two different coefficients, averaged over all sections, is zero. These assumptions enable us to express the average attenuation per unit length caused by mode conversions in a wave guide line composed of many such sections in terms of the r.m.s. values of the Fourier coefficients used to describe the departure of the individual sections from perfect circularity. By making specific assumptions about the r.m.s. values of the amplitudes of the various harmonic components of distortion, we can calculate numerically the theoretical mode conversion losses in a long line.

Let us therefore consider a section of pipe whose deformation is given by a finite Fourier series:

$$\epsilon\rho_1(\varphi,z)=\tfrac{1}{4}\epsilon\sum_{s=0}^{S}\sum_{t=0}^{T}\epsilon_s\epsilon_t\left[\left(a_{st}\cos\frac{2\pi tz}{l}+b_{st}\sin\frac{2\pi tz}{l}\right)\cos s\varphi+\left(c_{st}\cos\frac{2\pi tz}{l}+d_{st}\sin\frac{2\pi tz}{l}\right)\sin s\varphi\right], \quad (19)$$

for $-\frac{1}{2}l\leq z\leq\frac{1}{2}l$ and $0\leq\varphi\leq 2\pi$. The coefficients a_{st}, b_{st}, c_{st}, and d_{st} are related to $\rho_1(\varphi,z)$ by the following scheme:

$$\begin{bmatrix}a_{st} & b_{st}\\ c_{st} & d_{st}\end{bmatrix}=\frac{2}{\pi l}\int_0^{2\pi}\int_{-\frac{1}{2}l}^{\frac{1}{2}l}\rho_1(\varphi,z)\begin{bmatrix}\cos\frac{2\pi tz}{l}\cos s\varphi & \sin\frac{2\pi tz}{l}\cos s\varphi\\ \cos\frac{2\pi tz}{l}\sin s\varphi & \sin\frac{2\pi tz}{l}\sin s\varphi\end{bmatrix}dzd\varphi. \quad (20)$$

The mean-square value of $\epsilon\rho_1(\varphi,z)$ is

$$\sigma^2=\frac{1}{2\pi l}\int_0^{2\pi}\int_{-\frac{1}{2}l}^{\frac{1}{2}l}\epsilon^2\rho_1^2(\varphi,z)dzd\varphi=\frac{\epsilon^2}{16}\left[\sum_{s=0}^{S}\sum_{t=0}^{T}\epsilon_s\epsilon_t a_{st}^2+2\sum_{s=0}^{S}\sum_{t=1}^{T}\epsilon_s b_{st}^2+2\sum_{s=1}^{S}\sum_{t=0}^{T}\epsilon_t c_{st}^2+4\sum_{s=1}^{S}\sum_{t=1}^{T}d_{st}^2\right]. \quad (21)$$

The quantities $C_{nm}^{\pm}$ and $S_{nm}^{\pm}$ which measure the mode conversion losses are given by (8) to be

$$C_{nm}^{\pm}=\frac{1}{4a^2}\sum_{t=0}^{T}\epsilon_t[a_{nt}f_{nmt}^{\pm}-ib_{nt}g_{nmt}^{\pm}],$$

$$S_{nm}^{\pm}=\frac{1}{4a^2}\sum_{t=0}^{T}\epsilon_t[c_{nt}f_{nmt}^{\pm}-id_{nt}g_{nmt}^{\pm}],$$

where

$$f_{nmt}^{\pm}=\int_{-\frac{1}{2}l}^{\frac{1}{2}l}\cos(h_{01}\mp h_{nm})z'\cos(2\pi tz'/l)dz'=\frac{(-)^t 2(h_{01}\mp h_{nm})l^2\sin\frac{1}{2}(h_{01}\mp h_{nm})l}{(h_{01}\mp h_{nm})^2l^2-4\pi^2t^2},$$

$$g_{nmt}^{\pm}=\int_{-\frac{1}{2}l}^{\frac{1}{2}l}\sin(h_{01}\mp h_{nm})z'\sin(2\pi tz'/l)dz'=\frac{(-)^t 4\pi tl\sin\frac{1}{2}(h_{01}\mp h_{nm})l}{(h_{01}\mp h_{nm})^2l^2-4\pi^2t^2}.$$

Hence

$$|C_{nm}^{\pm}|^2=\frac{1}{16a^4}\sum_{r=0}^{T}\sum_{t=0}^{T}\epsilon_r\epsilon_t[a_{nr}f_{nmr}^{\pm}-ib_{nr}g_{nmr}^{\pm}]\times[a_{nt}f_{nmt}^{\pm}+ib_{nt}g_{nmt}^{\pm}], \quad (22)$$

$$|S_{nm}^{\pm}|^2=\frac{1}{16a^4}\sum_{r=0}^{T}\sum_{t=0}^{T}\epsilon_r\epsilon_t[c_{nr}f_{nmr}^{\pm}-id_{nr}g_{nmr}^{\pm}]\times[c_{nt}f_{nmt}^{\pm}+id_{nt}g_{nmt}^{\pm}]. \quad (23)$$

On inserting these values into Eq. (9) and summing over n and m as in Eq. (11) we have an explicit expression for the total power converted into other modes, as a function of the Fourier coefficients a_{st}, b_{st}, c_{st}, and d_{st} describing the inner surface of the pipe.

Now let us imagine that we have a large number of sections of pipe, each of which will for the present be assumed to have the same length l. Let the kth section be represented by a finite Fourier series of the form (19), with coefficients

$$a_{st}^{(k)},\ b_{st}^{(k)},\ c_{st}^{(k)},\ d_{st}^{(k)}\quad(k=1,2,3,\cdots). \quad (24)$$

For all values of k, s, and t we may define, in accord with (20),

$$b_{s0}^{(k)}\equiv c_{0t}^{(k)}\equiv d_{s0}^{(k)}\equiv d_{0t}^{(k)}\equiv 0. \quad (25)$$

We assume that the coefficients (24) which define the various sections of pipe (excluding those which vanish identically by (25)) are *statistically independent random variables in k with mean zero and standard deviation* σ_{st}. In other words, using angular brackets to denote averages over k, so that

$$\langle f\rangle=\lim_{K\to\infty}(1/K)\sum_{k=1}^{K}f(k),$$

we assume that

$$\langle a\rangle_{st}=\langle b\rangle_{st}=\langle c\rangle_{st}=\langle d\rangle_{st}=0$$

and

$$\langle a_{st}^2\rangle=\langle b_{st}^2\rangle=\langle c_{st}^2\rangle=\langle d_{st}^2\rangle=\sigma_{st}^2, \quad (26)$$

while the average value of the product of any two coefficients with different subscripts is zero. We emphasize that these assumptions concerning the statistical behavior of the coefficients (24), while they may seem to possess a considerable degree of plausibility, are introduced at this stage as mathematical hypotheses;

TABLE II.

s \ t	σ_{st}/σ_0 0	1	2	3	4
0	25	20	15	10	5
1	20	16	12	8	4
2	15	12	9	6	3
3	10	8	6	4	2
4	5	4	3	2	1

we are not here concerned with proving their validity for any particular wave guide line.

It is easily seen from (21) and (26) that the average value of σ^2 taken over a large number of sections of pipe is given in terms of the quantities σ_{st}^2 by

$$\langle\sigma^2\rangle=\epsilon^2\left[\frac{1}{16}\sigma_{00}^2+\frac{1}{4}\sum_{t=1}^{S}\sigma_{s0}^2+\frac{1}{4}\sum_{s=1}^{T}\sigma_{0t}^2+\sum_{s=1}^{S}\sum_{t=1}^{T}\sigma_{st}^2\right], \quad (27)$$

provided that $\sigma_{st}=0$ for $s>S$ and/or $t>T$. In principle, of course, we may take S and T as large as desired.

If we add together Eqs. (22) and (23) and average the result over k, then using (25) and (26) and the assumed statistical independence of the different coefficients we obtain:

$$\langle|C_{nm}^{\pm}|^2+|S_{nm}^{\pm}|^2\rangle$$

$$=\frac{\epsilon_n}{16a^4}\left\{(f_{nm0}^{\pm})^2\sigma_{n0}^2+4\sum_{t=1}^{T}\left[(f_{nmt}^{\pm})^2+(g_{nmt}^{\pm})^2\right]\sigma_{nt}^2\right\}$$

$$=\frac{\epsilon_n l^2\sin^2\tfrac{1}{2}(h_{01}\mp h_{nm})l}{4a^4}\left\{\frac{\sigma_{n0}^2}{(h_{01}\mp h_{nm})^2l^2}\right.$$

$$\left.+4\sum_{t=1}^{T}\left[\frac{(h_{01}\mp h_{nm})^2l^2+4\pi^2t^2}{\left[(h_{01}\mp h_{nm})^2l^2-4\pi^2t^2\right]^2}\right]\sigma_{nt}^2\right\}. \quad (28)$$

Hence finally we get from (9), (11), and (13) the following expression for the average attenuation per unit length in a line composed of a great number of sections of pipe of length l, each deviating in a random way from a perfect circular cylinder:

$$\langle\alpha\rangle=\frac{4.343\epsilon^2}{l}\sum_{n=0}^{S}\sum_{m}D_{nm}\left[\langle|C_{nm}^{+}|^2+|S_{nm}^{+}|^2\rangle\right.$$

$$\left.+\langle|C_{nm}^{-}|^2+|S_{nm}^{-}|^2\rangle\right]\text{ db/unit length.} \quad (29)$$

In (29) the summation over m is taken to include all the modes which are above cut-off for a given value of n (except that the TE_{01}^{+} mode is omitted).

In view of the algebraic complexity of the final expression for $\langle\alpha\rangle$, it is worth while to point out some dimensional considerations which will permit us to introduce scale factors. If we fix our attention on the attenuation per wave-length $\langle\alpha\rangle\lambda$, it is not difficult to show that (29) may be written in the form

$$\langle\alpha\rangle\lambda=F(\lambda/a,\ l/\lambda;\ \sigma_{00}/a,\ \sigma_{10}/a,\ \sigma_{01}/a,\ \sigma_{20}/a,\ \cdots), \quad (30)$$

where the function F depends only on the indicated dimensionless ratios. In other words, if we multiply all linear dimensions of the wave guide line by a given scale factor and simultaneously multiply the frequency by the reciprocal of the same factor, the attenuation per wave-length due to mode conversion losses remains constant. We shall make use of this relationship presently.

The question may be raised here whether the function F which appears in (30) depends critically upon the assumed length (in wave-lengths) l/λ of the individual sections of pipe. Physically it seems very unlikely that the mode conversion losses in an extended line whose individual sections are hundreds of wave-lengths long would be much altered by moderate fractional changes in the lengths of these sections. On the other hand, it is easy to set up idealized configurations in which the theoretical mode conversion losses do depend markedly on phase relations determined by the length of the section in which the conversions take place, and it is perhaps not *a priori* clear by inspection of (29) that similar effects do not occur in this more complicated case. To settle the question it is possible to average the right side of (29) over a selected range of values of l. Thus we find that the average attenuation per unit length owing to mode conversions in a line composed of a great number of sections of pipe whose deviations from circularity are random in the sense defined above, and whose lengths are distributed uniformly between l_1 and l_2, is

$$\langle\alpha(l_1,l_2)\rangle=\frac{4.343\epsilon^2}{4a^2(l_2-l_1)}\sum_{n=0}^{S}\sum_{m}\epsilon_nD_{nm}$$

$$\times\left[\sum_{t=0}^{T}\epsilon_t^2(I_{nmt}^{+}+I_{nmt}^{-})\sigma_{nt}^2\right]\text{ db/unit length,} \quad (31)$$

where

$$I_{nmt}^{\pm}=\frac{1}{a^2}\int_{l_1}^{l_2}l\sin^2\tfrac{1}{2}(h_{01}\mp h_{nm})l\frac{(h_{01}\mp h_{nm})^2l^2+4\pi^2t^2}{\left[(h_{01}\mp h_{nm})^2l^2-4\pi^2t^2\right]^2}dl$$

$$=\frac{1}{4(h_{01}\mp h_{nm})^2a^2}\left\{\ln\tfrac{1}{4}\left|(h_{01}\mp h_{nm})^2l^2-4\pi^2t^2\right|\right.$$

$$-\mathrm{Ci}\left[\left|(h_{01}\mp h_{nm})l-2\pi t\right|\right]-\mathrm{Ci}\left[\left|(h_{01}\mp h_{nm})l+2\pi t\right|\right]$$

$$+2\pi t\,\mathrm{Si}\left[(h_{01}\mp h_{nm})l-2\pi t\right]-2\pi t\,\mathrm{Si}\left[(h_{01}\mp h_{nm})l+2\pi t\right]$$

$$\left.-\frac{4\pi^2t^2\sin^2\tfrac{1}{2}(h_{01}\mp h_{nm})l}{\tfrac{1}{4}\left[(h_{01}\mp h_{nm})^2l^2-4\pi^2t^2\right]}\right\}_{l_1}^{l_2}. \quad (32)$$

Before we can calculate numerical values of $\langle\alpha\rangle$, it is necessary to reduce considerably the number of parameters involved in the general expression (29). If we knew the relative magnitudes of the mean-square Fourier amplitudes σ_{nt}^2 occurring in (28), it would be a simple matter to express their absolute magnitudes in terms of $\langle\sigma^2\rangle$ by (27) and thus to express the mode con-

version losses in terms of the latter quantity. Unfortunately information about the individual σ_{st}'s is not at present available. It may be argued that in view of the structural rigidity of commercial copper pipe the amplitudes of the higher harmonics in the distortion must tend rapidly to zero, but this tells us little about the behavior of σ_{st} for the first few terms of the series. In the absence of more detailed information and for the purpose of obtaining a numerical result, we shall arbitrarily assume that only the constant term and the first four harmonics in both the circumferential and the axial directions occur in the expression (19) for the distortion of a typical section of pipe; and we shall further assume that the r.m.s. amplitudes of these harmonics are given by

$$\sigma_{st}=(5-s)(5-t)\sigma_0,\ 0\leq s,\ t\leq 4, \tag{33}$$

where σ_0 is a length proportional to the r.m.s. deviation of the wave guide line from an average circular cylinder. The relative magnitudes of the non-vanishing σ_{st}'s are thus assumed to be as shown in Table II:

It is easy to determine from (27) and (33) that the mean-square deviation of the wave guide line from an average cylinder is given by

$$\langle\sigma^2\rangle=1314.1\epsilon^2\sigma_0^2.$$

Numerical calculations have been carried out, under the assumptions just described, to obtain the mode conversion losses in transmission of TE_{01} power through a long wave guide composed of 20-foot sections of 5-inch (outside diameter) pipe at both X-band and K-band wave-lengths. For the X-band case we take

$$\lambda=3.20\text{ cm},\quad \lambda/a=0.532,$$
$$a=2.366\text{ in.},\quad l/\lambda=190.5.$$
$$l=20\text{ ft.},$$

Substitution of these values into (29) gives, after a lengthy calculation,

$$\langle\alpha\rangle=4.92\langle\sigma^2\rangle/a^2\text{ db/cm}, \tag{34}$$

where $\langle\sigma^2\rangle$ and a^2 are expressed in the same units. The numerical coefficient in (34) represents the combined effect of 14 forward modes (excluding TE_{01}^+) and 15 backward modes; but it turns out that the TE_{31}^+ and TE_{21}^+ modes together account for 97.6 percent of the total (TE_{31}^+, 85.8 percent; TE_{21}^+, 11.8 percent). It will in general be true that pipe deformations which are long compared to the wave-length convert power from the TE_{01} mode mostly into those (transverse electric) modes whose phase velocities are nearest the TE_{01}. Physically it is evident that unless the phase velocities of two modes are nearly equal, they will phase in and out so rapidly that over a distance of several wave-lengths the net power transfer will be small.*

If the r.m.s. deviation $\langle\sigma^2\rangle^{\frac{1}{2}}$ of the pipe from a perfect circular cylinder is expressed in mils, then since $a=2.366$ in., (34) becomes

$$\langle\alpha\rangle=0.879\times10^{-6}\langle\sigma^2_{\text{mils}}\rangle\text{ db/cm}. \tag{35}$$

This value may be compared with the theoretical attenuation α_0 due solely to heat losses. We find from the usual wave guide formulas[8] that for the TE_{01} mode at 3.2 cm in a copper pipe of diameter 4.732 in. and resistivity 1.72×10^{-6} ohm cm,[9]

$$\alpha_0=1.076\times10^{-5}\text{ db/cm}, \tag{36}$$

so that the ratio of mode conversion losses to theoretical heat losses, each expressed in db/cm, is

$$\langle\alpha\rangle/\alpha_0=0.0817\langle\sigma^2_{\text{mils}}\rangle. \tag{37}$$

A discrepancy of 8 percent of the theoretical copper losses could be accounted for by mode conversions, under the assumptions that led to (34), if the r.m.s. deviation of the pipe from perfect circularity were 1 mil. We may point out that if the circumferential variations in the pipe surface were sinusoidal, a 1-mil value of $\langle\sigma^2\rangle^{\frac{1}{2}}$ as here defined would correspond to a maximum variation of 2.83 mils in the radius, or, in the case of an even harmonic, to a difference of 5.66 mils between maximum and minimum internal diameters.

We should stress that the numbers just obtained depend rather strongly upon the assumptions which we made concerning the relative magnitudes of the various σ_{st}'s; in particular, the results are sentitive to variations in the relative amounts of second and third harmonics in the circumferential distortion, since these harmonics couple the two modes, TE_{21} and TE_{31}, whose phase velocities are closest to TE_{01}. It may be of interest to record the results of a calculation made under the assumption that all of the σ_{st}'s corresponding to harmonics of degree not greater than four are present in equal amounts; i.e.,

$$\begin{aligned}\sigma_{st}&=\sigma_1,\ 0\leq s,\ t\leq 4,\\ &=0,\text{ otherwise.}\end{aligned} \tag{38}$$

Then we find from (27) that

$$\langle\sigma^2\rangle=18.06\epsilon^2\sigma_1^2,$$

and from (29) and (36), after extensive computation,

$$\langle\alpha\rangle/\alpha_0=0.205\langle\sigma^2_{\text{mils}}\rangle,$$

which is two and one-half times the value of $\langle\alpha\rangle/\alpha_0$ given by (37). Although the "tapered" distribution of amplitudes (33) seems physically much more reason-

* On the other hand, unpublished calculations have indicated that the effect of a surface irregularity which is *short* compared to the wave-length is to couple the TE_{01} mode most strongly to those modes which are near cut-off. With such an irregularity one might expect pronounced resonance phenomena if the frequency were varied through the cut-off frequency of a particular higher mode.

[8] Reference 4, p. 390.

[9] The effective resistivity of metallic surfaces at centimeter wave-lengths is appreciably higher than the d.c. resistivity of the bulk metal, because of surface roughness and corrosion. See E. Maxwell, J. App. Phys. **18**, 629 (1947), and S. P. Morgan, Jr., J. App. Phys. **20**, 352 (1949). In estimating mode conversion losses from measurements of total line attenuation it is first necessary to take account of these augmented heat losses.

TABLE III. Values of the coefficients D_{nm} for $\lambda\ a=0.532$.

m \ n	0	1	2	3	4
1	1.7305	1.085	3.770	8.592	16.27
2	6.824	7.363	13.38	22.97	38.21
3	22.77	23.86	43.16	112.3	—
4	—	244.3	—	—	—

TABLE IV. Values of the coefficients D_{nm} for $\lambda/a=0.208$.

m \ n	0	1	2	3	4
1	0.2401	0.1562	0.5325	1.798	2.146
2	0.8208	0.9710	1.642	2.514	3.607
3	1.7830	2.499	3.559	4.845	6.384
4	3.208	4.858	6.400	8.230	10.39
5	5.249	8.270	10.47	13.07	16.19
6	8.207	13.16	16.35	20.24	25.06
7	12.78	20.41	25.43	31.97	40.98
8	21.16	32.36	41.96	—	—

able than the "flat" distribution (38), it must be remembered, in view of our lack of experimental measurements, that the actual distribution in commercial copper pipe may be quite different from either of these assumed distributions.

In order to compare mode conversion losses in the same pipe at different frequencies, we turn now to K-band wave-lengths and take

$$\lambda=1.25\text{ cm},\quad \lambda/a=0.208,$$
$$a=2.366\text{ in.},\quad l/\lambda=488.$$
$$l=20\text{ ft.},$$

If we assume, as in obtaining (34), that the σ_{si}'s are given by (33), a calculation similar to the preceding one gives

$$\langle\alpha\rangle=2.94\langle\sigma^2\rangle/a^2\text{ db/cm},\tag{39}$$

or, if $\langle\sigma^2\rangle^{\frac{1}{2}}$ is expressed in mils,

$$\langle\alpha\rangle=0.525\times10^{-6}\langle\sigma^2{}_{\text{mils}}\rangle\text{ db/cm}.\tag{40}$$

In deriving the numerical coefficient of Eq. (39) contributions have been included from the 37 forward modes whose phase velocities are nearest to that of the TE_{01} mode; the contributions of the other modes would be too small to affect the third significant figure. It appears during the calculation that 98.2 percent of the mode converted power is carried by five modes (TE_{31}^+, 51.8 percent; TE_{21}^+, 27.3 percent; TE_{12}^+, 12.4 percent; TE_{11}^+, 4.7 percent; TE_{11}^+, 2.0 percent).

Equations (39) and (40) may be compared respectively with (34) and (35); we see that in absolute magnitude the mode conversion losses at 1.25 cm are only 0.597 times the losses due to mode conversions in the same pipe at 3.2 cm. But the copper losses for the TE_{01} mode diminish even more rapidly as the frequency is increased;* at 1.25 cm the theoretical attenuation of this mode in a 4.732-inch pipe is

$$\alpha_0=2.51\times10^{-6}\text{ db/cm}.$$

Hence the ratio of mode conversion loss to theoretical heat loss at 1.25 cm is

$$\langle\alpha\rangle/\alpha_0=0.209\langle\sigma^2{}_{\text{mils}}\rangle,\tag{41}$$

and this is 2.56 times the relative mode conversion loss at 3.2 cm.

As a check on the preceding calculations, we have determined from (31) and (32) the average mode conversion power carried by the TE_{21}^+ and TE_{31}^+ modes at 3.2 cm for pipe sections ranging in length from 15 to 25 feet. Thus substituting

$$\lambda=3.20\text{ cm},\quad l_1=15\text{ ft.},$$
$$a=2.366\text{ in.},\quad l_2=25\text{ ft.},$$

we find that

$$\langle\alpha(l_1,l_2)\rangle\approx4.67\langle\sigma^2\rangle/a^2\text{ db/cm},\tag{42}$$

where the right side is a very close lower limit to the actual value of $\langle\alpha(l_1,l_2)\rangle$. Similarly, taking

$$\lambda=1.25\text{ cm},\quad l_1=15\text{ ft.},$$
$$a=2.366\text{ in.},\quad l_2=25\text{ ft.},$$

and considering the five modes nearest in phase velocity to TE_{01}, we find

$$\langle\alpha(l_1,l_2)\rangle\approx3.03\langle\sigma^2\rangle/a^2\text{ db/cm}.\tag{43}$$

On comparing (42) with (34) and (43) with (39) we see that the results obtained by considering 20-foot sections of pipe are within a few percent of the average results for lengths between 15 and 25 feet.

Finally we may inquire the effect of mode conversions on the TE_{01} wave at K-band in a smaller guide, say a 2-inch pipe instead of 5-inch. We get approximately this case if we scale down the results for X-band in a 5-inch pipe, using the dimensional relation (30) and the calculations which led to (34). The latter equation may be written

$$\langle\alpha\rangle\lambda=15.75\langle\sigma^2\rangle/a^2\text{ db/wave-length},\tag{44}$$

and this relation holds for the values

$$\lambda=1.25\text{ cm},\quad a=0.924\text{ in.},\quad l=7.81\text{ ft.},$$

since the ratios λ/a and l/λ are the same as those for which it was derived. But at $\lambda=1.25$ cm, (44) gives

$$\langle\alpha\rangle=12.60\langle\sigma^2\rangle/a^2\text{ db/cm},$$

or, if $\langle\sigma^2\rangle^{\frac{1}{2}}$ is expressed in mils,

$$\langle\alpha\rangle=14.76\times10^{-6}\langle\sigma^2{}_{\text{mils}}\rangle\text{ db/cm}.$$

Since the theoretical copper losses for the TE_{01} mode at 1.25 cm in a guide of inside diameter 1.848 in. lead to an attenuation

$$\alpha_0=4.41\times10^{-5}\text{ db/cm},$$

we find for the ratio of mode conversion losses to heat losses,

$$\langle\alpha\rangle/\alpha_0=0.335\langle\sigma^2{}_{\text{mils}}\rangle.\tag{45}$$

* In practice however surface roughness effects become more significant as the skin depth for eddy currents is reduced.

Comparing (45) with (41), we see that when we go from a 4.732-inch pipe to a 1.848-inch pipe at 1.25 cm, we increase the relative mode conversion losses, for a fixed value of $\langle\sigma^2{}_{\text{mils}}\rangle$, by a factor of 1.60.

ACKNOWLEDGMENTS

I wish to thank Mr. A. C. Beck and Mr. A. P. King for permission to quote certain of their unpublished experimental results. I am indebted to Dr. W. A. Tyrrell for helpful suggestions during the course of this work, and to Mrs. Jean A. Smith for carrying out most of the numerical calculations.

APPENDIX I

Excitation of Transverse Electric Modes by Tangential Electric Field at Boundary

Let the tangential components of the electric field vanish over the surface $\rho=a$ of a circular wave guide everywhere except in a finite region S where they are given by

$$E_\varphi=E(a,\varphi,z), \quad E_z=0. \tag{A1}$$

The stream function $\Psi(\rho,\varphi,z)$ corresponding to these assigned boundary values may be found by the following formal procedure:

Let the stream function giving the boundary value

$$E_\varphi=E_0(a,\varphi,z)=\delta(\varphi-\varphi')\delta(z-z'), \tag{A2}$$

where δ is the unit impulse-function, be

$$\Psi_0(\rho,\varphi,z;\varphi',z')$$
$$=\sum_{n=0}^{\infty}\left[\int_{(C)} A_n(\gamma)J_n[(\beta^2+\gamma^2)^{\frac{1}{2}}\rho]e^{\gamma z}d\gamma\right]\frac{\epsilon_n}{2\pi}\cos n(\varphi-\varphi'),$$

where the contour (C) in the γ plane will be specified presently and $A_n(\gamma)$ is a function to be determined. Now

$$E(a,\varphi,z)=[\partial\Psi_0/\partial\rho]_{\rho=a}=\sum_{n=0}^{\infty}\left[\int_{(C)} A_n(\gamma)(\beta^2+\gamma^2)^{\frac{1}{2}}J_n'[(\beta^2+\gamma^2)^{\frac{1}{2}}a]e^{\gamma z}d\gamma\right]\frac{\epsilon_n}{2\pi}\cos n(\varphi-\varphi'). \tag{A3}$$

But if we write $\delta(\varphi-\varphi')$ as a Fourier series in φ and $\delta(z-z')$ as a contour integral,[10] (A2) becomes

$$E_0(a,\varphi,z)=\lim_{\substack{s\to 0\\ t\to 0}}\sum_{n=0}^{\infty}\left[\frac{1}{2\pi i}\int_{(C)}\frac{\operatorname{sh}\frac{1}{2}\gamma s}{\frac{1}{2}\gamma s}\times\exp[\gamma(z-z')]d\gamma\right]\frac{\epsilon_n}{2\pi}\frac{\sin\frac{1}{2}nt}{\frac{1}{2}nt}\cos n(\varphi-\varphi'), \tag{A4}$$

the contour (C) in the γ-plane being along the imaginary axis indented to the right at the origin, as in Fig. 3. We determine $A_n(\gamma)$ by comparing (A3) and (A4), and obtain, on letting s and t pass to zero under the signs of summation and integration, the result

$$\Psi_0(\rho,\varphi,z;\varphi',z')$$
$$=\sum_{n=0}^{\infty}\left[\frac{1}{2\pi i}\int_{(C)}\frac{J_n[(\beta^2+\gamma^2)^{\frac{1}{2}}\rho]\exp[\gamma(z-z')]d\gamma}{(\beta^2+\gamma^2)^{\frac{1}{2}}J_n'[(\beta^2+\gamma^2)^{\frac{1}{2}}a]}\right]\frac{\epsilon_n}{2\pi}\times\cos n(\varphi-\varphi')$$
$$=\sum_{n=0}^{\infty}\frac{\epsilon_n I_n}{2\pi}\cos n(\varphi-\varphi'),$$

where

$$I_n=\frac{1}{2\pi i}\int_{(C)}\frac{J_n[(\beta^2+\gamma^2)^{\frac{1}{2}}\rho]\exp[\gamma(z-z')]d\gamma}{(\beta^2+\gamma^2)^{\frac{1}{2}}J_n'[(\beta^2+\gamma^2)^{\frac{1}{2}}a]}. \tag{A5}$$

It is easily shown that the integrand in (A5) is a single-valued function of γ, so that I_n can be evaluated in terms of the residues at the poles of the integrand. These poles are at the points* $\gamma=\pm\Gamma_{nm}$, where $k_{nm}=(\beta^2+\Gamma_{nm}^2)^{\frac{1}{2}}a$ is the mth positive root of $J_n'(x)=0$ and Γ_{nm} is the corresponding natural propagation constant in the guide. The contour (C) is indented to the right of the poles on the negative imaginary γ-axis and to the left of the poles on the positive imaginary γ-axis; then if $z>z'$ it is closed with an infinite semi-circle in the left half-plane, thus including an infinite number of poles on the negative real axis. With the aid of l'Hospital's rule and Bessel's equation it is easy to show that

$$\lim_{\gamma\to-\Gamma_{nm}}\frac{\gamma+\Gamma_{nm}}{J_n'[(\beta^2+\gamma^2)^{\frac{1}{2}}a]}=\frac{k_{nm}{}^2}{\Gamma_{nm}a^2(k_{nm}{}^2-n^2)J_n(k_{nm})},$$

so that the contribution of the pole at $\gamma=-\Gamma_{mn}$ to the stream function $\Psi_0(\rho,\varphi,z;\varphi',z')$ is

$$\frac{k_{nm}{}^2\epsilon_n J_n(\chi_{nm}\rho)\cos n(\varphi-\varphi')\exp[-\Gamma_{nm}(z-z')]}{2\pi\Gamma_{nm}a(k_{nm}{}^2-n^2)J_n(k_{nm})} \tag{A6}$$

for $z>z'$. If $z<z'$ the contour (C) is to be closed with an infinite semicircle in the right half-plane; the end result

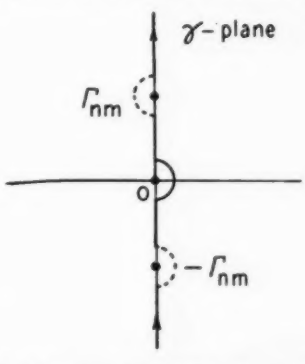

FIG. 3. The contour (C) in the γ-plane.

[10] Reference 4, pp. 34–35.

* For $n=0$ there are also poles at $\gamma=\pm i\beta$, but the contribution of these poles to the stream function is of the form constant $\times\exp(\pm i\beta z)$, which leads to no non-vanishing fields.

is to change the sign of the exponent in the last factor of (A6). Hence in general

$$\Psi_0(\rho,\varphi,z;\varphi',z')=\sum_{n=0}^{\infty}\sum_{m=1}^{\infty}\frac{\epsilon_n k_{nm}^2 J_n(\chi_{nm}\rho)\cos n(\varphi-\varphi')\exp[-\Gamma_{nm}|z-z'|]}{2\pi\Gamma_{nm}a(k_{nm}^2-n^2)J_n(k_{nm})}. \tag{A7}$$

Having the stream function which corresponds to an impulse-function boundary value of E_φ, we are able to write down at once the stream function for the general field given by (A1); it is

$$\Psi(\rho,\varphi,z)=\int\int_S E(a,\varphi',z')\Psi_0(\rho,\varphi,z;\varphi',z')dz'd\varphi',$$

which corresponds by (A7) to Eq. (5) of Section II.

APPENDIX II

Some values of the quantities D_{nm} defined by (10) have been calculated for particular choices of λ/a and are given in Tables III and IV.

Wettability, a Function of the Polarizability of the Surface Ions

L. R. Sonders, D. P. Enright, and W. A. Weyl
The Pennsylvania State College, School of Mineral Industries, State College, Pennsylvania
(Received October 28, 1949)

The wettability of crystals, glasses, and even of water itself can be temporarily decreased by bringing ions of high polarizability into their surfaces. Base exchange experiments are described where the hydrogen ions present in the surface layers of bentonite (a clay mineral of high exchange capacity) and of a soda-lime glass are replaced by different cations. This substitution seems to have no particular effect on the hydrophilic and rheological properties of the carriers as long as their surfaces are kept in contact with water. After drying, however, the surfaces which contain ions of high polarizability become hydrophobic, at least temporarily. A porous clay film will no longer absorb water instantaneously after having been treated with Ni^{2+}, Mn^{2+}, Hg^{2+}, or similar ions with incomplete outer electron shells. Contact angles with water up to 70° could be observed for a short period for Hg^{2+} and Pb^{2+} clays.

Glass capillary tubes which have been treated with non-noble gas-type ions show a capillary rise which is much smaller than that observed with the tubes which have been treated with HCl and water only. This depression of the capillary rise, too, is temporary and can be observed only if the glass wall has been thoroughly dried previous to the experiment and if the capillary rise is measured in the upward direction.

An explanation is presented for these and allied phenomena on the basis of the polarization of ions in the strongly asymmetrical forcefields of interfaces. The experiments are correlated with the hysteresis of the contact angle and with observations concerning adhesion phenomena and catalytic activities of heavy metal ions at interfaces.

I. INTRODUCTION

THE present difficulty in the understanding and in the correct interpretation of surface phenomena, such as heterogeneous catalysis, adhesion and wetting properties of solids, is partly the result of not being able to directly measure the surface forces emanating from a solid without changing the surface structure. For example, the forcefields emanating from the surfaces of alkali halides cannot be measured by bringing the salts onto a platinum surface and then determining their adhesion, because a metal surface in contact with NaCl is not identical with one in contact with KI. It is now well established that the electrical properties of metal films are changed if they are brought in contact with different gases or solids. The checkered forcefield of the cube face of NaCl or of a glass surface polarizes the metal surface by inducing higher electron densities opposite the cations and lower electron densities opposite the anions. The metals respond to the external forcefield by producing image forces and these in turn affect the surface structures of the alkali halides.

This uncertainty about the forcefields of surfaces and their change with the environment is not generally appreciated. A surface of galena (PbS), for example, exerts different forces upon its environment depending on its chemical composition. The galena surface undergoes a structural change if one medium, say air, is replaced by another, for example, water. The forcefields of the highly polarizable Pb^{2+} and S^{2-} ions can assume directional properties. This structural change in the galena surface affects its contact angle with a liquid and, as a result, the contact angle depends on whether the liquid is advancing over or receding from the solid surface. Adam[1] in his authoritative book writes on this hysteresis phenomenon as follows: ". . . mathematical works on Capillarity rarely mention it at all. It may, however, be observed without any apparatus with almost any rain drop traveling down an ordinarily dirty window pane. This difference between advancing and receding angles is often called the 'hysteresis' of

[1] N. K. Adam, *The Physics and Chemistry of Surfaces* (Oxford University Press, London, 1941), third edition, p. 180.

the contact angle. Early references to it in the literature are scarce; Rayleigh referred to it in 1890; Pockels measured it for several liquids; Sulman studied it in connection with the flotation of minerals. It is well known to those who have measured surface tension by the rise in a capillary tube, for the rise is often less if the liquid is pushing its way up from below than if it is falling from a point above its final equilibrium height.

"The cause of the 'hysteresis' of contact angles is still obscure. It looks superficially as if there was a frictional resistance to motion of the liquid edge over the solid."

It is the object of this paper to explain this hysteresis of the contact angle. Experiments with solid-liquid and liquid-gas interfaces are described and their explanation is based on the polarizability of ions and the effect which the asymmetrical forcefield of an interface exerts upon the direction of valency forces.

A note on this subject has been published as a Letter to the Editor.[1a]

II. THE POLARIZABILITY OF IONS AND SOME OF ITS MANIFESTATIONS

The polarizability of a molecule is frequently measured by its response to the alternating electromagnetic field of light. It can be easily computed from refractive index, molecular weight, and density. The polarizability is a measure for the change which takes place in the outer electronic orbits if an atom, molecule, or ion is exposed to an external electrical field. The polarizability of an ion depends on its size, charge, and on its electron configuration. The rules governing polarization of ions have been derived by Fajans[2] and his school.

Without going into details, some of these rules shall be mentioned.

(a) Anions are more polarizable than cations of the same configuration. For example, the ions which have the electron structure of the inert gas atom, neon, show polarizabilities which decrease with increasing nuclear charge.

$$O^{2-} > F^{-} > Ne > Na^{+} > Mg^{2+}.$$

(b) For ions of the same electrical charge and of comparable electron configuration, the polarizability increases with the size (Table I).

(c) The polarizability of cations of approximately equal size is larger for those of 18 outer electrons than for those of the noble gas type, but is greatest for those cations which have only one or two outer electrons.

$$Sr^{2+}(8 \text{ outer electrons}) < Cd^{2+}(18 \text{ outer electrons}) < Pb^{2+}(18+2 \text{ outer electrons}).$$

The mercurous ion Hg^{+} has only one outer electron and its polarizability is, therefore, extremely high.

The polarizability of an ion can be described as its ability to adjust its own forcefield to that of the environment. This concept has been used by Weyl[3] for explaining adhesion phenomena and solubilities involving two incompatible media. A metal, for example, ordinarily is not soluble in a fused glass. Glasses, say soda-lime-silicates, consist only of noble gas-type ions having rather low polarizabilities. If a strongly polarizable cation such as Pb^{2+}, Bi^{3+}, Sn^{2+}, or Tl^{+} is introduced into the glass, a metal such as gold or copper becomes soluble to a certain extent. These ions act as "metallophilic groups" comparable with hydrotropic substances or with emulsifiers. In the asymmetrical forcefield, which exists between the neutral metal atom and the negatively charged O^{2-} ion, metallophilic ions are strongly polarized. Their electron density no longer possesses the spherical symmetry of the ion in the gaseous state, but has become strongly asymmetrical as far as the outer or valency electrons are concerned.

The deformation of a strongly polarizable ion, such as a Pb^{2+} ion, can be described in the language of the chemist as a disproportionation. Its inner shells (*K* to *O* shell) are not directly affected by chemical changes. It is the *P* shell of a lead atom with its four 6*s* electrons which is primarily responsible for its chemical properties. The four outer electrons of the *P* shell can be donated to electron acceptors. The result of this electron transfer is the formation of the fourfold positively charged Pb^{4+} ion. If only two of the four valence electrons are surrendered to an electron acceptor a Pb^{2+} ion is formed. Outside of the 18 electrons of the *O* shell, such a Pb^{2+} ion, has still two 6*s* electrons. On approach of a negatively charged oxygen ion these two outer electrons are repelled. As a result, the electrical or valence forces of the Pb^{2+} ion are no longer equally distributed in space. The one side of the Pb^{2+} from which the two electrons are repelled has a lower electron density and resembles in its structure the Pb^{4+} ion (18 outer electrons). The

TABLE I. Molar refraction of gaseous ions in cc (after Bauer and Fajans).[a]

		He	Li^{+}	Be^{2+}
		0.521	0.08	—
O^{2-}	F^{-}	Ne	Na^{+}	Mg^{2+}
6.95	2.44	1.00	0.47	0.26
S^{2-}	Cl^{-}	A	K^{+}	Ca^{2+}
22.7	9.06	4.20	2.25	1.40
Se^{2-}	Br^{-}	Kr	Rb^{+}	Sr^{2+}
28.8	12.66	6.39	3.79	2.58
Te^{2-}	I^{-}	Xe	Cs^{+}	Ba^{2+}
40.9	19.21	10.43	6.53	4.73

[a] See reference 2(a).

[1a] Enright, Sonders, and Weyl, J. App. Phys. **20**, 1011 (1949).

[2] (a) K. Fajans, *Chemical Forces and Optical Properties of Substances* (McGraw-Hill Book Company, Inc., New York, 1931). (b) N. Bauer and K. Fajans, J. Am. Chem. Soc. **64**, 3023 (1942).

[3] W. A. Weyl, J. Soc. Glass Tech. **32**, 247–259 (1948).

TABLE II.

Glass type	Gain in weight (1 cm² glass powder in 4 hr.)
Lead borate (51.7 percent PbO)	4.9 mg
F. 620 (45 percent PbO)	5.6 mg
Window glass	32.0 mg
Bottle glass	35.0 mg

TABLE III. Influence of adsorbed cations on the capillary rise of water in glass tubes.[a]

Adsorbed cation	Example for the capillary rise in mm for different treatments				Average decrease in rise (percent) for different treatments		
	Blank	24 hr.	48 hr.	120 hr.	24 hr.	48 hr.	120 hr.
Ba^{2+}	62	62	59	56	0	5.4	9.2
Tl^{+}	63	63	63	57	0	0	10.2
Fe^{3+}	60	56	55	53	8.5	10.8	12.5
Co^{2+}	64	60	57	55	5.8	10.5	13.1
Zn^{2+}	61	57	55	53	6.9	11.7	13.8
Cu^{2+}	64	58	55	55	9.0	13.3	14.4
Cd^{2+}	60	57	52	50	5.4	13.5	15.7
Cr^{3+}	63	58	53	53	7.5	13.9	10.1
Mn^{2+}	62	55	52	50	10.1	16.5	18.0
Ni^{2+}	62	55	49	48	12.2	20.2	21.8
Hg^{2+}	60	46	40	40	24.1	32.8	32.8
Pb^{2+}	61	44	39	37	29.0	38.1	40.8

[a] The value for the blank (H^{+} glass) varied between 60 and 64 mm depending on the diameter of the tube. All data presented are averages of several experiments carried out with different tubes.

other side characterized by a higher electron density resembles the neutral Pb atom.

One can describe this deformation or polarization of the lead ion by the scheme:

$$Pb^{2+} = \tfrac{1}{2}Pb^{4+} + \tfrac{1}{2}Pb.$$

This is analogous to other "internal oxidation-reduction" reactions such as:

$$2Sn^{2+} = Sn^{4+} + Sn \quad \text{or} \quad Hg_2Cl_2 = HgCl_2 + Hg.$$

The strongly polarized Pb^{2+} ion, therefore, exerts strong ionic forces toward the oxygen ion at its one side but is "neutral" at the opposite side. The side to which the two 6*s* electrons have been repelled has the property of atomic lead and, as a result of its high electron density at this side, it may form a "metallic bond" with a metal atom and, thus, keep atomic Au or Cu in solution.

A similar state of polarization was found to exist for Pb^{2+} and other strongly polarizable cations in surface layers. The polarization of surface ions affects the surface tension, hygroscopicity, catalytic properties, as well as adhesion forces.

Summarizing, we may say that polarizable ions change their electron distribution and with it their "chemical affinities" when brought into the asymmetrical forcefield of a surface or of an interface. In contrast to the gaseous ion or to the hydrated ion which has an electron density function of spherical symmetry, the polarized surface ion exerts directional valence forces because its electron density distribution has become asymmetrical.

III. WETTABILITY OF A SOLID SURFACE

Whether or not a solid brought into a liquid goes into solution depends on its lattice energy and the heat of solvation. Solubility is an equilibrium phenomenon and, as such, it is fairly well understood. There seems to be no relationship, however, between the solubility of a crystal and its wettability by the solvent. Anhydrous chromium chloride may be cited as a typical example. This compound is soluble in water and forms several hydrates, when allowed to crystallize from its aqueous solutions. Nevertheless, it is not easily wet by water and one cannot obtain a reproducible contact angle between $CrCl_3$, H_2O, and air. Even the uncontaminated freshly sublimed anhydrous $CrCl_3$ will float on water for hours without being wet. This phenomenon is due to the state of polarization of the large Cl^- ions in the surface layer where they are exposed to the positive forcefields of Cr^{3+} ions on one side only. The Coulomb forces of these polarized surface Cl^- ions are directed only toward the interior and, therefore, they are not available for hydration. The air film covering the $CrCl_3$ is gradually replaced by water, and the presence of "contrapolarizing" cations is required in order to make the $CrCl_3$ crystal hydrophilic. Addition of HCl accelerates this process because now the Cl^- ions come into a more symmetrical forcefield; they have a Cr^{3+} ion on the one side and a H^+ ion on the other.

Just as striking is the behavior of freshly precipitated mercuric iodide HgI_2. This compound contains the two very polarizable ions Hg^{2+} and I^-. When precipitated from aqueous solution the iodide behaves like any other hydrophilic precipitate, for example, $BaSO_4$, AgCl, etc. However, on filtering, the HgI_2 changes into a hydrophobic material as soon as it comes in contact with air. In the asymmetrical forcefield crystal-air, the polarizable ions adjust their own forcefields to that of the interface by directing their valence forces primarily toward the interior of the crystal. This structural change causes the surface-free energy of the crystal to be lowered.

The low surface-free energy or the lack of strong attraction forces of glasses containing some strongly polarizable heavy metal ions causes them to be less hygroscopic than others which contain only noble gas-type ions of low polarizability. This phenomenon was discovered by Hubbard.[4]

When developing a more logical test for optical glasses which correspond to actual service conditions instead of treating a lens with hot nitric acid, Hubbard found that the hygroscopicity of otherwise "chemically poor" glasses can be much lower than that of a bottle glass of known high chemical resistivity as can be seen from Table II. Glasses containing only noble gas-type ions exert strong surface forces because their low polarizability makes it impossible for them to adjust their Coulomb forces to the asymmetrical forcefield of the

[4] D. Hubbard, J. Research Nat. Bur. Stand. **36**, 365–375 (1946).

surface. A surface ion of such a glass has incomplete coordination and extends unsaturated valence forces into space. As a result, oncoming water molecules have a greater chance to be attracted and chemisorbed at such a glass surface: the glass is hygroscopic. However, a glass containing Pb^{2-} ions does not extend strong forces toward the atmosphere and, as a result, only a smaller number of collisions with oncoming H_2O molecules will lead to adsorption.

The difference between a lead glass and a soda-lime glass is not very convincing evidence that it is the polarizability of the surface ions which determines primarily the wettability of a solid and, as such, is responsible for the hysteresis of the contact angle. Experiments were carried out, therefore, with a soda-lime silicate glass and a clay of high base exchange capacity, both of which can be easily changed in respect to surface forces by bringing different cations into their surfaces.

IV. CAPILLARY RISE IN GLASS TUBES CONTAINING DIFFERENT CATIONS AT THEIR INNER SURFACE

The surface of a soft (soda-lime-silicate) glass in contact with water consists of OH^- groups. These hydroxy-groups extend hydrogen bonds toward any liquid containing one or more OH^- groups (water, glycerol, sulfuric acid) so that these liquids completely wet the glass and give a zero contact angle. The importance of the OH^- groups for the wettability of a glass surface can be easily demonstrated.

Concentrated sulfuric acid to which a trace of potassium dichromate has been added is heated in a test tube. The chromate oxidizes organic impurities and produces a clean glass surface which is completely wetted by the liquid. Sulfuric acid molecules can attach themselves to this surface by hydrogen bonds. Adding a trace of sodium fluoride to the sulfuric acid causes the OH^- groups to be replaced by F^- ions according to the equation:

$$-\overset{|}{\underset{|}{Si}}-OH+HF=-\overset{|}{\underset{|}{Si}}-F+H_2O.$$

The dehydrating effect of the concentrated sulfuric acid causes this reaction to proceed to completion. After a few seconds, the inner surface of the test tube has become depleted of OH^- groups and is now covered with fluorine ions. With the OH^- groups missing, the surface lacks the ability to form hydrogen bonds with the H_2SO_4 molecules and, as a result, the sulfuric acid forms little droplets on the glass surface and behaves like water in a greasy container. The substitution of F^- for OH^- has completely changed the interfacial forces between glass and sulfuric acid, because the fluorine ion under the strongly polarizing influence of the silicon ion cannot exert a Coulomb force upon the H_2SO_4 molecules which is sufficiently strong to overcome the cohesion forces of the liquid and to produce wetting.

TABLE IV. Temporary hydrophobicity imparted to a clay film by adsorbed ions.

Cation	Approximate contact angle	Average time for spreading
H^+	0°	Immediate spreading
Li^+	0°	Immediate spreading
Na^+	0°	Immediate spreading
K^+	0°	Immediate spreading
Mg^{2+}	20°	1–3 min.
Ca^{2+}	20°	1–3 min.
Sr^{2+}	20°	1–3 min.
Be^{2+}	20°	1–3 min.
Al^{3+}	20°	1–3 min.
Ba^{2+}	40°	5–10 min.
Tl^+	40°	5–10 min.
Zn^{2+}	40°	5–10 min.
Cd^{2+}	40°	5–10 min.
Cu^{2+}	40°	5–10 min.
Co^{2+}	40°	5–10 min.
Cr^{3+}	40°	5–10 min.
Ni^{2+}	60°	10–12 min.
Mn^{2+}	60°	10–12 min.
Pb^{2+}	70°	15–30 min.
Hg^{2+}	70°	15–30 min.
Laurylamine	80°	No spreading after 120 min.

In the absence of water the silicon fluoride layer is stable and, if the glass tube with the sulfuric acid is sealed, the inner surface retains its repellency indefinitely. However, in the presence of water, hydrolysis takes place and the OH^- groups are restored. The glass surface again is completely wet by water; that means it has a zero contact angle.

In contact with the aqueous solution of a salt some of the H^+ ions of the glass surface can be replaced by other cations; for example, Hg^{2+} or Pb^{2+}. This base exchange is accomplished by treating glass capillaries of about 0.3-mm inner diameter first with diluted HCl and, after rinsing them with water, exposing them to a salt solution for several days. After rinsing with distilled water and drying at 110°C, the glass surface was modified by adsorbed cations. The number of ions adsorbed on the glass depends on the time of exposure, the nature of the compounds, its concentration, and on the temperature. Rinsing of the glass after the adsorption is necessary in order to remove the excess salt and the loosely adsorbed anions. Unfortunately, this procedure introduces a certain error because the substitution of H^+ by other cations is a reversible reaction.

The capillary rise was then determined by carefully inserting the treated glass tubes into water and measuring the rise in the *upward direction.*

The salts containing cations of the noble gas-type did not exert a measurable effect on the capillary rise, namely, the nitrates of Li^+, Na^+, K^+, Be^{2+}, Mg^{2+}, Ca^{2+}, Sr^{2+} and Al^{3+}. The effect of other cations can be seen from Table III.

The experiments on the capillary rise of water in glass tubes which had been treated with various cations

shows how the polarizability of the cation determines the temporary interfacial tension value. With the exception of the large and, therefore, polarizable Ba^{2+} ion, all cations with eight outer electrons (noble gas-type ions) did not affect the wettability of the surface to a noticeable extent. As the capillaries were allowed to stand in the water a gradual rise was observed and the time required for reaching the equilibrium value varied from one ion to another. It was greatest for Hg^{2+} (144 hr.) and Pb^{2+} (120 hr.), less for Ni^{2+} (72 hr.) and Cd^{2+} (48 hr.).

As water molecules distill from the meniscus onto the glass surface, the forcefield of the polarized surface ions gradually becomes more symmetrical and with increasing symmetry the strength of attraction forces emanating from the surface ions increases. As a result the liquid rises, replaces the gas film as well as the adsorbed cations and gradually the original glass surface (OH^- groups) is restored.

V. WETTABILITY OF CLAY SURFACES

The same phenomenon of "temporary hydrophobicity" can be observed for clay minerals. Because of its high base exchange capacity, Wyoming bentonite was selected for these experiments. The clay was purified by electrodialysis and allowed to stand with the electrolyte for 48 hr. under occasional agitation by a mechanical stirrer. The concentration of the electrolyte was chosen so as to provide 200 milliequivalents of the cation per 100 grams of the dry clay.

The homogeneous clay suspensions containing the various cations adsorbed at their surface were then sprayed onto porous ceramic tiles by means of a DeVilbiss spray gun. This method produced smooth clay films of controlled thickness. The porosity of the tile removes both the excess electrolyte and water from the clay film.

The clay-covered tiles were then dried at 110°C for 24 hr. Their wettability was tested by dropping freshly distilled water upon the clay, estimating the contact angle of the water droplet right after its application and determining the time necessary for its complete disappearance.

As the bentonite shows practically no anion exchange capacity it was immaterial which salt was used for introducing the cations. The experiments showed that no significant difference exists between nitrates, chlorides, and sulfates. Nitrates were chosen for the base exchange experiments.

Table IV summarizes the results. The cations are divided into several groups according to their increasing effectiveness based on the contact angle. Table IV brings out the parallelism which exists between the effect of these ions on the wettability of a clay film and on the capillary rise in glass tubes.

In order to show the effect of a long chain hydrocarbon group on the wettability and the spreading time, a clay was treated with a solution of the organic base, laurylamine. As far as the contact angle is concerned, Pb^{2+} and Hg^{2+} ions come very close to this substance. However, in contrast to the temporary hydrophobicity imparted by the polarized cation, the lauryl group causes the clay surface to become permanently water repellent.*

VI. WETTABILITY OF A WATER SURFACE

The phenomenon that a drop of a liquid, for example, one falling from a reflux condenser onto the surface of a boiling liquid, does not immediately unite, but may be seen floating for several seconds, is well known to every chemist and has been described in the textbooks on surface chemistry. It can be explained on the basis that gas films or vapor films are present at the surface. The removal of adsorbed gas molecules or the rearrangement of adsorbed vapor molecules so that they fit into the structure of the liquid are time consuming processes.

We have found that polarizable cations, such as Pb^{2+} or Hg^{2+} dissolved in water affect its surface properties in a manner similar to surface active agents, such as sodium stearate or laurylamine. It can be demonstrated that there is no basic difference between the effects of mercuric acetate and sodium stearate upon the forcefield emanating from a water surface. However, the long chains of the stearic acid molecules cannot turn around very rapidly, but the state of polarization of the Hg^{2+} ions change instantaneously with the symmetry of the forcefield. As a result, the similarity between the effects of the two compounds can be demonstrated best by a dynamic rather than by a static method.

The influence of polarizable cations on the surface forces of water affects the tendency of a stream of water flowing out of an orifice to trap air bubbles. Distilled and degassed water was allowed to flow from a burette into a glass container. Both burette and container were equipped with overflow tubes which ensured constancy of the two water levels. By a screw attachment the container could be gradually lowered or raised and the variable distance between the orifice of the burette and the water level could be measured. As long as the tip of the burette was kept close to the water level of the container a steady flow could be observed and no gas bubbles were trapped. By gradually increasing the distance between the tip of the burette and the water level of the container, one reaches a point where gas bubbles become entrapped and carried under the water surface. It was found that for one and the same apparatus and orifice this critical height, H, could be reproduced with fair accuracy. Taking the essential precautions, such as using boiled and degassed water, avoiding contamination and using degreased glass ware (no stopcock grease), the values for H were reproducible within one percent.

* Viscosity measurements of the different clay suspensions did not reveal any unusual features for those clays which contained Pb^{2+} or Hg^{2+} at their surfaces.

The phenomenon can be explained as follows. Depending on the height and on the speed of the flowing water a surface film is formed which has its own characteristic structure. Its structure is the result of two antagonistic effects, namely, the tendency of the system to assume a molecular arrangement which decreases its surface-free energy and the thermal motion favoring a random orientation.

Gas molecules are being adsorbed at the water surface and their desorption is a time consuming process. The desorption of the gas film, however, is essential before the surface of the streaming water can unite with that of the stagnant water. For slowly flowing water the rate of combination of the two water surfaces is slower than the gas desorption. However, as H and with it the time of exposure of the water to air and the velocity of the falling water is increased, a point is reached where the speed of the uniting water surfaces exceeds the rate of desorption. As a result the gas film is carried below the water level where it assumes spherical shape under the influence of the surface tension: gas bubbles are formed.

The addition of sodium stearate to the flowing or to the stagnant water or to both causes their surface structures to change, the surface tension of the water is lowered. In other words, the ratio of attraction forces toward air to attraction forces toward the liquid is increased if a surface active compound such as sodium stearate is added to the water. A one-tenth molal sodium stearate solution was found to trap the airfilm at a height which was nearly 20 percent lower than that for the pure water. A solution of laurylamine (two percent by volume) decreased the value of H nearly 15 percent.

This method of studying the surface forcefields of solutions was found to be very sensitive as can be seen from Table V which shows the effects of a 0.5 molal and a 1.0 molal salt solution on the critical height, i.e., the one above which a gas film is trapped and carried under the water surface. In contrast to the experiments on the wettability of glass and of clay, it was found that even the Na^+ and K^+ ions showed some influence on the wettability of water. In addition, it was found that the nature of the anion is not without influence as can be seen from a comparison between the values for a sodium nitrate and a sodium acetate solution.

A 1.0 molar solution of $NaNO_3$ causes H to decrease 1.2 percent due to the weak polarizability of the hydrated sodium ion. The NO_3^- ion has no effect as can be seen from the addition of HNO_3. The sodium acetate in 1.0 molal solution was found to decrease the value of H by 2.4 percent which means that the acetate group must have about the same effect as the Na^+ ion.

The response of this method to changes in the constitution of aqueous solutions makes it an interesting tool for studying complex formation and related phenomena. For example: depression of H for 0.25 molar mercuric chloride, 9.1 percent; depression of H for 0.25 molar potassium chloride, 0; depression of H for 0.25 molar KCl+0.25 m $HgCl_2$, 4.8 percent.

TABLE V. Effect of dissolved salts on trapping of airfilm by flowing water.

Salt		0.5 molal solution		1.0 molal solution	
Cation	Anion	H mm	Percent decrease	H mm	Percent decrease
H^+	NO_3^-	83	0	83	0
Li^+	NO_3^-	83	0	83	0
Na^+	NO_3^-	83	0	82	1.2
K^+	NO_3^-	82	1.2	79.5	4.2
Be^{2+}	NO_3^-	83	0	83	0
Mg^{2+}	NO_3^-	83	0	83	0
Ca^{2+}	NO_3^-	82.5	0.6	80.5	3.0
Sr^{2+}	NO_3^-	81.5	1.8	79	4.8
Ba^{2+}	Br^-	80	3.6	75	9.7
Al^{3+}	NO_3^-	83	0	83	0
Zn^{2+}	NO_3^-	81	2.4	78	6.0
Cu^{2+}	NO_3^-	80.5	3.0	77	7.2
Cd^{2+}	NO_3^-	79	4.7	74.5	10.2
Fe^{3+}	NO_3^-	79.5	4.2	74	10.9
Mn^{2+}	NO_3^-	78	6.0	71	14.5
Cr^{3+}	NO_3^-	78	6.0	70.5	15.1
Co^{2+}	NO_3^-	77	7.2	70.5	15.1
Ni^{2+}	NO_3^-	76.5	7.7	69.5	16.3
Pb^{2+}	NO_3^-	70.5	15.1	54.4	34.4
Tl^+	CH_3COO^-	69.5	16.3	52	37.3
Hg^{2+}	CH_3COO^-	65.5	21.1	50	39.8

These data indicate that the highly polarizable Hg^{2+} ion which is responsible for the strong decrease of H is made less effective in the presence of KCl. The chemistry of these compounds suggests the formation of $(HgCl_4)^{2-}$ ions or of a similar complex anion which is less polarizable than the cation Hg^{2+}.

For experiments of this type, it is important to control the temperature fairly accurately because an equilibrium such as

$$HgCl_2+2KCl \rightleftharpoons K_2(HgCl_4)$$

is temperature sensitive. In general it was found that the temperature is not a major factor. For our experiments, no special precautions had to be taken to control the temperature accurately because even a 10°C deviation from room temperature would have caused H to vary less than one percent. For pure water, H was found to increase 2.4 percent if the temperature was lowered from 32° to 3°C.

VII. CONCLUSIONS

All surface phenomena such as adhesion, wetting of solids by liquids, and heterogeneous catalysis are governed by the polarization properties of ions. Perfect crystals, liquids, or gases provide a symmetrical environment for ions and molecules at least as far as their bulk is concerned. Interfaces, such as solid-gas or liquid-gas, are the seat of highly asymmetrical forcefields which cause the polarizable ions to undergo a strong change in their electronic orbits. This change will not look very spectacular when described by the elec-

tron density function of the atom because it affects only the tail end of this curve, i.e., the part which represents the outer orbitals. However, these orbitals are the seat of optical and chemical properties and, consequently, they determine light absorption, fluorescence, electrical conductivity, as well as oxidation and reduction phenomena. An ion which is exposed to the one-sided polarizing influence of an interface becomes optically and chemically a different individual. It has different light absorption and different fluorescence. If the polarizability of an ion is sufficiently high it may lose those properties which are the result of its electrical excess charge. A Tl^+ or Pb^{2+} ion is easily hydrated, because their excess charges orient and attract the dipoles of water. However, the same ions adsorbed at a dry clay or a dry glass surface have an electron density distribution which is different from the ions in their gaseous state or from the ions when symmetrically surrounded by water. The O^{2-} ions of the carrier repel the valency electrons of these cations thus increasing their forcefield toward the solid and decreasing their forces emanating into space. The polarized cations lower the surface free energy of the solid and by becoming neutral towards the exterior—the repelled electrons counteract the effect of the positive excess charge —they have lost the property to attract water molecules. It is this decrease of the Coulomb forces directed toward the exterior which causes the solid to appear water repellent. Strictly, there are no repulsion forces acting in the surface which make the carrier hydrophobic but the attraction forces have become too weak to overcome the cohesion of the liquid.

Solids containing large and, therefore, polarizable ions, e.g., I^-, S^{2-}, etc., especially when crystallizing in layer lattices (PbI_2, CdI_2, MoS_2), are not easily wet and due to their weak forcefields they assume properties usually associated with lubricants.

In contrast to organic materials with long hydrocarbon chains, the inertness of polarized ions is only temporary. Every one who has walked along a dusty road on a dry hot summer day and been caught by a sudden rain may have observed this phenomenon of temporary hydrophobicity. The dry dust is not easily wet by water and the first rain drops may roll around like mercury. However, after it has rained a few minutes the rain soaks into the ground and soon the mud tells us that the dust did not have permanent hydrophobic properties.

Polarizable ions can adjust their own forcefields to that of the environment. Their Coulomb forces are symmetrical when symmetrically surrounded by ions of the opposite charge. In the asymmetrical forcefield of an interface, however, their electron distribution and with it their valency forces assume directional properties. A heavy metal ion adsorbed at a surface which repels its electron cloud, so that the polarized ion has a higher electron density toward the exterior, assumes the properties of a neutral metal atom. As such, it may be used as a bridge between an ionic substance, for example, glass, and the metals silver, gold, or copper. Polarizable ions are used to enhance the adhesion between glass and metal. Before silvering a glass it is treated with tin compounds in order to make the silver film adhere better.

Enright, Marboe, and Weyl[5] used the decomposition of H_2O_2 into H_2O and oxygen for demonstrating the metallic character of adsorbed heavy metal ions. Hydrogen peroxide is readily decomposed when brought in contact with a noble metal, Au or Pt. Dissolved ions, such as Hg^{2+} or Ag^+, have no effect on this reaction. However, if these ions are adsorbed at the surface of an ionic carrier (glass or alumina) they become positive catalysts. Ions of this type act as negative catalysts or catalytic poisons when adsorbed at the surface of platinum, because in its forcefield they form metallic bonds with the metal (high electron density between cation and metal surface) and extend a strong positive forcefield toward the solution which is ineffective as a catalyst for this reaction.

The experiments with flowing water prove that the water-gas interface has a similar deforming influence on polarizable ions at the glass or clay surface. Very probably this interface plays an important role in certain gas-liquid reactions which are catalyzed by heavy metal ions. The rate of oxidation of ferrous sulfate by air or oxygen gas is greatly increased if 0.01 molar cupric ions are present. In a similar fashion the hydration of acetylene gas in diluted acid leading to acetaldehyde is catalyzed by Hg^{2+} ions.

[5] Enright, Marboe, and Weyl, "Influence of the carrier on the catalytic activity of adsorbed heavy metal ions," Tech. Report No. 1, Contract No. N6onr 269 Task Order 8 N.R. 032-265 (October, 1948).

Distribution of Ionization in Materials Irradiated by Two and Three Million-Volt Cathode Rays

J. G. Trump, K. A. Wright, and A. M. Clarke
Department of Electrical Engineering, Massachusetts Institute of Technology, Cambridge, Massachusetts
(Received November 4, 1949)

Measurements are reported on the distribution of ionization in depth of aluminum produced by steady beams of two and three million-volt electrons. The variation of cathode-ray current density in a plane transverse to the beam, the effect on this transverse distribution of additional aluminum scattering foils, and a practical method of cathode-ray dosage computation are given.

INTRODUCTION

In the study of the physical and biological effects of high energy cathode rays[1] it is desirable to know the actual distribution of the ionization energy in the absorber material. An earlier paper[2] reported measurements on the distribution of ionization in depth of water, aluminum, copper, and lead produced by monoenergetic electron beams over the energy range from 0.3 to 1.5 million volts. In the present studies, ionization distribution in depth of aluminum and intensity distribution across the beam were measured for steady streams of electrons in the two and three million-volt range. In order to secure greater uniformity across the field, a study was made of the effect of scatter produced by aluminum foils inserted in the beam. A method of dosage computation which facilitates the determination of maximum, average, and minimum cathode-ray dose on a sample of given size is included.

CATHODE-RAY SOURCE

A pressure-insulated Van de Graaff electrostatic accelerator[3] was used as the source of high energy electrons. These were directed toward the absorber in a continuous stream, homogeneous in energy and controllable over the range from 1 to 3.5 million volts. The electrons emerged from the tube through an aluminum window 0.003 inch thick on which they impinged as parallel particles over an area of about 5 mm diameter. Voltage was measured by a generating voltmeter which had been calibrated at 1.63 million volts by making use of the beryllium (γn) reaction and observing the threshold with a BF_3 counter.

MEASUREMENT TECHNIQUE

A thin parallel-plate ionization chamber was used to measure the distribution of ionization in depth caused by the high energy electrons in their passage through aluminum. The chamber consisted essentially of a stretched aluminum diaphragm 0.0006-inch thick, insulated and separated by 1 mm from a thick aluminum plate which formed the other electrode. The area of the air gap was large compared with that of the cathode-ray beam at the region of measurement. As shown in Fig. 1, the chamber was mounted close beneath the cathode-ray window of the accelerator tube. Thin aluminum sheets were inserted between the cathode-ray window and the ionization chamber to give the effect of placing the chamber at progressively greater depths below the surface of the absorbing material.

A constant beam current I_1 of high energy electrons was directed at the absorber system. Two microamperes of beam current produced maximum ionization currents I_2 or I_3 of approximately 40 μa. I_2 represents the negative ionization current plus the portion of the beam current which passed through the aluminum sheets, and I_3 the positive ionization current minus the portion of the beam current which was absorbed in the aluminum sheets.

Linearity of the ionization chamber was checked by using a fixed thickness of aluminum absorber above the chamber and observing the constancy of the ratio I_2/I_1

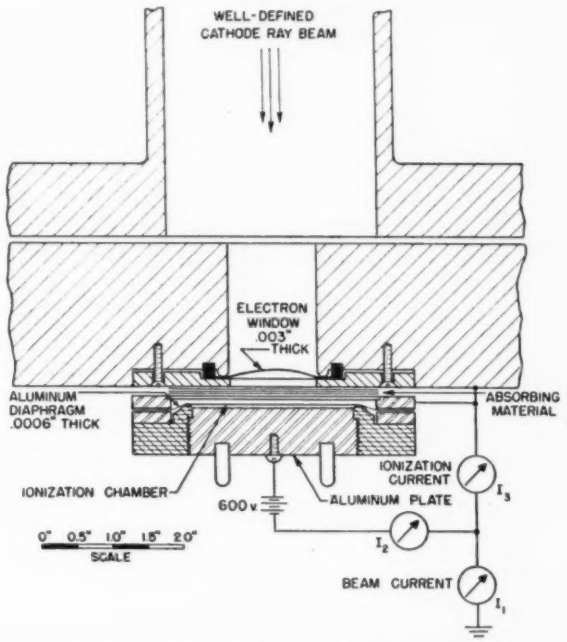

FIG. 1. Apparatus for measuring the distribution of ionization in depth of aluminum produced by high energy electron beams.

[1] J. G. Trump and R. J. Van de Graaff, J. App. Phys. **19**, 599 (1948).
[2] Trump, Van de Graaff, and Cloud, Am. J. Roentgenology and Rad. Therapy **43**, 728 (1940).
[3] J. G. Trump and R. W. Cloud, Am. J. Roentgenology and Rad. Therapy **49**, 531 (1943).

over a wide range of beam currents I_1. The collecting voltage was maintained constant at 600 volts, this voltage having been found to be well above the amount for saturation. This check indicated linearity of response to within ± 2 percent for the range of currents used in the experiment.

The distribution of current density in a plane transverse to the beam was measured with the arrangement shown in Fig. 2 by collecting the current passing through spaced holes in an aluminum plate at a distance of 40 cm from the exit window of the accelerator tube. The minimum or inherent scattering of the electron beam was caused by both the 0.003-inch aluminum window and the 40 cm of intervening air. Faraday cages were placed beneath the individual holes spaced radially at $\frac{1}{4}$-inch intervals from the center of the plate. Holes which did not have Faraday cages beneath were plugged to eliminate stray currents. The $\frac{1}{8}$-inch diameter holes in the lower aluminum plate were drilled so

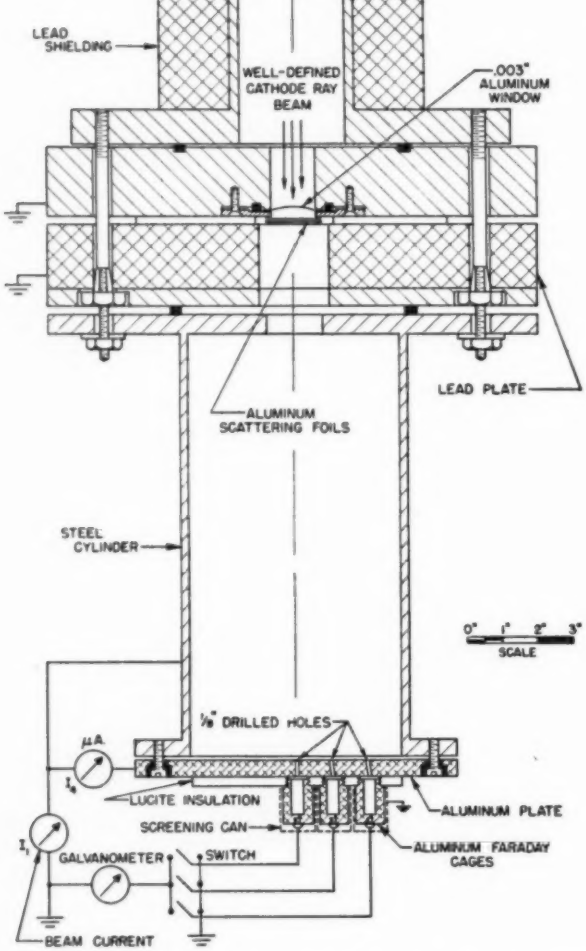

FIG. 2. Apparatus for determining the cathode-ray current density transverse to the beam and the effect of additional aluminum scatterer.

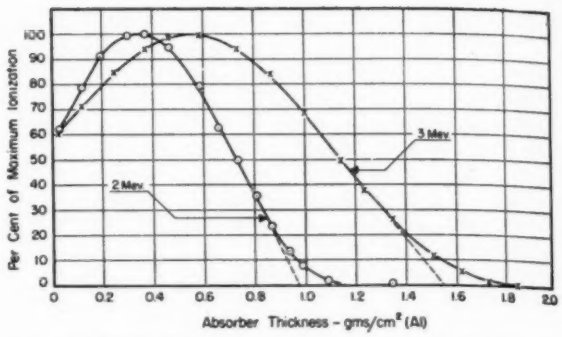

FIG. 3. Distribution of ionization in depth of aluminum produced by cathode rays with energies of two and three million volts.

that their angles with respect to the beam axis were determined by the center of the exit window and the radial distance of the holes from the center of the plate. It was found necessary to shield the individual Faraday cages from ionization in air caused by x-rays. For these measurements the total beam current I_1 was held constant at 50 μa, and the resultant Faraday cage currents of the order of 10^{-8} amp. were read on a galvanometer.

IONIZATION DISTRIBUTION IN DEPTH

Figure 3 shows the ionization distribution in depth of aluminum produced by electron beams of two and of three million volts energy. It is observed that the ionization has a broad maximum at about one-third the greatest range, this previously reported distribution[2] arising from the high scattering tendency of the primary electrons within the absorber. The penetrating power of electrons in aluminum is close to 1 g/sq. cm per two million volts, as determined by the interpolated curve intercept. From other studies[2] at lower electron energies, a corresponding range was found for water, aluminum, copper, and lead, and the general shapes of the ionization distribution curves were closely similar. The range in centimeters can be obtained by dividing the range in g/sq. cm by the density of the absorber material. The tail of the distribution curve is due primarily to those few electrons which have made relatively undeviated paths through the absorber. Ionization due to x-rays produced within the absorber can easily be shown to constitute a negligible addition to the measured ionization currents.

Since the area of the ionization chamber was large in comparison with that of the beam, the curves of Fig. 3 represent approximately the distribution of ionization in depth along the axis of the beam and more accurately the total ionization at each depth. In addition to its primary dependence on electron energy and absorber density, the distribution of ionization energy in an absorber irradiated by essentially parallel and monoenergetic electrons is profoundly affected by electron scattering. Although the ionization density is greatest near the end of the path of a single electron,

the effect of scattering on a beam of such particles is to shift the region of highest ionization and energy absorption to a depth of about one-third the maximum penetration for that energy.

BEAM INTENSITY DISTRIBUTION ACROSS THE FIELD

Figures 4 and 5 show the intensity distribution of two and three million-volt cathode-ray beams in a transverse plane 40 cm from the exit window. The upper curve of each figure shows the distribution resulting from the inherent scatter consisting of the 0.003-inch aluminum window and 40 cm of atmospheric air. The remaining curves show the beam-spreading effects of additional aluminum scatterer placed immediately below the window.

The greater directivity and reduced scatter obtained at the higher beam energies is evident from a comparison of Figs. 4 and 5. In the irradiation of an area four inches in diameter at the 40-cm distance, two million-volt

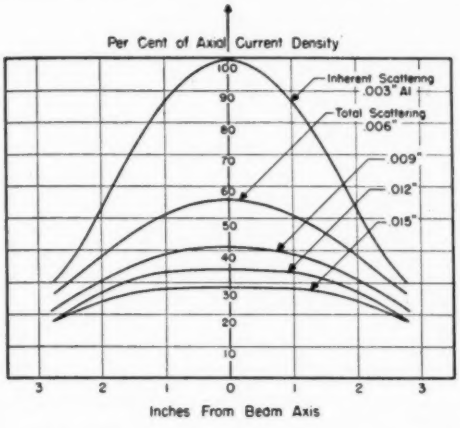

FIG. 4. Distribution of current density for two million-volt cathode rays in a transverse plane 40 cm from the 3-mil aluminum window.

cathode rays with inherent scatter would deliver 52 percent of the axial intensity to the sample edges, while a three million-volt beam would deliver but 30 percent to the edges. Additional scatterer inserted in the beam rapidly increases the uniformity of beam intensity over the selected area, but is attended by loss of charge to outside regions. Modification of the intensity distribution to the transverse plane can readily be accomplished by the addition of solid scatterer or an increase in the air path to the absorber. Because the ratio of scatter to absorption increases with atomic number, it would be preferable to use foils of gold or other high atomic-number metal as the scattering material.

DOSAGE COMPUTATIONS

At the present time there exists a considerable interest in the physical, chemical,[4] and biological[5] effects of high energy cathode rays on living and non-living materials. For such irradiation studies, the cathode-ray equipment may be set up as in Fig. 2 with a solid lower aluminum plate. A current-collecting disk is placed on, and preferably flush with, the top of this plate, but electrically insulated from it. A suitable shutter is used to provide accurate control of the exposure time.

In principle, the cathode-ray dosage rate can be specified with great exactness inasmuch as it is determined by the number of impinging electrons per second and their accelerating voltage. In practice, account must be taken of the distribution of the ionization energy both in depth and across the transverse plane of the absorber. For the case of stationary samples, dosage computations can readily be made with the aid of information contained in Figs. 3–5. The dose delivered to liquids in continuous flow or to solids on a moving belt may often be derived more simply by direct comparison with the known chemical or bactericidal effects of cathode rays as determined on stationary samples.

The total cathode-ray power falling on a disk of diameter D is EI where E is the accelerating potential and I the total beam current to the disk. The average power P absorbed per gram of material distributed uniformly over this disk to a depth R expressed in g/sq. cm is

$$P=[EI/\pi(D/2)^2R]K_1K_2\text{watts/g},$$

where K_1 is the fraction of the total power absorbed in range R and K_2 is a factor close to unity which takes account of the possible change in electron backscatter from the disk area after a sample of the same diameter has been placed upon it. The value of K_1 may be obtained from Fig. 3 by dividing the area under the curve for a sample thickness R by the total area of the curve of energy E. The value of K_2 requires the measurement of electron backscatter for different materials,[6] but can be kept close to unity by making both disk and sample

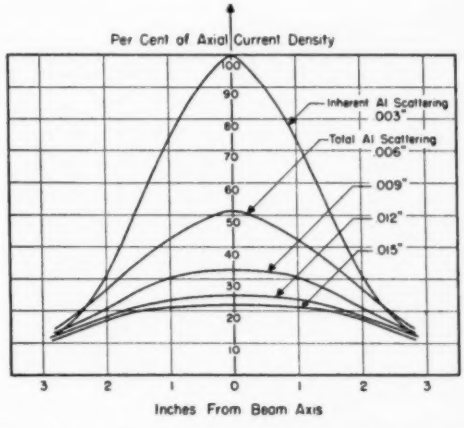

FIG. 5. Distribution of current density for three million-volt cathode rays in a transverse plane 40 cm from the 3-mil aluminum window.

[4] A. O. Allen, AEC Report MDDC-363 (September, 1946).
[5] Dunn, Campbell, Fram, and Hutchins, J. App. Phys. **19**, 605 (1948).
[6] J. G. Trump and R. J. Van de Graaff, Phys. Rev. **75**, 44 (1949).

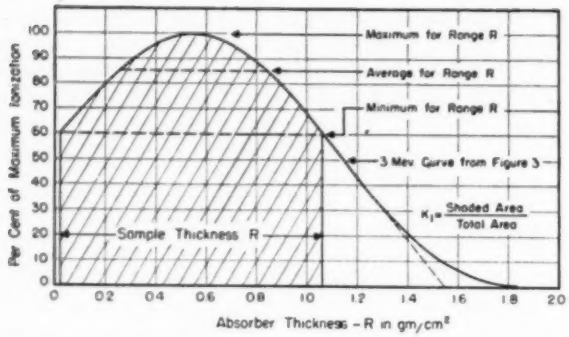
Per Cent of Maximum Ionization
Maximum for Range R
Average for Range R
Minimum for Range R
3 Mev Curve from Figure 3
K_1= Shaded Area / Total Area
Sample Thickness R
Absorber Thickness – R in gm/cm²

FIG. 6. Ionization-in-depth curve for three million-volt cathode rays applied to a 1.03-g/cm² sample to determine maximum, average, and minimum doses.

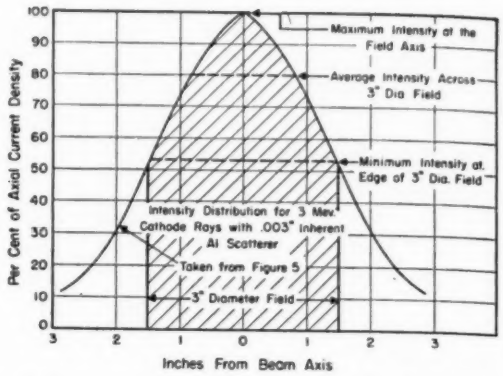
Per Cent of Axial Current Density
Maximum Intensity at the Field Axis
Average Intensity Across 3" Dia Field
Minimum Intensity at Edge of 3" Dia. Field
Intensity Distribution for 3 Mev Cathode Rays with .003" Inherent Al Scatterer
Taken from Figure 5
3" Diameter Field
Inches From Beam Axis

FIG. 7. Transverse beam intensity curve for three million-volt cathode-ray beam applied to a three-inch diameter sample at 40-cm distance to determine maximum, average, and minimum intensities.

cover of the same low atomic number material, such as aluminum.

Cathode-ray dose is best expressed in ergs and joules for physical studies, but may be specified in equivalent roentgens for biological studies. The conversion factors for these units of radiation energy are 1 joule $=10^7$ ergs; 1 roentgen equivalent physical[7] (rep) $=83$ ergs per gram of tissue; 10^6 reps $=8.3$ joules per gram of tissue. The irradiation time is found by dividing the desired dose expressed in joules by the average dosage rate P.

Maximum and minimum doses can be calculated from the average by applying the appropriate dose ratios both for the distribution in depth and the transverse distribution as given in Figs. 3–5. Consider the specific case in which it is desired to irradiate a stationary sample three inches in diameter (7.62 cm) with three million-volt cathode rays. The current to the three-inch collecting disk is taken as 10 μa. For convenience, the sample depth R in g/sq. cm is chosen so that the entrance and exit doses are the same percent of the maximum dose. From the three million-volt curve of Fig. 3 or 6, R is found to be 1.03 g/sq. cm. The ratio of the area included under this curve to depth R to the total area gives coefficient $K_1=0.84$. If care has been taken to use low atomic-number materials and to mount the sample for minimum effect on backscatter, then K_2 can be taken as unity. Then

$$P=3\times10^6\times\frac{10\times10^{-6}}{\pi(7.62/2)^2}\,\frac{0.84\times1}{1.03}=0.54\ \frac{\text{watts}}{\text{g}}$$

and the time required to deliver an average dose of 10^6 reps is

$$t=8.3/0.54=15.4\ \text{sec.}$$

From the distribution-in-depth curve of Fig. 6 the average dose is found to be 85 percent of the maximum, and the minimum 60 percent. From the intensity distribution across the beam of Fig. 7, with only inherent scattering, the average intensity is found to be 80 percent of the maximum, and the minimum 52 percent. Therefore the minimum dose is $(0.6\times0.52)/(0.85\times0.8)$, or 46 percent of the average, and the maximum dose is $(1\times1)/(0.85\times0.8)$, or 147 percent of the average. The spread between maximum and minimum doses may be controlled by suitable selection of absorber depth, width, scatterer, and irradiation distance.

ACKNOWLEDGMENTS

We desire to pay tribute to Arthur M. Clarke, our associate on this paper, whose death on January 19, 1949, ended seven years of devoted and effective work in the High Voltage Research Laboratory. The help of Dr. E. W. Webster in making some of the measurements is gratefully acknowledged. This work was assisted by the Joint Program of the ONR and the AEC.

[7] R. D. Evans, Nucleonics **1**, 39 (October, 1947). Proposals that 1 rep be associated with the absorption of 93 ergs per gram of water or tissue and that the value of 83 ergs per gram be restricted to absorption in air will be considered at the Sixth International Congress of Radiology in London, July 1950.

Letters to the Editor

Metal Transfer in the Cutting Process*

MILTON C. SHAW AND CHARLES D. STRANG, JR.
Department of Mechanical Engineering, Massachusetts Institute of Technology, Cambridge, Massachusetts
January 27, 1950

THERE are generally thought to be two distinct types of continuous chip formed in single point metal cutting—that produced in the presence of a so-called built-up edge and that produced when no built-up edge is present. The built-up edge is a metal appendage which accumulates at the cutting point of the tool when the metal is cut under conditions conducive to high friction and welding. The built-up edge can be found adhering to either the tool face or the workpiece and is frequently macroscopically visible. Figure 1 is a photo-micrograph of a polished

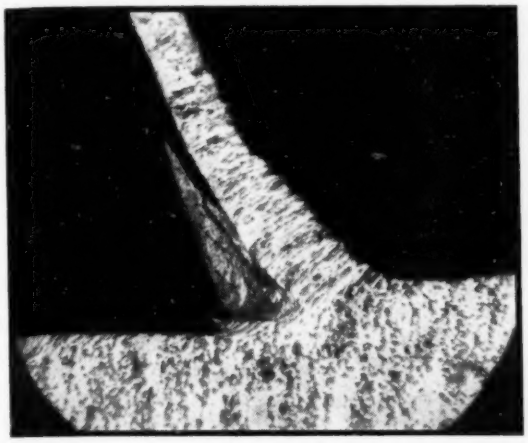

FIG. 1. Photo-micrograph showing built-up edge, magnification, 60 times.

and etched specimen obtained by cutting a sample of annealed SAE 4027 steel in air with the end milling cutter shown in Fig. 2. The large built-up edge can be seen at the junction of the chip and the freshly cut surface.

The chip shown in the photo-micrograph of Fig. 3 was produced under conditions least favorable to the formation of a built-up edge. The workpiece and the tool were submerged in carbon tetrachloride, one of the most effective cutting fluids known, and the cutting velocity was adjusted to be in the range where the carbon tetrachloride has sufficient time to react (below approximately 40 ft. per min.) with the metal being cut to form a low shear strength solid lubricant. This compound is thought to prevent or decrease metal-to-metal contact between chip and tool face and so prevent formation of a built-up edge. No built-up edge is evident in Fig. 3 nor was any transferred metal visible on the cutting tool when it was examined under the microscope. In spite of this, the autoradiograph of Fig. 4 shows that considerable material from the workpiece has been welded to the face of the tool.

This autoradiograph was produced by machining a specimen of SAE 4027 steel which had previously been made radioactive by neutron irradiation in the pile at Oak Ridge. A new tool, identical to the first, was used for this experiment and was carefully cleaned and washed in water to remove any loose chips or residual radioactive iron chloride produced as the metal was machined under carbon tetrachloride. The cutting end of the tool was placed in contact with a sheet of x-ray film and exposed for a period of two

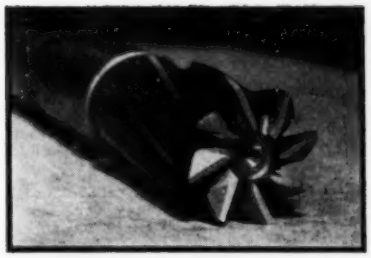

FIG. 2. End milling cutter.

weeks. Figure 4 is a positive print and the white areas indicate the presence of the radioactive built-up edge. It will be seen that the built-up edges does not extend across the full width of the tool face inasmuch as the workpiece was annular in cross section.

This simple experiment establishes the fact that even under the most ideal conditions of cutting fluid action, some welding occurs between the chip and tool face with attendant transfer of metal and further that the presence or absence of a built-up edge is merely a matter of degree. While the invisible built-up edge indicated by Figs. 3 and 4 is insignificant from the standpoint of cutting geometry, it is of considerable interest with regard to friction and tool wear. Although carbon tetrachloride does not entirely prevent metal to metal contact and welding at the chip-tool interface, it does act to reduce greatly the amount of welding or transfer and the size of the built-up edge. The iron chloride that is formed when carbon tetrachloride reacts with the metal during cutting probably reduces the real area of metal-to-metal contact and at the same time may produce a transferred layer that is weak in shear, consisting in part of steel and iron chloride.

Under usual cutting conditions, the built-up edge is welded to the tool face whereas it is generally found attached to the chip when the operation is suddenly stopped for the purpose of preparing photo-micrographs as shown in Fig. 1. This paradox may be readily explained on the basis of decreased shear strength with increased temperature. During cutting, the temperature at that surface of the built-up edge furthest from the tool face is higher than that at the tool face and slip consequently takes place in the region of temperature-reduced shear strength. When a photo-micrograph specimen is prepared by suddenly stopping the tool in the act of producing a chip, the metal quickly cools and the shear strength of the highly worked metal at the interface of the built-up edge and the chip exceeds that at the tool face. Therefore, when the tool is withdrawn, the built-up edge is usually found adhering to the chip rather than to the tool. On the other hand, remnants of built-up edge are often found on the face of a tool which has continued cutting to the very end of the workpiece.

The relatively large amount of metal transfer (built-up edge) which occurs when cutting metal in air as compared to that observed in dry friction experiments[1] may also be explained by the

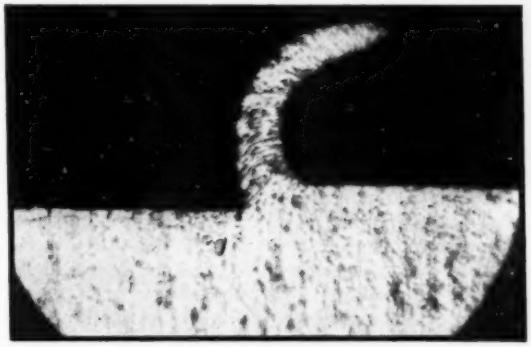

FIG. 3. Photo-micrograph of chip formed beneath the surface of carbon tetrachloride. Magnification, 60 times.

FIG. 4. Autoradiograph of end milling cutter used to machine radioactive steel.

decrease in shear strength with increase in temperature. When cutting metal, considerable energy is expended in plastic deformation along the shear plane. The energy thus dissipated causes an increase in the internal energy along the shear plane, a consequent rise in temperature and hence a decrease in shear strength. The portion of the material in the built-up edge adjacent to the tool face is at a lower temperature and hence has a greater shear strength. The presence of the plastic deformation in the shearing process thus acts to allow the transfer of an unusually large quantity of metal from the chip to the tool face before the built-up edge produced becomes unstable and passes off with the chip.

In the field of metal cutting research, as in many other branches of physics and engineering, the use of radioactive materials provides a means for detecting changes of very small magnitude. This technique should prove particularly valuable in studies of the chemical reactivity of cutting fluids, the general nature of cutting fluid action, and in detecting very small rates of tool wear.

* The radioactive steel used in these experiments was irradiated at Oak Ridge under authorization of the United States AEC and was made available through the generosity of Professor J. T. Burwell, Jr. and the Chrysler Corporation.

[1] J. T. Burwell, Jr., "Radioactive tracers in friction studies," Nucleonics 38 (December, 1947).

The Potential Distribution in Pulsed Oxide-Coated Cathodes and Its Consequences for the Velocity Distribution of the Emitted Electrons

R. LOOSJES, H. J. VINK, AND C. G. J. JANSEN
Philips Research Laboratories, N. V. Philips' Gloeilampenfabrieken, Eindhoven, Netherlands

January 23, 1950

OUR investigations[1] concerning the total potential drop across a pulsed, activated oxide* coating of 25 micron thickness showed that a potential difference of e.g. 200 v at a current density of 10 amp./cm² at 827°C can exist.

Further investigations[2] by means of probe potential-measurements showed that, when using a rather pure nickel core containing a few tenths percent of different impurities, there was no appreciable interface potential difference and only a moderate potential drop of e.g. 6 v at 10 amp./cm² at 900°C across 85 microns of an oxide coating of 270 micron total thickness was set up during a pulse.

From these results it was concluded that, at least under the given circumstances, the potential distribution in a pulsed, activated oxide coating is of the form reproduced in Fig. 1. It was supposed that the rather steep potential drop near the surface could give rise to a spread of the electron velocities over tens or hundreds of volts, (a) because of electrons starting not only from points on the surface like *A*, but also emerging from points more inside the porous coating like *B*, or (b) because of all the electrons starting from points like *A*, while the potential at these points would be rather variable in connection with local variations in the properties of the surface layer of the coating. We therefore worked out a method for investigating the electron velocity distribution by means of electrostatic deflection.[3] Great care was taken not to lose any group of electrons especially those with the smaller velocities.

Preliminary results showed that the spread of the velocities of the electrons emitted from a pulsed, activated oxide-coated cathode is much greater than could be expected if the distribution

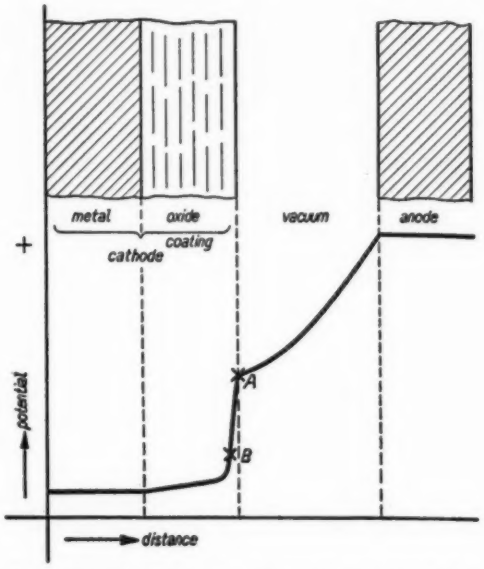

FIG. 1. Potential distribution in an oxide-coated cathode.

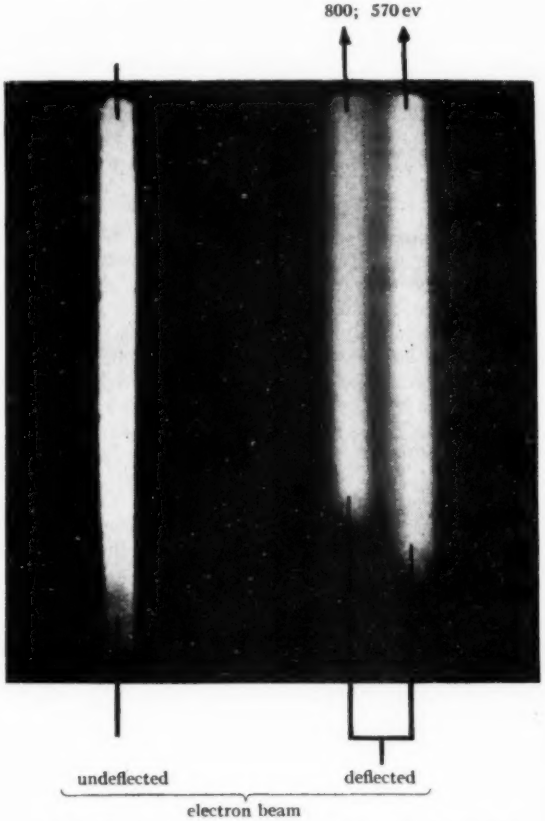

FIG. 2. Electron velocity spectrum of a pulsed oxide cathode. $V_a = 860$ v; $I_a = 14$ amp./cm²; $T = 942$°C.

were Maxwellian. Thus our working hypothesis was confirmed. For example, using square microsecond pulses of 10 amp./cm² at 850°C and an oxide coating of 60 micron thickness the energy difference between the fastest and the slowest electrons detectable was 140 ev, the fastest ones still having an energy 60 ev smaller than that which could be computed from the total cathode-anode potential difference.

From all our results it follows that whereas in our cathodes no interface resistance is detectable, a high resistance layer must exist near the surface of the coating. An explanation for this phenomenon might be (a) the fact that the surface is cooler than the bulk of the coating, (b) the fact that the composition of the surface layer is different from that of the bulk,[4] and/or (c) an exhaustion of the electrons in the surface pores by the emission, since according to our theory of the conduction[5] of the oxide coating these same electrons are mainly responsible for the conduction.

We do not think that our results are in contradiction with those of Eisenstein[6] found with a retarding field method.

Another, but unexpected result of our investigations into the electron velocity distribution was the fact that the distribution spectrum was in most cases found to be more or less concentrated in two and even three "lines" instead of being continuous (see Fig. 2). The reason for the occurrence of these "lines" is not yet clear. It might be that electrons are emitted mostly from the surface of the coating and from the "bottom" of the pores in the surface. In view of the high voltages involved even the possibility of emission of secondary electrons from places on the surface, like A, cannot be excluded.

At low temperatures, e.g. 700°C, the spread in the velocities disappears. This can be explained by the fact that with decreasing temperature the thermionic emission falls off more rapidly than the electronic conduction.[5]

* Composition: 52.5 percent by weight BaO, 47.5 percent by weight SrO.
[1] R. Loosjes and H. J. Vink, Philips Res. Rep. **2**, 190–204 (1947).
[2] R. Loosjes and H. J. Vink, to be published in Le Vide.
[3] C. G. J. Jansen and R. Loosjes, unpublished.
[4] A. Eisenstein, J. App. Phys. **17**, 654–663 (1946). H. Huber and S. Wagener, Zeits. f. tech. Physik **23**, 1 (1942).
[5] R. Loosjes and H. J. Vink, Philips Res. Rep. **4**, 449–475 (1949); J. App. Phys. **20**, 884 (1949).
[6] A. S. Eisenstein, J. App. Phys. **20**, 776–790 (1949).

A Sampling of 1949 Books

THE output of new scientific books during 1949 is indeed impressive both in number of books published and in their quality. It seems as though the exposition pent up during the war years is now gradually escaping, and as a result we have an up-to-the-minute survey or treatise in almost every branch of physics. The sampling presented here is a selection from the new books that have come across the Editor's desk during late 1948 and 1949, and is not in any sense a complete list. In each case a few comments are given which may assist the reader in deciding whether or not the book has further interest for him. For easy reference the books are classified as to subject matter.

MATHEMATICS AND MATHEMATICAL PHYSICS

Principles of Mathematical Physics

By WILLIAM V. HOUSTON (new second edition). Pp. 363+xii. McGraw-Hill Book Company, Inc., New York, 1948. Price $5.00.

The purpose of this text is to introduce the student to the more powerful methods of handling physical problems by giving him an opportunity to apply them to simple cases. Designed for intermediate courses, the book is intended to fill the gap between elementary courses in physics and more advanced courses on special subjects. The abundance of problem material forming an integral part of the text is again emphasized, in this second edition, as a principal teaching aid. The student is encouraged to develop the theory for himself by working out these problems, and is urged to depend as far as possible upon his own resourcefulness, insight, and ingenuity.

The chapters on electricity and magnetism have been expanded, and the m. k. s. system of units has been used throughout.

The Mathematical Analysis of Logic

By GEORGE BOOLE (reprinted). Pp. 82. Philosophical Library, New York, 1949. Price $3.75.

This is the first reprinting of a monograph published a century ago and now extremely rare. This short book is believed to have been the first to set on a scientific basis the mathematization of logic and thus prepare the way for the formal study of the foundations of pure mathematics itself.

Elementary Mathematics from an Advanced Standpoint, Vol. II—Geometry

By FELIX KLEIN. Translated from the German by E. R. Hedrick and C. A. Noble. Pp. 214+ix, Figs. 141. Dover Publications, New York, 1949. Price $2.95.

Unlike an ordinary textbook on geometry, this book is intended to give the instructor a comprehensive view of the whole field of geometry, help stimulate his own creative thinking on the subject, and provide him with a broader understanding which he will be able to apply profitably in the classroom, laboratory, or in general reading. The book is divided into three sections: the Simplest Geometric Manifolds, Geometric Transformations, and Systematic Discussion of Geometry and Its Foundations.

Proceedings of Symposia in Applied Mathematics

Pp. 219+vii. American Mathematical Society, New York, 1949. Price $5.25.

This book consists of a series of papers on non-linear problems in the mechanics of continua, including hydrodynamics, elasticity, and plasticity.

Problem Book in the Theory of Functions, Vol. I

By KONRAD KNOPP. Pp. 126. Dover Publications, New York, 1949. Price $1.85.

Used in conjunction with Professor Knopp's previously published *Theory of Functions*, this new English translation of the Problem Book provides the teacher and student with excellent aid in any first course of study covering the theory of functions of a complex variable. This book may also be used to supplement any other textbook in the field.

Introduction to the Theory of Fourier's Series and Integrals

By H. S. CARSLAW (third revised edition). Pp. 368+xiii, Figs. 39. Dover Publications, New York, 1949. Price $3.95.

In preparing this new printing of the third edition, the author has contributed a number of corrections noted since the last printing. This volume contains new tests for uniform convergence of series, a more thorough treatment of term by term integration and the Second Mean Value Theorem, enlarged sets of examples on Infinite Series and Integrals, a new section dealing with the Riemann-Lebesque theorem and its consequences, and a special treatment of the Lebesque definite integral which compares it with the classical Riemann integral.

Modern Operational Calculus

By N. W. MCLACHLAN. Pp. 218+xiv, Figs. 29. The Macmillan Company, New York, 1949. Price $5.00.

Integraltafel. Erster Teil: Unbestimmte Integrale

By WOLFGANG GRÖBNER AND NIKOLAUS HOFREITER. Pp. 166. Springer-Verlag, Vienna, 1949.

Introduction to Applied Mathematics

By FRANCIS D. MURNAGHAN. Pp. 389. John Wiley and Sons, Inc., New York, 1948. Price $5.00.

This is a detailed and self-contained study of the mathematics used in modern physics and engineering. The author gives a relatively full account of vector and matrix calculus, harmonic analysis, spherical harmonics, and Bessel functions. There is a thorough discussion of boundary value problems and integral equations, culminating in Rayleigh's principle; a treatment of mechanical problems by means of the calculation of variations; and a detailed explanation of operational calculus. The book is designed for graduate students and scientific workers with diversified interests.

Numerical Calculus

By WILLIAM EDMUND MILNE. Pp. 393+x. Princeton University Press, Princeton, 1949. Price $3.75.

This book is especially designed for the use of actuarial students, statisticians, applied mathematicians, and others who are forced to seek numerical solutions. It presupposes only a knowledge of the

essentials of algebra, analytical geometry, trigonometry, and elementary calculus. The object is practical, for while numerical calculus is based on the concepts of pure mathematics, it is recognized that the worker must produce a numerical result. This book would be a useful text for undergraduate courses in finite differences and methods of approximation.

Tables of Bessel Functions of Fractional Order, Vols. I and II

By Computation Laboratory of the National Bureau of Standards. Pp. 413 and 365. Columbia University Press, New York, 1948 and 1949. Price $7.50 and $10.00.

These volumes are a continuation of a series published by the Computation Laboratory of the National Bureau of Standards.

Vorträge über Determinanten und Matrizen mit Anwendungen in Physik und Technik

By Werner Schmeidler. Pp. 155. Akademie-Verlag, Berlin, 1949.

Tables of Inverse Hyperbolic Functions

By the Staff of the Computation Laboratory, Harvard University. Pp. 290. Harvard University Press, Cambridge, 1949. Price $10.00.

This is believed to be the first adequate presentation of tables of the inverse hyperbolic functions between the covers of a single volume. The inverse hyperbolic sine, cosine, and tangent are explicitly tabulated to nine decimal places. Differences are available to provide second-order interpolation to this accuracy, and the other inverse hyperbolic functions are readily obtainable. These tables will meet the growing demand in the fields of physics, statistics, engineering, and applied mathematics generally. The book contains the tables, an introduction to the method of calculation, and what is believed to be a complete bibliography of all existing tables of these functions, with critical notes on their range and reliability.

Tables of Generalized Sine- and Cosine-Integral Functions, Parts I and II

By the Staff of the Computation Laboratory, Harvard University. Pp. 462 and 560. Harvard University Press, Cambridge, 1949. Price $10 and $10.

The tables in these two volumes were computed by the automatic sequence controlled calculator, which was presented to Harvard University in 1944 by the International Business Machines Corporation. These tables, which are carried to six decimal places, are invaluable time-savers in the investigation of such questions as self- and mutual impedances, radiation resistance, and distribution of current in antennas and antenna arrays of various types.

Tables of the Bessel Functions of the First Kind of Orders 52 through 63

By the Staff of the Computation Laboratory, Harvard University. Pp. 544. Harvard University Press, Cambridge, 1949. Price $8.00.

Tables of Sines and Cosines to Fifteen Decimal Places at Hundredths of a Degree

By the Staff of the National Bureau of Standards. Pp. 95. Superintendent of Documents, Washington, 1949. Price $0.40.

Tables of Scattering Functions for Spherical Particles

By the Staff of the National Bureau of Standards. Pp. 119. Superintendent of Documents, Washington, 1949. Price $0.45.

The Slide Rule

By Lee H. Johnson. Pp. 242+x, Figs. 138. D. Van Nostrand Company, Inc., New York, 1949. Price $3.00.

This book presents a technique of operation for the Duplex slide rule which makes full use of its versatility and efficiency. A chapter on the Mannheim type is also included.

A Concise History of Mathematics, Vols. I and II

By Dirk J. Struik. Pp. 299+xviii (total), Figs. 49 (total). Dover Publications, New York, 1948. Price $1.50 per volume, $3.00 set.

The author has compressed the history of mathematics into two small volumes. He stresses the continuity and affinity of the Oriental civilizations rather than the mechanical divisions of Egyptian, Babylonian, Chinese, Indian, and Arabian. He is particularly careful to point out the distinctions between established facts, hypotheses, and tradition, especially in Greek mathematics.

Mathematics Dictionary

Glenn James and Robert C. James, editors (revised and enlarged edition). Pp. 432+v. D. Van Nostrand Company, Inc., New York, 1949. Price $7.50.

This dictionary has been designed as a reference work for students and for practicing physicists, chemists, engineers, and statisticians. To the coverage of terms included in the earlier version of the book there have now been added the basic terms in: metric differential geometry, theory of functions of real and complex variables; advanced calculus, differential equations, theory of groups, theory of matrices, theory of summability, point-set topology, analytic mechanics, theory of potential, and statistics. The appendix contains the tables most frequently referred to by mathematicians, physicists, chemists, engineers, and statisticians.

Regular Polytopes

By H. S. M. Coxeter. Pp. 321+xx. Pitman Publishing Corporation, New York, 1949. Price $10.00.

This book attempts to answer questions about the five regular solids. A knowledge of high school mathematics is all that is required for understanding it. There are excursions into such varied subjects as algebra, vector analysis, plane and spherical trigonometry, analytical geometry, integral calculus, crystallography, and topology.

Giant Brains, or Machines That Think

By Edmund C. Berkeley. Pp. 270+xvi. John Wiley and Sons, Inc., New York, 1949. Price $4.00.

Machines that calculate, make decisions, choose between different courses of action, determine most of their own instructions, machines that learn, remember, reason, machines, in other words, that seem almost to think—these machines are the subject of this book. The book describes several existing large-scale mechanical computers, but it is more than a purely descriptive work. Here computing machines are set in perspective; the reader can evaluate their importance to himself and to society. The author compares the machines with human brains and with various types of languages; he indicates their possibilities for the future and the problems of control to direct them toward the greatest good. More than 250 references to the literature are given.

Description of a Relay Calculator

By the Staff of the Computation Laboratory, Harvard University. Pp. 366+xvi. Harvard University Press, Cambridge, 1949. Price $8.00.

This is a description of the relay calculator formerly known as Mark II, that was built by the Computation Laboratory for the

Bureau of Ordnance of the United States Navy. The calculator is now in operation at the Naval Proving Ground, Dahlgren, Virginia. Tape-controlled and completely automatic, the calculator can handle numerical quantities consisting of ten significant digits within the range 10^{-15} to 10^{+15}. It is operated by timed electric impulses provided by a cam unit. All components are duplicated so that the machine may be operated as two independent calculators, solving two problems simultaneously, or as one calculator working on a single problem. The volume includes a complete description of the design and construction of the calculator, a manual of operation, and a discussion of problem preparation and solutions of typical examples. There are 36 plates and many figures illustrating details of construction and wiring.

MECHANICS

Principles of Mechanics

By John L. Synge and B. A. Griffith (second edition). Pp. 530+xvi, Figs. 164. McGraw-Hill Book Company, Inc., New York, 1949. Price $5.00.

This is the second edition of a well-known text in intermediate mechanics. Most readers will be delighted with the philosophical ideas expressed from time to time throughout the book. It concerns the usual chapters in statics, kinematics, dynamics, first considered in a plane and then in a space. Vector methods are used throughout. Three welcome chapters near the end of the book concern Lagrange's equation, special theory of relativity, and theory of dimensions.

Dynamic Principles of Mechanics

By David Rittenhouse Inglis. Pp. 174+x, Figs. 64. The Blakiston Company, Philadelphia, 1949. Price $4.00.

This text is intended for juniors and seniors. Many of the chapters are selected because they illustrate principles fundamental to the understanding of certain important parts of atomic and molecular physics and chemistry. Vector methods are used throughout eight chapters entitled Kinematics of a Particle, Dynamics of a Particle, Coupled Oscillators and Normal Coordinates, Inverse-Square Force and Planetary Motion, A Dynamical System of Several Particles, Statics, Rotation of a Rigid Body, and Impact.

Vectorial Mechanics

By E. A. Milne. Pp. 382+xiii, Figs. 112. Interscience Publishers, Inc., New York, 1948. Price $7.50.

Professor Milne's book is one for advanced students. In his words, he is expounding the view that vectorial mechanics is suitable not only for elegant proofs of general theorems but as a powerful weapon of workaday mathematical investigation, both in research and in solving problems of the type set in English examinations. There are chapters not only on vector analysis but also on tensors. The three main sections of the book deal with vector algebra, systems of line vectors, and dynamics.

Mechanics

By John W. Breneman (new second edition). Pp. 144+xi, Figs. 214. McGraw-Hill Book Company, Inc., New York, 1948. Price $2.50.

The subject covered in this book is usually referred to as engineering mechanics. The text is on a rather elementary level and considers fundamental principles, equilibrium, with examples in bridges and trusses, screws and threads, friction, centroids, curvilinear motion, with a final chapter on work, energy, and power. Helpful tables are provided in appendices concerning trigonometric functions, elements of sections, and so forth.

The Measurement of Stress and Strain in Solids

By the Institute of Physics (London). Pp. 114+x, Figs. 54. Institute of Physics, London, 1948.

This little volume was based on the proceedings of a conference arranged by the Manchester and District Branch of the Institute of Physics in July, 1946. Some of the papers read to the conference were intended to be survey papers, while others were more concerned with the details of the application of the various techniques to specific problems. Twelve papers are included in this book, including three survey papers on electrical resistance strain gauges, recent developments in photoelasticity, and other methods for measurement of strain, such as extensometers and the use of brittle lacquer coatings.

Reissner Anniversary Volume

Polytechnic Institute of Brooklyn, Department of Aeronautical Engineering and Applied Mechanics, editor. Pp. 493+viii. J. W. Edwards, Ann Arbor, Michigan, 1949. Price $6.50.

This volume consists of a collection of contributions to applied mechanics by the friends and former students of Hans J. Reissner on the occasion of his 75th birthday. In addition to the biographical sketch of Dr. Reissner, there are collections of papers in the fields of aerodynamics, dynamics, electricity, elasticity and structures, mathematical methods, plasticity, and propulsion. The reader will find represented in this list many of the great names in mathematical physics.

Elements of Strength of Materials

By S. Timoshenko and Gleason H. MacCullough (third edition). Pp. 426+ix, Figs. 386. D. Van Nostrand Company, Inc., New York, 1949. Price $5.00.

Whereas the original edition of this work presents both the elementary and advanced aspects of the subject, the present work is considerably abridged and is designed primarily for undergraduate courses in elementary strength of materials in engineering colleges.

Applied Mechanics and Statics

By George W. Housner and Donald E. Hudson. Pp. 220+ix. D. Van Nostrand Company, Inc., New York, 1949. Price $3.00.

This book has been prepared as a textbook for the use of sophomore engineering students. The emphasis is on fundamental principles, but the book is not to be considered as a treatise or reference book. The general topics treated are the composition and resolution of force systems, equilibrium, principles of virtual displacement, center of gravity, friction, statically determinant structures, and statically undeterminant structures, with an appendix containing a short bibliography and tables of centroids, moments, and products of inertia.

Mechanics, Statics, and Dynamics

By Merit Scott. Pp. 394+xi. McGraw-Hill Book Company, Inc., New York, 1949. Price $4.50.

The purpose of this text is to serve as a bridge between the first course in college physics and later studies making use of higher mathematics. It is intended also to serve as a reference book, and the initial chapters deal with vector notation and vector analysis. The book is divided into two sections, the first concerning statics and the second, dynamics. Motion is considered, first in one, then in two, and finally in three dimensions.

Elements of Mechanical Vibration

By C. R. Freberg and Emory N. Kemler (second edition). Pp. 227+xiii. John Wiley and Sons, Inc., New York, 1949. Price $3.75.

This is the second edition of the authors' text on mechanical vibration, which concerns primarily the more elementary phases of vibrations and attempts to reduce them to a form in which they can be applied to practical problems. The book is concerned particularly with those problems which can be solved by the use of the simpler forms of differential equations, approximation methods, or the mobility method. Some of the chapter headings are: Vibrations without Damping, Damped Vibrations, Vibration Isolation and Absorption, Equivalent Systems, Beams, Sound, The Mobility Method, and Mechanical and Electrical Models of Vibration Systems.

Mechanical Vibrations

By William Tyrrell Thomson. Pp. 222+viii, Figs. 212. Prentice-Hall, Inc., New York, 1948. Price $5.00.

This text is written primarily for class instruction and follows closely material presented in the course in mechanical vibrations offered to senior and graduate students at the University of Wisconsin. An elementary knowledge of calculus, dynamics, and strength of materials is presupposed, but not familiarity with differential equations. The chapters include: Undamped and Damped Free Vibrations, Forced Vibrations with One, Two, and Many Degrees of Freedom, Vibration of Elastic Bodies, and a chapter on Electromechanical Systems and Analogues.

Design of Machine Elements

By M. F. Spotts. Pp. 402. Prentice-Hall, Inc., New York, 1948. Price $6.65.

This book is intended as a two-semester text for third- and fourth-year engineering students. A brief review of strength of materials is given, in order to emphasize to the student the importance of certain fundamental rules. The chapters include stress concentration and repeated loading, theory of torsion, springs, screws, belts, brakes, clutches, welded and riveted connections, lubrication, ball and roller bearings, spur gears, helical, beveled, and worm gears, and a final very useful chapter on engineering materials.

Analysis and Lubrication of Bearings

By Milton C. Shaw and E. Fred Macks. Pp. 618+xvi. McGraw-Hill Book Company, Inc., New York, 1949. Price $10.00.

The purpose of this book is aptly indicated by a quotation in the preface by A. G. M. Mitchell: "To the machine designer, all bearings are, of course, only necessary evils. . . . Their merit consists in absorbing as little power as possible, wearing out as slowly as possible, occupying as little space as possible, and costing as little as possible." With this philosophy in mind, the general principles of bearing load are developed, and a number of representative examples are discussed. Dimensional analysis is introduced, and there are chapters devoted to hydrodynamic lubrication, rolling contact bearings, boundary lubrication, and a final chapter devoted to a discussion of a representative group of bearing test machines.

Computation Curves for Compressible Fluid Problems

By C. L. Dailey and F. C. Wood. Pp. 33+x, Figs. 33. John Wiley and Sons, Inc., New York, 1949. Price $2.00.

An Introduction to the Mechanics of Viscous Flow

By H. F. P. Purday. Pp. 185+vi, Figs. 79. Dover Publications, Inc., New York, 1949. Price $2.75.

This book is intended as a text to present for the student the application of modern fluid dynamics to problems of lubrication and heat transfer. The author's main object is to show by the simplest means how to calculate velocities, pressures, and boundary resistances arising in laminar fluid motion, and how to adapt the results to serve the theories of bearing lubrication and heat transfer. The book was published in England under the title, *Streamline Flow*.

Deformation and Flow—An Elementary Introduction to Theoretical Rheology

By Markus Reiner. Pp. 346+xix. Interscience Publishers, Inc., New York (U.S. agents), 1949. Price $6.50.

The author explains that this book does not attempt to cover the whole field of rheology. To material mainly of interest to the chemist there has been added other material which should interest the structural or mechanical engineer. The book emphasizes theory, but includes three numerical examples of the application of theory upon one problem each of viscosity, plasticity including strain-hardening, and creep. These were taken from experimental investigations.

The Physics of Rubber Elasticity

By L. R. G. Treloar. Pp. 254. Oxford University Press, New York, 1949. Price $6.00.

This is the fourth volume in a new series entitled "Monographs on the Physics and Chemistry of Materials." The series is intended to summarize the recent results of research in materials and allied subjects, in a form useful to physicists in university and industrial laboratories. The present volume attempts to set down as concisely as possible the essential advances in the study of the elasticity of rubber. The statistical or kinetic theory of elasticity is developed, and is shown to give a satisfactory account of the fundamental mechanical and photoelastic properties of rubber. The book also includes a discussion of the phenomena of crystallization, stress relaxation and flow, the dynamic properties of rubber, and the solution of engineering problems involving large elastic deformations.

Plasticity as a Factor in the Design of Dense Bituminous Road Carpets

By L. W. Nijboer. Pp. 184+xv, Figs. 51. Elsevier Publishing Company, Inc., New York, 1948. Price $5.25.

The importance of a thorough knowledge of the mechanical properties of bituminous road materials is pointed out, and a study is made of the plastic properties of this material. A new test method is developed on the principles of soil mechanics.

HEAT AND THE THEORY OF GASES

Introduction to Statistical Mechanics

By Ronald W. Gurney. Pp. 268+vii, Figs. 59. McGraw-Hill Book Company, Inc., New York, 1949. Price $5.00.

This is an advanced text for graduate students of physics and chemistry. Against a background of atomic physics, the book studies the behavior of large groups of particles, showing how the behavior of matter in bulk follows directly from the properties of the individual atoms. The author has devised methods whereby the student is enabled to grasp the basic principles and the nature of partition functions. A feature of the book is the treatment of metallic alloys, especially the solutions in the alpha- and gamma-phases of iron which form the basis of steel metallurgy. Problems appear at the end of each chapter.

Mathematical Foundations of Statistical Mechanics

By A. I. Khinchin. Translated from the Russian by G. Gamow. Pp. 179+viii. Dover Publications, New York, 1949. Price $2.95.

This book is a mathematical treatment of statistical mechanics on the basis of modern concepts of the theory of probability and a

maximum utilization of its analytical apparatus. The book is written for the mathematician, and its purpose is to introduce him to the problems of statistical mechanics in an atmosphere of logical precision. Among the topics treated in a somewhat novel fashion are the ergodic problems, properties of entropy, and intramolecular correlation.

Scientific Foundations of Vacuum Technique

By Saul Dushman. Pp. 882+xi. John Wiley and Sons, Inc., New York, 1949. Price $15.00.

This book is a broad study of all phases of achieving, maintaining, and measuring very low gas pressures. In the author's words, it presents a survey of "fundamental ideas in physics, chemistry, and (to a smaller extent) metallurgy which will be found useful to both scientists and engineers in dealing with problems in the production and measurement of high vacua."

Vacuum Equipment and Techniques

A. Guthrie and R. K. Wakerling, editors. Pp. 264+xvii. McGraw-Hill Book Company, Inc., New York, 1949. Price $2.50.

This book is concerned with the development and study of high vacuum equipment by the personnel of the University of California Radiation Laboratory for use in electromagnetic separation plants. The problems involved were of a magnitude which made it necessary to do a considerable amount of pioneering work on both equipment and testing. One topic of particular interest is the use of the vacuum analyzer and helium leak detector which were developed for use in the project and proved to be very sensitive instruments.

Glass-to-Metal Seals

By J. H. Partridge. Pp. 238+xii, Figs. 167. The Society of Glass Technology, Sheffield, England, 1949. Price £1 15s. 0d, plus 6d. postage.

This book brings together scattered data about glasses, metals, metal oxides, and the techniques employed in making glass-to-metal seals. It also includes a chapter on the sealing of ceramic materials to metals. The sealing of different glasses to one another and of glasses to ceramic materials are described. The problems of the stresses in the seals and the variation of those stresses when the devices embodying them are in service are also thoroughly examined.

Vacuum Manipulation of Volatile Compounds

By R. T. Sanderson. Pp. 162+viii, Figs. 40. John Wiley and Sons, Inc., New York, 1948. Price $3.00.

This book brings together, in a form designed for easy reference, all the varied essentials which make up the chemical vacuum technique. Through the book this technique becomes readily accessible to the investigator who has no more than the ordinary chemical background. The reader is given a firm foundation for working with high vacuum apparatus and is supplied with all the data necessary for the construction and operation of such apparatus. The book includes vapor pressures, at the same easily producible low temperatures, of almost 400 of the many pure compounds which can conveniently be studied by use of the described manipulative techniques.

A Textbook of Heat

By L. D. Weld. Pp. 436. The Macmillan Company, New York, 1948. Price $5.00.

This is an up-to-date textbook of heat and elementary thermodynamics for upperclassmen. The aim has been to keep the treatment well within the comprehension of students familiar with differential and integral calculus. A carefully selected list of references for supplementary reading is given at the end of each chapter.

Engineering Developments in the Gaseous Diffusion Process

By Manson Benedict and Clarke Williams. Pp. 127+xx. McGraw-Hill Book Company, Inc., New York, 1949. Price $1.25.

This volume describes some of the new engineering procedures and devices developed in connection with the design and construction of gas diffusion plants for separation of uranium isotopes. Topics treated include: special plant instruments and devices including the mass spectrometer for continuous analysis of gas mixtures flowing through a plant, and a recording ionization chamber for detecting traces of radioactive components in a gas mixture; mass spectrometer and engineering methods for testing vacuum-tight systems; engineering processes for handling fluorine and heat transfer ideas applicable to the freezing of liquids.

Heat Transfer

By Max Jakob. Pp. 758+xxix. John Wiley and Sons, Inc. New York, 1949. Price $12.00.

This is a comprehensive work suitable both as a reference work and as a textbook. It shows the development of the ideas which have led to the present knowledge of the subject. The book is international in scope, with particularly thorough coverage of German literature, and should serve the needs of mechanical, chemical, electrical, and civil engineers, and physicists alike.

Third Symposium on Combustion and Flame and Explosion Phenomena

By the Standing Committee on Combustion Symposia. Pp. 748+xiii. The Williams and Wilkins Company, Baltimore, Maryland, 1949. Price $13.50.

This volume contains 100 papers, arranged under eleven categories, which were presented at the Symposium held at the University of Wisconsin in September, 1948. Thirty-eight of the papers were received from European countries.

Steam Power Plants

By Philip J. Potter. Pp. 503+xii. The Ronald Press Company, New York, 1949. Price $6.50.

The aim of this textbook is to present the fundamentals of engineering as applied to the design of steam power plants. No attempt has been made to illustrate all of the various designs of equipment that are available on the market nor to compare similar designs of competitor manufacturers. Descriptions of equipment have been kept to a minimum, and discussions of empirically designed apparatus—such as coal and ash handling systems—have been omitted. Problems and examples have been taken from practical situations to illustrate the principles developed throughout the text.

Thermodynamic Charts for Combustion Processes. Part I Text; Part II Charts

By H. C. Hottel, G. C. Williams, and C. N. Satterfield. Pp. 75, Charts 23. John Wiley and Sons, Inc., New York, 1949. Price $2.60 and $2.40.

ACOUSTICS

Acoustic Measurements

By Leo L. Beranek, Pp. 914+vii. John Wiley and Sons, Inc., New York, 1949. Price $7.00.

In addition to an exposition of acoustic measuring techniques, this book combines data published for the first time with information previously found only in isolated publications. Topics

range from the calibration of microphones and loudspeakers to evaluation of over-all audio systems, and to chapters on the audiometer, speech articulation tests and the sound level meter. The book presents the source of the theory of many electroacoustic phenomena, a description in detail of the basic types of acoustic measuring devices, such as microphones, sources, acoustic impedance bridges and analyzers, and a discussion of the relative advantages and disadvantages of alternate methods for accomplishing electroacoustic measurements.

Sound Absorbing Materials

By C. Zwikker and C. W. Kosten. Pp. 174+ix, Figs. 92. Elsevier Publishing Company, Inc., New York, 1949. Price $3.00.

This book examines the properties that impart sound absorbing qualities to materials or composites, describes their theoretical and experimental study, and shows how these qualities can be conferred upon structures and how they can in many cases be predicted for given surfaces. This latter can be done from mechanical factors such as porosity, compliance, air-resistance, shape, etc. The authors stress the importance of acoustic impedance, which can with advantage be expressed and studied graphically by means of impedance contours. The acoustic behavior of a wide range of materials is discussed and explained.

Theory of Hearing

By Ernest Glen Wever. Pp. 484+xiii, Figs. 136. John Wiley and Sons, Inc., New York, 1949. Price $6.00.

This book is a result of the electrophysiological investigation of the ear's behavior, an investigation begun in 1930 by the author and C. W. Bray and now being carried out actively in many laboratories. The book reviews the development of auditory theory from earliest times and attempts an impartial presentation of all the classical theories of importance. It takes up the principal forms of these theories and brings them face to face with the modern facts about the ear and its actions. It also presents a new point of view in which the two main types of theory—the place and frequency theories—are fused into one and then evaluated with respect to the facts of hearing.

Elements of Sound Recording

By John G. Frayne and Halley Wolfe. Pp. 686+vii, Figs. 480. John Wiley and Sons, Inc., New York, 1949. Price $8.50.

This book covers in detail those subjects which belong peculiarly to the restricted field of sound recording and reproducing and which are not discussed in books devoted to the allied fields of electronics, radio engineering, etc. However, since those interested in studying sound recording have widely different kinds of training and experience, some closely related subjects such as electrochemical analogies, acoustics, vacuum tubes, and audio amplifiers are discussed briefly. For added clarity, numerical examples are used in a number of instances to illustrate the use of design formulas. Complex mathematical analysis is limited to those subjects in which it is desirable for a basic understanding of the point under discussion. The topics covered range from the nature of sound to stereophonic recording.

Installation and Servicing of Low Power Public Address Systems

By John F. Rider. Pp. 208. John F. Rider Publisher, Inc., New York, 1948. Price $1.89.

Inasmuch as the majority of public address installations are those requiring low power equipment—from both an acoustical and economic viewpoint—the apparatus discussed in this book in the main is confined to a rating of 50 watts or lower. Yet a great amount of the subject matter applies equally well to systems of higher power. The book opens with a discussion of the fundamentals of sound and the problems encountered in the public address field; this is followed by an explanation of microphones, phonograph pick-ups, and radio receivers as inputs to an amplifier, then the various types of audio amplifiers, with a chapter devoted to impedance matching.

ELECTROMAGNETIC WAVES AND ELECTRONICS

Principles of Electricity and Electromagnetism

By G. P. Harnwell. Pp. 670+xvi. McGraw-Hill Book Company, Inc., New York, 1949. Price $6.00.

This is a thorough revision of a well-known text for advanced students, and incorporates many important developments in electricity during the past decade. The emphasis is on the phenomena rather than the application of mathematical techniques to particular soluble problems. Increased attention is accorded to the application of the principles of electricity and magnetism to atomic phenomena. Sections have been added on ultra-high frequency techniques, especially those which represent important extensions of the field as covered in the previous edition. No effort has been made to cover the field of radar, but the basic techniques involved are specifically described in this edition. Discussions of wave guides, resonant cavities, and other new topics are included.

Principles of Electricity

By Leigh Page and Norman I. Adams, Jr. (second edition). Pp. 619+xiii, Figs. 323. D. Van Nostrand Company, Inc., New York, 1949. Price $5.50.

This second edition has been brought up to date by the addition of new topics such as the cyclotron, the betatron, and the wave guide, and by the omission of a few topics of diminishing interest. The Gaussian system of units has been employed throughout the book.

Elektrizitätslehre

By R. W. Pohl. Pp. 297. Springer-Verlag, Berlin, 1949.

The Extrapolation, Interpolation, and Smoothing of Stationary Time Series with Engineering Applications

By Norbert Wiener. Pp. 163+ix. John Wiley and Sons, Inc., New York, 1949. Price $4.00.

This book represents an attempt to unite the theory and practice of two important fields of work—time series in statistics, and communication engineering. These fields are widely different in vocabulary and in the training of personnel, and they have drawn their inspiration from two entirely distinct traditions. However, it is believed that they have a unification of theory and method. The author points out that the statistician is completely familiar with methods involving probability theory and correlation, but unable to use the engineer's methods; the communication engineer is just as familiar with the use of the complex plane, but unable to use the statistician's techniques. It is the purpose of this book to introduce methods stemming from both of these existing techniques and to fuse them into a common technique which is more effective than either one alone.

Electric and Magnetic Fields

By Stephen S. Attwood (third edition). Pp. 475+xi. John Wiley and Sons, Inc., New York, 1949. Price $5.50.

This book was written to provide a smooth transition from the study of mathematics, mechanics, and physics to advanced, professional-level electrical engineering. The author has divided this new edition into four parts. The electric field is discussed first. Next the magnetic field is treated and the field formulas are devel-

oped under the assumption of constant permeability. In the third part the ferromagnetic field introduces the modification of the basic magnetic relations necessary to account for the use of magnetic material in which permeability cannot be considered constant. The fourth section treats in an elementary manner the interactions between electric and magnetic fields that simultaneously occupy the same space. The formulas in the book have been recast in the rationalized form of the m.k.s. system.

Basic Electrical Engineering

By George F. Corcoran. Pp. 449+vii. John Wiley and Sons, Inc., New York, 1949. Price $4.50.

This is a textbook of electrical engineering which maintains throughout a level suitable for beginners. Each electrical or magnetic concept is exactly defined at the place of its introduction. Arrangement of subject matter is likewise planned to suit the beginning course. First d.c. theory is considered, with d.c. circuit analysis by the mesh and nodal methods. This is followed by electrical field theory, magnetic field theory, inductance, capacitance, and non-linear circuit elements. There is a wide range of problems with each chapter.

Electronics in Engineering

By W. Ryland Hill. Pp. 274+viii. McGraw-Hill Book Company, Inc., New York, 1949. Price $3.50.

This text is designed for senior and graduate students in engineering and allied sciences who find the need for an understanding of electronics and its applications to measurement and control in their respective fields. The treatment is sufficiently analytical to interest such students, and yet contains enough practical applications to illustrate the uses of electronics to the various engineering fields. The book provides material for a one-quarter or one-semester course covering vacuum and gas-filled tubes, rectification, amplification, feedback, the cathode-ray oscilloscope, and simple control and instrumentation techniques.

Electrical Engineers' Handbook; Electric Power. Vol. I

Harold Pender and William A. Del Mar, editors (fourth edition). Pp. 1700+xii. John Wiley and Sons, Inc., New York, 1949. Price $8.50.

The editors point out that the growth of knowledge and the greater degree of specialization in the various phases of electrical engineering have necessitated a considerable enlargement of this well-known handbook. An effort has been made to keep the book compact and readable.

Learning Electricity and Electronics Experimentally

By Leonard R. Crow. Pp. 525+xi. Universal Scientific Company, Vincennes, Indiana, 1949.

The author of this book aims to use the experimental or project approach to the subject of electricity, employing the simplest possible language. Some of the specific points treated in the book are energy and electrical effects, magnetism and electromagnetism, electromagnetic induction, magnetic flux control, rotating magnetic fields, current control by magnetic saturation.

Theory of Oscillations

By A. A. Andronow and C. E. Chaikin. Pp. 358+ix, Figs. 313. Princeton University Press, Princeton, 1949. Price $6.00.

This is a condensed and edited translation of the first comprehensive treatment of non-linear oscillations ever to be published. The original work, by two leading members of the Soviet Institute of Oscillations, was published in Russian in 1937. Since the field of non-linear oscillations is not as well known as it deserves to be, numerous examples are given, and a special index of physical examples is included. Practical applications are emphasized, and the examples given in the original Russian edition are preserved. The book begins with a treatment of linear systems, giving the newcomer to the field familiar ground from which to work, but it rapidly progresses to various types of non-linear systems, using both mechanical and electrical examples. The book will be useful to electrical, aeronautical, and mechanical engineers, to mathematicians and physicists, and to any scientists working with oscillatory phenomena.

Micro-Waves and Wave Guides

By H. M. Barlow. Pp. 122+x, Figs. 70. Dover Publications, New York, 1949. Price $1.95.

The first part of this volume presents a physical picture of wave-guide modes, synthesized from constituent plane waves in association with ordinary transmission line elements. The coaxial cable, representing the common meeting ground of wave-guide modes and the simple transverse electromagnetic wave, is discussed. The final section deals with the measurements and applications of micro-waves, giving the reader an appreciation and knowledge of the methods adopted in actual practice.

Radar Systems and Components

By the Technical Staff of Bell Telephone Laboratories. Pp. 1042+xiv. D. Van Nostrand Company, Inc., New York, 1949. Price $7.50.

About one-half of Bell Telephone Laboratories' total research effort during the war was devoted to radar. The Laboratories shared with the Radiation Laboratory at Massachusetts Institute of Technology the responsibility for the bulk of research and development in this field in the United States. In order that the scientific advances achieved might be recorded in detail (so far as security considerations would permit), the papers appearing in this volume were prepared and were originally published in the *Bell System Technical Journal*. While the work described was directed toward radar development as its immediate objective, it has a broad application to the new field of microwave transmission.

Aerials for Metre and Decimetre Wavelengths

By R. A. Smith. Pp. 218+xii, Figs. 125. Cambridge University Press, New York, 1949. Price $3.75.

The author of this book points out that the extension of radio technique to extremely short wave-lengths greatly increased the scope of aerial design. Half-wave and full-wave dipoles have manageable dimensions when the wave-length is less than 12 meters, and arrays for many special purposes may be designed. In this book the upper limit has been set at 12 meters, the longest wave-length used for radar. The lower limit has been fixed at 10 cm. A limited number of applications have been selected to illustrate general principles.

Electrical Transmission of Power and Signals

By Edward W. Kimbark. Pp. 461+xi. John Wiley and Sons, Inc., New York, 1949. Price $6.00.

This is the first textbook to apply transmission-line theory to all three fields of power, telephone, and ultra-high frequency transmission. It contains transmission-line (hyperbolic function) charts, tables and graphs of the characteristics of power-line conductors, power transmission and distribution lines, telephone lines and cables, submarine telegraph cables, and radiofrequency lines. This volume is a useful reference book for professional engineers and will be found of value in electrical transmission courses.

Elements of Electromagnetic Waves

By Lawrence A. Ware. Pp. 203+x. Pitman Publishing Corporation, New York, 1949. Price $3.50.

This text was prepared to meet the need for an elementary introduction to the basic ideas of electromagnetic theory, employ-

ing the rationalized m.k.s. units. It is intended as first-course material for either juniors or seniors, and the only prerequisites are calculus and the fundamentals of alternating-current theory. The text is prepared to serve as an introduction to the more advanced treatments of the subject.

Radio-Frequency Heating Equipment

By L. L. Langton. Pp. 196+ix, Figs. 95. Pitman Publishing Corporation, New York, 1949. Price $3.75.

This book deals with the design of equipment for radiofrequency heating, and also with some applications of the technique. The reasons underlying the advantages gained by using the technique in these applications are fully discussed; this serves as a guide to the advantages to be expected when the technique is applied elsewhere.

Terrestrial Radio Waves; Theory of Propagation

By H. Bremmer. Pp. 343+x, Figs. 91. Elsevier Publishing Company, Inc., New York, 1949. Price $6.75.

This book describes the mathematical methods by which the electromagnetic field of a radio transmitter can be computed, taking into account the curvature of the earth's surface. Special attention is paid to the physical interpretation of the mathematical deductions. The complicated formulas which are basic for numerical computations of the "ground-wave" have been collected in a practical form in a separate chapter.

Earth Conduction Effects in Transmission Systems

By Erling D. Sunde. Pp. 373+xiii. D. Van Nostrand Company, Inc., New York, 1949. Price $6.00.

This presentation is primarily concerned with fundamental methods in the analysis of earth conduction effects and basic principles underlying protective measures against resultant circuit disturbances. For conciseness and better exposition of basic formulas and considerations, much of the mathematical detail has been omitted in most derivations or covered by reference to other literature.

The Mathematics of Circuit Analysis

By Ernest A. Guillemin. Pp. 590+xiv. John Wiley and Sons, Inc., New York, 1949. Price $7.50.

This volume contains a collection of a variety of principles and methods essential to a thorough understanding of electrical network theory. It is designed specifically as a source book to supplement the usual undergraduate engineering mathematics curriculum. It is appropriate also for use as a textbook in a course in higher mathematics for engineers.

Communication Circuits

By Lawrence A. Ware and Henry R. Reed (third edition). Pp. 403+x. John Wiley and Sons, Inc., New York, 1949. Price $5.00.

In this third edition the authors cover the essentials of the transmission and lead logically to such subjects as filters, impedance matching, and wave guides. Features of this edition include the use of rationalized m.k.s. system of units; a radical revision of the chapter on transmission-line parameters; a treatment of attenuation in wave guides based on Poynting's theorem; the addition of many new problems. Although a knowledge of calculus and the elements of a.c. theory has been assumed, the more advanced mathematics that is needed for certain portions has been included in the appendices.

Pulses and Transients in Communication Circuits

By Colin Cherry. Pp. 317+xvi, Figs. 129. Chapman and Hall, Ltd., London, 1949. Price 32s. net.

This book is meant as an introduction to circuit transient analysis for communications engineers, which will bridge the gap between simple conventional alternating current theory and operational methods of analysis. It is intended to give students of steady-state circuit theory the essential groundwork, using, wherever possible, rigorous physical arguments and only elementary mathematics. Mathematical language and notation are avoided as much as possible. Electrical wave forms are dealt with, rather than analytical functions, thus giving the book a geometrical flavor.

Networks, Lines and Fields

By John D. Ryder. Pp. 462+x, Figs. 195. Prentice-Hall, Inc., New York, 1949. Price $5.50.

In this text the author has attempted to expand upon the subjects of networks, resonance, and wave filters in such a way as to develop in the undergraduate student a definite familiarity with "network theory," or the description of network performance by certain measured or defined parameters. The rationalized m.k.s. system of units is used throughout.

Radio Engineering

By E. K. Sandeman. Pp. 775+xxiv. John Wiley and Sons, Inc., New York, 1948. Price $6.50.

Originally planned as instructions for maintenance engineers at B.B.C. transmitting stations, this book is designed to give beginners in radio the working principles they need. Experienced engineers and designers of radio equipment and circuits will find it a useful reference volume. Practical ends are stressed, either in the form of technical facts, designs, or methods or else in the form of essential formulas.

Electric Circuits and Machines

By B. L. Robertson and L. J. Black. Pp. 434+vii. D. Van Nostrand Company, Inc., New York, 1949. Price $5.00.

This is a textbook intended primarily for third-year students of mechanical engineering, or for non-electricals in general, to give them a strong minor in electrical engineering.

Radio at Ultra-High Frequencies, Vol. II

By Alfred N. Goldsmith *et al.*, editors. Pp. 485. RCA Review, RCA Laboratories Division, Princeton, New Jersey, 1948. Price $2.50.

This is the eighth volume in the RCA Technical Book Series and the second on the general subject of radio at the higher frequencies. The present volume covers the period 1940–47. Papers are presented in seven sections: antennas and transmission lines; propagation; reception; radio relays; microwaves; measurements and components; navigational aids. The appendices include a bibliography in the field of ultra-high frequency radio, and summaries of all papers appearing in Vol. I, which is now out of print.

Electrical Measurements in Theory and Application

By Arthur Whitmore Smith. Pp. 371, Figs. 250. McGraw-Hill Book Company, Inc., New York, 1948. Price $4.25.

This is a thorough revision and modernization of a well-known standard text, incorporating many changes to clarify the explanations and present improved methods. The meter-kilogram-second (m.k.s.) system has been used for the definitions of the units of the electrical and magnetic quantities, resulting in great simplification of the approach to these definitions. Several new measurement methods have been added, especially for the measurement of capacitance and inductance.

Advances in Electronics, Vol. I

L. MARTON, editor. Pp. 475+xi. Academic Press, Inc., New York, 1949. Price $9.00.

This volume is the first of a series of yearly publications devoted to articles in the general field of electronics. The aim is to publish critical and integrated reviews on physical and engineering electronics. The editors and publishers of the book were obliged to use a somewhat arbitrary definition of the word "electronics," and thus limit the choice of materials to a reasonably restricted field. In this volume the topics covered are: oxide-coated cathodes, secondary electron emission, television pick-up tubes and the problem of vision, the deflection of beams of charged particles, modern mass spectroscopy, particle accelerators, ionospheric research, cosmic radio noise, propagation in the f-m broadcast band, electronic aids to navigation.

Electronics: Experimental Techniques

BY W. C. ELMORE AND MATTHEW L. SANDS. Pp. 417+xviii. McGraw-Hill Book Company, Inc., New York, 1949. Price $3.75.

This volume describes the most useful and the most successful circuits for making nuclear and other physical measurements. In addition to the description of complete circuits—pulse amplifiers, counting circuits, sweep circuits, timing circuits, testing equipment, etc.—the book contains a discussion of the circuit elements that constitute the basis of the complete circuits.

Theory and Design of Electron Beams

BY J. R. PIERCE. Pp. 197+xiii. D. Van Nostrand Company, Inc., New York, 1949. Price $3.50.

This book represents an effort to collect the minimum amount of theoretical material necessary for a good understanding of electron flow and electron focusing in devices other than electron microscopes and image tubes. Much of the elementary material found in books on electron optics is included. There is, however, no extensive treatment of aberrations. Instead, there is considerable emphasis and material on space charge and thermal velocities. Problems are included, partly so that the book can be used as a text, but more so that "the reader will have to do things for himself in order to understand them."

Fundamentals of Radio-Valve Technique

BY J. DEKETH. Pp. 535+xxii, Figs. 384. N. V. Philips' Gloeilampenfabrieken, Eindhoven, The Netherlands, 1949. Price $5.00.

In this book the author aims at giving technicians and research workers an account which will be of value to those who make, use, or maintain apparatus employing electronic valves. The mathematical treatment is restricted, and the subjects treated include resonance, short-wave technique, and low frequency modulation.

Microwaves and Radar Electronics

BY ERNEST C. POLLARD AND JULIAN M. STURTEVANT. Pp. 426+vii. John Wiley and Sons, Inc., New York, 1948. Price $5.00.

No extensive background in communications or electronics is required for use of this book. The usual student background in physics, chemistry, and electrical engineering is sufficient. The essential facts about microwave circuits are developed on the fundamental basis of electricity and magnetism, rather than from an extension of the theory of circuits with lumped parameters. Pulse circuits are considered as a unified subject, since the fundamental problems and basic methods of solving such problems accompany all types of pulse circuits. Much attention has been devoted to the applications of microwave and radar electronic techniques which have been considered in various scientific periodicals since the end of the war.

Industrial Electronics Reference Book

BY ELECTRONICS ENGINEERS OF THE WESTINGHOUSE ELECTRIC CORPORATION. Pp. 680. John Wiley and Sons, Inc., New York, 1948. Price $7.50.

This reference book presents the basic theory and the vital application principles of industrial electronics. It is intended to help the reader to appraise accurately the possibilities as well as the limitations of new electronic devices, and also to help technicians to develop new applications and projects which will have a better chance of giving the desired results. The authors deal mostly with basic electronics application information and treat the specific apparatus less fully because of the many changes still taking place. The generous use of illustrations in the volume helps to elucidate every phase of the text material.

The Characteristics of Electrical Discharges in Magnetic Fields

A. GUTHRIE AND R. K. WAKERLING, editors. Pp. 376+xviii. McGraw-Hill Book Company, Inc., New York, 1949. Price $3.50.

This volume was prepared in an effort to collect the results of studies carried out in the California Radiation Laboratory on the characteristics of electrical discharges in magnetic fields. The primary emphasis is placed on the case of electrical discharges in the vapors of uranium compounds. The book does not cover all of the investigations, although the most significant studies are included. More than half of this book is devoted to work carried out by members of a British scientific mission.

Basic Electronics

BY ROYCE G. KLOEFFLER AND MAURICE W. HORRELL. Pp. 435+xiv. John Wiley and Sons, Inc., New York, 1949. Price $5.00.

The authors cover the fundamental theory of electronics in condensed form, assuming the reader has a knowledge of elementary physics, but no previous training in electronics. The authors' approach covers both the power and communication fields. Included among the subjects discussed are the developments of the transistor and mechano-electronic transducer. As a convenience to the reader, the authors have included curves and data of the basic tubes. This means that most of the problems can be solved without referring to any of the tube handbooks.

Photoelectricity and Its Application

BY V. K. ZWORYKIN AND E. G. RAMBERG. Pp. 494+xii. John Wiley and Sons, Inc., New York, 1949. Price $7.50.

This volume replaces the second edition of *Photocells and Their Application* by V. K. Zworykin and E. D. Wilson. It retains the aim of its predecessor—to present the reader with practical reliable data on the properties, preparation, and applications fo photoelectric devices. Throughout, the emphasis is on practical aspects.

Theory of Dielectrics

BY H. FRÖHLICH. Pp. 180+vi, Figs. 47. Oxford University Press, New York, 1949. Price $4.50.

This book, which is mainly written for applied scientists, is intended to give a systematic account of the theory of dielectric properties, and thus to provide a background against which applications can be made. The reader is assumed to have a certain ele-

mentary knowledge of atomic and molecular physics, statistical mechanics, electrostatics, and little mathematics beyond the calculus.

Atmospheric Electricity

By J. Alan Chalmers. Pp. 175, Figs. 36. Oxford University Press, New York, 1949. Price $3.75.

This book is intended to serve both as an introduction to the study of atmospheric electricity and as a short work of reference. It was written primarily for physicists but should prove useful to meteorologists and others interested in the subject. There are chapters on the ions in the atmosphere, the earth's vertical field, the conductivity of the air, the year-around current, point discharge currents, precipitation currents, the transfer of charge, the thunder cloud, the lightning flash, and the separation of charge.

TV Picture Projection and Enlargement

By Allan Lytel. Pp. 179+xi. John F. Rider Publisher, Inc., New York, 1949. Price $3.30.

This book, with its numerous illustrations, will appeal to those interested in television servicing. The author discusses the fundamentals of light, the Schmidt projection system, and refractive projection systems.

Understanding Television

By Orrin E. Dunlap, Jr. Pp. 128. Greenberg, Publisher, New York, 1948. Price $2.50.

This little book discusses the steps that led to television, the mechanisms which match the human eye, the necessity for high antennas and relay stations, the coaxial cable, and the receiver itself. The author describes how a television program is put together, both in the studio and in the field.

OPTICS AND SPECTROSCOPY

Introduction to Theoretical and Experimental Optics

By Joseph Valasek. Pp. 454+x. John Wiley and Sons, Inc., New York, 1949. Price $6.50.

This is a four-part book, covering geometrical optics, physical optics, radiation and spectra, and experiments relating to each of these fields. In line with the author's special interests, the subjects of x-rays, photographic optics, and ophthalmic lenses are treated in greater detail than is customary in books dealing with optics. This book holds useful information for many engineers and physicists working in industry and in research laboratories. It serves as an introduction to optical engineering, a field which is steadily growing more important. For example, students of photography, mechanical engineers who use optical methods of stress analysis, and optical mineralogists all can use the principles of optics contained in this book. Although the author assumes the reader has a knowledge of calculus and general physics, he keeps the mathematical treatment as elementary as possible.

Optik

By R. W. Pohl. Pp. 356, Figs. 565. Springer-Verlag, Berlin, 1948.

Physical Aspects of Color

By P. J. Bouma. Pp. 312, Figs. 113. Elsevier Publishing Company, Inc., New York, 1947. Price $5.50.

The physiologist, the psychologist, the physicist, the illumination engineer, and the chemist each has studied the problem of color perception from his own point of view and expressed the results in his own particular technical language. The author of this book has aimed to cast the subject matter in such a form that it may well enrich the knowledge of many a scientist and at the same time serve as a guide to the beginner—presumed to possess a secondary school knowledge of mathematics and physics—for the study of problems of chromatics. Starting from the established laws of color mixing, the author gives a complete insight into the origin and perception of colors in a logical and systematic manner.

Elementary Photography

By Guilford G. Quarles (new second edition). Pp. 345+xii, Figs. 86. McGraw-Hill Book Company, Inc., New York, 1949. Price $4.50.

As before, this text provides a treatment of photography between very elementary ones and those of an advanced, technical nature. The book assumes no previous knowledge of the subject, and an effort has been exerted to make the new edition even more easily understandable to the student and more teachable from the point of view of the instructor. A major revision of the order of the chapters has been made in order to bring the student as quickly as possible to active photography—i.e., the making of pictures.

Die Optik in der Feinmehtechnik

By Kurt Räntsch. Pp. 317, Figs. 299. Carl Hanser-Verlag, Munich, 1949.

Photographic Optics

By Arthur Cox. Pp. 412+xi. Pitman Publishing Corporation, New York, 1949. Price $5.75.

The subtitle of this book is "The Technique of Definition." The photographer should be able to discriminate between lenses in the same way he does between films and filters. This practical book, written in simple language and containing many diagrams and tables, deals with the importance of lenses in obtaining the best results with the camera, and shows how the proper type of lens must be used in the right kind of camera for each kind of subject. The photographer is shown why the correct focal length, best aperture, and sufficient covering power are considerations that eventually decide the picture.

Spectroscopic Properties of Uranium Compounds

By G. H. Dieke and A. B. F. Duncan. Pp. 290+xviii. McGraw-Hill Book Company, Inc., New York, 1949. Price $2.75.

This volume represents a comprehensive study of the spectroscopic properties. Correlation of absorption measurements with those obtained from fluorescence spectra have seldom been made for such a large amount of data. This work should be an important source of information and data in the development of future theories of the solid state.

Practical Spectroscopy

By George R. Harrison, Richard C. Lord, and John R. Loofbourow. Pp. 605+xiv. Prentice-Hall, Inc., New York, 1948. Price $6.65.

In this book the authors have avoided the historical method of approach and instead have attempted to give a comprehensive view of the status and possibilities of experimental spectroscopy as it exists today. In Chapter I they "view the field as from a great altitude, to enable the reader who is unacquainted with the methods and accomplishments of spectroscopy to judge for himself which parts, if any, may be of importance to him." In the remainder of the book they reconsider the various topics in considerably greater detail.

Practical Spectroscopy

By C. Candler. Pp. 190+viii. The Jarrell Ash Company, Boston (U.S. agents), 1949. Price $6.10.

This book is intended as a course of instruction in all branches branches of practical spectroscopy. The subject matter has been written primarily around the Hilger Barfit wave-length spectrometer. However, it is believed that this should not detract from its interest to those equipped with other apparatus. Experiments are given at the close of each chapter.

Absorption Spectrophotometry

By G. F. Lothian (third edition). Pp. 196, Figs. 71. Hilger and Watts, Ltd., London, 1949. Price $7.60.

Although this work forms the third edition of an already well-known publication, *The Practice of Absorption Spectrometry*, it has been so completely revised and largely rewritten that it is virtually a new work. It is a valuable handbook for the investigator who is employing spectrophotometry and contains much that will be of interest to those who are contemplating the use of that method. It describes the apparatus to be used and also shows the accuracy to be anticipated and the essential conditions for realizing that accuracy. Examples of work done in selected fields are included.

Infrared Determination of Organic Structures

By H. M. Randall, Nelson Fuson, R. G. Fowler, and J. R. Dangl. Pp. 239+v, Plates 354. D. Van Nostrand Company, Inc., New York, 1949. Price $10.00.

This volume is intended to supply some of the background which is required by investigators, whether they are chemists, biochemists, or physicists, using infra-red spectra to determine molecular structure. Methods of approach have been outlined; the possibilities inherent in the method have been explored; currently established correlations between structure and the absorption spectrum have been itemized; the instruments and techniques have been described.

An Introduction to Molecular Spectra

By R. C. Johnson. Pp. 296+xiii, Figs. 151, Plates 8. Pitman Publishing Corporation, New York, 1949. Price $7.50.

The author has attempted to provide a textbook on molecular spectra for the student who has graduated in physics or chemistry, or who is approaching graduation, and desires an understanding of the subject within the limits of ordinary mathematical equipment at that stage. At one or two points the author has introduced the results of wave mechanics, but has not assumed familiarity in the use of this method.

Contribution to the Study of Molecular Structure

In both French and English. Several contributors, in commemoration of Victor Henri. Pp. 314. Maison Desoer Editions, Liege, Belgium, 1948.

Luminescent Materials

By G. F. J. Garlick. Pp. 254+viii, Figs. 127. Oxford University Press, New York, 1949. Price $5.50.

This book describes recent research on the physical properties of luminescent materials. It is concerned with experimental and theoretical studies of such phenomena as fluorescence, phosphorescence, thermoluminescence, and the effects of infra-red radiation on phosphors. Associated phenomena, such as photoconductivity, dielectric changes, and the action of strong electric fields are also discussed. The preparation, constitution, and classification of materials according to their luminescence characteristics are given an important place in the text.

ATOMIC AND NUCLEAR PHYSICS

Foundations of Nuclear Physics

With bibliography compiled by Robert T. Beyer. Pp. 272. Dover Publications, New York, 1949. Price $2.95.

Here are thirteen important papers on nuclear physics, presented unabridged and in the original language of their authors. Selected from scientific journals published both in this country and throughout the world, these are the essential primary source materials in this field. This volume also contains a comprehensive guide (120 pages in length) to published material on nuclear physics in which entries are classified according to subject matter.

Wave Mechanics and Its Applications

By N. F. Mott and I. N. Sneddon. Pp. 393+xii, Figs. 68. Oxford University Press, New York, 1948. Price $10.00.

The aim of this book is to give a straightforward account of wave mechanics designed for those who want to use it. There are chapters dealing with applications to atomic and molecular structure, radiation, and collision problems, and the properties of solids. Modern relativistic quantum mechanics is also discussed. The book should be useful as a textbook to the theoretical physicist beginning research in the subject, and to his experimental colleagues as a reference book, while several chapters could usefully be studied by an advanced student of physics in his final year.

Theory of Atomic Nucleus and Nuclear Energy-Sources

By G. Gamow and C. L. Critchfield. Pp. 344+vi, Figs. 62. Oxford University Press, New York, 1949. Price $9.00.

This is the third edition of Gamow's *Structure of Atomic Nucleus and Nuclear Transformations*, of which the second edition has been out of print since 1944. The book has been practically rewritten. The authors have attempted to write it in an inductive way, starting from the properties of elementary particles from which the nuclei are made and working up to more and more complex nuclear properties. Considerable space has been devoted to thermonuclear reactions and their application to cosmological problems.

Two Lectures: I. The Present Situation in the Theory of Elementary Particles. II. Electron Theory of Superconductivity

By W. Heisenberg. Pp. 52. Cambridge University Press, New York, 1949. Price $1.00.

The two lectures here printed were delivered at the Cavendish Laboratory as an introduction to discussions on two different topics in atomic theory. The first lecture tries to explain why the well-known divergencies in meson theory and nuclear physics may be considered, not as a difficulty, but rather as a natural and therefore satisfactory feature of the present "correspondence" theory. The second lecture deals with an application of quantum mechanics, the theory of superconductivity. The views presented in it may be considered as an attempt to combine different features of the previous rather discordant theories into a consistent picture of the phenomenon.

The Physical Principles of the Quantum Theory

By Werner Heisenberg. English translation by Carl Eckart and Frank C. Hoyt (reprint of 1930 edition). Pp. 184+viii, Figs. 19. Dover Publications, New York, 1949. Price $2.50.

In this book the author, a Nobel prize winner, gives a physical picture of quantum theory, covering not only his own contribu-

tions but also those of Compton, Simon, Schrödinger, Einstein, Wilson, Rupp, Davisson, Germer, Thomson, Bohr, and others. Although there is a mathematical appendix, only elementary formulas and calculations have been used in the text itself, so far as practical.

Nuclear Radiation Physics

By R. E. Lapp and H. L. Andrews. Pp. 487+xiv. Prentice-Hall, Inc., New York, 1948. Price $6.00.

This volume is the outgrowth of an elementary manual originally written by the present authors and published within the Military Establishment as "Radiological Safety." Basically, the authors have tried to present a logical and simple interpretation of the phenomena of nuclear physics. In each chapter illustrative examples are given in order to serve as an introduction to the calculations of radioactivity and to guide the student in the technique of solving the problems that appear throughout the text. An essentially non-mathematical approach has been employed, in the hope that the subject matter would not be too involved for non-physicists.

The Theory of Groups and Quantum Mechanics

By Hermann Weyl. Pp. 422+xvii. Dover Publications, New York, 1949. Price $4.50.

The author of this book postulates the importance of the theory of groups in discovering the general laws of quantum theory. Showing how concepts arising in the theory of groups find their application in physics, he illustrates his argument with many examples. Included are discussions of Schrödinger's wave equation, de Broglie's waves of a particle, the Jordan-Holder theorum and its analogs, Burnside's theorem, Lie's theory of continuous groups of transformations, the Pauli exclusion principle and the structure of the periodic table, quantization of the Maxwell-Dirac field equations, and Young's symmetry opreators.

The Theory of Atomic Collisions

By N. F. Mott and H. S. W. Massey (second edition). Pp. 388+xv, Figs. 69. Oxford University Press, New York, 1949. Price $8.75.

This new edition contains a systematic treatment of the new "dispersion" method developed for nuclear collisions and of its application to a wide variety of nuclear phenomena—the scattering and radiation capture of neutrons and protons by various nuclei as well as the scattering of alpha-particles. Nuclear fission is also discussed.

Atoms in Action

By George Russell Harrison (third edition). Pp. 406+x. William Morrow and Company, New York, 1949. Price $5.00.

This "layman's guide to modern science," an account of our most important physical discoveries and their contributions to everyday life, has been completely revised and expanded. It includes new material on atomic energy, radar, and electronics. As in previous editions, the author explains difficult technical matters in simple, graphic language.

Elementary Modern Physics

By Gordon Ferrie Hull. Pp. 503+xvi. The Macmillan Company, New York, 1949. Price $5.25.

This book is intended to gather together, for the use of students, the main developments in physics in recent years—to present the experimental facts and the more elementary theories.

Artificial Radioactivity

By P. B. Moon. Pp. 102+x, Figs. 28. Cambridge University Press, New York, 1949. Price $2.50.

This monograph gives an outline of the main phenomena and techniques of radioactivity, as met with in the study of the light-weight and medium-weight radioactive nuclei that can now be made in great variety. It is chiefly intended for readers who wish to be put into touch with the recent literature on the subject. The radioactive properties of a good many individual nuclei are discussed.

The Science and Engineering of Nuclear Power, Vol. II

Clark Goodman, editor. Pp. 317. Addison-Wesley Press, Boston, 1949.

Whereas Vol. I of this work was primarily a general survey of the fundamentals of chain-reacting systems, the present volume considers specific aspects in some detail such as source materials, isotope separation, vacuum techniques, pile kinetics, rockets, health physics, and future developments. The contents should be of value to all scientists and engineers seriously interested in the industrial applications of nuclear energy. The editor states that the contents of these two volumes "alone should be sufficient proof that 'atomic secrets' are largely figments formed in the minds of well-meaning persons who happen to be ignorant of this special field. A workable basis for the free exchange of ideas must be found. Mankind cannot continue to stand in mortal fear of the greatest scientific accomplishment of our time."

Atomic Energy Levels, Vol. I

By Charlotte E. Moore. Pp. 309+xliii. Circular 467 from the National Bureau of Standards, Washington, D. C., 1949. Price $2.75.

This volume is a compilation of all known data on the energy levels of elements of atomic number 1 through 23. It was designed to meet the needs of workers in nuclear and atomic physics. astrophysics, chemistry, and industry. This volume is the first of a series being prepared by the Bureau as part of a general program on atomic energy levels derived from observations of the optical spectra of atoms and ions. Spectra are presented in order of increasing atomic number, and under a given atomic number they are listed in order of increasing stages of ionization. For each spectrum a selected bibliography covering the analysis is given.

Excited States of Nuclei

By S. Devons. Pp. 152+ix, Figs. 27. Cambridge University Press, New York, 1949. Price $2.50.

This monograph was written mainly from the experimental standpoint. It gives a description of experimental methods and examines typical experimental results in detail. An attempt has been made to include examples taken from recent research and particularly to provide a broad picture of the situation which is up to date.

Trilinear Chart of Nuclear Species

By William H. Sullivan. John Wiley and Sons, Inc., New York, 1949. Price $2.50.

This publication was originated in the Chemistry Division of Clinton Laboratories during November 1946 and sponsored initially by it and by the Argonne National Laboratory. Its preparation was also facilitated and supported by the AEC and by the National Research Council.

Ionization Chambers and Counters: Experimental Techniques

By Bruno Rossi and Hans H. Staub. Pp. 243+xviii. McGraw-Hill Book Company, Inc., New York, 1949. Price $2.25.

Part I of this volume discusses the general physical principles underlying the operation of ionization chambers and counters, with special emphasis on subjects that are of importance in modern detection techniques. Original results are included which were obtained at the Los Alamos Laboratory in the course of assembling important nuclear data. Part II presents detailed discussions for a number of detectors developed and used by the authors and others at Los Alamos for the study of different kinds of radiations.

Radioactive Measurements with Nuclear Emulsions

By Herman Yagoda. Pp. 356+ix, Figs. 75. John Wiley and Sons, Inc., New York, 1949. Price $5.00.

This volume is a description of the theory and practice of nuclear emulsion technique—the use of photographic emulsions in studying radioactivity. The author gives a detailed description of many practical methods for the use of such emulsions, and in addition he explains the theory which underlies the operations involved. The book describes carrier precipitation methods, emanations, alpha-star formation, and radiocolloid adsorption phenomena. The bibliography of 700 items is another valuable feature of the book.

Cosmic Ray Physics

By D. J. X. Montgomery. Pp. 370+viii. Princeton University Press, Princeton, 1949. Price $5.00.

This volume presents a survey of the entire field of cosmic-ray studies. Because of the uncertainty of theory in the regions of energy involved and the complexity of the phenomena, the emphasis of the book is experimental with theory subordinated. The various experimental techniques are discussed and explained, and numerous illustrations are used throughout. The book presupposes a knowledge of general physics equivalent to that of an upperclass undergraduate or a beginning graduate student.

On the Theory of Stochastic Processes and Their Application to the Theory of Cosmic Radiation

By Niels Arley. Pp. 240, Figs. 53. John Wiley and Sons, Inc., New York, 1949. Price $5.00.

The purpose of this book is to investigate in further detail the so-called fluctuation problem in the theory of cosmic radiation. Part I deals with the theory of stochastic, or random, processes. It is aimed at giving a further generalization of Feller's and Lundberg's theories for the purpose of application of stochastic processes to the theories of cosmic-ray showers. Part II discusses in detail the fluctuation problem in the theory of the cosmic-ray showers treated in the first part.

Introduction to Radiochemistry

By Gerhart Friedlander and Joseph W. Kennedy. Pp. 412+xiii. John Wiley and Sons, Inc., New York, 1949. Price $5.00.

Included in the early chapters of this book is descriptive information about atomic nuclei, nuclear reactions, and the machines used for the acceleration of nuclear projectiles. Later chapters introduce in logical sequence the quantitative treatment of radioactive decay processes, the various types of radioactive disintegration, the radiations emitted, their interactions with matter, and their detection. The book presupposes no previous knowledge of nuclear physics. At the end of each chapter are lists of references which call attention to standard works and recent literature on specific topics. Exercises are also included at the end of each chapter.

Radioactive Tracer Techniques

By George K. Schweitzer and Ira B. Whitney. Pp. 241+vi, Figs. 13. D. Van Nostrand Company, Inc., New York, 1949. Price $3.25.

This manual is designed to serve as a guide for laboratory work and instruction in the utilization of radioactive tracers. The first four chapters deal with topics pertaining to all radioactive laboratory work. Next basic experiments are presented. The remainder of the book is devoted to material illustrating chemical, physical, and biological tracer methods.

Isotopic Tracers and Nuclear Radiations with Applications to Biology and Medicine

By William E. Siri (with contributions by five others). Pp. 653+xiv, Figs. 136. McGraw-Hill Book Company, Inc., New York, 1949. Price $12.50.

This book has been developed to bridge the gap between those books intended solely for the nuclear physicist and those which merely describe the results of research in which radioactive isotopes and nuclear radiations were used. To this end, the authors have presented the theory, the methods of measurement, and the principles of applications of tracers and radiations without stressing unnecessary and complicated features of nuclear physics or rapidly outdated experiments in biology.

Fear, War, and the Bomb

By P. M. S. Blackett. Pp. 244. Whittlesey House, McGraw-Hill Book Company, Inc., New York, 1949. Price $3.50.

The author, winner of a 1948 Nobel prize, asserts that the world today has an atom neurosis. He believes that we are handcuffed by fear, and that before we can achieve lasting peace, that fear must be replaced by a firm belief in the long life of civilization. The author believes that the atomic bomb cannot bring about a cheap, quick military knockout in a war between Russia and the United States, nor is that war imminent. When this book was first published in Great Britain it aroused an immediate storm of controversy. The author, a former member of Great Britain's advisory committee on atomic energy, holds a position sharply at variance with the official attitudes of the British and American governments.

Constructive Uses of Atomic Energy

S. C. Rothmann, editor. Pp. 258+ix, Figs. 11. Harper and Brothers, New York, 1949. Price $3.00.

This book describes atomic energy applications in such fields as industrial power, chemistry, metallurgy, aviation, ceramics, soil-fertilizer research, and biological, pharmaceutical, and medical research. It is a collection of fourteen articles by scientists in atomic research.

SOLID STATE PHYSICS

Progress in Metal Physics, I

Bruce Chalmers, editor. Pp. 401+viii. Interscience Publishers, Inc., New York, 1949. Price $9.50.

The purpose of this volume, which is to be the first of an annual series, is to present authoritative reviews of the present state of knowledge in specialized aspects of the field that includes both physical metallurgy and metal physics. Nine authors have contributed chapters.

Fourier Technique in X-Ray Organic Structure Analysis

By A. D. Booth. Pp. 106. Cambridge University Press, London; The Macmillan Company, New York, 1948. Price $2.75.

This book gives a comprehensive account of the technique of organic crystal structure determination by Fourier methods, and

indicates the relative scope of the various techniques. The treatment is from fundamentals, but the reader is assumed to have an adequate knowledge of geometric crystallography and of the theory of space groups.

Crystals and X-Rays

By K. Lonsdale. Pp. 199+viii, Figs. 138. D. Van Nostrand Company, Inc., New York, 1949. Price $3.75.

This book is based on a course of public lectures given at University College, London, in the spring of 1946, and is designed to interest those who do not now use x-ray crystallography but who might well do so; and to instruct those who are making use of x-ray crystallographic methods.

On the Systems Formed by Points Regularly Distributed on a Plane or in Space

By M. A. Bravais. English translation by Amos J. Shaler. Pp. 113+viii, Figs. 42. The Crystallographic Society of America, care of Philips Laboratories, Irvington, New York, 1949. Price $3.40 to members, $3.90 to non-members.

With this volume the Crystallographic Society of America begins publication of its Memoir Series. This work by Bravais, concerned with the development of the fourteen space lattices, marked an important milestone in the science of crystallography.

The Adsorption of Gases on Solids

By A. R. Miller. Pp. 133+ix, Figs. 38. Cambridge University Press, New York, 1949. Price $2,50.

This book has been based upon "Some Problems in Adsorption" by J. K. Roberts, a *Cambridge Physical Tract* published in 1939. Since the original tract was written, certain statistical theories have been developed in connection with this work and other advances have been made. Hence it seemed desirable to rewrite the book. Nearly half of the present work is new material.

Prüfen und Messen der Oberflächengestalt

By Johannes Perthen. Pp. 257, Figs. 115. Carl Hanser-Verlag-München, Munich, 1949.

Metals Reference Book

Colin J. Smithells, editor. Pp. 735+xvi. Interscience Publishers, Inc., New York, 1949. Price $13.50.

The object of this book is to provide a convenient summary of data relating to metallurgy and metal physics. So far as possible the data are presented in the form of tables or diagrams with the minimum of descriptive matter, although short monographs have occasionally been included where information could not otherwise be adequately presented. The values given are those which contributors have selected as the most reliable after a critical review of the published data. A limited bibliography at the end of each section enables the reader to refer to the more important original sources.

Treatise on Powder Metallurgy, Vol. I. Technology of Metal Powders and Their Products

By Claus G. Goetzel. Pp. 778+xxvii, Figs 300. Interscience Publishers, Inc., New York, 1949. Price $15.00.

This is the first of three volumes intended to serve as an introduction into the field for the novice who wants detailed information, as a reference book for the initiated, and for the engineer who has to solve immediate problems.

Hydrogen in Metals

By Donald P. Smith. Pp. 367+xiii. The University of Chicago Press, Chicago, 1948. Price $10.00.

This monograph takes up the absorption and retention of hydrogen by massive metal. Rates of absorption, from gas and at the cathode, are discussed, as well as the factors which influence them. Existing solubility data are presented in numerous tables and graphs, with critical comment.

Metallic Creep and Creep Resistant Alloys

By A. H. Sully. Pp. 278+xii, Figs. 138. Interscience Publishers, Inc., New York, 1949. Price $5.50.

In this book the author has attempted to present the viewpoints of both the industrial worker and the academic researcher in the field of creep resistant alloys. The development of the existing theory of the strength of metals is described with special reference to creep, and an attempt has been made to explain certain metallurgical factors affecting creep on the basis of this theory. A detailed summary of experimental techniques for the study of creep phenomena has also been included as well as a survey of the creep properties of most of the well-known ferrous and non-ferrous alloys. Some speculations on future developments in creep resisting alloys are made.

Technology of Light Metals

By A. von Zeerleder. Pp. 366+xiv, Figs. 396. Elsevier Publishing Company, Inc., New York, 1949. Price $7.50.

This handbook deals with the working up of aluminum and magnesium alloys from the ore to the semimanufactured goods, taking into consideration the possibilities of the latest metallurgical improvements. To prevent this book from becoming too voluminous, some less important portions of the 1936 edition have been eliminated, with more space devoted to the most recent testing and working methods.

Metal Rectifiers

By H. K. Henisch. Pp. 156+xi, Figs. 55. Oxford University Press, New York, 1949. Price $3.75.

This is the second volume of a series intended to summarize the recent results of long-range research in materials and allied subjects, in a form useful to physicists in universities and industrial laboratories. The book deals with the theory and practice of dry rectification, especially those aspects of the subject which are parts of physics rather than of engineering. Attention is paid especially to the theories of rectification put forward by Schottky, Wilson, and others, and to the experimental work which is relevant to their verification.

Titanium

By Jelks Barksdale. Pp. 591+xii, Figs. 15. The Ronald Press Company, New York, 1949. Price $10.00.

The purpose of this book is to meet the need for a working reference volume on titanium. Abstracts of the literature on titanium were studied by the author, and essential information incorporated into the text. Exact references to all the material consulted are included.

Industrial Rheology and Rheological Structures

By Henry Green. Pp. 311+xii, Figs. 78. John Wiley and Sons, Inc., New York, 1949. Price $5.50.

Believed to be the first of its kind, this book is a manual and practical working guide for making rheological and structural microscopic investigations. It can be used by university or industrial laboratory where researchers deal with such articles as printing inks, paints, oils, varnishes, biochemicals, resins, plastics, food, cement, and asphalt.

Engineering Laminates

ALBERT G. H. DIETZ, editor. Pp. 797. John Wiley and Sons, Inc., New York, 1949. Price $10.00.

This book contains valuable information for everyone concerned with the design, manufacture, and use of structural materials. The book completely explains the mechanics of laminate materials from basic properties, through physical and chemical properties, to industrial uses. Discussions of wood, metallic, and rubber-based laminates are included. Throughout the book the authors have emphasized engineering properties, design, manufacture, and use. The book has a contributing staff of 24 engineers, architects, builders, metallurgists, designers, and professors.

High-Polymer Physics—a Symposium

HOWARD A. ROBINSON, editor. Pp. 572+xiii. Remsen Press Division, Chemical Publishing Company, Inc., Brooklyn, New York, 1948. Price $12.00.

Thirty-nine physicists and chemists, all rather prominent experts in their special fields, contributed to this symposim on hte relatively new subject of high-polymer physics. The results discussed come largely from industrial research laboratories rather than from college research groups. The physicist had to help the chemist, and vice versa, to explain the phenomena encountered in high polymers. This volume is the product of their cooperation.

APPLIED PHYSICS NOT INCLUDED ELSEWHERE

Mathematical Biophysics

BY NICOLAS RASHEVSKY (revised edition). Pp. 669+xxiii. University of Chicago Press, Chicago, 1948. Price $7.50.

This study is intended to lay the foundation for a mathematical biology, analogous in its methods to mathematical physics and based on the physical interpretations of biological phenomena. In this new edition the author has included recent developments in the field of mathematical biophysics and has incorporated most of the material formerly published in his *Advances and Applications of Mathematical Biology*. This edition contains 200 pages of new material, including the theory of embryonic development, the theory of cancer, and an elaboration on the theory of cell division. Also included are a number of new chapters on learning, abstractions, logical thinking, and perception of visual patterns.

Biological Reactions Caused by Electric Currents and by X-Rays

BY J. TH. VAN DER WERFF. Pp. 203, Figs. 38. Elsevier Publishing Company, Inc., New York, 1948. Price $5.00.

This book is a theoretical study of the phenomena of excitation in the nerve by different electric currents and of the biological reactions caused by x-rays, both based upon a common principle.

The Atmospheres of the Earth and Planets

GERARD P. KUIPER, editor. Pp. 366+vii, Figs. 91. The University of Chicago Press, Chicago, 1949. Price $7.50.

Physical Principles of Oil Production

BY MORRIS MUSKAT. Pp. 922+xv. McGraw-Hill Book Company, Inc., New York, 1949. Price $15.00.

The purpose of this book is to formulate and correlate present information concerning the physical principles and facts underlying the mechanics of oil production. A further purpose has been to stimulate and encourage additional research and study of the subject to fill in the many gaps in our present knowledge, clarify the many aspects which are still subject to speculation and conjecture, generalize the simplified and idealized treatments of special problems, and to improve the correlation between laboratory theories and field observations. The approach of the book consists in the detailed analysis of the physical concepts and principles which are developed as foundations for the interpretation and study of actual oil field performance. Many examples from actual oil field operation demonstrate the basic characteristics of the various types of producing mechanism and operation.

Seismicity of the Earth and Associated Phenomena

BY B. GUTENBERG AND C. F. RICHTER. Pp. 273+vii, Figs. 34. Princeton University Press, Princeton, 1949. Price $10.00.

This is an account of the relative seismicity of various parts of the earth during the limited period (since about 1904) for which sufficiently accurate data are available. Geographical and geological relations of the principal earthquake zones and areas are discussed, including correlation with mountain structures, oceanic deeps, gravity anomalies, and active volcanoes. A new checklist of active volcanoes is included. The origin of earthquakes is discussed, particularly with reference to folding and thrusting in the structural arcs of Pacific type.

Oscillations of the Earth's Atmosphere

BY M. V. WILKES. Pp. 76+ix, Figs. 23. Cambridge University Press, New York, 1949. Price $2.50.

This monograph discusses all that is known to date of the oscillations of the atmosphere. It treats of the lunar and solar air tides, their measurement, manifestations, and causes; the theory of oscillations in a rotating atmosphere; the numerical evaluation of air tides; the outward flux of energy; the height of the earth's atmosphere; the temperature variation, etc. Observational and mathematical methods of arriving at a knowledge of the properties of the atmosphere are referred to as they arise, and the book concludes with a general discussion of results.

Some Recent Researches in Solar Physics

BY F. HOYLE. Pp. 134+xii, Figs. 8. Cambridge University Press, New York, 1949. Price $3.00.

The aim of this monograph is to provide an account of the present state of solar physics. The first two chapters are largely devoted to an account of the observational material concerning sunspots, the solar cycle, the chromosphere, and the corona. In the third and fourth chapters a new theory of the origin and structure of the chromosphere and corona is presented, while in the remainder of the book such diverse topics as electromagnetism in the solar atmosphere, solar and terrestrial relationships, the emission of radio waves by the sun, and the origin of the general solar magnetic field are discussed.

The Solar System Analysed

BY F. C. ATTWOOD. Pp. 88. The Dawson Printing Company, Ltd., Auckland, New Zealand, 1947.

This brief book is subtitled "Old Laws from a New Angle." Chapters deal with the beginning of the solar system, the solar nebula, the origin of the earth's rotation, and so on through a concluding chapter named "Speculation."

Our Sun

BY DONALD H. MENZEL. Pp. 326, Figs. 178. The Blakiston Company, Philadelphia, 1949. Price $4.50.

In language that is easily understood, this volume explains the basic methods for finding out about the sun. It vividly pictures solar activity and the vast explosions occurring in the sun's atmosphere. Included are the many new advances in solar research heretofore restricted from publication because of military classification. The author discusses the relationship between the sun and our natural resources; its probability as a source of heat and fuel; the sun and atomic power; and its effect on radio transmission and weather forecasting.

The Face of the Moon

By Ralph B. Baldwin. Pp. 239+xiv, Figs. 26, Plates XVII. The University of Chicago Press, Chicago, 1949. Price $5.00.

"How and when did the moon arrive at its present state of dilapidated grandeur?" In this interesting volume the author examines and rejects all but one of the processes previously suggested to account for the lunar craters, rays, mountain ranges, and lava flows. He selects as the most probable cause the impacts of giant meteorites on the rocky lunar face and their resultant explosions. Chapters are devoted to a description of the strange and beautiful formations found on the moon, to a discussion of modern and ancient meteoritic craters known to exist on earth, to an analysis of the impact theory in the light of knowledge of man-made explosion pits, to an investigation of the possible effects of a lunar atmosphere, to the dating of the major changes on the face of the moon, and to a consideration of the possibility of meteoritic infalls on other planets.

Hydrology

By C. O. Wisler and E. F. Brater. Pp. 419+xi, Figs. 132. John Wiley and Sons, Inc., New York, 1949. Price $6.00.

This textbook presents the fundamental principles of hydrology as they have been developed up to the time of writing. The distribution graph, the unit hydrograph, the theory of infiltration capacity, and many other recent developments are presented. The many applications cited throughout the book make it useful to the general practicing engineer, forester, and agriculturist, as well as to the student who is looking for the basic principles of hydrology. The book provides information which can be used in the determination of the maximum flood flow that may be expected every few years, as in airport drainage and storm sewer design. For the design of a spillway for an important dam, or any flood control work, the authors present methods for determining the maximum flow that will occur with rare frequency, such as once in a thousand years.

Surface Tension and the Spreading of Liquids

By R. S. Burdon. Pp. 92+xi, Figs. 22. Cambridge University Press, New York, 1949. Price $2.50.

The first edition of this book was published in 1940. In this new edition the author has added accounts of all important work published recently. Chapter subjects include the nature of surface forces; measurement of surface tension; the surface of liquid metals; spreading; general conditions; spreading on the surface of mercury; spreading on water; liquids on the surface of solids.

Experimental Immunochemistry

By Elvin A. Kabat and Manfred M. Mayer. Pp. 567+xv, Figs. 88. Charles C. Thomas, Publisher, Springfield, Illinois, 1948.

The authors of this book have undertaken the task of assembling for the first time in one place the scattered techniques which have been developed to fill the needs of immunochemical problems. Main emphasis is placed on quantitative analytical methods. To meet the needs of students as well as of chemists who may not be thoroughly familiar with immunology, and of bacteriologists and immunologists who may not be well acquainted with microchemical methods, introductory and background material in both fields has been included.

Bibliography of Research on Heavy Hydrogen Compounds

Harold C. Urey and Isidor Kirshenbaum, editors; compiled by Alice H. Kimball. Pp. 350+xvi. McGraw-Hill Book Company, Inc., New York, 1949. Price $3.25.

This volume is a collection of about 2000 references to published literature on the subject of the heavy hydrogen isotope. The material is classified according to subject in such a manner that previous work in the field may be readily found. The volume should prove useful to anyone concerned with research on isotopes and their application to specific problems.

Physical Methods of Organic Chemistry, Parts I and II

Arnold Weissberger, editor (second edition). Pp. 1072+xii and 1024+xi. Interscience Publishers, Inc., New York, 1949. Price $12.50 each.

This familiar work has been completely revised and augmented, and as before, appears in two volumes. The new edition has new chapters on temperature measurement, temperature control, vapor pressure, the ultra-centrifuge, electrophoresis, and turbidimetry. The chapters on viscosity, osmotic pressure, diffusivity, dipole moments, radioactivity, and mass spectrometry have been entirely rewritten. All other chapters have been thoroughly revised.

Outlines of Physical Chemistry

By Farrington Daniels. Pp. 713+viii, Figs. 164. John Wiley and Sons, Inc., New York, 1948. Price $5.00.

This is the seventh revision of what was originally the well-known "Getman and Daniels" text on physical chemistry. The illustrations in this edition have been revised in keeping with the author's emphasis on practicality. Hypothetical diagrams illustrating physical chemical phenomena have been replaced with data from laboratory measurements. One-fourth of the numreous problems have been replaced or revised.

Sources of Engineering Information

By Blanche H. Dalton. Pp. 109. University of California Press, Berkeley, 1948. Price $4.00.

This is a guide to engineering literature and data designed as a concise reference for engineering students, practicing engineers, research workers, and librarians. Its arrangement is based on studies of the use of an actual library collection. The book includes information on every type of engineering.

Rocket Propulsion Elements

By George P. Sutton. Pp. 294+ix. John Wiley and Sons, Inc., New York, 1949. Price $4.50.

Airplane Performance, Stability, and Control

By Courtland D. Perkins and Robert E. Hage. Pp. 493+vii. John Wiley and Sons, Inc., New York, 1949. Price $7.00.

This book is divided into two major parts, the first dealing with the problems of airplane design for performance, and the second involving the design of the airplane for adequate stability and control characteristics. In the first part, basic aerodynamics is summarized so that an estimation of airplane drag can be made for subsonic, transonic, and supersonic speeds; propulsion characteristics of the reciprocating engine, turbine propeller, turbojet, ramjet, and rocket are presented; performance methods are analyzed for the basic forces acting on an airplane utilizing any of the above power plants. In the second part of the book, the comparatively new art of designing the airplane for adequate flying qualities has been dealt with, with only subsonic flight being discussed. A modern analysis of the dynamics of the airplane is included.

GENERAL AND HISTORICAL

Reports on Progress in Physics, Vol. XII

Pp. 382. The Physical Society, London, 1949. Price to non-Fellows £2 2s. (postage 1s.).

This volume, containing papers by 19 authors, includes the following subjects: mass spectrometry, nuclear paramagnetism,

phosphors and phosphorescence, spontaneous fluctuations, recent nuclear experiments with high voltage x-rays, linear accelerators, viscosity and related properties in glass, theory of the oxidation of metals, fracture and strength of solids, multipole radiation in atomic spectra, collisions between atoms and molecules at ordinary temperatures, low temperature physics, slow neutron absorption cross sections of the elements, and molecular distribution and equation of state of gases.

Fundamentals of Physical Science

By Konrad Bates Krauskopf (second edition). Pp. 676+xii, Figs. 330. McGraw-Hill Book Company, Inc., New York, 1948. Price $4.50.

The preparation of this second edition was prompted chiefly "by a desire to bring the book up to date in several rapidly advancing fields of physical science." Notable changes are a complete rewriting of the chapter on the atomic nucleus, addition of a section on the uncertainty principle, introduction of Brönsted's theory in the discussion of acids and bases, and increased emphasis on air-mass analysis in weather forecasting.

Physics in the Modern World

By Henry Semat. Pp. 434. Rinehart and Company, New York, 1949. Price $5.00.

This book is addressed specifically to students of the arts and social sciences who are interested in learning and understanding the methods of the physical sciences. This volume is the outgrowth of three years of experience in teaching "Physics in the Modern World" to non-science students at the College of the City of New York. (Similar courses of the same length are given in chemistry, biology, and geology-astronomy.)

The Nature of Physical Theory

By P. W. Bridgman (reprint of 1936 edition). Pp.138+vi. Dover Publications, New York, 1949. $2.25.

This book is a study of modern scientific theory which views the problem of correlating reality with the various theoretical structures set up in the past fifty years. It analyzes the inadequacies of physical theories in supplying the answers to all questions, but points out the real service these concepts render within limited frames of reference. The author investigates and weighs the contributions of Newton, Bohr, Einstein, Heisenberg, and others. He discusses such basic concepts as the wave and corpuscular theories, the "clocks" of relativity, the "laws" of probability, and the mathematical system itself.

Science at War

By J. G. Crowther and R. Whiddington. Pp. 185, Figs. 51, Plates 51. Philosophical Library, Inc., New York, 1948. Price $6.00.

This is a detailed account of science's contribution to the war effort, based on the official archives and documents assembled by the scientific advisory committee to the British Cabinet. This volume should be of fundamental interest to the American scientist as well as to the intelligent layman interested in science. Among the basic topics dealt with in the book are radar, the atomic bomb, operational research, science, and the sea.

The Principles of Scientific Research

By Paul Freedman. Pp. 222, Figs. 11. Macdonald and Company, Ltd., New York, 1949. Price $3.05.

This book is addressed chiefly to young men and women embarking on or concerned with scientific research, but it is also intended for business executives in whose power, to a considerable extent, the successful conduct of scientific research lies.

The Universe and Dr. Einstein

By Lincoln Barnett. Pp. 127. William Sloane Associates, New York, 1948. Price $2.50.

This book is a report on what the men at the forefront of science know about the nature of the universe. The story of the search for essential truth about the universe is here told simply, in the vocabulary of the intelligent layman. This book can be understood by the high school student of physics and chemistry and still could be read with profit by outstanding scientists of today.

Man and This Mysterious Universe

By Brynjolf Bjorset. Pp. 174+vii. Philosophical Library, New York, 1949. Price $3.75.

This small book is intended as a synthesis of the many aspects of modern civilization, bringing within its scope the contribution of the East as well as of the West, showing how it has grown from the civilization of the past and how it will probably develop in the future. The author has traveled for thirty years and lived in more than fifty countries.

After Dinner Science

By Kenneth M. Swezey. Pp. 182. Whittlesey House, McGraw-Hill Book Company, Inc., New York, 1948. Price $3.00.

For everyone interested in popular science, here is a book full of pictures and fascinating scientific experiments that can be performed with ordinary household materials and without any previous scientific knowledge. The author takes the mystery out of science. With photographs and easy-to-understand explanations he shows the reader how he himself can demonstrate the basic laws of scientific phenomena. This is a volume that the whole family can enjoy.

Mendeleyev—the Story of a Great Scientist

By Daniel Q. Posin. Pp. 345+xii. McGraw-Hill Book Company, Inc., New York, 1948. Price $4.50.

This is the first biography in English of this famous Russian chemist and physicist. It reveals an almost unbelievable story of triumph in a man with a burning desire to be a scientist. It was Mendeleyev who first unlocked the doors of Russia's great natural resources. As a young man he had begun his studies handicapped by illness and poverty. Studying and teaching in the daytime, he spent most of the night in his laboratory. He discovered a plan of unity among the chemical elements which led him to fromulate the Periodic Table. When he died at 73, he had been acclaimed by every country in the world.

Albert Einstein, Philosopher-Scientist

Paul Arthur Schilpp, editor. Pp. 781+xvi. The Library of Living Philosophers, Northwestern University, Evanston, Illinois, 1949. Price $8.50.

This volume contains Albert Einstein's autobiography. In addition, contributions from 25 scholars and scientists in eleven countries (among them six Nobel Prize winners) discuss various aspects of Einstein's scientific work and achievements. In Part III of the volume Einstein replies to the comments, analyses, and criticisms of his contemporaries. An exhaustive bibliography of Einstein's writings is included.

Scientific Autobiography and Other Papers

By Max Planck. Pp. 192. Philosophical Library, New York, 1949. Price $3.75.

This is a collection of the last writings of one of the greatest physicists of our time. The essays that make up this small volume deal with problems such as: true and fictitious issues in science; meaning and limit of exact science; physics and causality; natural sciences and the religious world. The autobiographical notes tell the story of Max Planck's own personal and scientific development.